U.PORTO

FEUP FACULDADE DE ENGENHARIA
UNIVERSIDADE DO PORTO

Design of a high-speed transmission for an electric vehicle

Carlos Daniel Pires Rodrigues

Dissertation submitted to
Faculdade de Engenharia da Universidade do Porto
for the degree of:

Mestre em Engenharia Mecânica

Advisor:
Prof. Jorge Humberto Oliveira Seabra

Co-Advisor:
Prof. José António dos Santos Almacinha

Unidade de Tribologia, Vibrações e Manutenção Industrial
Departamento de Engenharia Mecânica
Faculdade de Engenharia da Universidade do Porto

Porto, Julho de 2018

The work presented in this dissertation was performed at the
Tribology, Vibrations and Industrial Management Unit
Department of Mechanical Engineering
Faculty of Engineering
University of Porto
Porto, Portugal.

Carlos Daniel Pires Rodrigues
E-mail: up201305002@fe.up.pt, cdpr@outlook.com

Faculdade de Engenharia da Universidade do Porto
Departamento de Engenharia Mecânica
Unidade de Tribologia, Vibrações e Manutenção Industrial
Rua Dr. Roberto Frias s/n, Sala M206
4200-465 Porto
Portugal

Abstract

For decades, the hegemony of internal combustion vehicles has led to an improvement, by the automotive industry, of transmissions, in order to increase the torque and reduce the rotational speed from the engine.

These transmissions are quite complex, having up to 7 speeds, with the aim of retrieving the highest possible efficiency from the considerably inefficient internal combustion engines.

Nowadays, environmental concerns and strong governmental regulations, as well as, buying incentives, have presented electric vehicles as a viable solution to consumers while being in line with the new global paradigm of sustainability.

Electric vehicles turn to electric motors to transform electric energy in mechanical energy. Since these motors are widely used in other industrial applications, they are already a mature technology. They have an ideal torque and power curves regarding vehicle operation. Due to these favourable characteristics, the transmission of an electric vehicle is simpler, presenting itself as a conventional reducer with respect to the overall geometry, having usually only one speed ratio between the input and the output.

However, the high rotational speed associated with compact electric motors, makes it necessary to take some factors into account when designing a transmission: gear design, lubrication method selection, as well as rolling bearing selection are just some of the concerns that will be further elaborated in this thesis, in order to reduce power losses, ensuring a good efficiency and, at the same time, control the noise generated.

The mechanical differential, which is present in all internal combustion vehicles, is a system that provides the vehicle with the capacity to change direction steadily, however it cannot be continually controlled. Thus, the idea of using an electronic differential seems interesting, since it would reduce the number of mechanical components and, through the ever-increasing network of sensors and data acquired by the vehicles themselves, it is possible to independently control the rotational speed of each front wheel continuously, leading to greater safety and comfort when the vehicle is changing direction.

Keywords: electric vehicles, transmission, gears, electronic differential, splash lubrication.

Resumo

Durante largas décadas, a hegemonia dos veículos de combustão interna levou a um aperfeiçoamento por parte da indústria automóvel das transmissões para aumentar o binário e reduzir a velocidade provenientes do motor.

Estas transmissões são bastante complexas, podendo ter até 7 velocidades, de forma a extrair o mais rendimento possível dos pouco eficientes motores de combustão interna.

Atualmente, preocupações ambienteais e fortes regulações governementais, bem como, elevados incentivos de compra, tornaram os veículos elétricos como uma solução viável para os consumidores e que vai de encontro ao novo paradigma mundial de sustentabilidade.

Os veículos elétricos recorrem a motores elétricos para transformar a energia elétrica em energia mecânica. Uma vez que estes motores são amplamente utilizados em outras aplicações industriais, já se apresentam como uma tecnologia madura. Eles possuem uma curva de binário e de potência ideal para os automóveis. Devido a estas características favoráveis, a transmissão de um veículo elétrico é mais simples, apresentando-se como um redutor convencional em termos geométricos, tendo apenas uma razão de velocidades entre a entrada e a saída. Porém, a elevada velocidade de rotação associada aos motores elétricos compactos, leva a que sejam necessários cuidados na concepção da transmissão: desenvolvimento das engrenagens, escolha do método de lubrificação ideal e escolha dos rolamentos são apenas algumas das questões que serão aprofundadas nesta dissertação, de forma a que as perdas de potência sejam reduzidas, garantindo uma boa efficiência e, ao mesmo tempo, controlar o ruído gerado.

O diferencial mecânico, presente em todos os veículos de combustão interna, é um sistema que proporciona a capacidade para um veículo curvar de forma correta, mas que não é possível regular enquanto veículo está em movimento. Assim, surgiu a ideia de usar um diferencial eletrónico, reduzindo o número de componentes mecânicos e, através da cada vez mais elevada rede de sensores e informação adquirida pelos próprios veículos, seja possível realizar um controlo independente e continuado das velocidades de rotação das duas rodas da frente, levando a uma maior segurança e conforto quando o veículo está a mudar de direção.

'Nós somos o que fazemos. O que não se faz não existe.'

Padre António Vieira

Acknowledgements

I would like to thank my thesis advisor Prof. Jorge Seabra and co-advisor Prof. José Almacinha of the Faculty of Engineering at University of Porto. They consistently allowed this thesis to be my own work and steered me in the right direction providing guidance and support, as well as recommendations and several revisions throughout the semester.

I would also like to thank all my friends which provide a very pleasant environment to evade, for short periods of time, the work atmosphere.

Finally, I give my warmest thanks to my family, in particular to my parents, for the continuous encouragement and everything that they have provided me along the years, and whose support after all is the most essential.

Contents

List of Figures

List of Tables

Acronyms

AC	Alternating Current
BEV	Battery Electric Vehicle
BLDC	Brushless DC
BMS	Battery Management System
BRS	Boost Recuperation System
CVT	Continuously Variable Transmission
DC	Direct Current
EM	Electric Motor
EREV	Extended Range Electric Vehicle
ESKAM	Electrically Scalable Axial-Module
EV	Electric Vehicle
FPM	Fluorocarbon rubber
FVA	Forschungsvereinigung Antriebstechnik, the Research Association for Drive Technology
GHG	Greenhouse Gas
HEV	Hybrid Electric Vehicle
iBAS	Integrated Belt Alternator Starter
ICE	Internal Combustion Engine
IM	Induction Motor
LSD	Limited Slip Differential
NBR	Acrylonitrile-butadiene rubber
NEDC	New European Driving Cycle
NVH	Noise, Vibration and Harshness
OEM	Original Equipment Manufacturer
PEV	Pure Electric Vehicle
PHEV	Plug-In Hybrid Electric Vehicle
PMSM	Permanent Magnet Synchronous Motor
PPTE	Peak-to-Peak Transmission Error
SRM	Switched Reluctance Motor
TUM	Technical University of Munich
WRSM	Wound Rotor Synchronous Motor

Nomenclature

Symbol	Description	Unit
a	Center distance	mm
A_{air}	Ventilated housing area	m^2
a_{d}	Reference center distance	mm
A_{ca}	External housing area	m^2
A_{fin}	Total fin area	m^2
A_{oil}	Internal housing area	m^2
A_{pro}	Projected fin area	m^2
A_{f}	Frontal area	m^2
b	Face width	mm
C_{ch}	Churning losses	W
C_{d}	Aerodynamic drag coefficient	-
C_{m}	Churning losses parameter	-
C_{rr}	Rolling resistance coefficient	-
C_{α}	Tip relief	µm
$C_{\alpha\mathrm{f}}$	Front tire cornering stiffness	µm
$C_{\alpha\mathrm{r}}$	Rear tire cornering stiffness	µm
C_{β}	Crowning	µm
$C_{\mathrm{H}\beta}$	Helix angle modification	µm
d	Shaft diameter, distance between left and right wheel	mm
d_{a}	Gear tip diameter	mm
d_{w}	Gear operating pitch diameter	mm
D_{hub}	Hub diameter	mm
D_{p}	Pitch diameter	mm
f_{ma}	Manufacturing allowance (axis misalignment)	-
$f_{\mathrm{H}\beta}$	Manufacturing allowance (gear lead variation)	-
f_{s}	Horizontal static friction	-
F_{a}	Aerodynamic drag, Axial force	N
F_{g}	Grading force	N
F_{r}	Radial force	N
F_{rr}	Rolling resistance	N
F_{t}	Tractive force	N
F_{x}	Shearing force X	N
F_{z}	Shearing force Z	N
F_{C}	Centrifugal force	N
Fr	Froude number	-
g	Gravitational acceleration (= 9,81)	$\mathrm{m}^2\,\mathrm{s}^{-1}$
Gr	Grashoff number	-

h	Submerged height, height of vehicle center of mass	mm
h_{ca}	Overall transmission height	mm
H_{f}	Flange height	mm
H_{t}	Gear tooth height	mm
i_1	First stage transmission ratio	-
i_2	Second stage transmission ratio	-
i_{g}	Overall transmission ratio	-
Ja	Axial distance between flange and gear	mm
k	Heat transfer coefficient	$\mathrm{W\,m^{-2}\,K^{-1}}$
K	Ackerman steering gradient	-
K_{a}	Application factor	-
K_{AF}	Root strength application factor	-
K_{AH}	Flank strength application factor	-
$K_{\mathrm{H\beta}}$	Face load factor	-
l_{fin}	Depth of one fin	mm
l_{x}	Flow length (path of flow filament along the housing wall)	mm
L	Length between front and rear axle	m
L_{Ca}	Roll length of the tip relief	µm
$L_{\mathrm{Ca*}}$	Length factor	-
m	Mass	kg
m_{n}	Normal module	mm
M_{x}	Bending moment X	Nm
M_{z}	Bending moment Z	Nm
N, n	Rotational speed	rpm
P	Distance between left and right front wheel kingpins	m
P_{m}	Electric motor power	kW
$\bar{P}_{\mathrm{res}}$	Average resistance power	kW
P_{VD}	Seal power loss	W
P_{VL}	Rolling bearing power loss	W
P_{VZP}	Gear power loss	W
P_{VZ0}	Churning loss	W
P_{V}	Total power loss	W
p_{x}	Axial pitch	mm
Q_{ca}	Housing heat dissipation	W
r_{t}	Tire radius	m
R	Turning radius	m
R_1	Turning radius of left-front wheel	m
R_2	Turning radius of right-front wheel	m
R_{p}	Gear pitch radius	mm
Ra	Average roughness	µm
Rz	Mean peak-to-valley roughness	µm
Re	Reynolds number	-
R_{m}	Tensile strength	$\mathrm{N\,mm^{-2}}$
S_{F}	Tooth root safety	-
S_{H}	Tooth flank safety	-
S_{m}	Gear submerged surface	$\mathrm{m^2}$
S_{md}	Wet surface of the gear flank	$\mathrm{m^2}$
S_{mf}	Wet surface of the gear teeth	$\mathrm{m^2}$
t_{a}	Acceleration time	s

T_{air}	Air temperature	K
T_{m}	Torque (electric motor)	Nm
T_{oil}	Oil temperature	K
T_{wall}	Housing wall temperature	K
T_{∞}	Ambient temperature	K
Ta	Taylor number	-
v	Velocity, Circumferential speed, Cornering speed	$\mathrm{m\,s^{-1}}$
v_{arg}	Air Velocity	$\mathrm{m\,s^{-1}}$
v_{ga}	Sliding velocity at tip	$\mathrm{m\,s^{-1}}$
V_0	Oil volume	$\mathrm{m^3}$
x_{i}	Gear profile shift	-
W_{f}	Front vehicle load	N
W_{r}	Rear vehicle load	N
Z	Gear number of teeth	-

Greek symbol	Description	Unit
α	Road grade	rad
α_{ca}	Air-side heat transfer coefficient	$\mathrm{W\,m^{-2}\,K^{-1}}$
α_{con}	Convection heat transfer coefficient	$\mathrm{W\,m^{-2}\,K^{-1}}$
α_{n}	Pressure angle	$^{\circ}$
α_{oil}	Oil-side heat transfer coefficient	$\mathrm{W\,m^{-2}\,K^{-1}}$
α_{rad}	Radiation heat transfer coefficient	$\mathrm{W\,m^{-2}\,K^{-1}}$
β	Helix angle	$^{\circ}$
Γ	Flange parameter	-
δ	Rotating inertia factor, Ackerman angle	-
δ_{fin}	Fin thickness	mm
ε	Housing emission ratio	-
ε_{α}	Transverse contact ratio	-
ε_{β}	Overlap ratio	-
ε_{γ}	Total contact ratio	-
ζ_{a}	Specific sliding at the tip	-
η	Efficiency	-
λ_{fin}	Fin thermal conductivity	$\mathrm{W\,m^{-1}\,K^{-1}}$
μ_{s}	Static friction coefficient	-
ν	Oil kinematic viscosity	$[\mathrm{mm^2/s}]$
ν_{air}	Air kinematic viscosity	$[\mathrm{mm^2/s}]$
ρ	Density	$\mathrm{kg\,m^{-3}}$
ω	Rotational velocity	rad/s

Chapter 1

Introduction

1.1 Introduction

The increasing necessity to preserve natural resources and environmental issues stimulate interest in the development of electric vehicles. These vehicles offer various advantages compared to internal combustion vehicles. They are more efficient, less noisy and simpler, providing a smooth drive experience.

While most of the existing vehicles work under some form of internal combustion engines, electric vehicles invoke the excellent performance specifications of an electric motor, such as high torque at low rotations and constant power during a large speed range.

High-speed electric motors are a valuable option to drive an electric vehicle. They are low weight and low cost while highly efficient. For an urban vehicle, they can deliver the necessary power to comply with the performance requirements. The major challenge is to integrate a high-speed motor and a gearbox, reducing significantly the speed and increase the torque.

Whereas, conventionally, multi-speed transmissions are employed, in electric vehicles single-speed transmissions with a fixed ratio are the standard, due to the characteristics of the electric motors.

The electric automotive industry is still in its early days, so, a great number of investigative research is required and already being performed to review specific areas so that consensus among the manufacturers and designers can be built.

1.2 Objectives

The main objective of the thesis is to design a high-speed gear transmission for a front-wheel drive urban passenger vehicle with a city drive cycle.

In a high-speed transmission, special attention has to be given to gear teeth geometry and rolling bearing selection to maximize the energetic efficiency, while, at the same time, control the noise generated, major factor in electric vehicles, since there is no noise from the internal combustion engine to suppress the transmission noise.

A further challenge is to design a simple transmission using standard manufacturing techniques, so that the manufacturing costs are reduced. To avoid the use of a mechanical differential, resulting in a minimization of the transmission weight and an increase in reliability, two electric motors associated with two independent transmissions are used. This requires an electronic differential, which acquires information from several vehicle sensors, for example, regarding wheel speed and weight distribution. The differential

kinematics are obtained through the variation of the speed output from the electric motors to the transmissions input.

Lubrication and thermal efficiency require close attention, in order to assess the best lubrication method and to estimate if the transmission is operating at a proper temperature spectrum.

Mechanical design regarding assembling and manufacturing drawings will also be considered and the necessary ones presented.

1.3 Layout

The document layout follows a chapter structure, the references are presented after the last chapter and the document has the required appendices at the end. The chapters layout is:

Chapter 2

In the chapter 2 a background research regarding the current situation of the electric vehicle market is presented. Electrification, automotive industry, energy storage and powertrain solutions as well as present projects are thoroughly discussed.

Chapter 3

In chapter 3 the general design characteristics are evaluated. The required vehicle specifications and vehicle performance are reviewed. An assessment is made regarding the overall kinematic chain (number of stages and geometry) of the transmission.

Chapter 4

Both cylindrical gear pairs are designed in chapter 4. Several factors have to be derived and estimated to comply with the necessary requisites, for instance, face width, normal module and helix angle. A comparison of different gear pairs for the respective stages is going to be made to select a final solution.

Chapter 5

In chapter 5, the required shafts are designed according to standard shaft layout. Special attention is given to the relative position of the shafts with respect to each other, since it affects the load distribution that the rolling bearings have to withstand. According to the resulting loads, the bearing selection and arrangement is going to be analysed. Finally, a shaft analysis regarding stress, deflection and critical speed is performed.

Chapter 6

Chapter 6 provides an examination of the gear modification sizing. Considerations about shaft deflection, manufacturing tolerances and noise behaviour are specified and the appropriate tooth trace and profile modifications are going to be evaluated, and, if there is a positive outcome, implemented.

Chapter 7

Chapter 7 deals with lubrication and sealing. The most suitable lubrication method is selected and solutions will be assessed for the previously chosen lubrication method. Afterwards, the lubricant is selected just as the necessary sealing system with the respective shaft seals.

Chapter 8

In chapter 8 a thermal analysis is carried out. Considering the total power losses and the heat dissipation, both at maximum torque and maximum speed operating conditions, the required oil temperature for these two extreme conditions is going to be calculated giving a good estimation of the oil temperature range inside the transmission, during normal operation.

Chapter 9

Housing design considerations, and several transmission components are presented in the chapter 9. Housing layout design remarks are going to be determined and important specifications regarding the listed parts, such as, screws, set pins, retaining rings and plugs will be presented.

Chapter 10

The chapter 10 is reserved to the final assembly of the transmission. In this chapter, all the components are going to be sequentially positioned in the transmission housing resulting in a fully functional transmission.

Chapter 11

The concluding chapter is the chapter 11 where considerations towards the application of the electronic differential are offered. The critical cornering speed for a minimum turning radius is going to be obtained and the variation of left and right wheel speed consider.

Chapter 2

Background Theory

2.1 Electric vehicles

Any vehicle where its transmission is powered (partially or in full) by a battery is designated an Electric Vehicle (EV). There are several types of EVs, each one with its own set of characteristics and different purposes. Thus, EVs can be divided in Pure Electric Vehicles (PEVs), Plug-In Hybrid Electric Vehicles (PHEVs), Extended Range Electric Vehicles (EREVs) and Hybrid Electric Vehicles (HEVs).

The absence of vibrations, noise and exhaust gases as well as greater reliability compared to Internal Combustion Engine vehicles (ICEs) favoured EVs until the beginning of the 20^{th} century. However, major improvements in the oil industry led to a decrease in gasoline prices. Obstacles, such as the arduous and dangerous start were overcame by the invention of the electric starter motor in 1912. The moving assembly line and mass production techniques developed by Henry Ford in 1913 push the price of ICE vehicles even lower and propelled the adoption of these vehicles as the standard choice for most consumers [1].

For a long time, the superior driving range and the affordable price of the ICE vehicles completely dominated the automotive market, until the oil crisis and environmental considerations, such as the need to drastically reduce greenhouse gas (GHG) emissions, took place and triggered a renovated interest for electric vehicles. Because of strong environmental concerns like significant rise of the global temperature and scarcity of fossil fuel reserves, several governments have established standards to limit the increasing temperature to less than 2 °C this century (Paris Agreement in 2015) [2].

The transportation sector plays a crucial role (23 %) in GHG global emissions [3]. Therefore, ten governments, which include the top vehicle markets worldwide, issued fuel economy and/or GHG emissions standards for light duty vehicles (see figure 2.1). Nowadays, 80 % of the vehicles sold worldwide are subjected to these standards [2]. Despite the positive reduction of CO_2 vehicle emissions, ambitious targets such as the European Union's (95 g/km, until 2021) demand an extensive adoption of vehicle transmission electrification [4].

Thanks to strong regulations facing ICE vehicles, as well as accelerated technological advancements in batteries and electrical powertrains, there has been a growing call for electric vehicles. Worth mention is the EV30@30 campaign, with the objective to reach 30 % sales share for EVs by 2030, which has the purpose to present several benefits linked to electrical mobility and help reach the established climate goals [5].

Furthermore, urbanization surge across the globe, mostly in developing countries, demands green mobility solutions to preserve favourable air quality in cities. Some

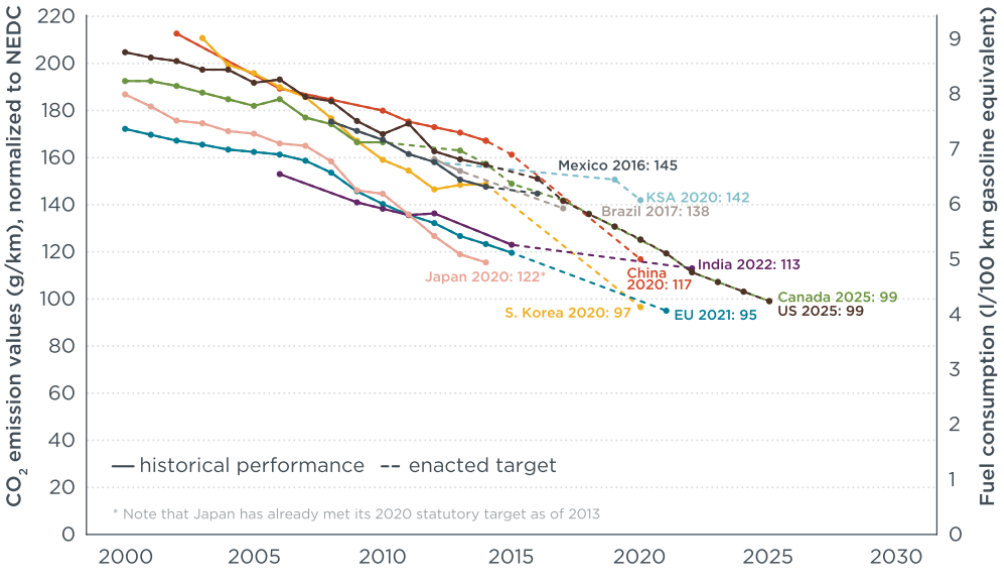

Figure 2.1: Historical fleet CO_2 emissions performance and current standards for passenger cars (gCO_2/km normalized to NEDC) [2]

restraints are already in place to control the air quality problem. For example, in Beijing (China), a plate lottery system is employed and, in Europe, several countries have environmental zones where some vehicles cannot circulate [6].

It is important to emphasize that the sole replacement of ICE vehicles by EVs will not make a drastic impact in reducing global GHG emissions. Considering that EVs run on electricity, to considerable influence emissions, this electricity needs to derive from renewable sources (for example: solar, wind and hydro) [7].

Despite the usual consumer concerns regarding EVs, such as, range anxiety, charging speed and high price it is clearly shown by figure 2.2 that these problems are being overcame and there is an increasing trust in EVs. Most buyers desire at least 400 km of range (full charged) for a pure/battery electric vehicle (PEV/BEV), charging infrastructure expansion that provides acceptable charging speed is crucial for big trips and, although, battery pack prices fell around 80 % in the last 6 years [6], the price of EVs will become more competitive with a further decrease in battery cost. Currently, government incentives are implemented to balance the discrepancy in prices and to push the sales of EVs instead of ICEs.

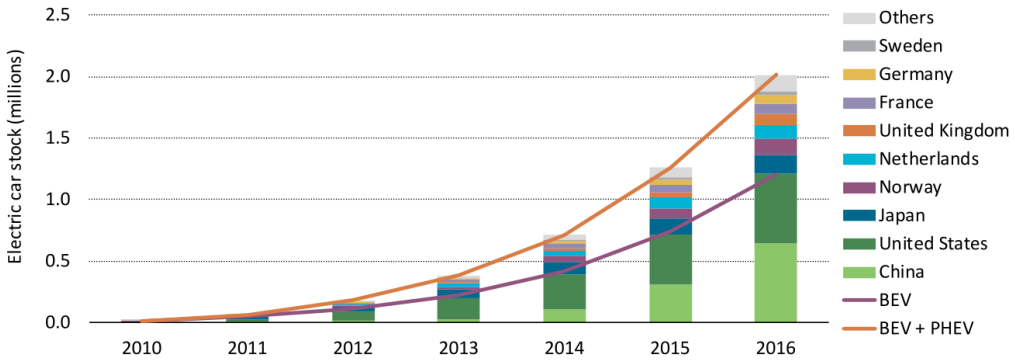

Figure 2.2: Evolution of the global electric car stock 2010 – 2016 [8]

Two countries are incontestably leading the shift to electric vehicles. In Norway, strong government benefits led to a market share of 39 % (2017), by far the highest [9]. China, the other emerging country in the EV market, was responsible, in 2016, for more than 40 % of the electric cars sales worldwide [8].

In Norway, the monthly electric vehicle market share, in last December (2017), reached a record value of 52 % [9]. While in other countries the government benefits are modest, in Norway they are bold. Some examples are free parking, no road tolls and competitive electric vehicle prices compared to equivalent ICEs. For instance, the 2017 Nissan Leaf costs around 245 900 kr ($\sim$ 26 000 €) in Norway [10], while in Germany costs 31 950 € (+23 %) [11].

Germany, as an established automaker country, represents an important catalyst in the adoption of a strong Europe EV market. With a 2 % market share of EVs, there is still a long way to go, but the trend is visible and the emissions scandal in the Germany industry triggered government action. Last year PEVs purchases increased 143,2 % and PHEVs sales rose 76,4 % while for diesel vehicles decreased 14 % [12]. At the start of 2017, 33 models from German manufacturers were on the market, and BMW, in Leipzig, is currently operating the world's first large-scale series production facility specifically for electric vehicles [13].

Taking this rise into account, it is expected that the automotive industry will have to deal with drastic disruption directly related to four factors – autonomous, connectivity, electrification and ride-sharing. Several challenges will arise from each of these factors and they need to be tackled effectively by the industry.

In the coming years, ICE will continue to be the central segment in the powertrain in most original equipment manufacturers (OEMs). However, as time goes on, and CO_2 penalties become more expensive compared to investing in carbon free technologies, the change to PEVs is clear and requires robust adaptation from the industry [6].

Unless there is a PEV break-through (for example: great reduction in battery price), the expected trend in the automotive market is a shift towards PHEVs. PHEVs are hybrid vehicles which can use only the battery, the ICE or a combination of both for driving. As the name states, they can be plugged-in and charged. Considering that the daily use of a passenger vehicle in the European Union is approximately 50 km leaning to 70 km (2020), with a PHEV is possible to run only on electricity most days, charging the vehicle at home during the night and, if necessary, use the conventional engine for unforeseen detours or long trips [4, 7]

Mild hybrid vehicles (cannot be driven merely on battery power but have systems to assist the ICE, such as regenerative braking and start-stop technology) will play a key role in the following years with respect to electrification, especially for full-line OEMs [14]. They bring several advantages regarding fuel efficiency and, consequently, CO_2 reduction with small integration effort and low additional cost, associated to several possible architectures [15].

Instant high torque at low speeds where there is a need for acceleration or grade climbing, and constant power once these demands are surpassed, are the ideal characteristics to operate a vehicle. From figure 2.3, it is evident that the use of an electric motor is more suitable and efficient to attend this requirements than the ICE counterpart.

The ICE can only operate starting from idle speed, the power increases with increasing revolutions per minute (rpm) and the torque-speed curve is rather flat requiring a multigear transmission to propel the vehicle. Considering this, the combustion process and, if manual transmission, the driving profile, leads to a rather low efficiency.

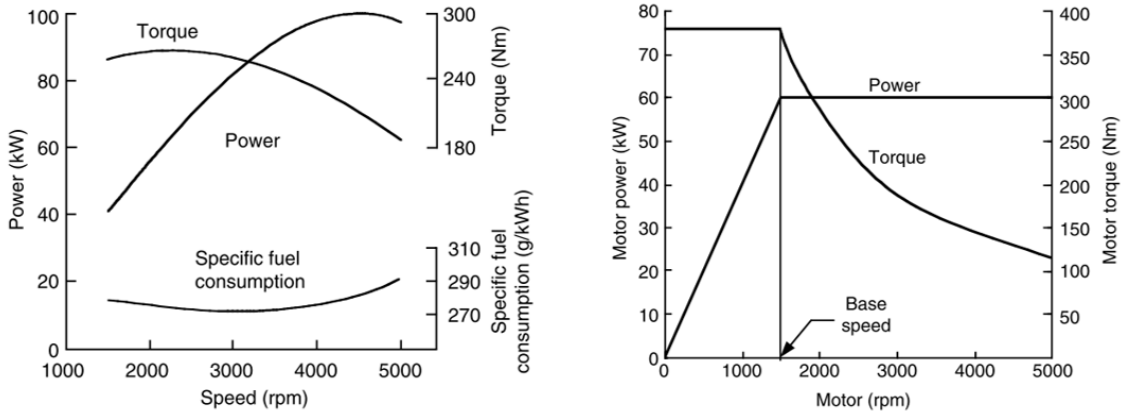

Figure 2.3: Typical performance characteristics of gasoline engine (left) and electric motor (right) [16]

Electric motors, with a torque-speed curve almost ideal, do not require a multigear transmission. They also start from zero speed and do not use any consumable fuel which contributes to a superior efficiency without polluting emissions.

Vehicle segments in Europe do not have strict formal regulations. The definition is vague, and passenger vehicles are subdivided in 9 categories (A–F, J, M, S). In figure 2.4, it is possible to correlate the mass with the vehicle segment. This dissertation focuses on small passenger vehicles (A and B segments), where Ford Fiesta, VW Polo, Fiat 500e and VW e-up! are well known examples [17, 18]. In table 2.1 the specifications of three vehicles (two ICE vehicles and one EV) from the same segment are presented.

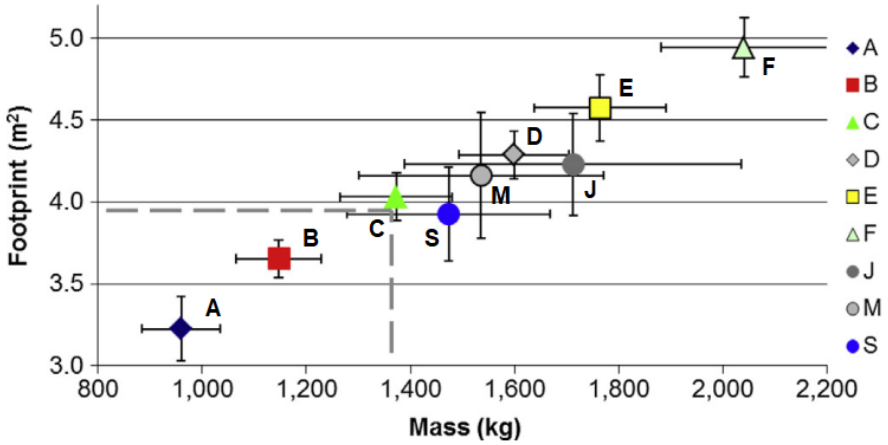

Figure 2.4: Average footprint[1] over average mass per vehicle segment in the EU 2010 Note: The error bars around the averages represent the standard deviation [17]

2.2 Electrification

Electrification is the term appointed to a vehicle where electricity powers more than the 12-volt battery, present in every common vehicle, as well as basic accessories (e.g. radio,

[1] footprint: vertical projection of the surface between the four wheels of the car

Table 2.1: Specifications for two ICE vehicles and the EV counterpart [19]

Parameter	VW Up! (45 kW)	VW Up! (56 kW)	VW E-up!
Motor	Gasoline (3 cylinders)	Gasoline (3 cylinders)	Electric
Max. Power (kW / rpm)	45 / 5000 – 6000	56 / 6200	61
Max. Torque (Nm / rpm)	95 / 3000 – 4300	95 / 3000 – 4300	210
Transmission	5 speed	5 speed	1 speed
Tare weight (kg)	940	940	1229
Top speed (km/h)	162	172	130 (limited)
Acc. 0–100 km/h (s)	14,4	13,5	12,4
Consumption	4,9 l/100 km (urban)	4,9 l/100 km (urban)	11,7 kW/100 km
Autonomy (km)	650 (calculated)	650 (calculated)	160 (NEDC)
Price Portugal (€)	12 132	12 804	27 769
Price Germany (€)	10 425	11 900	26 900
Price Norway (€)	16 600	20 500	23 300

windows).

The efficiency of an ICE vehicle can be enhanced through engine improvement, transmission improvement, mild hybridization and use of lightweight materials. Taking only into consideration improvements on ICEs they are not sufficient to achieve future regulatory targets.

The elementary form of electrification can be seen in mild hybrid vehicles, where an electric machine is used as a generator which recovers braking energy (regenerative braking). This energy can be stored and, afterwards, applied in the electrical system or when accelerating the vehicle.

While the internal combustion engine technology is at full efficiency from upgrades throughout the last century, electrification is just in the beginning which grants room for improvement. Even though the ICE is at maximum performance, it cannot by itself meet current regulatory legislation established. This restraint associated with the high price of PEVs results in a need for electrification in the forthcoming years.

The main advantage of an electric drive is the capacity to generate high torque at low speeds, thus it is an ideal complement to an ICE since the torque is delivered at high speeds. The hybridization of a vehicle has the aim to perform always at optimum speed to reduce emissions and fuel consumption [20].

Companies in the automotive market, like BorgWarner, Bosch and Continental regard 48 Volt (V) mild hybridization as an impact technology in the near future and are working on solutions towards it. BorgWarner predicts that 48 V systems will impact more than 60 % of the global PHEV/HEV market in the next ten years. Examples of solutions in the BorgWarner's portfolio are eBooster® electrically driven compressors and integrated belt alternator starters (iBAS) which capture and handle waste energy in an efficient way contributing to a better efficiency and higher power [21]. Progress in fuel economy can be as high as 20 % depending on the application.

Bosch is investing in a 48 V battery that stores braking energy by means of a boost recuperation system (BRS). This energy is applied when the driver accelerates (electronic boost) which results in less fuel consumption and CO_2 emissions [22]. Combined with the battery, Bosch has also designed a 48 V hybrid powertrain that, compared to other hybrid systems, is more economic. The additional 150 Nm of torque helps during acceleration and can reduce consumption up to 15 % [20].

Continental expects that electromobility is going to be vital in future mobility, hence the focus on electrification, particularly 48 V technologies. A decisive factor is the ease with which the 48 V belt starter generator integrates with the pre-existing ICE, because of the high power to size ratio of the electric motor. This small but powerful electric motor is viable since the stator is water cooled and has high efficiency. This technology is standard in recent models, Audi A8 and Renault Scénic, the latter has combined fuel consumptions of 3,5 liters (of diesel) per 100 km and CO_2 emissions as low as 92 g/km [23, 24].

2.3 Automotive industry

Nowadays, automakers are strongly dependent on base vehicle upgrades from costumers. There are several possible combinations, with different engines and transmissions as well as safety features and comfort upgrades (see figure 2.5). The subsequent market for parts and services also plays a vital role in the revenue of OEMs.

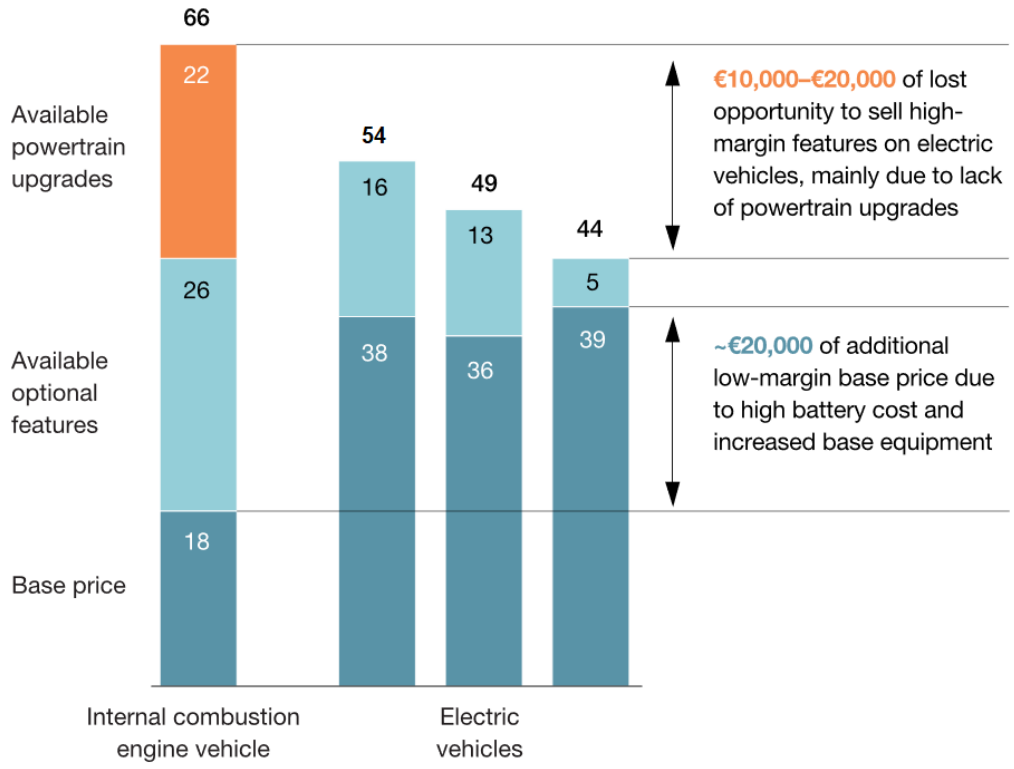

Figure 2.5: Examples of sales prices in German market, € thousands (not including external incentives) [25]

As a result of base EVs being expensive it is common that a lot of safety and comfort features are already included. Moreover, EVs come with limited available configurations and the aftermarket maintenance is sparse and far economic, for consumers, compared to ICEs.

Native electric vehicle models have an indisputable advantage compared to models based on ICE. They can exploit new arrangements for the powertrain and battery pack and not be tied to the current disposition of components. This new approach leads to improved battery packaging culminating in extended range and more interior space [25].

The inferior complexity of electric relatively to ICE powertrains leads to exposure

from OEMs which stand out through driving performance and creates an opportunity for suppliers and new OEMs to step up. As of today, Tesla and BYD (new competitors), are in the top 5 of EV manufacturers. While a PEV powertrain has around 200 components, an ICE one has 1400, additionally, the main components in a PEV (electric motor and battery packs) employ a highly automated process which is less dependent on labor [26].

Although automotive OEMs generally build and assemble engines and transmissions themselves, in this transition phase, most of PEV powertrains are acquired from suppliers due to inadequate production capacity and insufficient technological knowledge.

Europe OEMs are a good example, since they amount to one quarter (25 %) of worldwide ICE powertrain production, yet, regarding EVs, they outsource the electric motor, are dependent on battery suppliers and the Lithium-ion (present in most EV batteries) production is scarce (3 %) [26].

With this in mind, it is evident that, even though consumers still prefer to purchase an EV from leading manufacturers, EVs brought disruptive consequences to the automotive industry and there is an urgency for a new business model for automotive OEMs.

The automotive industry, to address these challenges, needs to connect the sequential product-development approach, developed in the last century, with a model like agile instead of a waterfall-based approach since it is faster and more iterative. It will have to collect and handle enormous amounts of data from consumers and vehicles to reimagine products and their production according to costumer's desires (4.0 Industry). Due to the new unexplored technology, cooperation between the manufacturers is decisive to an active and robust progress in these still unfamiliar areas.

Key points for OEMs [4]:

- Collaboration with software manufacturers and map providers to create driving assistance systems and develop autonomous driving;
- Sustainability, use of renewable materials and life cycle assessment are of utmost importance;
- Electrification and electric vehicles developments, with strong focus in 48 V technologies and PHEVs, are already in motion, since, as it is perceived by OEMs, in the near future they will fully substitute conventional ICE vehicles;
- Accelerated changes in the market bring the need to introduce vehicles quickly, leading to a higher dependency in computer simulations;
- Developing countries such as Brazil, India and China play a crucial role in the future automotive market.

2.4 Energy storage

Energy storage systems follow a set of conditions in order to be applied in vehicles, specially electric vehicles. Specific energy[2] and specific power[3] (both characteristic of battery chemistry and packaging), efficiency and cost are the primary requisites which need to be taken into account when designing an electric vehicle battery. Specific energy

[2]Nominal battery energy per unit mass (Wh/kg), it determines the weight required to achieve a given electric range.

[3]Maximum available power per unit mass (W/kg), it determines the weight required to achieve a given performance.

is essential in PEVs considering it is directly associated to vehicle range. In HEVs, there is a focus in specific power to provide good vehicle performance [16].

In figure 2.6 and table 2.2, there is a comparison between the most commonly employed energy storage devices in today's vehicles.

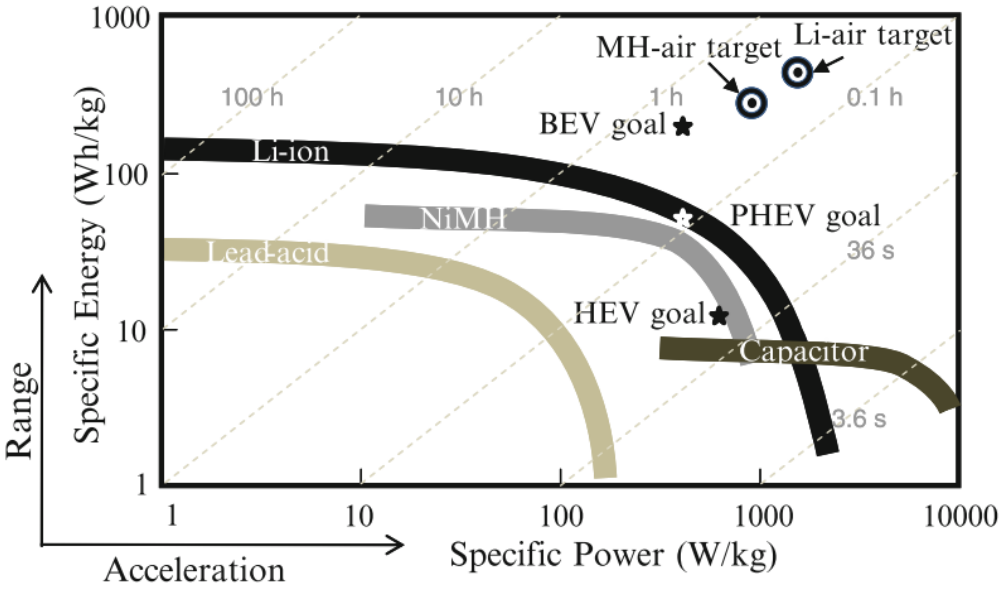

Figure 2.6: Plot of a few electrochemical energy storage devices used in the propulsion application [7]

Table 2.2: Properties of several energy storage types [20]

Storage type	Specific energy (Wh/kg)	Energy density (Wh/L)	Specific power (W/kg)	Life cycles to 80 % (charge-discharge)
Lead-acid	20 – 35	54 – 95	250	800
Nickel-metal hydride (NiMH)	65	150	200	1000
Lithium-ion (Li-ion)	140	250 – 620	300 – 1500	>1000
Hydrogen fuel cell	400	–	650	–
Ultra-capacitor	1 – 10	–	1000 – 10000	–

2.4.1 Battery

Batteries are the critical component in any EV; they must handle high power and high energy capacity while remaining at a reasonable price. Other relevant requirements are the weight and the limited space available. Despite the price decline (77 %) in recent years [6], battery is the component which pushes EVs price to a value higher than related ICEs.

Lead-acid batteries have been used for more than a century and despite all the research in energy storage, they are still the best choice for low-voltage applications. Since they have low cycle life and low energy density, their use is prohibitive according to today EV's requirements [7, 27].

The dominant battery technologies used in today EVs are nickel metal hydride (NiMH) and lithium-based (Li), mostly lithium-ion (Li-ion). NiMH batteries are employed mainly in HEVs because of their low cost, high reliability and high durability.

Li-based batteries are employed in PHEVs and PEVs in virtue of higher energy density and specific energy, compared to NiMH, allowing a vital extended range. To ensure safety, battery management system (BMS) is always employed with these batteries [20, 27].

For small passenger vehicles, typical battery properties values are: energy capacity 12 to 30 kWh, voltage 270 to 410 V, specific energy 55 to 100 Wh/kg. Battery cooling can be liquid, passive or by air [18].

2.4.2 Fuel cell

Unlike chemical batteries, fuel cells generates electric energy while fuel is supplied, instead of storing it in large quantities. Longer driving range, without time consuming charging time, puts fuel cell vehicles ahead of PEVs. Direct conversion to electric energy without combustion poses as an advantage towards ICEs. The most efficient fuel design employed in these vehicles is hydrogen, as fuel combined with oxygen.

Fuel cells are very reliable, with outstanding energy density and silent in operation but quite expensive to construct. Intricate storage and high pressure are the main problems that require development so that fuel cells can become a viable solution for energy storage. The access to hydrogen by consumers also lacks a favourable solution [20, 28].

2.4.3 Ultra-capacitor

They are low-size and very high capacity capacitors. They can be charged in a very short period of time and the energy can also be used very quickly, for example, in fast acceleration.

In conventional vehicles, they can substitute large alternators for meeting intermittent high-peak power demands related to power steering and braking. They recover braking energy which usually dissipates as heat and it can be used to reduce losses in electric power steering [20].

2.5 Powertrain

Powertrain system of PEVs combine an electrical and a mechanical subsystem. The electrical system uses energy from the batteries to power one or more electric motors recurring to power electronics (e.g. converters, inverters). The mechanical system usually consists of a clutch, a transmission and a differential. Moreover, due to the favourable characteristic of the electric motor in respect to the torque-power curve desirable to run a vehicle, the restrictions around the ICE are not present anymore and several powertrain configurations are possible (see figure 2.7).

PEVs powertrain structures can be divided in two main classes – one-motor or two-motor based powertrains (see table 2.3).

One-motor based powertrains have been adopted, preferentially, for commercial PEVs due to similarities with traditional ICEs where the transmission has been continually optimized, therefore requiring less overall modifications.

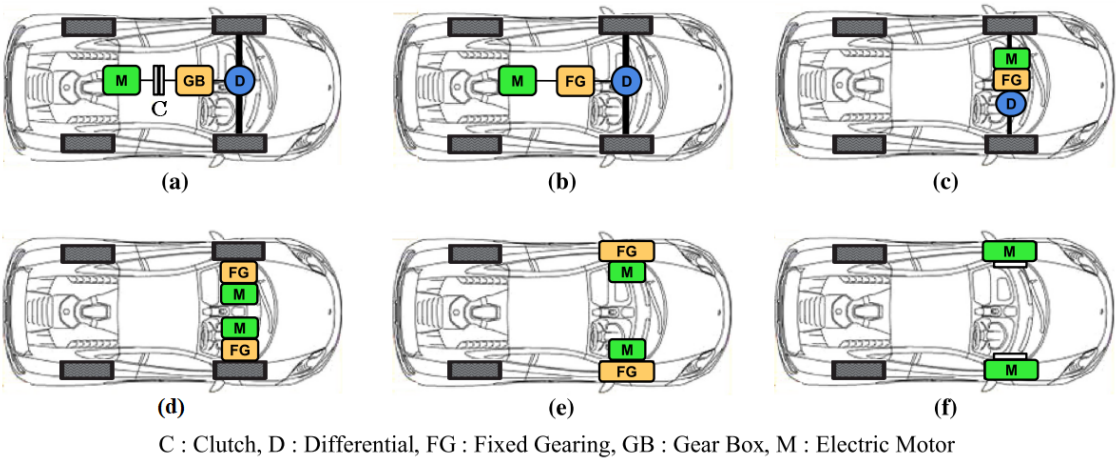

Figure 2.7: Six types of EV configurations [29]

Table 2.3: Categories of EV powertrain structures [29]

One-motor based EV powertrains (see figure 2.7)
(a) Conventional type: The EV propulsion system consists of a differential (D), a gearbox (GB), a clutch (C) and an electric motor (M). This configuration can be considered as a counterpart of an ICE vehicle with rear-engine-front-wheel drive, where the ICE is replaced by an electric motor.
(b) No transmission type: Rear-engine-Front-wheel (RF) This configuration, with fixed gearing (FG) used instead of a clutch and gearbox, is quite similar as the conventional one.
(c) No transmission type: Front-engine-Front-wheel (FF) The electric motor, fixed gearing and differential are placed together in the front, just like ICE vehicles with front-engine-front-wheel drives.
Two-motor based EV powertrains (see figure 2.7)
(d) No differential type: Two electric motors are employed for individual front wheel to eliminate a differential. The two motors are connected to the front wheels through mechanical fixed gearing.
(e) In wheel type with fixed gear (FG): This type is similar to the no-differential type in (d), except different location of the electric motors. Electric motors are embedded in wheels for the in-wheel type.
(f) In wheel type without fixed gear (FG): Mechanical gearing is completely removed for this type. The vehicle speed directly depends on the motor speed.

Two-motor powertrains identify themselves with simplified mechanical structures at the expense of complex electrical arrangements. The need for a differential can be eliminated, if each electric motor is independent and connected only to a single wheel.

2.5.1 Electric motor

Electric machines, in traditional vehicles, work as starters and alternators to provide the necessary energy for the engine to reach its idle speed and to any electric auxiliary loads (e.g. lights and radio). In electric vehicles, they are a fundamental component in the transmission.

An electric motor converts the electric energy, provided by the battery, into mechanical energy to move the vehicle. It can also work as a generator, harvesting the mechanical power from the transmission to recharge the battery and, in hybrid vehicles, convert the mechanical energy from the engine to electric energy which is delivered to the battery. Generally, they have a very wide operating range and, compared to ICE, are more efficient.

The classic torque-power curve which an electric motor must follow is presented in figure 2.8, it can be divided in three essential stages – constant torque, constant power and high speed region.

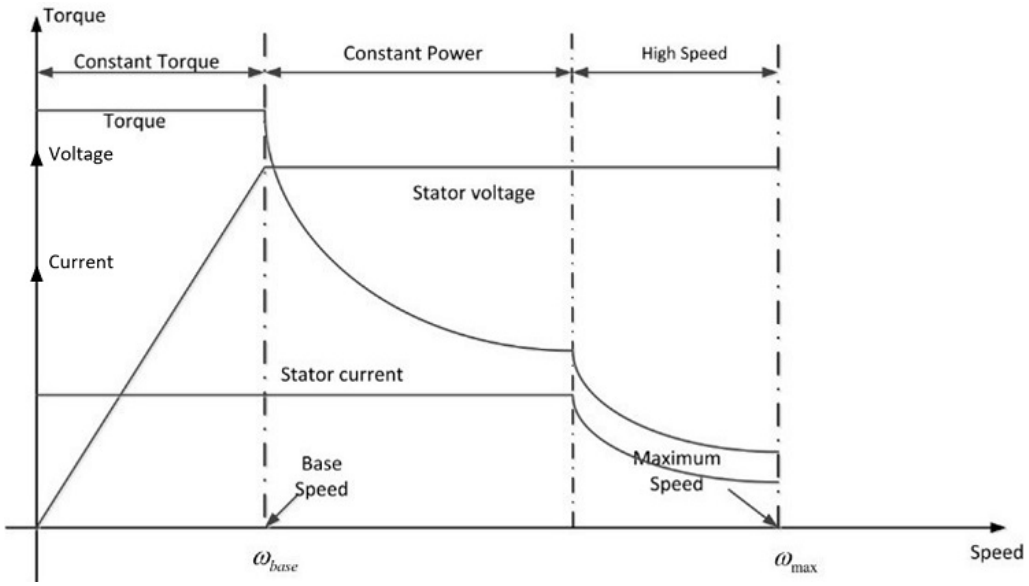

Figure 2.8: Typical torque speed curve of an electric traction motor [30]

During the first stage, constant torque is applied until base speed is reached when inverter output voltage reaches its limit. The greater the constant torque phase, the higher the vehicle acceleration.

For the second stage, since the inverter is at both maximum voltage and current, it cannot deliver more power to the electric motor. So, to increase the vehicle speed beyond the base speed point, the output torque has to decrease by weakening the flux.

The last stage, high speed region, where vehicle speed is very high, the power cannot be kept constant and the inverter reduces the current provided to the electric motor [30].

Regarding small passenger PEVs, typical values for the electric motor are: maximum power 30 to 70 kW, maximum torque 130 to 200 Nm and maximum speed 7000 to 12 000 rpm [18, 31].

Nearly all manufacturers adopt liquid cooling for the electric motors to avoid corrosion, overheating and freezing. The liquid usually consists of 50 % ethylene glycol and 50 % deionized water. Air and oil are also used, but in a very small scale [18].

Regardless of the type of electric motor, they all have two main components, the stator and the rotor. The rotor is linked to the output shaft where motor torque is generated.

Electric motors can be split into two main categories: alternating-current (AC) motors and direct-current (DC) motors.

Today, the main choice for PEVs is the permanent magnet synchronous machine (PMSM), which is a three-phase AC motor, because of its suitable properties related to efficiency, size and control simplicity [18, 20, 27].

Despite the dominance of PMSM in the EV industry, other relevant types of electric motors currently in use are induction motors (IM) and switched reluctance motors (SRM), see figure 2.9.

There are other arrangements worth mentioning such as DC motors, wound rotor synchronous motors (WRSM) and hybrid PMSM (synchronous reluctance machine with added permanent magnets).

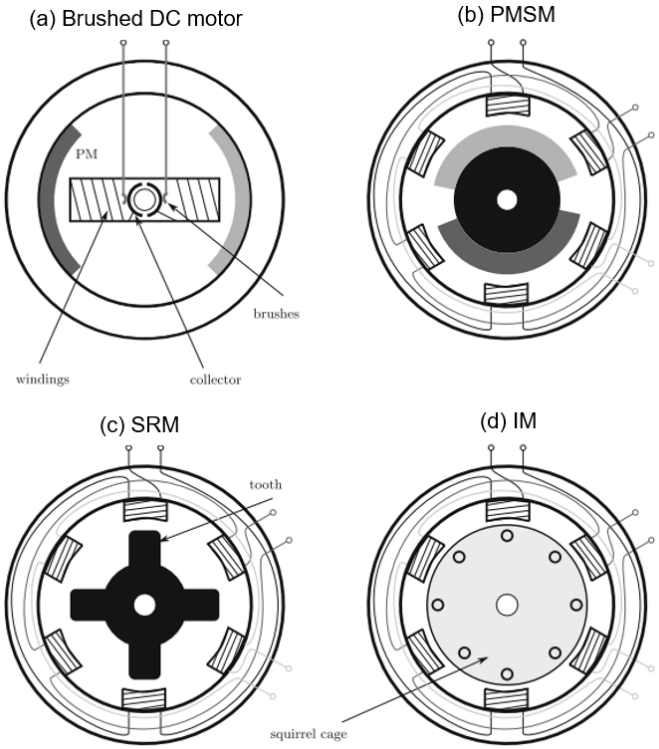

Figure 2.9: Schematics of four types of motors:
Brushed DC motor (a), Permanent Magnet Synchronous Motors (b), Switched Reluctance Motor (c), Induction Motor (d). Adapted from [27]

Originally, DC motors were the preferred choice because of its control simplicity, decoupling of flux and torque and the unnecessary need of an inverter. Drawbacks like maintenance (brushes and rings) and low efficiency have led to its discontinuity. WRSM have the advantage of reducing starting current and increasing starting torque, but they require maintenance (brush gear) and are expensive. Hybrid PMSM brings a boost to base torque as well as an increased efficiency and power, which remains constant until maximum speed. Torque ripple and low power factor come up as disadvantages [27, 32, 33].

Permanent Magnet Synchronous Motor (PMSM)

The main advantages of PMSMs are higher efficiency, specific power and power density. They also are more compact than induction motors. However, a small constant power

region is associated with these motors. Controlling the conduction angle of the power converter at speeds higher than the base speed[4], it is possible to increase the efficiency and widen the speed range. It can be extended to three or four times the base speed. One of the drawbacks is the possibility of demagnetization due to armature reaction or excessive heat.

Brushless DC motors (BLDC) are often confused with PMSM since they are identical in respect to the torque generation principle. Both are synchronous machines that perform the excitation of the rotor through permanent magnets. The main difference is the waveform of the stator currents – rectangular in BLDC and sinusoidal in PMSM [20, 28].

Some recent EVs have interior mounted magnets instead of being at the rotor surface, this provides several advantages such as higher torque (additional reluctance torque) and the magnets are protected against centrifugal force allowing higher rotational speed.

PM motors can also be classified with respect to the magnetic flux – radial flux, axial flux or transverse flux. While radial flux motors are the most common, axial flux ones are getting traction and are easily integrated as in-wheel motors due to the reduced axial dimension. Transverse flux PM motors are still in development phase, so, they are quite inexpressive in the electric vehicle automotive industry [27, 32, 33].

Induction Motor (IM)

The IM are asynchronous AC motors and have been increasingly endorsed by OEMs because of the cost liability of rare-earth elements, present in the magnets, which have seen an increase in price due to high demand and scarcity. They can have a wound rotor but, frequently, the squirrel cage is chosen since it is more reliable, robust and requires almost no maintenance.

Tesla vehicles, Roadster and Model S, use these motors since with high power rating they achieve higher performance, and the torque and speed can be controlled more smoothly, providing more stability and comfort.

Disadvantages consist of break-down torque (in the constant power region), inferior efficiency compared to PMSM and low power factor [18, 27, 32].

Switched Reluctance Motor (SRM)

SRM motors are presently perceived by OEMs as a possible future solution. In general, they are known for its simple control and construction, fault tolerance, high efficiency and intrinsic wider constant power region. They possess, as well, an excellent torque-speed characteristic and can work at high temperatures and great rotational speed. Like for induction motors, there is no need for rare earth magnets and the drawbacks associated with its use.

Some obstacles still need to be surpassed like significant torque ripple and electromagnetic interference. In virtue of more accurate switch control, the high noise problem is already solved [20, 28, 32].

Comparison

The brushed DC motor, despite starting the EV era due to its advanced technical maturity and low cost, provides the lowest power density, inadequate reliability and it has poor efficiency. As already stated, it also requires maintenance. All these faults led to a search for new solutions and, ultimately, to its obsolescence in the EV industry.

[4]Motor's speed from which it produces the maximum designed power output

PMSM, due to the highest power density – highest power for the same motor weight – among the mentioned EM, leads the EM market for EVs. It has the maximum efficiency in a limited speed range (generally at low speeds), hence its use in small passenger vehicles (A – B segment) which are mainly used in city traffic conditions.

At low production costs, the finest reliability and best overall efficiency over the entire speed range are characteristics of the IM machine. It is the preferred choice when one of the requisites is good efficiency over a wide speed range (vehicles in segments C to F, for example, Mercedes-Benz B-Class, Toyota RAV4 and Tesla S [18]). As main disadvantages, conservative power density and field oriented control, significant costs drive away the low-end vehicle market off.

SRM machine is similar to IM regarding efficiency and power density. However, as previously indicated, high torque ripple (at low speeds) still is an exclusion criterion for most manufacturers [34].

In table 2.4 is presented a comparison between the electric motors commonly adopted by OEMs, which provides a clear view over the most significant properties, and the efficiency maps of figure 2.10 confirm the segment market tendencies.

Table 2.4: Evaluation of four electric machine types [34]

	DC	IM	PMSM	SRM		
power density	⊖⊖	⊙	⊕⊕	⊙	⊕⊕	very good
efficiency	⊖	⊕	⊕⊕	⊕	⊕	good
costs	⊕	⊕⊕	⊖	⊕	⊙	neutral
reliability	⊖	⊕⊕	⊙	⊕	⊖	bad
technical maturity	⊕	⊕	⊙	⊙	⊖⊖	very bad
controlability, costs	⊕⊕	⊙	⊕	⊖		

DC – direct current; IM – induction motor; PMSM – permanent magnet synchronous motor; SRM – switched reluctance motor

2.5.2 Transmission

Transmission is a key component in vehicles, its main function is to transmit power from the engine to the wheels, it converts torque and engine speed so that the vehicle performance requisites are achieved. There is a wide variety of transmission configurations – manual, automatic, continuous variable transmission (CVT) which can be further subdivided. Major components commonly present in transmission include: clutch, gearbox, differential and drive shaft [35].

Due to its features and importance, transmissions are inherently related to "fuel" consumption, reliability and ease of operation. All these points play a crucial role in today's automotive industry and, while simple innovations are not likely to happen, there is a strong urge in electronic transmission control to reach improved operation.

In conventional ICEs, considering the engine characteristics, a manual or automatic transmission with a considerable amount of speeds is required to effectively deliver torque and power. EVs, which depend on an electric drive (like PEVs), have, at most, a two-speed transmission, hence reducing energy losses through gear-shifting.

Predominantly, in PEVs, a single speed transmission is employed which turns the clutch dispensable. The common transmission ratio range of latest PEV models, with one electric motor, is between 7 and 10 [18].

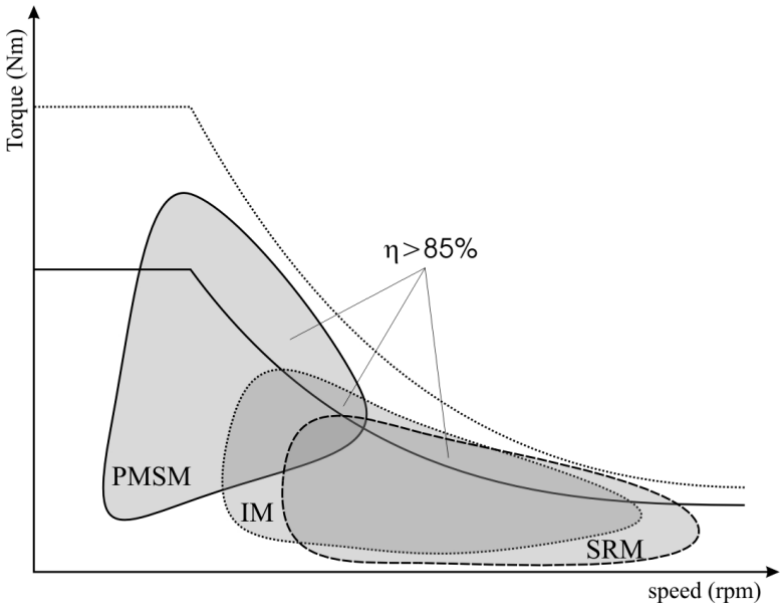

Figure 2.10: Exemplary efficiency maps of different electric motors with constant power [34]

Fixed ratio single speed transmission

This transmission (see figure 2.11) is the most widely used system in behalf of structure simplicity and the remarkable effectiveness of the electric motor over combustion engines, namely, high stall-torque[5] and ability to deliver constant power in a wide speed range. Additionally, it provides a pleasant driving experience at an affordable price [36, 37]. Despite being adequate for the majority of vehicles, gear ratio design is a commitment between range, performance (for example: stall torque) and top speed desired.

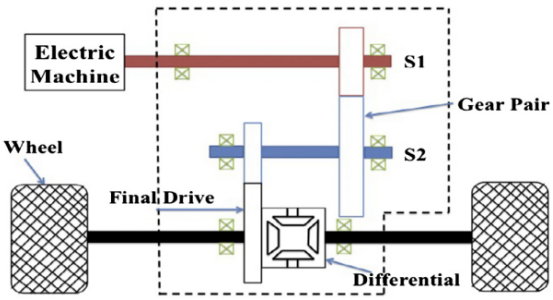

Figure 2.11: Single speed transmission in a PEV powertrain. S1, S2 – shafts [37]

Two speed transmission

Even though, multi-speed transmissions typical drawbacks, such as increased cost and mass, decreased efficiency and torque interruption when gear shifting, suggest that they are counter-productive for electric vehicles, innovative arrangements can offer advantages over single transmissions.

[5]Torque that a motor produces at zero rotating speed and with P_{out} (output power) equal to zero.

Two speed transmission provide higher wheel torque at low rpm, consequently, the electric motor stall torque may be inferior resulting in a smaller motor. Global efficiency increases leading to extended driving range. Moreover, acceleration and gradeability increase as well. Finally, the presence of a second gear allows a superior vehicle top speed [36, 38].

One of the innovative structures uses a dual clutch system (see figure 2.12). The use of two clutches facilitates the torque transference, overcoming the torque interruption problem. Since there are only two speeds, each clutch is connected to each speed directly, therefore there is no need for a synchronizer and its control. The extra gear set and clutches have a negative effect in efficiency and overall mass [37].

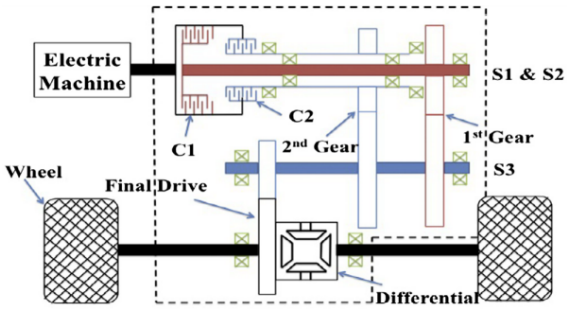

Figure 2.12: Two speed dual clutch transmission in PEV powertrain. S1, S2, S3 – shafts. C1, C2 – clutches [37]

The twinspeed transmission (see figure 2.13) has two integrated planetary gear sets, one selectable clutch and a single stage final drive (with differential). It has a shift strategy implemented which results in an excellent combination of efficiency and performance. In general, it increases the effective area of high efficiency in actual driving [36].

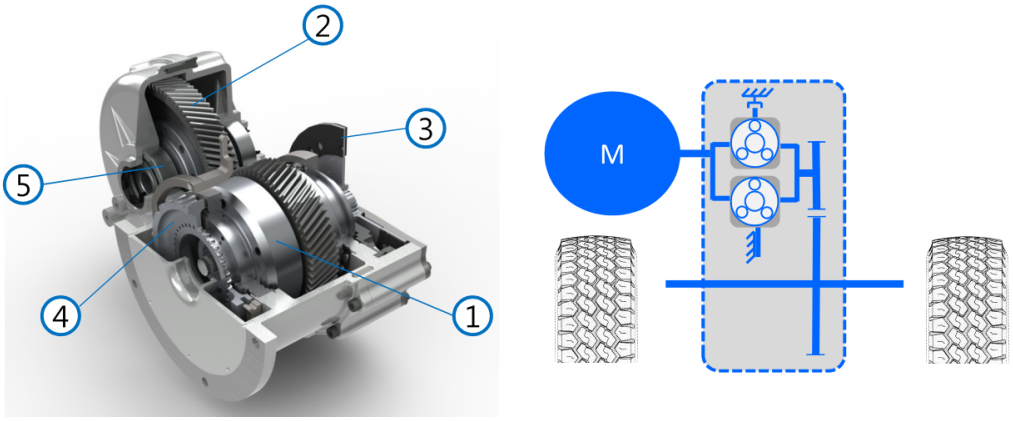

Figure 2.13: Twinspeed transmission with two planetary gear sets. 1 - Two integrated planetary gear sets, 2 - Single stage final drive, 3 - Controlled dry friction brake, 4 - Selectable dog clutch, 5 - Differential gear [36].

Continuously Variable Transmission (CVT)

CVT (figure 2.14) has an infinite number of ratios (between the stipulated limits) and the unique possibility to alter gear ratios without power flow interruption. Usually a CVT has a steel belt which connects two variable diameter pulleys, the transmission ratio

changes with the adjustment in pulley diameter, allowing the best possible speed over the whole vehicle driving range ensuing higher motor efficiency [37]. Another convenience is the potential to decouple top speed and acceleration, ultimately leading to improved performance.

However, extra weight and manufacturing costs need to be considered when designing such a transmission.

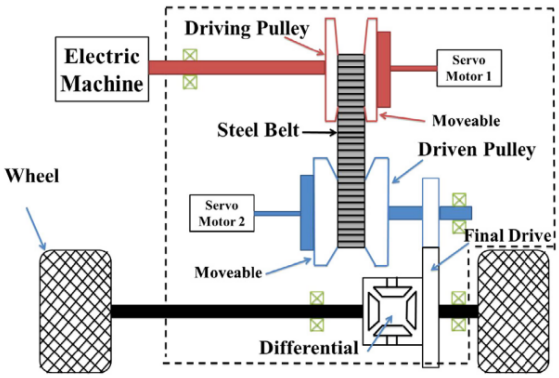

Figure 2.14: Continuously variable transmission with servo-electromechanical actuation system [37]

2.5.3 Differential

All vehicles need some sort of differential. It is indispensable when turning a vehicle. To safely turn, the outside wheels must spin faster than the inside wheels, which is provided by the differential. At the same time, they act as the final gear reduction in a vehicle and transmit the power to the wheels.

There are several types of differentials, designed for certain conditions, such as on and off-road driving. The most common is an open differential which is preferred in normal road conditions, but if one wheel loses traction, it will send all the power to the wheel with the least resistance. Locking differential works as an open differential, but if locked it locks the axle resulting in equal torque being sent to each wheel [39].

Limited slip differential (LSD) works as a trade-off between the open and the locking differential. It limits the difference in rotational wheel speed to counter the problem where all power goes to one wheel. Within LSDs, one particular example is the electronic limited slip differential which determines the ideal amount of torque needed for the given driving conditions through the vehicle's engine unit [39].

Most vehicles have a front-mounted engine, which leads to a preferred front-wheel drive (see figure 2.15) due to its lighter weight, and predictable handling characteristics. In these vehicles, the differential is interconnected with the reducer having a simpler design and sparing the need for a drive shaft and/or center differential.

Today, rear-wheel drive (see figure 2.16) vehicles are found in sports and luxury cars. A good example is the automotive company BMW. Despite being more complex systems, the precise handling performance is still a decisive point for some costumers. When connected to a front-mounted engine, a drive shaft and rear differential are required. The rear differential is very similar to a front differential, yet it cannot be coupled with the reducer, leading to more components, complexity and lower efficiency.

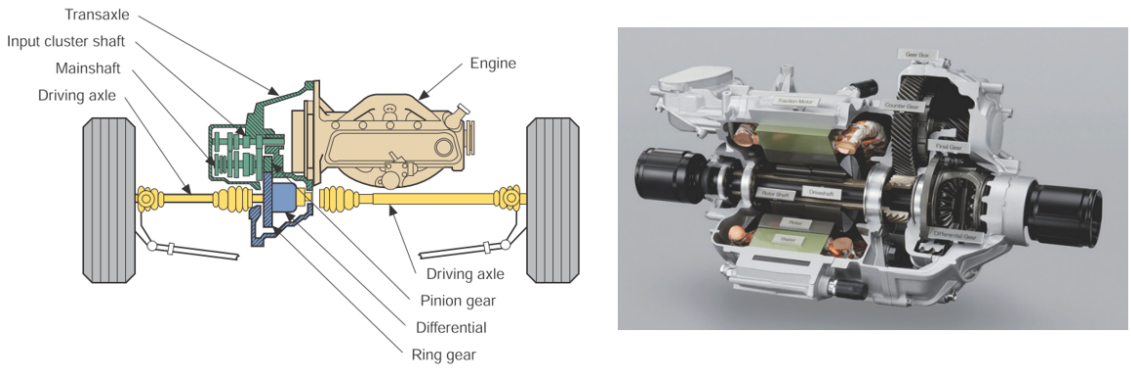

Figure 2.15: Typical front-wheel drive powertrain components: in an ICE vehicle (left) [40] and in a PEV vehicle (right) [20]

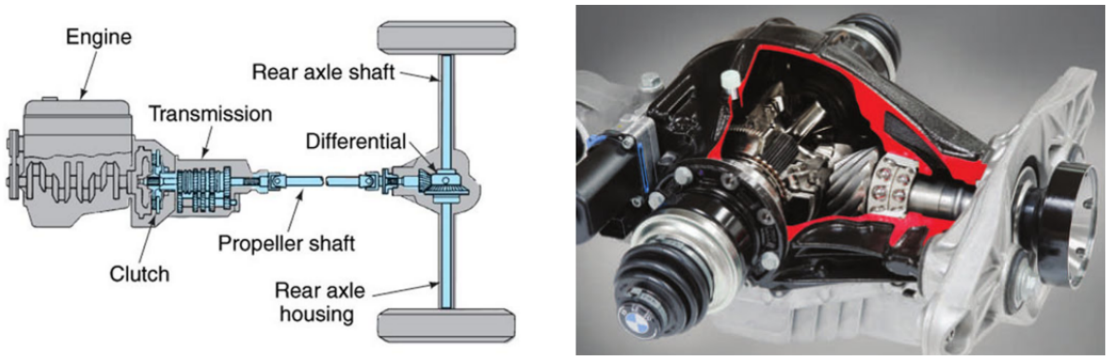

Figure 2.16: Rear-wheel drive powertrain components (left) [41] and BMW rear differential (right) [40]

Torque vectoring

A torque vectoring differential has the capability to transmit torque independently between the wheels. This capacity brings advantages such as increasing stability and responsiveness.

While before it was only used in racing vehicles, the technology development led to an adoption from automotive manufacturers, specially in all-wheel drive vehicles, saving the need to use brakes or cutting power to control wheel spin

PEVs, also regard torque vectoring as an important step forward regarding vehicle performance when cornering [42]. Dual motor systems without differential (see figure 2.17), where each wheel is independently controlled by each motor through independent transmissions can improve the transient response of the vehicle, require a complex motor control system but are not subjected to the intricate differential system. Other torque vectoring systems adopt planetary gear sets and/or clutches integrated with the common differential (see figure 2.18).

2.5.4 Projects

Electric vehicle transmissions, even if conceptually similar to conventional transmission, hold the possibility to new and creative solutions, not yet implemented in the EV market. Conventional ICE vehicle transmissions are expensive, heavy and bulky which is not ideal

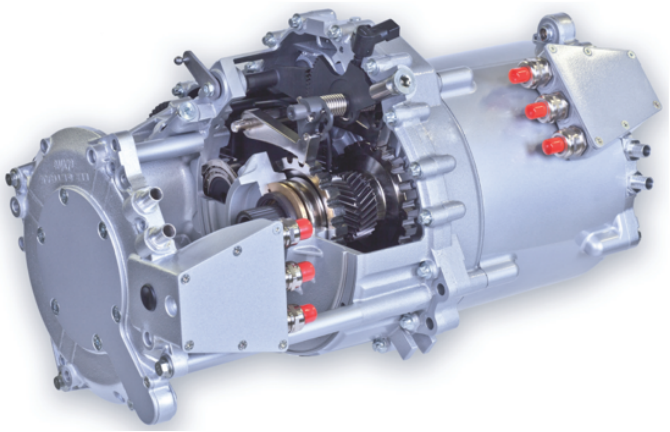

Figure 2.17: GETRAG 1eDT330 electrical transmission with independent transmission components and electric motors [43].

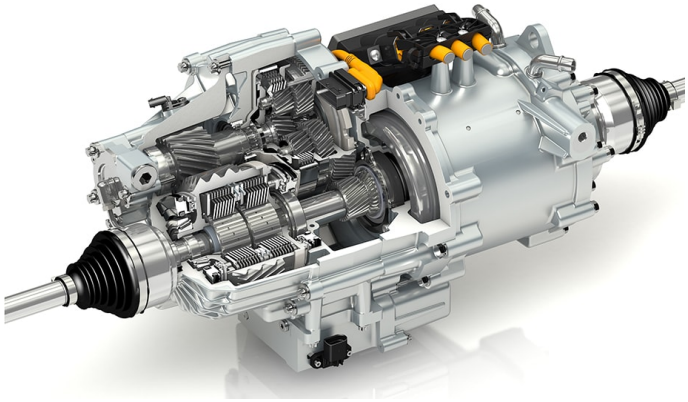

Figure 2.18: GKN electric axle - 'eTwinsterX' [44].

for EVs. In this section, a few projects and their main objectives are discussed.

Electrically Scalable Axial-Module (ESKAM)

The main aim of this German project is to develop scalable drive and axial modules for electric vehicles. From materials, production and manufacturing down to efficiency and power delivered, all is revised and thought to arrive at the best possible solution.

Initially, it was designed for a medium-weight inner city delivery vehicle with modest performance characteristics. Two electric motors – each with maximum drive speed 20 000 rpm, peak power 32 kW and peak torque 46 Nm – are connected to an axle reducer with a single 2-step reduction gear with a 19,25 ratio [45] (see figure 2.19).

Scalability is the project core since it brings the possibility to ease implementation in several vehicles with different performance requisites, without changing the concept basis.

Major advantages include – twin-drive concept, no differential needed (torque vectoring), axial module that can be adapted and customized and usage of lightweight components [46].

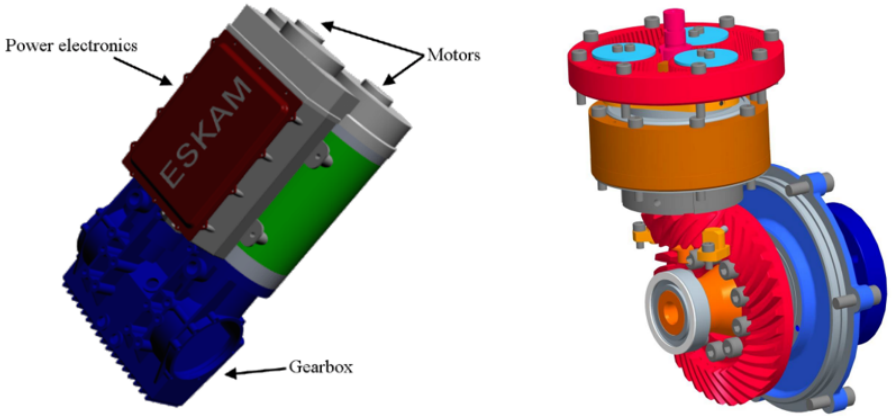

Figure 2.19: ESKAM axle module with integrated motors (left) [46]. Gearbox (right) [45].

Speed2E

At the Technical University of Munich (TUM), the Speed2E project arise from the ambition to study the relevance of high-speed transmission in electric powertrains. High input speeds are closely related to exceptional power density, reducing size and weight of electric motors. Such high speeds bring challenges regarding, for instance, efficiency, gear load-carrying capacity and noise, vibration and harshness (NVH) behaviour [47].

The transmission has been designed for a C-segment vehicle (top speed 160 km/h), two identical PMSM with up to 30 000 rpm and 60 kW peak power are employed, one drives the first sub-transmission which consists of a two-stage helical gear drive with a fixed gear ratio of 21. The other PMSM run the other sub-transmission which integrates three helical gear sets with a dog clutch that enables shifting between two speeds. The final drive is common for both sub-transmissions and it has a conventional bevel gear differential (see figure 2.20).

The way the setup was designed grant different application strategies regarding load-distribution in the powertrain. The stated challenges, provided sufficient data is gather from the assessed strategies, are efficiently reached [47, 48].

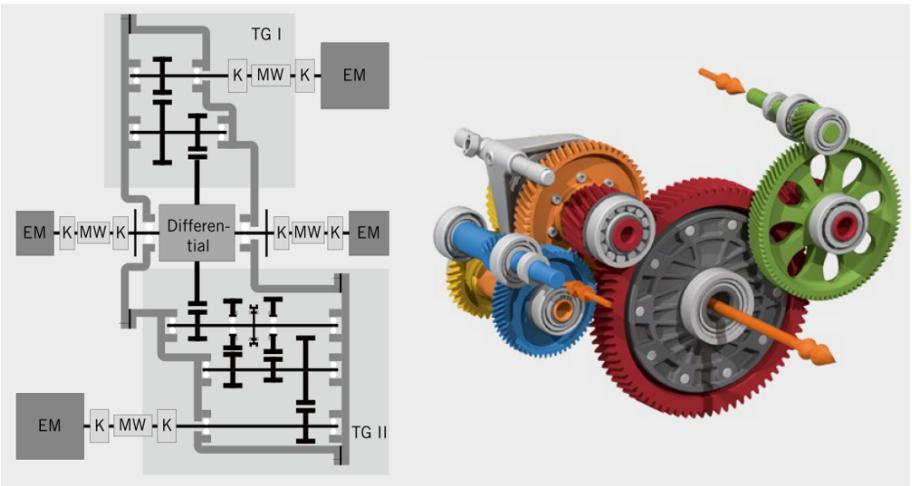

Figure 2.20: Schematic design of the drive train (left) and gear set (right) [47].

Visio.M

Visio.M is a project from TUM which is fundamentally different from conventional transmissions. It proposes a torque vectoring system, for small segment vehicles that provides significant advantages.

One electric motor functions has the drive machine, generating propulsion or recuperation through an axle gear and a spur gear differential which splits evenly the torque between the wheels. Another, smaller electric machine, denominated superimposing machine, coupled to a planetary gear set provides the possibility to control the torque sent to the wheels when necessary. The superimposing gear together with the spur gear differential is an active differential [49] (see figure 2.21).

The separation of the two dynamics, generation of axle torque and torque distribution to the wheels, contributes to a significant controllability and performance over conventional systems.

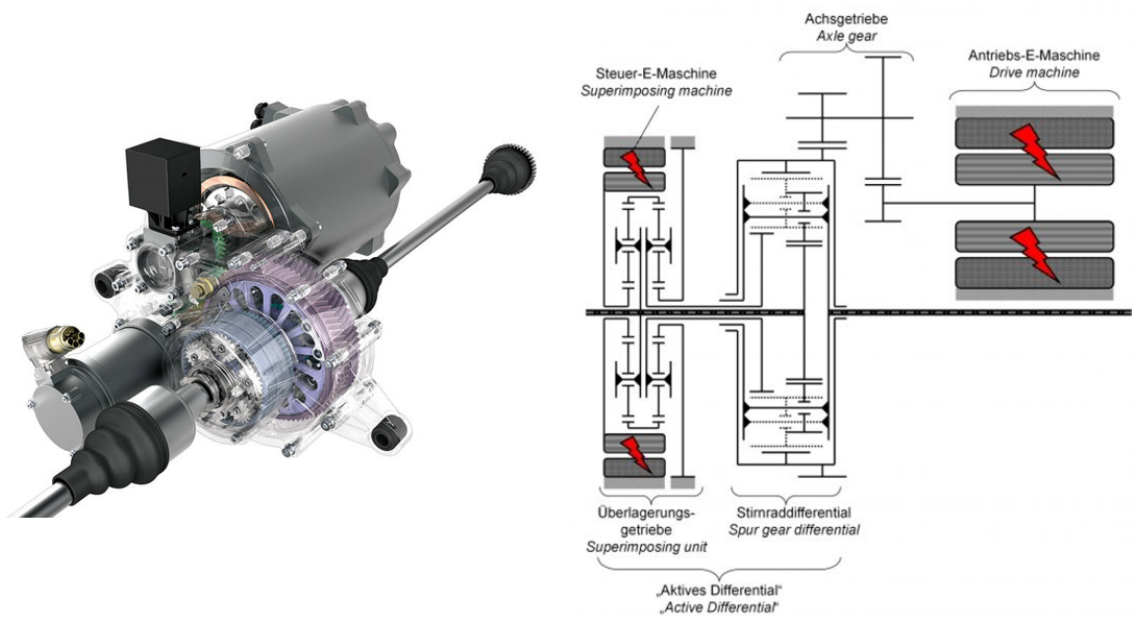

Figure 2.21: Dual motor transmission from Visio.M project (left) and transmission diagram (right) [49].

Chapter 3

Project characteristics

The dissertation main objective is to design a high-speed transmission for an electric vehicle. It has the purpose of reducing the input speed from the electric motor and, at the same time, increasing the torque to comply with the requirements to propel the vehicle.

The electric motor is increasingly efficient, to accomplish it, the rotational speed has to increase and values around 20 000 rpm are becoming usual in the automotive industry. This speed change leads to an adjustment of usual components (e.g. bearings and seals) regarding the altered operating conditions. Even though, special solutions already exist, its cost is still prohibitive for the expanding electric automotive market which has already a high price tag associated.

Additional cautions, such as, the need to preserve lubrication in key areas, since the lubrication regimes are susceptible to rotational speed, also need to be accounted for. Other important challenge is the energy loss increase, specially churning losses in a sump lubricated transmission, which considerably increases in a high speed system. Furthermore, the greater transmission ratios and surface velocities, require special attention with respect to the design of the cylindrical gears pairs [50].

3.1 Vehicle specifications

The focus is in small passenger vehicles (A and B segment) with an urban driving profile. Nowadays, commuting from home to the work place, with small driven distances (under 100 km), is the most common driving profile. Despite that, the majority of consumers, intrinsically, still desire to own a vehicle with an excessive driving range and performance characteristics that are, in fact, only used in long trips. Contradictorily, these costumers want as well, in the same vehicle, to have excellent fuel consumption and low emissions. This problem can be easily solved, if a driver acquires a small passenger vehicle for his everyday commute and rent a higher segment one for sporadic long trips.

The small passenger vehicle performance requirements are, typically, the following [51]:

- Top speed: 120 – 145 km/h
- Gradeability[1]: 20 – 30 %
- Acceleration (0 – 100 km/h): 10 – 16 s

[1] Vehicle's ability to climb slopes.

3.2 Electric motor

Electric motors have high efficiency through all speed range, in particular, high-speed electric motors, with greater power density contribute to a reduction in weight and cost.

From the main three types of electric motors used in the automotive industry, the permanent magnet synchronous motor (PMSM) appears to be the leading choice in segments A and B [18]. It has a high efficiency in the low-medium speed range, where the vehicle will operate most of the time (figure 2.10).

Most of electric motor suppliers (e.g. ABB, ABM, Siemens, ...) are focused in motors with a continuous power of at least 30 kW, so that one single motor can deliver the required power to the vehicle. However, since this project is going to study the adoption of two electric motors, the company Zytek Automotive provides a good solution with a electric motor which provides 15 kW of continuous power and 25 kW of peak power, combining low weight with an adequate motor performance (table 3.1 and figure 3.1).

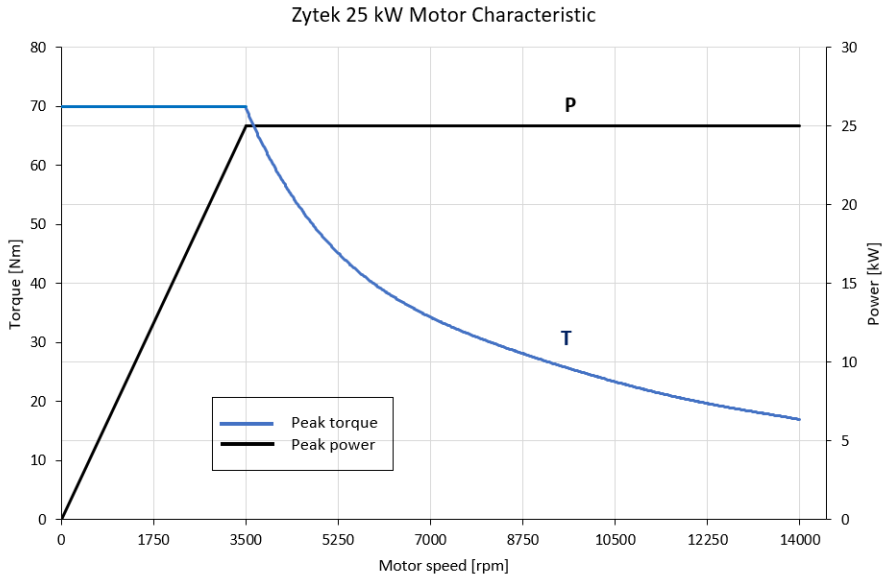

Figure 3.1: Torque-power peak curve of the Zytek 25 kW electric motor [52]

Table 3.1: Technical data for the Zytek Automotive 25 kW electric motor [52]

Parameter	Motor Zytek Automotive
Type	3 phase AC permanent magnet synchronous
Power (Peak/Continuous) [kW]	25 / 15 (Peak for 30 s)
Torque (Peak/Continuous) [Nm]	70 / 47 (Peak for 30 s)
Base Speed [rpm]	3500
Maximum Speed [rpm]	14 000
Cooling	Water/Glycol
Weight [kg]	12,8 (without leads)

3.3 Vehicle performance

Designing a power transmission structure demands thorough consideration of individual components (e.g. shaft, gears, bearings), which are not independent, leading to an interdependent and iterative design process [53].

Initially, the main three indicative vehicle performance attributes are considered to determine power and torque requirements, as well as, the overall transmission ratio.

In table 3.2 the values used in the ensuing calculations are presented, some of the vehicle properties, such as curb weight, frontal area, tire radius were taken from [16, 51].

Table 3.2: Vehicle properties, coefficients and other factors [16, 51]

Results	Value
Top Speed [km/h]	135
Gradeability (start) [%]	30
Gradeability (at 90 km/h) [%]	6
Acceleration (0 – 100 km/h) [s]	16
Overall transmission ratio	12
1^{st} transmission ratio	4
2^{nd} transmission ratio	3

3.3.1 Maximum speed and gradeability

The maximum speed of a vehicle is the constant cruising speed that it can attain on a flat road. From the maximum speed of the electric motor ($N_{\max} = 14\ 000$ rpm) and with a maximum speed ($v_{\max}$) of 135 km/h (37,5 m/s), using equation (3.2) the maximum overall transmission ratio (i_g), of around 12, is obtained.

$$v_{max} = \frac{\pi N_{max} r_t}{30\, i_g} \quad (m/s) \tag{3.1}$$

Rearranging:

$$i_g = \frac{\pi N_{max} r_t}{30\, v_{max}} \approx 12 \tag{3.2}$$

To reach the required velocity, the vehicle must overcome aerodynamic and rolling resistance which oppose its desired direction (the grading force is not relevant since the flat road case is being considered) (see figure 3.2). Equation (3.3) describes the resistive force (F_a) exercised by air, denominated, aerodynamic drag. Through equation (3.4) the force from rolling resistance of tires (F_{rr}) can be derived. Finally, vehicle's weight originates the grading force (F_g) (see equation (3.5)) which characterizes the opposing (climbing) or supporting (descending) movement. These three forces can be combined in a single component, the resistive force, commonly referred to as road load.

$$F_a = \frac{1}{2}\rho A_f C_d (v_{vehicle} - v_{wind})^2 \tag{3.3}$$

$$F_{rr} = C_{rr} mg \cos\alpha \approx C_r mg \tag{3.4}$$

$$F_g = mg \sin\alpha \tag{3.5}$$

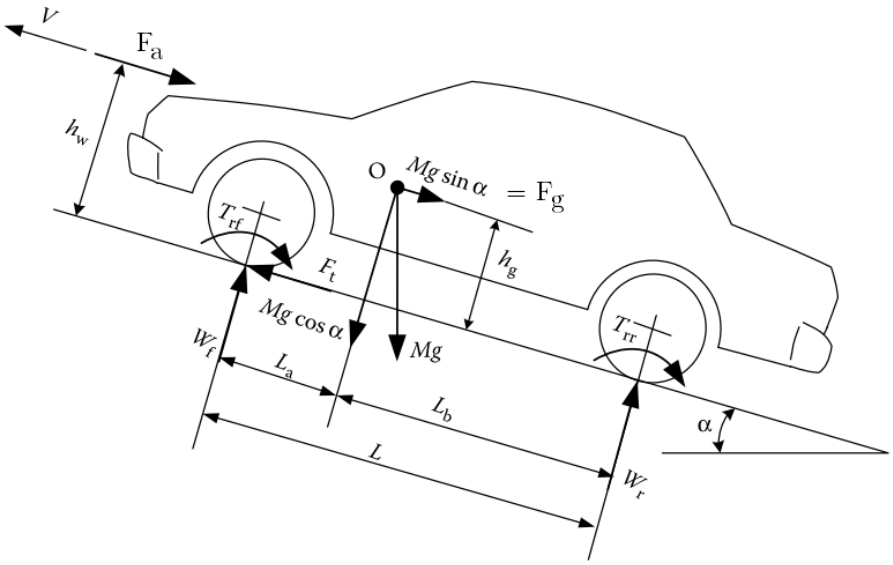

Figure 3.2: Forces acting on a vehicle moving uphill [16]

The tractive force (F_t) on the driven wheels can be expressed by equation (3.6) where the numerator specifies the torque transmitted from the electric motor to the wheels, and the denominator is the tire radius (r_t).

$$F_t = \frac{T_m i_g}{r_t} \tag{3.6}$$

To not prolong and hinder this preliminary assessments, the following simplifications are introduced:

- In equations (3.1), (3.2) and (3.6), no transmission efficiency is considered;
- In equation (3.3), the (v_{wind}) is not considered;
- In equation (3.4), the parameter $\cos\alpha$ is considered approximately one, since the road grade is relatively small ($\alpha < 16{,}7\ ^\circ$).

According to the previous equations, road load as function of vehicle speed, is derived. From figure 3.3, some conclusions can already be drawn:

- Three main operational points, 1, 2 and 3 are presented, which represent the respective road load at different vehicle speeds and grades;
- The vehicle can move up to 30 km/h at 30 % grade, 90 km/h at 6 % grade and 135 km/h in a flat road, for a motor with a continuous power of 30 kW.

3.3.2 Acceleration performance

Acceleration time is an important performance factor for passenger cars, generally this requirement defines the power required for the electric motor [16]. It evaluates the time that a vehicle takes from a stand still until it reaches a stipulated high speed (usually 100 km/h) on a flat road.

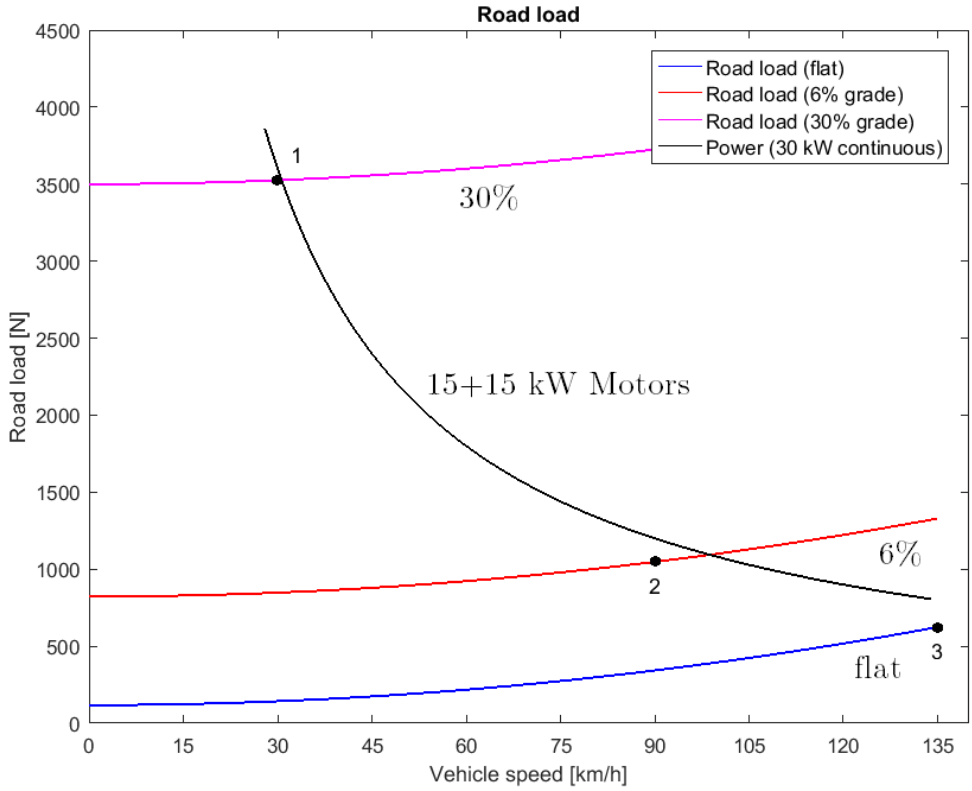

Figure 3.3: Road load as function of vehicle speed

From equation (3.7), where (v_{base}) is the vehicle base speed (which can be calculated from equation (3.1), substituting (v_{max}) and (N_{max}) with (v_{base}) and (N_{base})) and P_{m} is the electric motor power (peak), an acceptable initial assessment of acceleration time can be estimated.

$$t_a = \frac{\delta\, m}{2P_m}(v_{final}^2 + v_{base}^2) \tag{3.7}$$

The rotational inertia factor, δ, is a constant and can be estimated by equation (3.8), where δ_1 is 0,04 and δ_2 is 0,0025 [16].

$$\delta = 1 + \delta_1 + \delta_2 i_g^2 \tag{3.8}$$

Equation (3.9) provides a good estimation of the average power required to overcome the rolling resistance and aerodynamic drag during the acceleration time for a given final speed (v_{final}) [16].

$$\bar{P}_{res} = \frac{2}{3}C_{rr}mgv_{final} + \frac{1}{5}\rho A_f C_d v_{final}^3 \tag{3.9}$$

Finally, the total power (P_{m}) needed to accelerate the vehicle from 0 to 100 km/h can be calculated using equation (3.10).

$$P_m = \frac{\delta m}{2t_a}(v_{final}^2 + v_{base}^2) + \frac{2}{3}C_{rr}mgv_{final} + \frac{1}{5}\rho A_f C_d v_{final}^3 \tag{3.10}$$

3.3.3 Preliminary results

According to equation (3.2) the overall transmission ratio (i_g) is approximately 12.

In table 3.3 a summary of the results of the three specified points in figure 3.3 is presented.

Table 3.3: Relevant calculations for three specified points (see figure 3.3)

Parameter	Point 1	Point 2	Point 3
Vehicle speed [km/h]	30	90	135
Road grade [%]	30	6	0 (flat)
Road load [N]	3525	1048	624
Power [kW]	29,4	26,2	23,4
Torque [Nm]	1092,4	324,9	193,4

After using equation (3.7), a value of roughly 14,5 seconds was the initial assessment of the vehicle acceleration, with this in regard, a value of 16 seconds was used in the following calculations, along with the overall transmission ratio of 12.

Finally, table 3.4 provides the calculations regarding the vehicle acceleration.

Table 3.4: Relevant calculations for acceleration

Parameter	Value
δ [-]	1,4
(v_{base}) [km/h]	34
Acceleration time [s]	16
(P_m) (eq. (3.7)) [kW]	45,2
$\bar{P}_{res}$ [kW]	5,3
(P_m) (eq. (3.10)) [kW]	50,6

After these initial assessments, it is shown that if two of the referenced electric motors are used, with a peak power of 25 kW each, they can achieve the desired performance requirements for the urban vehicle.

3.4 Transmission

The transmission is influenced by the vehicle, electric motor and road profile [35]. Technical and economical factors are of major importance when designing a transmission. Along the years, extensive research and development have been employed in transmission design to reduce losses and to transmit power from the engine to the wheels effectively. Even though, complex automotive transmissions (with up to 7 speeds) have been developed for internal combustion engine vehicles, in the electric vehicle industry, single speed transmissions are the standard, reducing complexity and granting the opportunity to explore other decisive factors, such as material selection and gear design.

The use of a dual motor system allows an extended range of possibilities for the transmission. Each motor can be individually connected to its own reducer, and an electronic differential can be implemented, in spite of a mechanical differential, to control the associated kinematics, which arise, for example, when the vehicle is cornering.

At the start of the design phase, the selection of an appropriate transmission arrangement is of extreme importance, since it will affect the subsequent decisions. Parallel gear sets are the standard choice in electric vehicle transmissions. They have greater mechanical efficiency and are more compact. One of the decisive factors is the number of stages, which is dependent on the overall ratio, which in turn is related to vehicle requirements and motor performance, as previously shown.

3.4.1 Number of stages and overall transmission ratio

A single stage parallel gear pair is generally limited to a ratio of 10:1, beyond this ratio, it becomes ineffective (large dimension and high cost) and it is more practical to increase the number of stages of the gear train [54]. Still, at ratios close to 4:1, problems arise related to the very small module required and its manufacturing issues [50].

With a maximum input speed of 14 000 rpm, the overall transmission ratio, previously calculated, is about 12. A three-stage transmission, given the moderate overall ratio, does not overcome in terms of global efficiency a two-stage transmission. It also has more components and its only benefit would be the smaller gears. Thus, the two-stage gear reducer is the preferred choice which will be further explored.

The global transmission ratio is the product of each stage ratio. In EV transmissions, unlike ICE vehicles, high operating speeds are predominant. In such a setting it is advantageous to adopt an higher ratio at the input stage. Therefore, the selected ratios are 4 and 3, for the first and second stage, respectively.

It is important to avoid integer ratios, non-integer gear ratios improve service life and reduce gear noise, since the engaging locations between teeth keep shifting at every rotation. The wear is distributed among all teeth and not continuously between the same teeth contact.

3.4.2 Geometry

Even though in an electric vehicle, due to lower number of components, there is more available space, the transmission geometry is of great importance. The absence of a mechanical differential results in a conventional two-stage reducer, with one input, one output and three parallel shafts that connect two gear pairs. This simple arrangement carries with it a great size reduction, allowing extra room for the battery pack, as well as, a weight minimization. Both of this aspects are directly related to an increase in the vehicle range, factor of utmost concern in electric automotive market. However, two independent transmissions are necessary to effectively make use of the electronic differential capabilities.

There are two possible geometries where the major difference is the input being in the same side of the output or in the opposite side (figure 3.4). One of the advantages of having the input and output in opposite sides is that it grants the possibility to reduce the distance between the wheel and the transmission.

The arrangement with the input and output on the same side has the advantage that both transmissions may be arranged together in just one housing while still mechanical independent, leading to a more compact total transmission (figure 3.5).

Figure 3.4 shows the arrangement of the cylindrical gear pairs inside the housing. As will be seen afterwards, helical gears will be used, and with them another issue arises, the helix direction for each gear.

In the intermediate shaft (B), the helix direction of the gear wheel (Z2) and pinion (Z3) must be the same, so that the axial forces counteract each other. Despite that both gears (Z2 and Z3) rotate in the same direction, the axial force transmitted from the pinion Z1 to

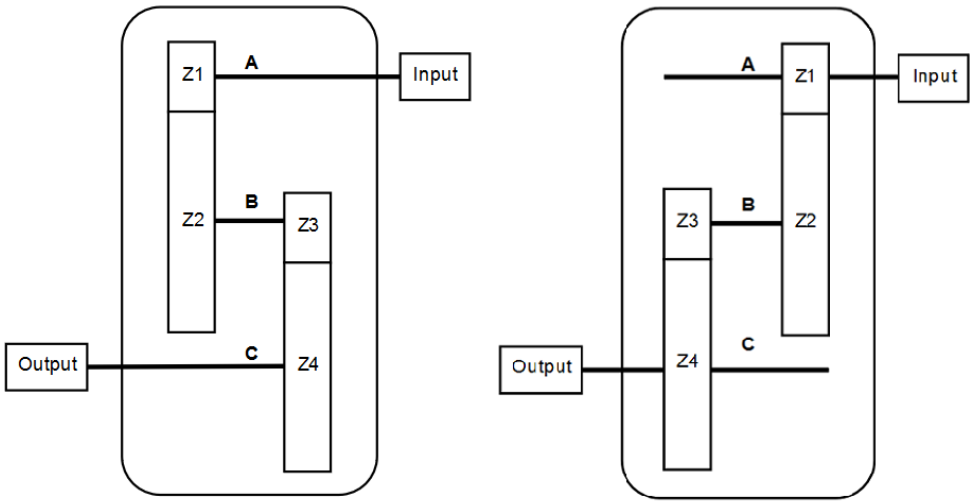

Figure 3.4: Two-stage parallel transmission arrangement with the input and output at opposites shaft ends

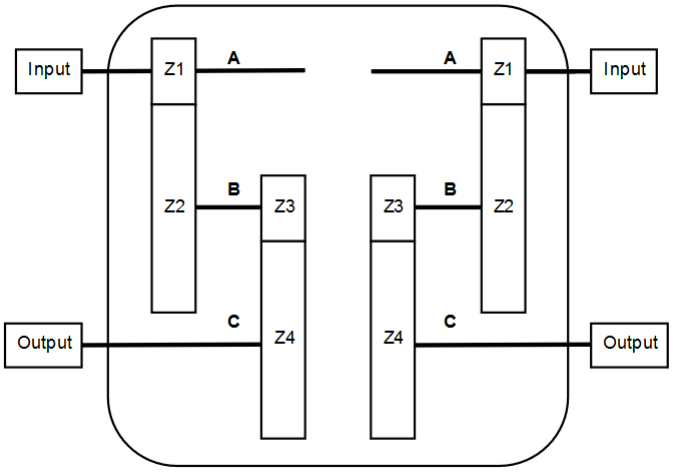

Figure 3.5: Two independent transmission arrangements in the same housing

the gear wheel Z2 has an opposite direction of the axial force that the pinion Z3 withstands from the meshing with the gearwheel Z4. In figure 3.6 there is a clear representation of the above mentioned (opposition between F_{x2} and F_{x3}).

All shafts are going to be supported by two bearings, placed in the shaft extremities, with the gear meshes between them, to provide a consistent and even support through the transmission.

The possible combinations, with the two arrangements in figure 3.4 and different helix direction for each, were tested whilst performing the gear and shaft designs. In the end, the chosen arrangement in this project is the one presented in figure 3.4 (a) since it was the one which yield better results in terms of overall force distribution. This layout is going to be applied to the right front-wheel transmission, which will be further discussed

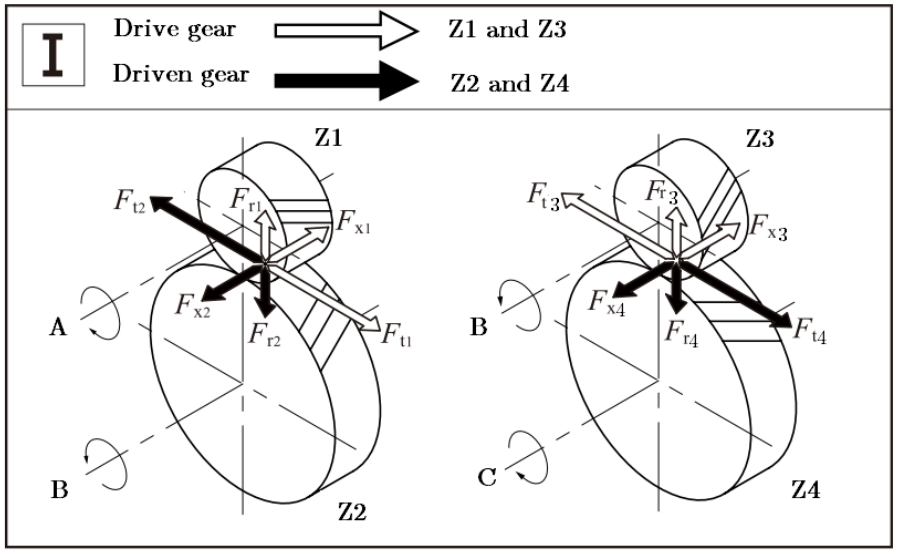

Figure 3.6: Direction of forces acting on a helical gear mesh. Adapted from [55]

in the next chapters. A mirror layout for the left front-wheel transmission should perform accordingly, since the rotational speed and elements are the same of the ones present in the right front-wheel transmission.

The electric motor is the input and it is linked to the shaft A, which supports the pinion Z1. This pinion drives the gear wheel Z2, which is supported, along with the pinion Z3, by the shaft B. Finally, the pinion Z3 drives the gear wheel Z4, connected to the shaft C, which transmits the torque to the output of the transmission.

Chapter 4

Gear design

Gears are a common element in several types of machinery. Gear design is very complex and, during the years, several approaches have been studied and standards have been compiled to achieve gear that are cheaper, quieter and lighter while being more powerful [56].

The continuous requirement of high-performance gear transmissions, has led to important progresses in gear tooth micro geometry, to obtain the optimal tooth contact localization towards higher load capacity and lower transmission error [57].

When designing a transmission, the designer initially works on the basis of the maximum engine torque [35]. After the initial design, maximum speed, maximum power and load spectrum are the next operating conditions to consider in the design phase.

To quickly design competitive gears, KISSsoft [58] will be used to perform the necessary gear calculations, review them according to general standards (ISO, DIN), as well as provide further optimization of the selected gear pairs.

4.1 Application factor

The application factor (K_a) adapts the load to satisfy incremental gear loads and impacts from external sources. These loads depend on the behaviour and characteristics of the driving and driven machines.

In this case, the driving machine is an electric motor with a uniform working characteristic, the driven machine is a urban vehicle which can be associated to a light shock environment. Taking into account the table 4.1, presented in ISO 6336:6 [59], the corresponding application factor is 1,25.

Table 4.1: Application factor (K_a) [59]

Working characteristic of driving machine	Working characteristic of driven machine			
	Uniform	Light shocks	Moderate shocks	Heavy shocks
Uniform	1,00	**1,25**	1,50	1,75
Light shocks	1,10	1,35	1,60	1,85
Moderate shocks	1,25	1,50	1,75	2,00
Heavy shocks	1,50	1,75	2,00	$\geq$ 2,25

Another standard (DIN 3990 Part 41 [60]), specific for car gearboxes, identifies two application factors, one for flank strength (K_{AH}) and other for tooth root strength (K_{AF}). The application factor, in this case, can have values lower than 1,0, in order to avoid a load

spectrum calculation. Considering that this standard is focused on conventional vehicle gearboxes, with several speeds, there is a distinction between the number of cycles for each speed. Therefore, the approach that seems more appropriate is to use the application factor from the ISO standard, since the load capacity calculation [61] will be based on it.

4.2 Road profile

An automotive transmission has, usually, an expected lifetime of 400 000 km, if correctly handled according to factory recommendations.

An adequate identification of the urban driving cycle, provides a more suitable transmission design regarding torque, power, speed and, therefore, a more precise lifetime prediction. Several organizations, mostly in Europe and in the United States, have contributed with a great amount of research, regarding driving patterns on different road types [51]. However, a lot of factors contribute to a definition of the driving pattern, for example, driver behaviour, road conditions, weather conditions and traffic conditions. The non-objectivity of these factors make a strict characterization very hard to achieve.

An estimate of an urban road profile is provided in table 4.2, where torque and power values are related to only one of the transmission's motors. The references [51, 62–64] provided the basis for this estimate.

Table 4.2: Single motor input for an urban road profile [51, 62–64]

	Input speed [rpm]	Power [kW]	Torque [Nm]	Factor [%]
$<$ 50 km/h	3500	18	50	25
50 km/h	5134	15	27,9	45
90 km/h	9241	15	15,5	21
135 km/h	14 000	25	17,1	9
$\sum$	—	—	—	100

The table 4.3 provides an approach of the transmission lifetime, both in terms of hours and distance covered. It was developed based in the previous table 4.2.

Table 4.3: Road profile [51, 62–64]

	Factor [%]	Time [h]	Distance [km]
$<$ 50 km/h	25	2857	100 000
50 km/h	45	3600	180 000
90 km/h	21	933	84 000
135 km/h	9	267	36 000
$\sum$	100	7657	400 000

One may conclude that, in a passenger vehicle with an urban road profile, the lifetime in hours that shall be met is around 7657 hours for a distance of 400 000 km.

4.3 Tooth root and flank safeties

An important step when designing cylindrical gears is to define the required safeties (particularly for tooth root and flank). Nowadays, when designing vehicle transmissions,

pitting performance is decisive, in order to not occur tooth failure, since it leads to immediate transmission failure [35].

The current calculation standards (DIN 3990 and ISO 6336) are also used to calculate the load-carrying capacity for small-module size gears. Despite that, the experimental analysis is predominantly based on a module (m_n) range between 2 and 20 mm. The number of experiments in fine-pitch gears is reduced and is mainly inferred by the general-size influence according to material properties. According to the mentioned standards, there is no increase of the load-carrying capacity when decreasing the module from values lower than 5 mm. In contrast, according to the general theory of material strength, there is a load-capacity increase of 15 % (when decreasing the module from 5 mm to 0,45 mm). By appropriate extrapolation of the of FVA Research Project 246, a 60 % load-carrying capacity increase is expected [65]. According to DIN and ISO standards there is also no increase expected for the pitting-carrying capacity for gears with a module smaller than 10 mm [65].

The standards DIN 3990 and ISO 6336 do not give any particular information about the necessary safeties for gears. The only specific data is presented in part 11 of DIN 3990, where the minimum safety for root and flank given is 1,4 and 1,0, respectively. Despite this, in accordance with empirical values, the required safeties are much smaller for precision gears (module lower than 1,5 mm) (for example: KISSsoft suggests for a module of 1 mm the root and flank safety to be 1,2 and 0,9, respectively).

In light of the above, and to be in the safety side, the standard DIN values will be used. So, for minimum root safety (SF_{min}) and flank safety (SH_{min}), the corresponding values are 1,4 and 1,0, respectively.

4.4 Material

Electric vehicle's transmissions, compared to conventional, have fewer gears which run at higher rotational speed. Since they also feature a reduced number of transmission speeds (usually single speed), the existing gears have to sustain severe life cycles compared to the ones from traditional transmissions.

Gears for vehicle transmissions are traditionally case-hardened. Gear finishing processes such as shaving, grinding and honing are mandatory and one must be selected according to the operational requirements. For low-noise and high-speed applications, after hardening, the gearwheels must be honed. Compared to the grinding process, honing presents superior wear characteristics and quietness, while being a less expensive system. Gears must have a surface hardness around 60 HRC and a core hardness of 30 HRC [56].

It is clear that gear material importance will increase, in order to comply with this, clean gear steels, which exhibit smaller inclusions and give equal strength in all directions to the material are one of the current solutions. Traditionally, to reduce the number of inclusions in steel, expensive secondary operations (e.g. vacuum arc remelting) have to be applied, increasing the material price to excessive values for the automotive industry.

One recent solution, which is implemented by an European producer (Ovako), turns to air melting techniques. Ovako's BQ (bearing quality) and IQ (isotropic quality) steels have a similar fatigue performance compared to high-priced processes steels and, thereby, greater than conventional steels. This quality comes at price, but despite the higher cost of Ovako's steels, the improvement of gear and, therefore, transmission performance, as well as the exclusion of some posterior machining operations (such as shot peening), may result in an overall cost benefit [66].

Another interesting material is the nitriding 31CrMoV9 steel. It has a high

load-carrying capacity is higher, compared to standard gear materials (e.g. 18CrNiMo7-6 and 16MnCr5). For small-module gears, the nitrided depth profile appears similar to that of the case depth profile of the case-hardened gears, the nitriding process may become much more important for these gears because of the obviously better-managed heat treatment.

The 18CrNiMo7-6 steel, according to the standard EN 10084:2008, has got a core hardness higher than 30 HRC. ISO 6336-5 refers an MQ quality (good quality) for this steel. These requisites can be achieved by steel manufacturers at a reasonable price, and so this steel is a very common choice in the automotive industry, and will be considered in this thesis.

4.5 Manufacturing Quality

The standards ISO 1328:1995 [67] and DIN 3961 [68] contain information related to gear quality classes, which range from 1 to 12, being 1 the highest class. To reduce gear noise at high operating speeds, the general class quality should not be greater than 7. According to Larburu [69] the gear quality for automotive applications ranges between classes 3 to 9. Moreover, the circumferential speed is also a criteria when choosing the gear quality class.

When the input shaft is rotating at maximum speed (14 000 rpm) the circumferential speed at the operating pitch circle is greater than 20 m/s and the class required must be, at most, 5. In the second gear pair, despite the higher applied loads, the rotational speed is much lower (maximum: 3500 rpm) and the gear class required is not so strict. Thus, the chosen gear quality class for the second gear pair is 6.

4.6 Tooth flank surface roughness

The standards DIN 4766 part 1 and part 2 [70, 71] give a range of expected values according to manufacturing processes. Despite not being very precise, it is a good starting point to get an idea of what values can be expected.

According to the technical report ISO/TR 10064-4:1998 [72] the roughness classes are not directly related to the gear accuracy grades from ISO 1328-1. Despite that, recommended limits are given for the roughness average value (Ra) and to the mean peak-to-valley roughness (Rz). Since the root is less stressed than the flank, typically the root value is three times higher than the flank value. The mean peak-to-valley roughness generally adopts a value around six times the roughness average value.

With this in mind, and evoking the superior gear quality of the first gear pair (gear quality 5) compared to the second (gear quality 6), the values adopted throughout the project are presented in table 4.4.

Table 4.4: Gear surface roughness

Gear pair	Zone	Ra [µm]	Rz [µm]
1 (Z1 & Z2)	Flank	0,3	2,0
	Root	1,0	6,0
2 (Z3 & Z4)	Flank	0,5	3,0
	Root	1,0	6,0

4.7 Module

The normal module (m_n) is the ratio of the pitch diameter to the number of teeth. It is the index of tooth size in the International System of Units (SI) and its standard unit measure is the millimetre.

Gears with a module 1,25 mm or lower are designated fine-pitch, low-module or small-module gears. Low-module gears with a larger number of teeth, compared to higher module gears, are more efficient and make less noise. Nevertheless, the characteristic small tooth size makes them more susceptible to manufacturing errors and tolerances (e.g. center distance tolerance), as well as operating conditions.

In the standard DIN 780-1 [73], a preferred series of modules is presented, which were used to perform several gear pair calculations, that, after reviewed and compared, lead to the final selected modules.

4.8 Helix angle

The classic electric vehicle transmission practice is to use standard helical gear units with a fixed transmission ratio. To transmit motion between parallel shafts, the helix angle is the same on each gear, but one gear has a right-hand helix and the other the complementary left-hand helix, or vice versa (see figure 3.6).

Helical gears with an adequate total contact ratio, ε_γ, (higher than 2,5) act as an active measure to reduce noise generation due to the more gradual engagement of the teeth during meshing [35]. This meshing of the teeth and smooth transfer of load from one tooth to another gives helical gears the ability to transmit heavy loads at high speeds.

Single-helical gears introduce both thrust and radial loads on the rolling bearings. By increasing the helix angle, thrust (axial) loads rise accordingly. An accurate choice of the helix angle is a key phase, since it will affect, for example, the subsequent bearing selection.

Double-helical or herringbone gears establish equal and opposite thrust forces, suppressing the thrust load in the shafts and rolling bearings, giving more freedom in their choice. These type of gears are associated with significant helix angles, β, (30° to 45°), which lead to smoother operation, however, the tooth strength decreases [56]. They are very unusual in automotive transmissions, mainly due to the associated large face width that is necessary to provide tooth strength. Additionally, acting axial forces usually can be easily supported by standard bearings.

4.9 Face width

Face width (b) is selected based on the load-carrying requirements, module (m_n) and helix angle (β), in order to meet the safety factors required.

The contact area, which is proportional to the gear face width, becomes a dominant aspect in the gear geometry, in comparison to the contact ratio, for helical gears. General expertise refers that, face width must be a minimum of two times the axial pitch (p_x) (see figure 4.1), in order to benefit from helical teeth action [53, 56].

The higher the face width, the higher the tooth root strength as well as the contact ratio, but, close requirement consideration, need to be taken into account since gears will be larger and heavier.

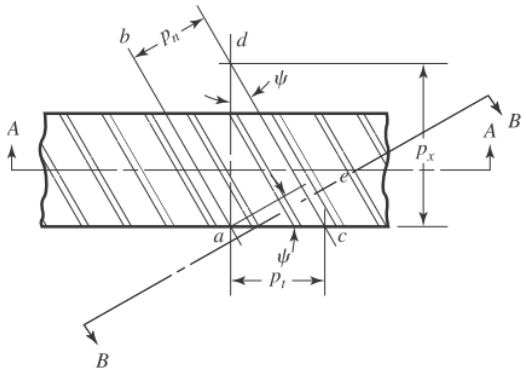

Figure 4.1: Axial pitch (p_x) of helical gears [53]

4.10 Profile shift

Gear teeth have a profile shift (x_i) to avoid undercut and balance the bending stresses in the pinion and gear. It has been defined to use a sum of profile shift coefficients equal or higher than zero, consequently, the center distance (a) will increase, relatively to the reference center distance (a_d). A greater tooth root width, hence, increased tooth root carrying capacity is associated with a positive profile shift.

The KISSsoft software, provides several possible calculations for the pinion and gear coefficients, according to the operational conditions desired. For the first cylindrical gear pair, due to the high rotational speed and high sliding velocity, the minimal sliding velocity criteria was applied. For the second cylindrical gear pair, the loads acquire more importance than the sliding velocity, so the optimum specific sliding criteria was used in order to have similar wear of the pinion and gear.

4.11 Contact ratio

The total contact ratio of helical gears (ε_γ) is the sum of transverse contact ratio (ε_α) and overlap ratio (ε_β).

$$\varepsilon_\gamma = \varepsilon_\alpha + \varepsilon_\beta \tag{4.1}$$

When the total contact ratio increases, the load carrying capacity also increases, while reducing the gear noise since it reduces the irregularity of resultant tooth rigidity and limits the meshing impact [35, 53].

The characteristic pressure angle (α_n) of 20° has limited values associated to the transverse contact ratio (ε_α), a minimum value of 1,0 and a maximum value of 2,0. The overlap ratio (see equation 4.2) present in helical gears, depends on face width and axial pitch, a value higher than 2 is associated to a good use of the helical gears capabilities. Conventionally, when using helical gears, the overlap ratio is higher than the transverse contact ratio.

$$\varepsilon_\beta = \frac{b}{p_x} \tag{4.2}$$

4.12 Comparison

The KISSsoft software, yields a large number of results, using the rough and fine sizing capabilities. These results are based on some initial parameters, such as desired load, speed and/or power. Nominal ratio is also an input and has been previously investigated. Then, the other major conditions, such as, normal module and helix angle, are introduced with a minimum and maximum value, so that the software can iterate between the intended range.

In the beginning, the extended parameter range returns a great number of results, which can be graphically analysed to get a general idea of the impact of the different inputs. After this analysis, the parameter range is substantially reduced, and some final results are selected to further investigate.

In tables 4.5 and 4.6, some results with the associated parameters and its values are presented. In the first stage cylindrical gear pair, for maximum torque, the set torque and input speed are, 70 Nm and 3500 rpm, respectively. For maximum speed, the rating values are 25 kW of power, and an input speed of 14 000 rpm. The face width (b) is also fixed, with a value of 30 mm for the pinion and gear. All of the selected results comply with the minimum safeties required and the other previously referred considerations and, further regards, such as the selected lubricant.

Table 4.5: Cylindrical gear pair for the first stage (Designs A – F)

	Unit	A	B	C	D	**E**	F
Normal module (m_n)	mm	1	0,9	1	0,9	**0,8**	1
Center distance (a)	mm	**85**	95	100	95	95	100
Helix angle (β)	°	**9**	11	12	11	12	12
Total profile shift ($\sum x$)	–	1,005	0,119	0,858	0,641	0,159	1,407
Transmission ratio (i_1)	–	4,030	3,929	3,974	4,024	3,936	3,949
Transverse contact ratio (ε_α)	–	1,500	1,500	2,000	2,000	2,000	**1,000**
Overlap ratio (ε_β)	–	1,494	2,025	1,985	2,025	**2,482**	1,985
Total contact ratio (ε_γ)	–	2,994	3,525	3,985	4,025	4,482	2,985
Maximum torque							
Axial force (F_a)	N	**663,7**	706,7	746,3	723,9	774,1	746,3
Sound pressure level	dB(A)	71,5	71,5	69,8	69,8	**69,6**	74
Power loss (P_{VZ})	W	106	79	130	129	113	**64**
Meshing efficiency (η)	%	99,585	99,691	99,492	99,497	99,565	99,750
Root safety (min.) (S_F)	–	1,642	1,628	1,712	1,509	1,511	1,476
Flank safety (min.) (S_H)	–	1,168	1,259	1,527	1,430	1,467	1,136
Maximum speed							
Sound pressure level	dB(A)	82,3	87,7	82,3	82,4	**81,5**	93
Power loss (P_{VZ})	W	79	58	96	95	82	**47**
Meshing efficiency (η)	%	99,686	99,766	99,615	99,619	99,670	99,810

Some important conclusions can already be drawn for both the first and second stage gear pairs:

- Axial force (F_a) increases with a greater helix angle (β);

Table 4.6: Cylindrical gear pair for the second stage (Designs G – I)

	Unit	G	H	**I**
Normal module (m_n)	mm	1,5	1,5	**1,25**
Center distance (a)	mm	130	130	130
Helix angle (β)	deg	12	13	12
Total profile shift ($\sum x$)	–	0,282	1,008	0,763
Transmission ratio (i_2)	–	3,024	2,976	2,961
Transverse contact ratio (ε_α)	–	1,683	1,592	**1,969**
Overlap ratio (ε_β)	–	1,765	1,909	**2,118**
Total contact ratio (ε_γ)	–	3,448	3,501	4,087
Maximum torque				
Axial force (F_a)	N	1861,3	2013,8	**1797,2**
Sound pressure level	dB(A)	69,2	69,2	**68,5**
Power loss (P_{VZ})	W	149	131	**156**
Meshing efficiency (η)	%	99,420	99,488	99,394
Root safety (min.) (S_F)	–	1,629	1,600	1,446
Flank safety (min.) (S_H)	–	1,324	1,334	1,478
Maximum speed				
Sound pressure level	dB(A)	74,3	74,6	**73,7**
Power loss (P_{VZ})	W	100	88	**106**
Meshing efficiency (η)	%	99,599	99,646	99,577

- The higher the contact ratio (ε_γ), the lower the sound pressure level;
- An overall contact ratio (ε_γ) higher than, approximately, 3 is required to be in line with the requirements;
- At maximum speed the sound pressure level greatly increases, as opposed to power loss (P_{VZ}), which decreases.

Despite that, the ratio of face width (b) to normal module (m_n) is considerable since the axial pitch (p_x) was set to be at least half of the face width (b), the significant face width value was required to increase load-carrying capacity and be within the stipulated safeties (S_F and S_H)

A low-loss gear pair (F) has the highest efficiency, with considerably reduced load-dependent losses in the tooth contact. Its transverse contact ratio (ε_α) has a characteristic minimum value of 1,000, since the considered pressure angle is 20°, and a great profile shift ($\sum x = 1{,}407$) to be within the requirements. However, this gear set has the drawback of having a significant sound pressure level associated, not desired in electric vehicle transmissions.

From these results, the gear pair E was selected for the first stage. It has the lowest normal module and sound pressure level (both in maximum torque and maximum speed). The considerable total contact ratio, ε_γ, (4,482) with an overlap ratio, ε_β, higher than the transverse contact ratio, ε_α, provides the gear pair with a low noise generation and favourable operating conditions. The axial force is the highest, but has a value compatible with the subsequent studied rolling bearings and shaft force analysis. The power loss and efficiency is regarded as acceptable.

In the second stage cylindrical gear pair, for maximum torque, the rating torque and input speed are drawn from the first stage selected gear pair (E), which yields 275,5 Nm and 889,2 rpm, respectively. For maximum speed, the rating values are 25 kW of power, and an input speed of 3556,8 rpm. The face width (b) is fixed, with a value of 40 mm for the pinion and gear. Just as the first stage, the selected results comply with the minimum safeties required and previous design considerations.

From table 4.6 the gear pair I was chosen for the second stage. The normal module of 1,25 mm to continue in the scope of fine-pitch gears. A thorough evaluation of axial force effect was required, particularly on the shaft C where no counteracting forces are in place. The axial force demands an appropriate support and bearing selection. With this in mind, the smaller axial force, F_{a}, with a value of 1797,2 N is desirable. As before, the selected total contact ratio is the highest (4,087) and, again, the overlap ratio is bigger than the transverse contact ratio. The sound pressure level also has the preferred smallest value between the selected options. In contrast, power loss and efficiency are the worst, despite that, since it is a relatively small difference, these parameters do not impact the selection.

4.13 Final results

Four elements (Z1, Z2, Z3, Z4) compose the final cylindrical gear pairs for the two-stage parallel transmission. The transmission has an overall transmission ratio (i_{g}) of 11,65.

Table 4.7 provides some reference values for the transmission, based on the selected helical gear pairs.

Table 4.7: General transmission results

Parameter	Maximum torque	Maximum speed
Overall meshing efficiency (η) [%]	98,96	99,25
Input speed [rpm]	3500	14 000
Output speed [rpm]	300,3	1201,3
Input torque [Nm]	70	17,1
Output torque [Nm]	815,8	198,7

In the next tables, some specific data regarding the resultant cylindrical gear pairs is listed. For a more detailed review, the appendix C can be consulted, where there are the complete reports from the KISSsoft software.

Table 4.8: Summary of the first stage cylindrical gear pair specifications

Parameter	Unit	Pinion (Z1)	Gear (Z2)
Normal module (m_n)	mm	0,8	
Pressure angle (α_n)	°	20	
Helix angle (β)	°	12	
Center distance (a)	mm	95	
Face width (b)	mm	30	
Transmission ratio (i_1)	–	3,936	
Transverse contact ratio (ε_α)	–	2,005	
Overlap ratio (ε_β)	–	2,482	
Total contact ratio (ε_γ)	–	4,487	
Number of teeth (Z)	–	47	185
Profile shift (x_i)	–	0,0907	0,0685
Operating pitch diameter (d_w)	mm	38,491	151,509
Tip diameter (d_a)	mm	40,701	153,018
Specific sliding at the tip (ζ_a)	–	0,329	0,410

Table 4.9: Summary of the first stage cylindrical gear pair specifications according to maximum torque and maximum speed

Parameter	Unit	Maximum torque	Maximum speed
Sliding velocity at tip (max.) (v_ga)	m/s	1,110	4,438
Circumferential speed (v)	m/s	7,04	28,178
Root safety (min.) (S_F)	–	1,511	2,467
Flank safety (min.) (S_H)	–	1,467	1,888
Sound pressure level	dB(A)	69,6	81,8
Power loss (P_VZ)	W	112	82
Meshing efficiency (η)	%	99,565	99,670
Transmittable power (max.)	kW	27,70	44,06

Table 4.10: Summary of the second stage cylindrical gear pair specifications.

Parameter	Unit	Pinion (Z1)	Gear (Z2)
Normal module (m_n)	mm	1,25	
Pressure angle (α_n)	°	20	
Helix angle (β)	°	12	
Center distance (a)	mm	130	
Face width (b)	mm	40	
Transmission ratio (i_2)	–	2,961	
Transverse contact ratio (ε_α)	–	1,972	
Overlap ratio (ε_β)	–	2,118	
Total contact ratio (ε_γ)	–	4,090	
Number of teeth (Z)	–	51	151
Profile shift (x_i)	–	0,3715	0,3910
Operating pitch diameter (d_w)	mm	65,644	194,356
Tip diameter (d_a)	mm	69,055	196,897
Specific sliding at the tip (ζ_a)	–	0,339	0,339

Table 4.11: Summary of the second stage cylindrical gear pair specifications according to maximum torque and maximum speed.

Parameter	Unit	Maximum torque	Maximum speed
Sliding velocity at tip (max.) (v_ga)	m/s	0,509	2,035
Circumferential speed (v)	m/s	3,03	12,14
Root safety (min.) (S_F)	–	1,446	2,745
Flank safety (min.) (S_H)	–	1,478	2,024
Sound pressure level	dB(A)	68,4	73,4
Power loss (P_VZ)	W	156	106
Meshing efficiency (η)	%	99,394	99,577
Transmittable power (max.)	kW	26,49	49,02

Chapter 5

Shaft design and bearing selection

The purpose of a shaft is to transmit torque along its axis, to support the elements located on it, and endure the forces which act on these elements [74]. In an automotive transmission, the torque is transmitted from an input gear to an output gear. The torque transmission between the shaft and the gears is achieved through machine elements, in particular, keys and splines.

Rolling bearings are universally applied in mechanical transmissions. They support the shaft, keeping it in the right position. They also withstand forces acting on the shaft, transmitting them to the housing, and allow the shaft to freely rotate, minimizing friction. For electric automotive transmissions, rolling bearings need to endure high rotational speed, considerable operating temperatures and, when using a light alloy housing (e.g. aluminium), a compensation regarding heat expansion is crucial.

5.1 Shaft layout

The common shaft layout is a stepped cylinder, also denominated a multi diameter shaft. With this structure, both manufacturing and element assembly are facilitated.

The general shaft considerations [35, 53] which must be taken into account when designing such a shaft are:

- Shaft length must be minimized in order to limit bending moments and deflections;
- Shaft shoulders are a proper way to axially locate shaft elements and withstand thrust loads;
- Components with load-carrying capacity, such as gears, must be positioned between supporting bearings (preferably two) and, close to the bearings itself. This leads to a reduced deflection and bending moment. Besides, this disposition is also related to an increase in shaft critical speed;
- Axial clearances between components are necessary with the aim of giving access for their disassembly and to let lubricant flow properly;
- Strict positioning of elements on the shaft is a key point, as well as accurate hold after positioning so that coupling components are correctly aligned;
- If the applied loads are not significant, it is possible to axially locate elements with retaining rings (circlips) (at the end of the shaft) in shaft grooves and with space sleeves (in the middle of the shaft);

- Diameter shifts in the shaft, must be kept below a ratio of D/d ≈ 1,4.

Shaft shoulders, with corresponding diameters transitions, where bearings inner rings are abut, must have relief grooves. The selected relief grooves are based on DIN 509 [75]. The type E undercut (see figure 5.1), which is appropriate for modest demands on the shoulder, is selected.

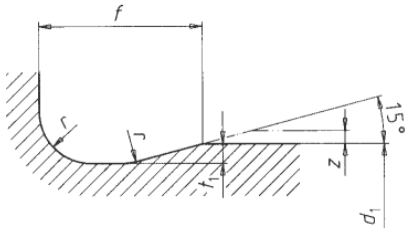

Figure 5.1: DIN 509 - Type E undercut [75]

In other internal corners, a transition radius was selected to provide a filleted corner, according to the transition ratio and shaft diameter. External corners must be chamfered, usually at 45 °. For cylindrical components, the chamfer leg c can be approximate using the equation 5.1, shaft diameter is represented by D [76].

$$c = 0,1\sqrt{D} \tag{5.1}$$

Standard values that must be employed, after rounding off, are:

$$c = 0{,}2; 0{,}5; 0{,}8; 1; 1{,}2; 1{,}5; 1{,}8; 2; 2{,}5; 3; 3{,}5; 4; 5 \tag{5.2}$$

All the above considerations were taken into account when performing the shaft layout design. This process is not straightforward, since continuously changes have to be made to meet the requirements, and, in the end to attain the best possible shaft layout to the several settings in question.

5.1.1 Material

The conventional materials for shaft are carbon and alloy steels. They have an high elasticity coefficient, and the required strength through forging or rolling. Pinion shafts, require both contact and bending strength of the teeth to withstand loading stresses, becoming necessary to use alloy steels and their respective treatments [74].

In [35], some examples of standard shaft materials are given: 25CrMo4, 34Cr4 and 16MnCr5.

Since shaft A and B are pinion shafts, the chosen material is the same as the selected for the gears, the 18CrNiMo7-6 steel, with a core hardness higher than 30 HRC, according to the standard EN 10084:2008. Shaft C, to control material cost, also is from the same steel.

5.1.2 Relative position and direction of rotation

The relative position between the shafts is usually altered to better accommodate the applied loads. The transmission initial position, is completely horizontal as presented in figure 5.2 After some iterations, performed in the KISSsoft software, the final shaft relative position is presented in figure 5.3. Despite not being the position that is less

stressed, since, as will be exposed, the selected lubrication method is splash lubrication which requires particular considerations. In fact, a more favourable arrangement would be obtained if gear Z2 as well as gear Z4 positions were lifted with respect to pinion Z1. However, in order to let lubrication flow properly through all gear teeth and to control churning losses, the presented arrangement had to be consider.

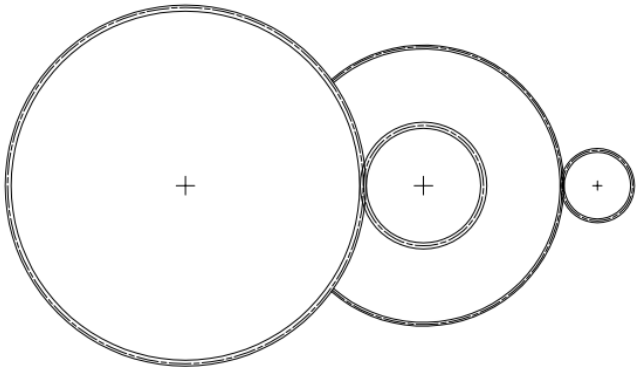

Figure 5.2: Initial shaft relative position

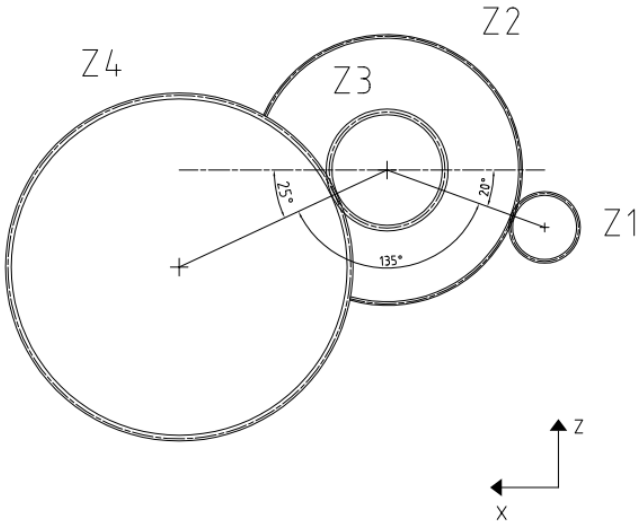

Figure 5.3: Final shaft relative position

The direction of rotation of a shaft, when working with helical gears, is also an important parameter in the design phase. Corresponding loads, change with clockwise (negative) or counter clockwise (positive) rotation, which affects the relative position between the shafts, as well as rolling bearing selection and final arrangement.

In figure 5.4, taken from KISSsoft, the direction of rotation is defined, according to the referenced axis. The shaft axis of rotation is the Y axis, along which the shaft is generated.

In both figures 5.5 and 5.6 the final transmission architecture with the respective shaft arrangement is presented. For the vehicle to move forward, the gear Z4 has to rotate in the same direction as the tire, in this case, positive direction. The presented transmission must be linked to the front right wheel of the vehicle, so that the weight is directed more close to the vehicle center. As can be seen in figure 5.6, even if the transmission is along

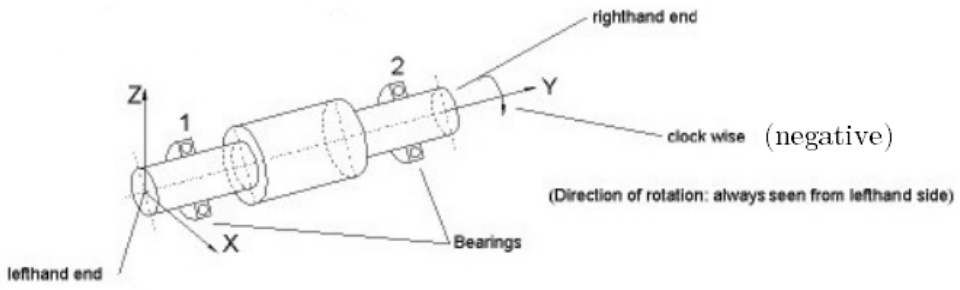

Figure 5.4: Direction of shaft rotation [58]

the rim/tire axis, the total height of the transmission does not constitute a problem, since there is a considerable space between the transmission and the road.

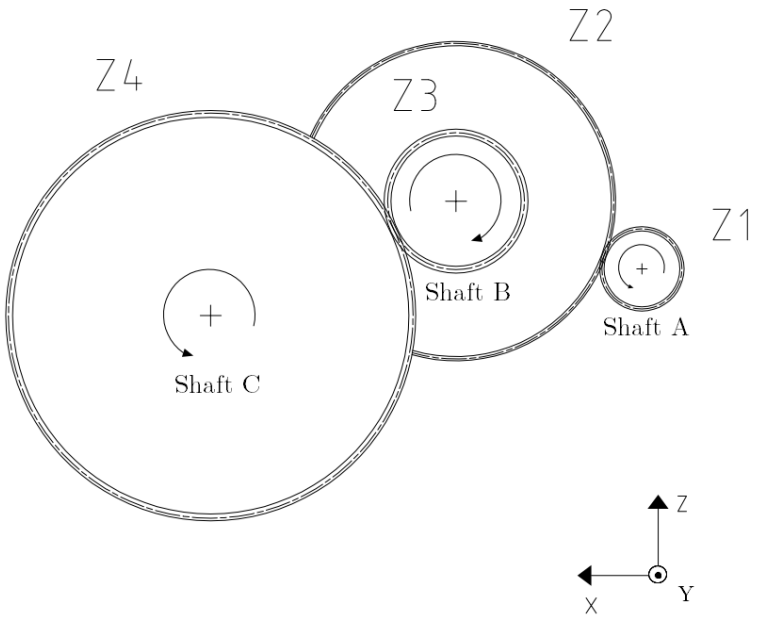

Figure 5.5: Final shaft arrangement and respective shaft rotational directions

5.1.3 Shaft ends

Shaft A and shaft C have couplings, since they are the input and output shaft, respectively. These couplings are located outside of the housing, consequently, the shafts must have shaft ends, where the splines will be manufactured.

The industry available shaft ends fall into two main areas: cylindrical and conical. In turn, the shaft ends of these areas can be subdivided in long or short series. Due to the relatively small length of the shafts and, in order to comply with this line of reason, the shaft ends used will be from the short series of the standard ISO/R 775 [77].

In the input shaft, the diameter of the section right before the shaft end is 25 mm, leading to a shaft end with a 20 mm diameter, which as 36 mm according to the short series length.

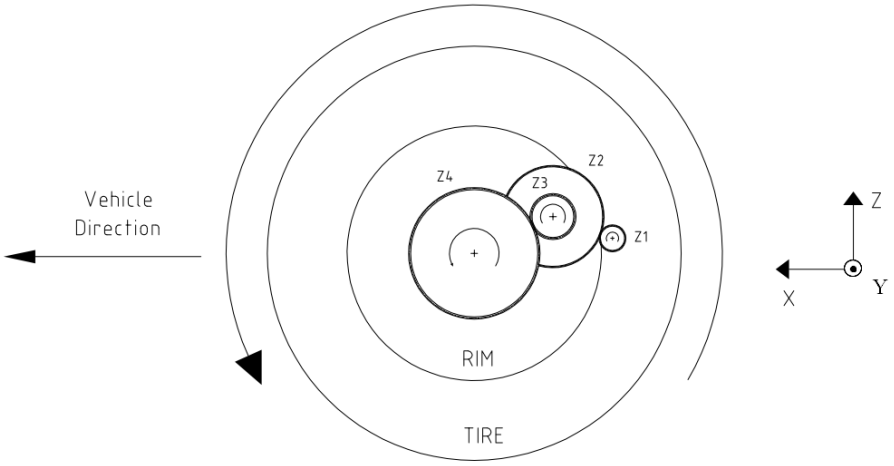

Figure 5.6: Vehicle forward direction with associated tire rotation and transmission architecture

In the output shaft, the diameter of the section right before the shaft end is 45 mm, the chosen diameter for the shaft end is 35 mm, which as 58 mm according to the short series length.

It can be concluded that there is a diameter transition between the shaft end and the nearby section. This transition favours the rolling bearings assembly, since it has to cover a shorter distance, and creates an opportunity to use a smaller radial shaft seal both in the input and output shaft.

The selected shaft ends, according to the designation in [78], for the input and output shaft are, respectively:

- Shaft end, cylindrical, short, diameter 20 mm without threaded hole;
- Shaft end, cylindrical, short, diameter 35 mm without threaded hole.

5.1.4 Splines

The input and output shafts are linked to an electric motor, and to a drive axle, respectively. This connection will be made through splines.

Splines, due to their complexity, are more expensive to manufacture than keys, which are also used for torque transmission. This statement is only valid for small-lot production, when mass production is considered, usually the case for the automotive industry, the tools required to manufacture splines are already in place, thus reducing the costs associated. Since the load distribution between teeth is equivalent in a spline connection, a longer fatigue life is expected compared to a key connection. Conventionally, they are applied to ensure high torque transmission. In this case, the useful advantage is the achievable loose slip fit, which allows significant axial motion between the connected elements while accurately transmitting torque [53].

The two most common spline types are: straight-sided and involute splines. The latter is clearly more advantageous, therefore, it is selected for the design of the transmission.

The major benefits of involute splines are [79]:

- Higher strength, both in bending and compression;

- Manufactured with high accuracy, using standard gear-cutting equipment;
- Involute splines of the same module are formed by the same hob cutter (or gear cutter);
- Possibility to correct, in order to increase strength and meet standard major diameters;
- Can be subjected to finish machining, when present on shafts.

For couplings, generally, involute short cut teeth are used. To increase strength ability, large pressure angles ($\alpha_n = 30$ °) are the most universally used. The standard DIN 5480 [80] applies to flank-centred fitted spline connections, where the teeth flanks are use to transmit the required torque and center the hub and shaft relative to each other.

The length of the input and output shaft splines are, respectively, 19 and 30 mm.

To manufacture the splines, an overtravel of the manufacturing tool has to be regarded and provisions made. A shaft groove is necessary to avoid this issue, and in [81] provides dimensional information regarding the height, width and radius of the groove for several shaft diameter ranges.

In accordance to the standard DIN 5480, fitted splined connection are designated by: the main standard number, N for a hub or W for a shaft, the reference diameter, the module, number of teeth and finally the tolerance class. The selected splines for the input and output shaft, respectively:

- DIN 5480 - W 19 x 0.8 x 22 x 5f;
- DIN 5480 - W 34 x 0.8 x 41 x 5f.

5.1.5 Key connections

Concerning shaft-hub connections, keys are the most widespread type which help transmitting torque. Stationary key connections provide the most efficient and economical connection [74] to transmit moderate to high torque.

Straight keys, with a rectangular cross-section and chamfered ends, following standard DIN 6885 [82], are selected for the connection between the gear wheels Z2, Z4 and shafts B, C, respectively. The assembly and disassembly of keyed components is usually straightforward, due to the existence of a slip fit onto the shaft [53].

Conventionally, medium-carbon steels are the key materials (e.g. C 45 (EN), C 50 E (EN)), with a tensile stress higher than 590 N/mm^2.

According to DIN 6885 A, the keys are designated by type, width, height and length. The selected keys for shaft B and C are, respectively:

- Parallel Key - DIN 6885 - A 12 x 8 x 28;
- Parallel Key - DIN 6885 - A 14 x 9 x 36.

A minimum ratio D_{hub}/d, where D_{hub} is the gear hub diameter and d is the shaft diameter, is required to ensure the proper hub strength at the section where the keyway is located. In [79] minimum values are given for this ratio. The gear Z2 hub diameter has to be greater than 58 mm ($D_{\text{hub}}/d = 1{,}46$), and the gear Z4 hub diameter must be higher than 72 mm ($D_{\text{hub}}/d = 1{,}44$).

5.2 Rolling bearings

In the following section, the bearing selection and arrangement, as well as the final selected bearings will be explored. During the bearing selection phase, several manufacturers were taken into account (SKF, Koyo, FAG and TIMKEN).

In the appendix E, the catalogue reference for each bearing can be consulted.

5.2.1 Rolling bearings selection criteria

To select the most appropriate rolling bearing type for a given application, several variants have to been taken into account. After some considerations, the selected rolling bearing type for all transmission bearings is the most widely used one, which is the deep groove ball bearing (single row). It can withstand considerable radial and axial loads in both directions, thereby rendering it notably versatile. The simple design leads to an inexpensive bearing, still they are robust in operation requiring little maintenance and can withstand very high speeds, relevant for electric vehicle transmissions.

Regarding the bearing manufacturers, Koyo provided, for a bearing with the same dimensional characteristics, higher load ratings (dynamic and static) which could lead to a smaller bearing choice compared to the group SKF. However, SKF was selected for the final bearings, since the necessary thermal limiting speed was achievable, in contrast to Koyo's.

Life of a rolling bearing is a crucial design criteria. It can be expressed as the number of operating hours endured by the bearing at a given speed, before metal fatigue occurs on one of the bearing elements (inner race, outer race or rolling element). The ISO 281 standard [83], is based on the life that 90 % of a large group of identical bearings can achieve, denominated the basic rating life. To get a base value for the rolling bearing service life, a calculation was performed, taking into consideration the estimated driving profile (see table 4.2 and 4.3). It was determined that a service life superior to 4000 hours for the rolling bearings, when the transmission is operating at maximum torque, is a good starting point to select a suitable rolling bearing.

The actual service life can divert substantially from the basic rating life, regarding modern high-quality bearings and their application. Thus, the mentioned standard has a modified life factor to complement disparities, which arise from application factors, such as, lubrication and degree of contamination [84].

Concerning the degree of contamination, bearing size, relative lubricant film thickness, size and distribution of solid contaminants and types of contaminants play an important role. ISO 4406 [85] classifies the contamination level in a lubrication system. For the current application, and its operating conditions, the chosen classification, for an oil lubrication without filtration, is -/15/12, where the second and third representative scale numbers are related to the number of particles equal to or larger than 6 µm, and than 14 µm, respectively.

In the input shaft A, the selected bearings, to comply with the load and, particularly, thermally safe speed requirements, could not present the simplest design provided by SKF. A reinforced ball set (prefix E) and a glass fibre reinforced PA66 cage, ball centred (prefix TN9) were mandatory to remain in the deep groove ball bearing setting, otherwise angular contact ball bearings, or hybrid deep groove ball bearings would also provide a good, but more expensive, solution.

The rolling bearings selected for the shafts B and C, have the simplest design, without variants, since they can accommodate the given loads and speeds adequately.

5.2.2 Arrangement

The rolling bearing arrangement has the objective of both supporting and locating the shaft relative to the stationary housing. The typical arrangement is the locating/non-locating bearing arrangement (figure 5.7), which provides clearance for thermal expansion and contraction of the shafts. In particular, the locating rolling bearing support is associated with the strict axial location of the shaft in both directions.

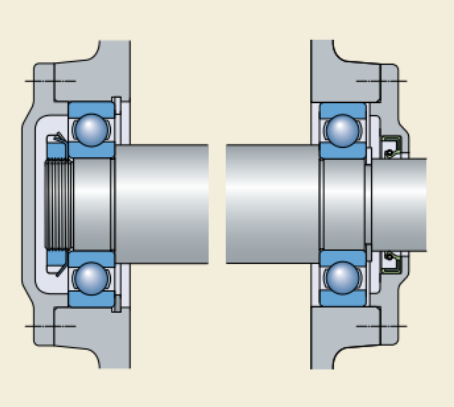

Figure 5.7: Locating/non-locating bearing arrangement [84]

Since deep groove ball bearings can withstand combined loads (radial and axial), they are appropriate both in the locating and non-locating position. The bearings in the non-locating position must carry only radial loads, to alleviate the expansion and contraction of the shaft. They also must have a loose fit between the outer ring and the housing, so that there is identical axial movement of the running shaft and bearing, thereby, not creating abnormal axial loads, which could lead to premature failure [84].

5.3 Rolling bearings selected

In the following tables 5.1 to 5.3, a summary of the rolling bearings selected for each shaft is presented, with some representative characteristics and results when operating at maximum torque.

Table 5.1: Summary of selected bearings for shaft A and operating parameters for maximum torque

	Non-locating bearing	Locating bearing
Designation	SKF 6305 ETN9	SKF 6205 ETN9
Type	Single row deep groove ball bearing	
Dimensions		
Inner diameter [mm]	25	25
External diameter [mm]	62	52
Nominal width [mm]	17	15
Characteristics		
Dynamic load rating [kN]	26	17,8
Static load rating [kN]	13,4	9,8
Reference speed [rpm]	24 000	28 000
Limiting speed [rpm]	16 000	18 000
Mass [kg]	0,22	0,12
Rolling bearing reaction forces		
Radial force (F_r) [kN]	2,765	1,125
Axial force (F_a) [kN]	0	0,776
Operating parameters		
Operating speed - ω_A [rpm]	3500	
Service temperature [°C]	65	
Modified life - Lnmh [h]	4669	4639
Static safety factor	4,85	8,27
Power loss [W]	21,42	23,24

Table 5.2: Summary of selected bearings for shaft B and operating parameters for maximum torque

	Non-locating bearing	Locating bearing
Designation	SKF 6308	
Type	Single row deep groove ball bearing	
Dimensions		
Inner diameter [mm]	40	
External diameter [mm]	90	
Nominal width [mm]	23	
Characteristics		
Dynamic load rating [kN]	42,3	
Static load rating [kN]	24	
Reference speed [rpm]	17 000	
Limiting speed [rpm]	11 000	
Mass [kg]	0,63	
Rolling bearing reaction forces		
Radial force (F_r) [kN]	4,321	5,736
Axial force (F_a) [kN]	0	1,028
Operating parameters		
Operating speed - ω_B [rpm]	889,23	
Service temperature [°C]	65	
Modified life - Lnmh [h]	14027	4875
Static safety factor	5,55	4,18
Power loss [W]	11,02	26,42

Table 5.3: Summary of selected bearings for shaft C and operating parameters for maximum torque

	Non-locating bearing	Locating bearing
Designation	SKF 6209	SKF 6309
Type	Single row deep groove ball bearing	
Dimensions		
Inner diameter [mm]	45	45
External diameter [mm]	85	100
Nominal width [mm]	19	25
Characteristics		
Dynamic load rating [kN]	35,1	55,3
Static load rating [kN]	21,6	31,5
Reference speed [rpm]	17 000	15 000
Limiting speed [rpm]	11 000	9 500
Mass [kg]	0,42	0,84
Rolling bearing reaction forces		
Radial force (F_r) [kN]	2,909	6,596
Axial force (F_a) [kN]	0	-1,797
Operating parameters		
Operating speed - ω_C [rpm]	300,31	
Service temperature [°C]	65	
Modified life - Lnmh [h]	19577	6192
Static safety factor	4,78	7,43
Power loss [W]	3,07	16,36

5.4 Shaft analysis

This section presents the final shafts design, their respective loads and the main values regarding shaft analysis. Stress, deflection and critical speed of the shafts are treated and conclusions drawn. An exhaustive review, regarding geometry, calculations and respective results, performed with the KISSsoft software, can be consulted in the appendix D.

5.4.1 Final shafts

Shaft A

The pinion shaft A has two supporting rolling bearings, the pinion Z1 and, the spline coupling at the shaft right end. The pinion Z1 is axially spaced from the left rolling bearing by 9 mm, so that necessary axial space for the position of the flanges is available. The major diameter of the shaft A is 32 mm and it is rotating clockwise (negative direction) (see figure 5.4). The inner ring of the left bearing is secured axially by a retaining ring. The final shaft layout is presented in figure 5.8. The figure 5.9 shows the torque diagram of shaft A and figure 5.10 presents the Y-direction forces (green) and the resulting X-Z forces (blue).

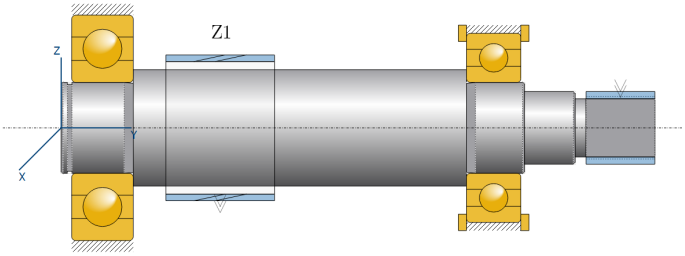

Figure 5.8: Shaft A final design layout [58].

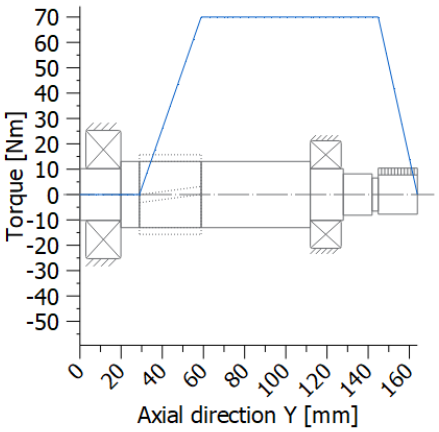

Figure 5.9: Torque diagram of shaft A [58]

When the shaft is operating at maximum speed (14 000 rpm) the minimum thermally safe operating speed is 14 241 rpm according to DIN 732 [86]. This calculation is essential, since the corresponding speed is close to the previous stated bearing limiting speed, which is a guide value for certain operating conditions. The parameters consider are: temperature

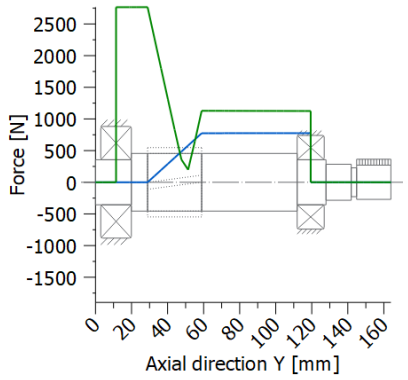

Figure 5.10: Force diagram of shaft A [58]

difference of 10 °C, circulatory lubrication, a mean bearing temperature of 80 °C and temperature around the bearing of 70 °C.

Shaft B

The pinion shaft B has a major diameter of 42 mm is supported by two deep groove rolling bearings and has the pinion Z3 integrated. The gear Z2, from the first stage cylindrical gear pair (Z1-Z2), is keyed to the shaft. To prevent relative rotation between the shaft and to enable torque transmission, there is a keyed joint between the shaft and the gear Z2. The pinion is axially located by a shaft shoulder on the right side and, in the left side, by the gear hub (in the figure 5.11 it is not clear, since it is not possible to create a larger hub in the software). The gear is axially located on the left by a spacer sleeve. As seen above, a retaining ring is used to axially locate the left rolling bearing inner ring. The final shaft layout is presented in figure 5.11. The figure 5.12 shows the torque diagram of shaft B and figure 5.13 presents the Y-direction forces (green) and the resulting X-Z forces (blue).

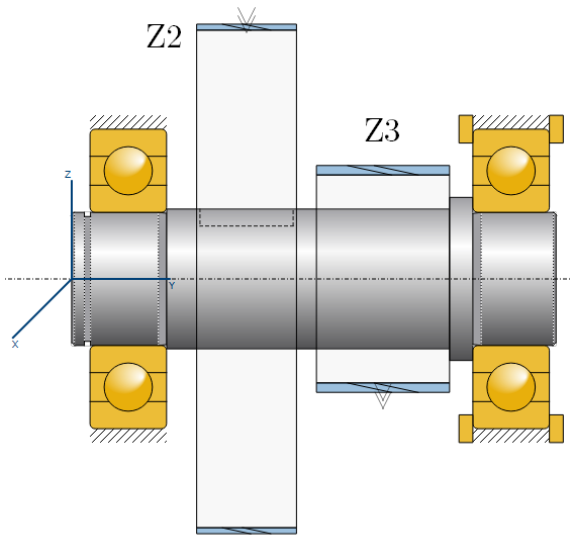

Figure 5.11: Shaft B final design layout [58]

When the shaft B is operating at maximum speed (3557 rpm), the minimum thermally

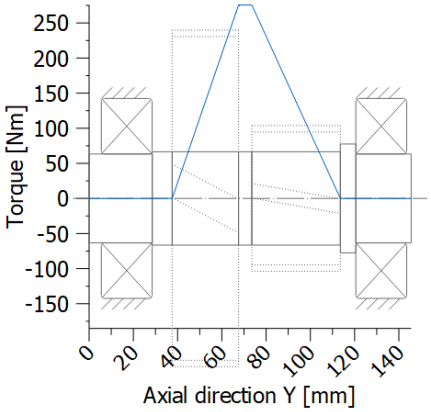

Figure 5.12: Torque diagram of shaft B [58]

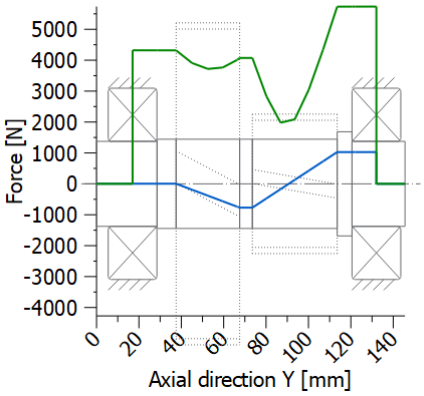

Figure 5.13: Force diagram of shaft B [58]

safe operating speed is 7240 rpm, according to DIN 732 [86]. Calculations performed for a temperature difference of 10 °C, considering circulatory lubrication, a mean bearing temperature of 80 °C and temperature around the bearing of 70 °C.

Shaft C

The shaft C also has two rolling bearings, the gear Z4 from the second stage cylindrical gear pair (Z3-Z4) which is also keyed to the shaft, which has a major diameter of 50 mm. The gear is axially located by a shaft shoulder and by a spacer sleeve. A retaining ring locates the left bearing axially. At the shaft end, there is a spline coupling, since this shaft is the output shaft. The final shaft layout is presented in figure 5.14. The figure 5.15 shows the torque diagram of shaft C and figure 5.16 presents the Y-direction forces (green) and the resulting X-Z forces (blue).

Shaft C when operating at maximum speed (1201 rpm) has a thermally safe operating speed of 1928 rpm. Calculations are performed for a temperature difference of 10 °C, considering oil level to middle of bearing, a mean bearing temperature of 80 °C and a temperature around the bearing of 70 °C, according to DIN 732 [86].

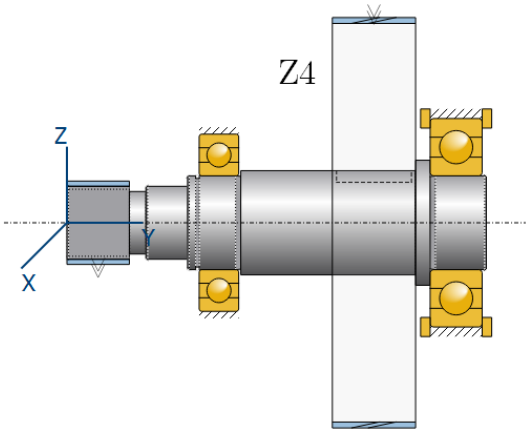

Figure 5.14: Shaft A final design layout [58]

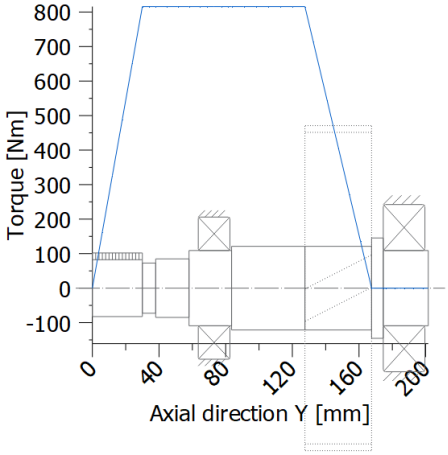

Figure 5.15: Torque diagram of shaft C [58]

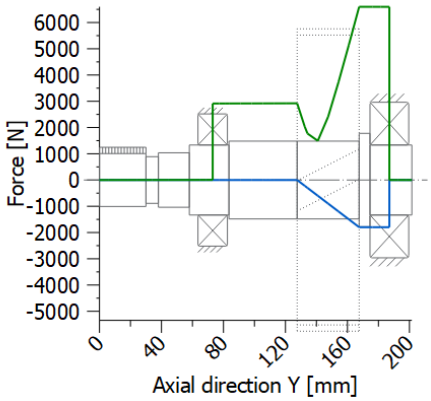

Figure 5.16: Force diagram of shaft C [58]

Forces

In the table 5.4 the applied forces and moments, generated by the cylindrical gear pairs are presented, according to the coordinate system from figure 5.4 and to the KISSsoft designation.

Table 5.4: Gear forces and moments [58]

	Z1	Z2	Z3	Z4
Axial force (F_a) [N]	-774,1	774,1	-1797,2	1797,4
Shearing force X (F_x) [N]	-2529,7	2529,6	-6542,3	5976,5
Shearing force Z (F_z) [N]	2949,9	-2949,7	-6211,8	6758,9
Bending moment X (M_x) [Nm]	5,1	20,1	-24,9	-59,7
Bending moment Z (M_z) [Nm]	-14,0	-55,1	-53,5	-164,1

5.4.2 Applied stresses (static and fatigue)

Despite all software and computational power, it would still be excessively time-consuming to evaluate shaft stresses at every point. Thus, a correct knowledge of the shaft critical locations is key to achieve a proper stress analysis. Through bending and torsion moment diagrams, some critical sections are significant which have to be considered. Generally, the axial stresses, from helical gears, are neglected since their magnitude is small compared to bending moment stresses.

Regarding stress analysis for fatigue, stress concentrations play a major role. They are mainly present at shaft shoulders and keyways, and are dependent on size specifications [53]. Shaft shoulders need appropriate fillets or undercuts to relieve a possible stress concentration point. Shaft bottomed grooves for retaining rings, if not correctly designed can also present a critical stress concentration. Keyways are near a critical section, where the gear (load-carrying component) is located, so they usually present a crucial zone.

In the table 5.5 a summary of the minimum static and fatigue results are presented, and in table 5.6 the corresponding shaft stressed zones. The following results are according to the strength calculation of the standard DIN 743 [87] using the software KISSsoft capacity.

Table 5.5: Summary of the static and fatigue analysis

	Minimum static safety		Minimum fatigue safety	
Shaft	Maximum torque	Maximum speed	Maximum torque	Maximum speed
A	3,02	12,41	4,15	17,04
B	10,96	44,89	5,59	22,82
C	1,58	6,48	1,71	7,02

5.4.3 Deflection

Deflection analysis is particular important in gears, in order to have a correct meshing contact when the transmission is continuously operating. The correspondent dynamic loads can lead to an excessive shaft deflection, resulting in an incorrect meshing from the pinion and gear, producing noise and incompatible transmission errors, from the uneven distribution of load over the face width.

Shaft deflection, also requires attention concerning bearings, since a significant misalignment can lead to excessive wear of bearing surfaces, resulting in premature failure.

The maximum permissible deflection for the transmission shaft is conventionally taken as [88]:

$$\delta = (0{,}001)\, L \quad to \quad (0{,}003)\, L \tag{5.3}$$

Table 5.6: Stressed zones in the shafts

Shaft	Min. static safety	Min. fatigue safety	Figure
A	Shoulder	Shoulder	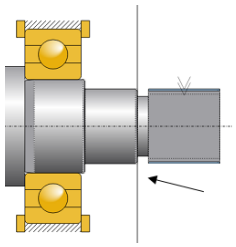
B	Smooth shaft	Keyway	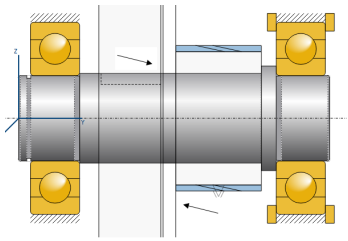
C	Shoulder	Shoulder	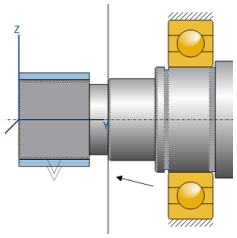

being L the length between the two supporting bearings. The allowable deflection at the gear depends on a large number of factors. Despite that, the usually followed requirement is [88]:

$$\delta = (0{,}01)\, m_n \tag{5.4}$$

where m_n represents the gear normal module.

In the next tables (5.7 and 5.8) the calculated and the allowable deflections (regarding the worst case scenario) are presented.

Table 5.7: Deflection analysis for the transmission shafts

Shaft	L [mm]	Allowable deflection [µm]	Maximum deflection [µm]	
			Maximum torque	Maximum speed
A	180	180	13,76	8,06
B	115	115	10,66	7,51
C	114	114	9,21	8,07

From table 5.8, the maximum deflection of the shaft does not present a problem when the transmission is operating at maximum speed. However, when at maximum torque, the deflection at the meshing zone of gears Z1 and Z2, exceeds the allowable deflection defined by the previous requirement (see equation 5.4), nevertheless the deflection is still quite small compared to the gear teeth dimensions. Several alternatives were studied to overcome this problem, such as, increase the number of supports, reduce the span length,

Table 5.8: Deflection analysis at meshing zones

Gear	Module [mm]	Allowable deflection [µm]	Maximum deflection [µm]	
			Maximum torque	Maximum speed
Z1	0,8	8	**12,9**	7,8
Z2	0,8	8	**9,5**	7,2
Z3	1,25	12,5	10,4	7,4
Z4	1,25	12,5	8,8	7,3

select a different rolling bearing. However, none of these solutions presented a proper resolution since it is rather challenging to achieve such a small shaft deflection.

Therefore, a practical solution is followed, which is based in performing micro geometry tweaks at the gear teeth, with the intention of accounting for the shaft deflections and manufacturing tolerances. The gear micro geometry modifications, increasingly used in the industry, are presented in the next chapter.

5.4.4 Critical speed

When a rotating shaft is dynamically unstable and vibrates intensely, it is at a critical speed. This speed corresponds to a resonance condition, where the rotational speed is equal to the natural frequency of vibration of the shaft. At these speeds, noise generation problems and serious structural problems may occur, from the considerable deflections which are unsuited for correct operation.

The shaft's flexural rigidity property EI is directly related to the deflection caused by centrifugal force from the eccentricity of a turning shaft. The eccentricity is present since the centre of mass of the transmission shaft does not coincide with the centre of rotation.

If a shaft goes through the critical speed condition briefly, it does not become a problem. In some industrial applications, the rotating shaft works at speeds higher than the corresponding critical speed, as long as it is continuously operating at these greater speeds. In automotive transmissions, it is not a good solution, since the rotational speed of the shaft is changing constantly, thereby it could possible work at critical speed for an excessive period of time.

As indicated in table 5.9, all shaft critical speeds are considerable higher than the maximum operating shaft speed ensuring a proper functioning of the transmission.

Table 5.9: Shaft critical speeds

Shaft	Eigenfrequency [Hz]	Critical speed [rpm]	Shaft speed (max.) [rpm]
A	4714	282 820	14 000
B	5020	301 231	3557
C	3633	217 969	1201

Chapter 6

Gear modification sizing

The final, but increasingly important, stage when designing a gear pair is to specify the flank line and profile modification. This micro geometry assessment has several optimization objectives, such as, reducing noise, increasing service life and efficiency.

A step by step approach is performed in the next sections, this approach is best suited for a simple analysis, compared to the Loaded Tooth Contact Analysis (LCTA), which is very complex. The major contributions of these modifications will be assessed. Firstly, the theoretical flank line modifications to even the load distribution through the face width, then, crowning to compensate the manufacturing tolerances, and finally, profile modification to reduce transmission error and, consequently, noise.

Noise from internal combustion engine is no longer present, so the contribution of transmission noise to overall vehicle noise becomes dominant, thereby rendering it as a very important factor in the electric vehicle industry.

The theoretical flank modifications, the crowning to compensate tolerances and the profile modifications will be addressed for the first stage cylindrical gear pair, and considering maximum torque operation. The second stage cylindrical gear pair was reviewed but, since it did not require major modifications it was left as before.

6.1 Theoretical flank modifications

Considering the face load factor without manufacturing allowances, according to ISO 6336-1, Annex E [61], in KISSsoft, it is possible to take into consideration the previous shafts and their calculations, in order to get a favourable flank line modification and achieve a uniform load distribution, offsetting the previously calculated significant shaft deflection.

Following KISSsoft proposition for tooth trace modifications, with exact sizing according to ISO 6336-1 Annex E: Centric crowning + helix angle modification, the following values ensue:

Table 6.1: Proposed tooth trace modifications

Modification	Pinion (Z1)	Gear (Z2)
Crowning (C_{β}) [µm]	0,4297	0,4297
Helix angle modification ($C_{H\beta}$) [µm]	-1,509	-1,509

In figure 6.1, there is a representation of crowning and helix angle modifications.

The load distribution is more uniform after applying the tooth modifications, likewise the highest load before modifications is 210 N/mm and decreases to 186 N/mm, as can be seen in figure 6.2.

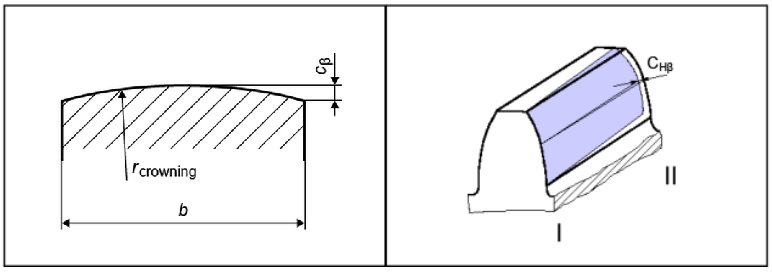

Figure 6.1: Crowning (left) and helix angle modification (right) [58]

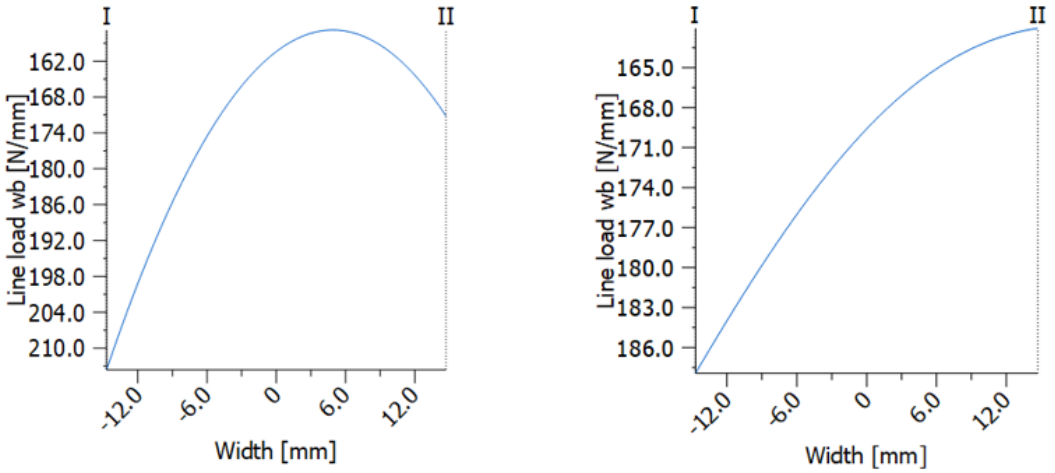

a) Before modifications

b) After modifications

Figure 6.2: Load distribution over face width, before and after modifications [58]

The face load factor $K_{H\beta}$ changes are presented in table 6.2:

Table 6.2: Face load factor $K_{H\beta}$

	Default	Without manufacturing allowances	Without manufacturing allowances (after modifications)
$K_{H\beta}$	1,2673	1,2454	1,0957

6.2 Crowning to compensate tolerances

Manufacturing tolerances that have an impact on the load distribution (according to ISO 6336) are $f_{H\beta}$ for the lead variation of the gears, and f_{ma} for the axis misalignment

in the contact plane.

In the annex E of ISO 6336-1, the factor $K_{H\beta}$ has to estimated five times, with respect to the different possible combinations: without tolerance and with the positive and negative combinations of $f_{H\beta}$ and f_{ma}. The highest $K_{H\beta}$ value estimated is employed in the load capacity calculations, constituting the worst-case scenario.

The crowning value for the gear is kept the same as the one presented in table 6.1, while the pinion crowning value is iterated. The initial crowning value that is considered, if no previous information is available, is equal to the suggested $f_{H\beta}$. After providing both gears teeth with the crowning modifications, and regarding the manufacturing tolerances, the load distribution over the face width is aggravated, and it is not so uniformly distributed as before. The final goal is to completely prevent edge contact in all the possible combinations. A trade-off between the several combinations, considering several crowning values, is seen as the aim of this gear modification, where the end result is an acceptable balance between the ultimate $K_{H\beta}$ values.

In figures 6.3 and 6.4 the load distribution results over the face width are presented. The light blue line (f_{ma} = 0 µm and $\sum f_{H\beta}$ = -8,8 µm), the strong blue line (f_{ma} = 0 µm and $\sum f_{H\beta}$ = 0 µm), and the green line (f_{ma} = 0 µm and $\sum f_{H\beta}$ = 8,8 µm)

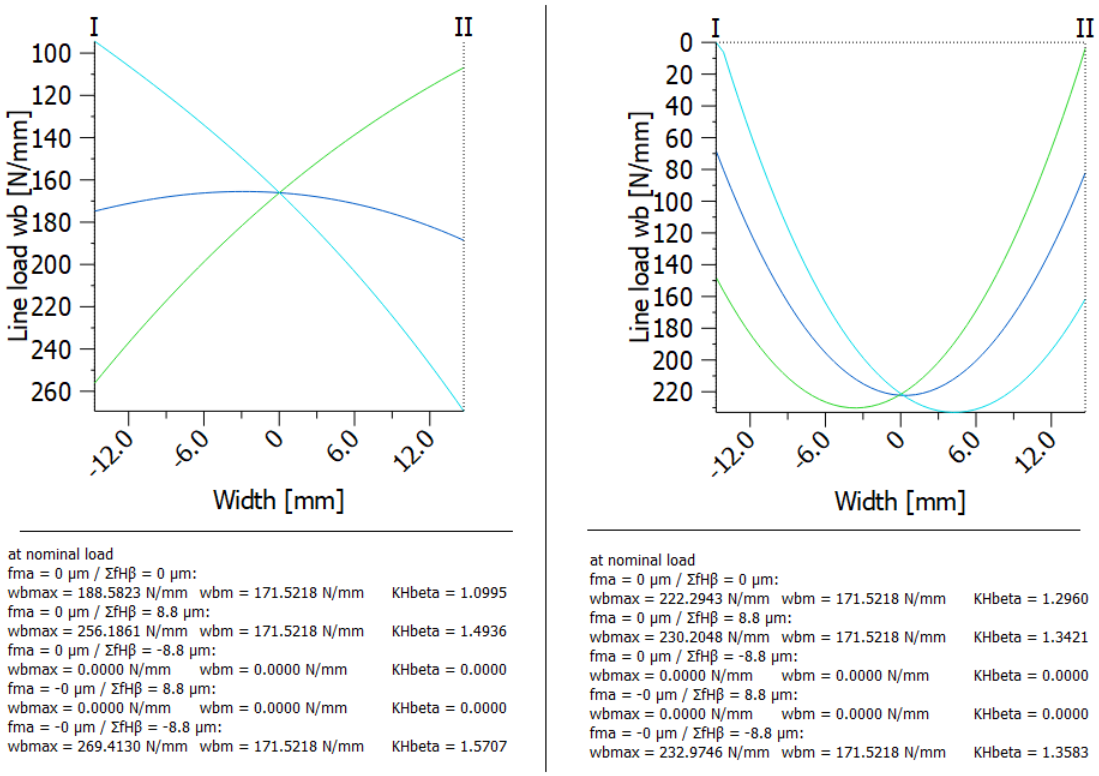

a) Previous

b) Proposed

Figure 6.3: Load distribution over face width considering manufacturing allowances with previous modifications (left) and proposed (right) [58]

From the figures 6.3 and 6.4, it can be concluded that the final version does not have any edge contact and the load distribution is more uniform across the three possible deviations, ensuring a better preventive behaviour.

In table 6.3, is presented a summary of the previous, proposed and final values for crowning and face load factor.

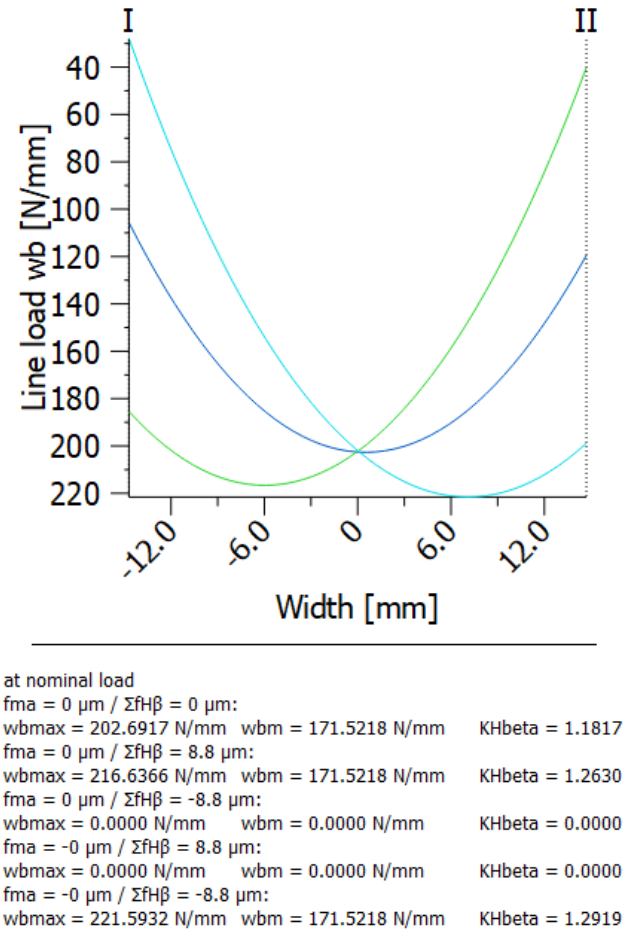

Figure 6.4: Load distribution over face width considering manufacturing allowances with the final modifications [58]

Table 6.3: Crowning modification and resultant highest face load factor $K_{H\beta}$

Parameter	Previous	Proposed	Final
Crowning [µm]	0,4297	9	6
$K_{H\beta}$ (highest)	1,5707	1,3583	1,2919

It is important to note that the previous face load factor, $K_{H\beta}$, with a value of 1,0957 without considering manufacturing allowances has significantly increased (to 1,5707) just by taking these allowances into consideration.The final value derived for the face load factor is 1,2919.

6.3 Profile modifications

The final step is to specify the profile modifications. They play a major role in gear losses, noise propagation, wear, among other conditions that require improvement depending on the final product specifications. For electric vehicle transmissions, peak-to-peak transmission error (PPTE) is a very important parameter since it is directly related with noise output.

Proposed values from KISSsoft for tip relief, with a long profile modification (arc-like), which are best suited for applications where noise is a determinant factor, are presented in table 6.4.

Table 6.4: Initial proposed values for tip relief

Parameter	Pinion (Z1)	Gear (Z2)
Tip relief ($C_{\alpha a}$) [µm]	3	3
Length factor (L_{Ca*})	1,1466	1,3386

In figure 6.5, there is a representation of the tip relief ($C_{\alpha a}$) and roll length of the tip relief (L_{Ca}). The length factor (L_{Ca*}) defines the length of the linear tip relief (L_{Ca}/m_n).

Figure 6.5: Arc-like profile modification [58].

A step analysis was performed in the KISSsoft software, where the minimum and maximum values for the specified parameters are presented in table 6.5.

Table 6.5: Tip relief minimum and maximum values for step analysis

Parameter	Minimum	Maximum
$C_{\alpha a}$ [µm]	1	3
L_{Ca*}	1	1,75

The results of the step analysis are presented in the next four figures, with two XY charts and two radar charts. The contact analysis which is carried out by the software is very time-consuming and the number of solutions considerably increases with the number of steps. Therefore, a simple analysis of the results and the factors influence will be performed. In a further design phase, the best solutions regarding the required parameters can be gather and later closely examined.

In figures 6.6 and 6.7, the horizontal axis represents the profile tip ($C_{\alpha a}$) value, and in the vertical axis is presented the peak-to-peak transmission error (PPTE) and efficiency (η), respectively. The color bar denotes the length factor (L_{Ca*}). The influence of tip

relief is clear, when it increases, the PPTE increases (which is unfavourable) along with the efficiency (which is positive). The length factor impact is not so sound, but it can be concluded that a higher value entails a higher PPTE as well as a better efficiency.

With a increase in PPTE there is an increase in noise generation, but also in efficiency, which also plays a major role in electric vehicle transmissions. Thus, it is perceptible that a trade-off between the noise suppression and efficiency requirements is necessary to consider the best proposed solution.

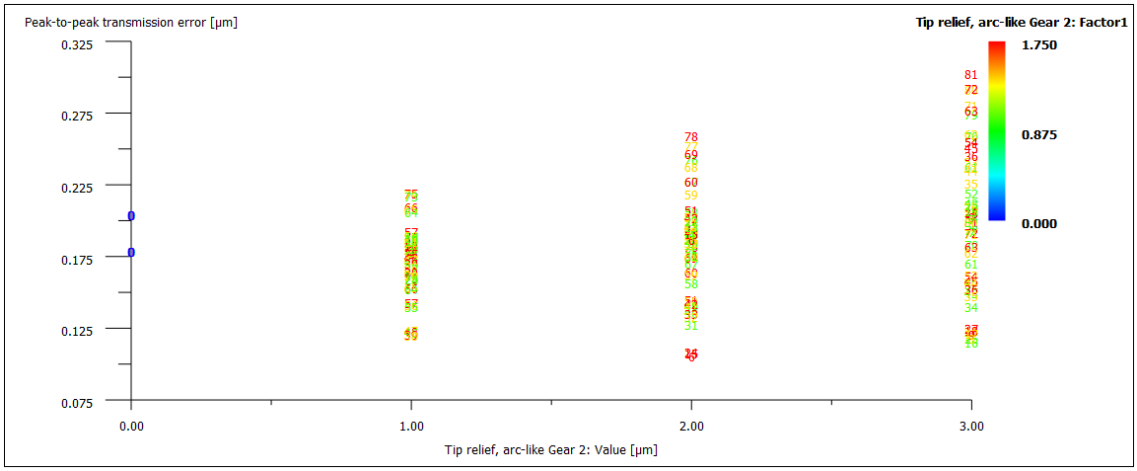

Figure 6.6: Peak-to-peak transmission error [58]

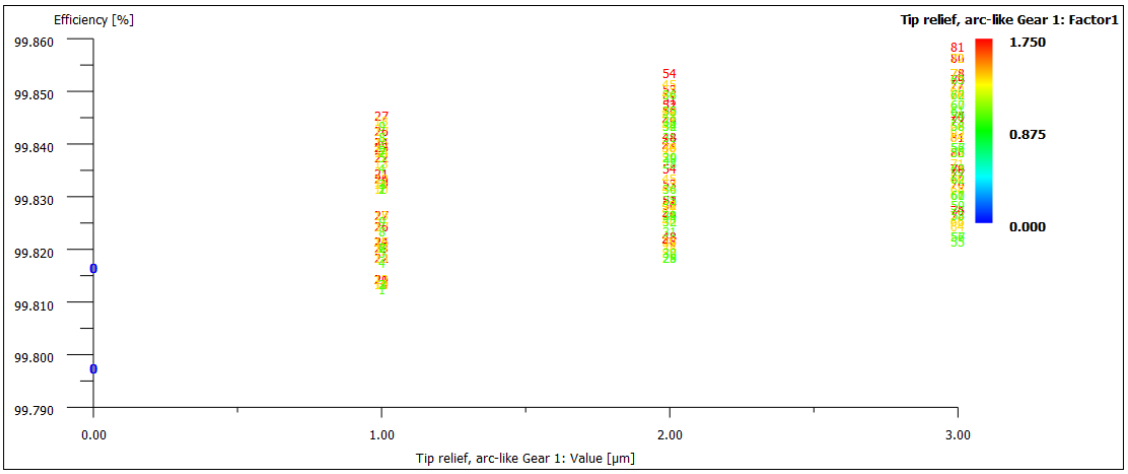

Figure 6.7: Efficiency [58]

Figures 6.8 and 6.9 present radar charts provided by KISSsoft, for the PPTE and efficiency, respectively. The red line represents the gear pair at 100 % load and the blue line at 80 % load. Both the efficiency and PPTE increase when the load decreases.

Table 6.6 presents a summary of the PPTE and efficiency values for 3 situations: the initial without any modifications, the modified gear with the modifications stated in the previous sections (C_{β} and $C_{H\beta}$) and, the final which has the proposed modifications (table 6.4). There is an approximate three times reduction of the PPTE from the initial to the final derived gear, and there is no great effect in efficiency, increasing only 0,03 %.

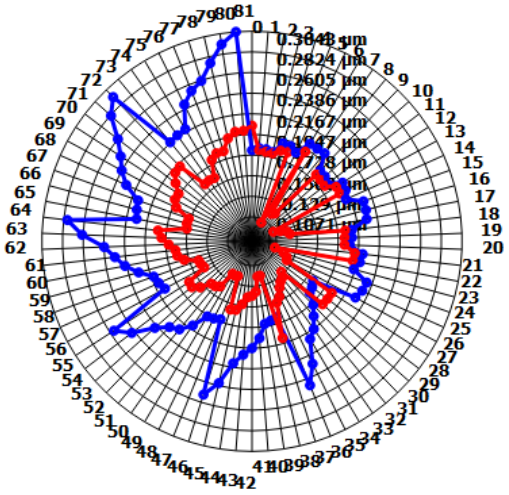

Figure 6.8: Peak-to-peak transmission error, radar chart with 100 % load (red) and 80 % load (blue) [58]

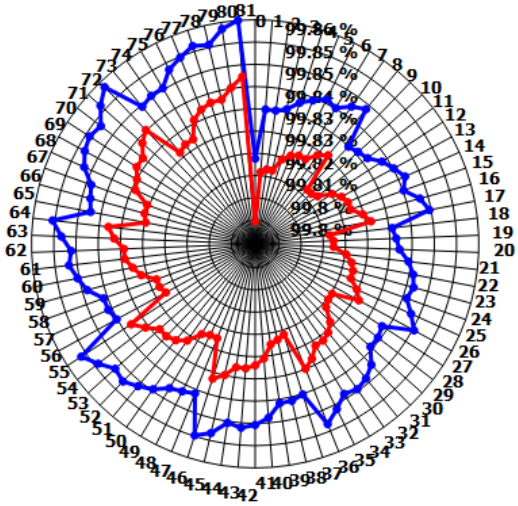

Figure 6.9: Efficiency, radar chart with 100 % load (red) and 80 % load (blue) [58]

Table 6.6: Summary of concluding values for the considered solutions

		PPTE [µm]	η [%]
First stage (Z1/Z2)	Initial	0,3352	99,77
	Modified	0,1217	99,77
	Final	0,1143	99,80
Second stage (Z3/Z4)		0,1619	99,38

Chapter 7

Lubrication and Sealing

A tribological system is composed by a base body (e.g. rolling element), a mating body (e.g. bearing ring) and an intermediary medium (e.g. a lubricating oil). The lubricant oil has to keep the base body apart from the mating body, under all considerable loads, to avoid excessive wear in the respective components which can lead to their early failure. There are three major lubricant regimes according to the Stribeck curve, as presented in figure 7.1, dry friction, mixed friction and hydrodynamic friction. Meshing gears preferably work in between mixed and hydrodynamics friction regimes (figure 7.2), also referred as an elastohydrodynamic lubrication regime (EHL), which is also preferred for other friction parts where elastic deflection of the contact surfaces is considered, such as ball bearings [35].

Nowadays, the automotive transmissions lubricant is not changed during the transmission lifetime. This requires a good knowledge of the applied loads, speed and the respective operating temperatures inside the transmission, so that a correct fluid can be selected, which would not cause components to wear quicker than expected.

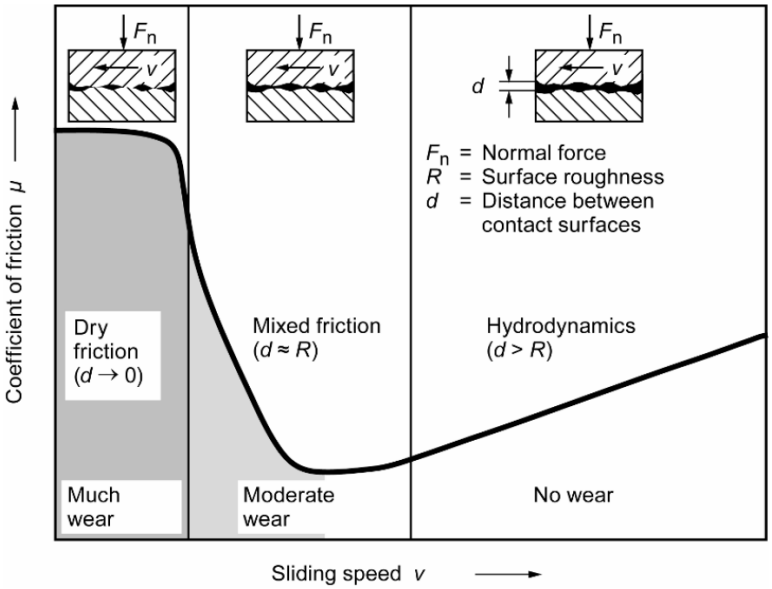

Figure 7.1: Relation between coefficient of friction and sliding speed (Stribeck curve) [35]

Vehicle transmissions are lubricated by oil. Solid lubricants (e.g. greases), generally, cannot withstand the acting forces and, since they are not a fluid media, the necessary

hydrodynamic film between the mating components is much more difficult to achieve and maintain during the long operating period. Another advantage of an oil lubricated transmission, is that the associated oil circulation sets an environment, where components which withstand higher loads can dissipate heat [35].

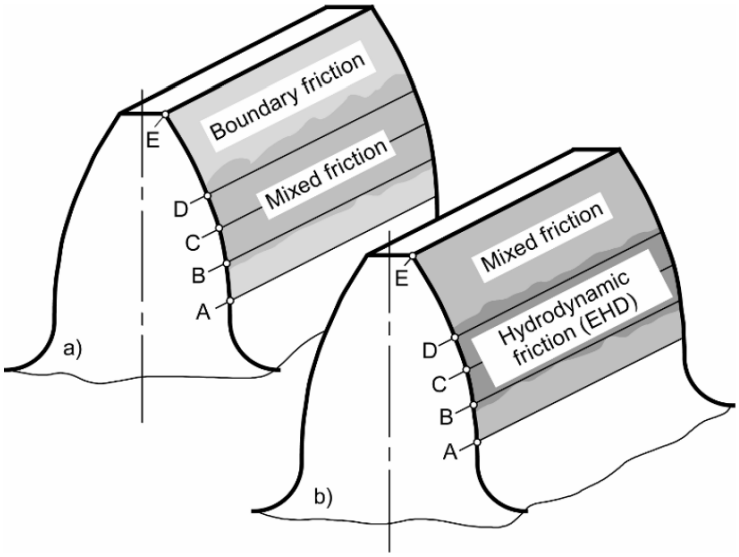

Figure 7.2: Typical friction zones on tooth flanks at high contact pressures. a) Low circumferential speed (up to 5 m/s); b) high circumferential speed. A - first point of contact; B - internal single contact point; C - pitch point; D - external single contact point; E - last point of contact [35]

7.1 Lubricant selection

The main influence parameter in transmission oil is the oil viscosity. Viscosity is regarded as the oil resistance to flow and shear and defines its internal friction. With an increase in viscosity, scuffing and pitting resistance increases, as well as damping capacity. In contrast, load-dependant losses generally decrease [35]. One has to keep in mind that problems can arise when oil viscosity is excessively high for a given operation, such as temperature outside of the defined range. This increase is directly related with the friction losses which are intensified along with oil viscosity.

Fluids with a lower viscosity are preferred, since they promote a greater cooling capacity due to the overall lower transmission temperature. Clearly, the lubricant selection is not precise but rather a trade-off between thermal efficiency and the necessary operational requirements.

In a high speed transmission, the oil must cope with the high sliding velocities and respective shearing, throughout the vehicle life [50].

A great number of constituents, in an oil base, is present in modern lubricants. A range of additives is used to improve performance in distinct conditions, and prevent common issues. Some examples of these additives are:

- EP (Extreme Pressure) additives which improve high-pressure functionality;
- VI (Viscosity Index) improver to enhance performance at high and low temperatures;

- Corrosion inhibitors which prevent oxidation related problems, such as rust and verdigris;

- Friction modifiers to reduce friction and, as a consequence, wear.

In manual transmissions, the oil used is denominated gear oil. This gear oil has higher viscosity than the automatic transmission fluid used in automatic transmissions and also currently employed in electric vehicle transmissions.

After consulting different oil manufacturer's catalogues, regarding viscosity specifications, additives and operating temperatures, the chosen transmission fluid is ATF DEX II Multivehicle, provided by the group Castrol which has a mineral oil base and the necessary additives. Specifications of the above mentioned oil are presented in appendix B.

7.2 Lubrication method

Generally, when correctly operating, the oil temperature in the oil bath inside the transmissions is between 60 – 90 °C.

Automotive transmissions, which are considered as a medium speed application, use splash lubrication as the conventional method to lubricate the gear teeth and bearings inside the housing [89]. This method will be implemented in the designed transmission. Compared to the oil spray method, it is clearly more economic because there is no need for extra components to direct and pump the oil to the specified locations. However, when operating at very high speeds, churning losses caused by the oil bath of the splash lubrication method, gear teeth pumping effect and aimless oil projection onto the housing walls may lead to thermal issues and a rise in bulk temperatures [90].

The great centrifugal force at place makes it challenging to manage the oil path and provide adequate quantities at specific locations. Mechanisms, such as, oil traps or feed ducts, sometimes have to be designed in the transmission housing so that the necessary oil reaches rolling bearings and other oil lubricated components. Although, quite often, the oil spray from the gearwheels is sufficient to meet the required demands [50].

The overall efficiency of the gear transmissions is very important in electric vehicles. To achieve a good performance, power losses have to be managed. Limiting the power loss related to oil churning is a good starting point. A correct oil volume inside the transmission is key to have the desired efficiency. Oil temperature changes with different oil levels, more specifically, for the same operating loads, if the oil level is decreased the global oil temperature increases [35, 89].

Sometimes, it is not desired, or even possible, to lower the oil level to the necessary height to effectively reduce churning losses, because of the increase in temperature which may be prohibitive. Thus, an alternative solution is carried out. It consists in using axial flanges or plates (figure 7.3) as obstacles to modify the oil flow inside the housing.

According to [90], if the axial clearance (Ja) between the flange and the gear is reduced, the churning losses decrease in accordance (see figure 7.4). This is owed to the reduction of the suction effect by the gear teeth. In order to obtain this outcome, the flange has to cover entirely the lateral surface of the pinion and respective gear. In [63] two important characteristics of this method were assessed: similar results are obtained for spur and helical gears, moreover, the use of two flanges, one on each side of the gear is much more effective in reducing losses that if using only one.

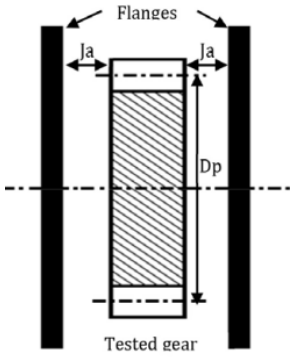

Figure 7.3: Flanges position relative to the gear [89]

From figure 7.4 it can also be assessed that the use of radial deflectors along the gear teeth (see figure 7.5) does not contribute to reduce churning losses, so the deflectors will not be considered.

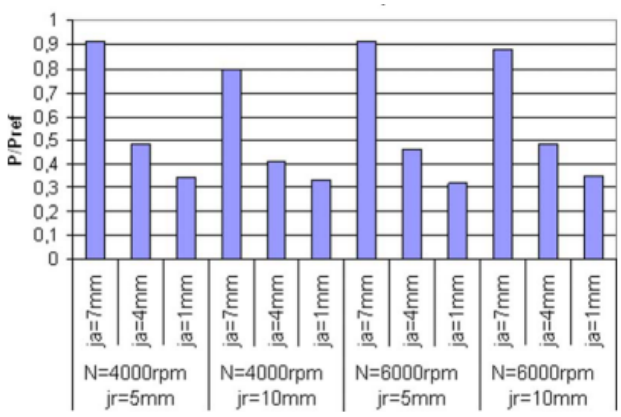

Figure 7.4: Influence of axial and radial clearances on churning losses (jr is the distance between the deflector and the tooth tip) [90]

The first stage of the transmission, particularly at high speed, causes considerable churning losses. Due to the substantially different speeds between the first and second stage, the flanges are only going to be applied in the first stage, where they produce a greater impact. A criteria (Γ) (eq. 7.1) relating two dimensionless parameters, Froude number (Fr) (eq. 7.2) and Taylor number (Ta) (eq. 7.3), is proposed in [63] to evaluate the flange axial distance to the gear (defined by Ja). If Γ is greater than 10, the flanges attain their maximum yield potential. To guarantee that the flanges are effective both on road (medium speed) and highway (high speed) conditions, a calculation of the Γ parameter is done for a transmission input speed of 3500 and 14 000 rpm, respectively. It is important to clarify, that it is the gear Z2, of the first stage, which is partially immersed in the oil bath, and not the pinion Z1 (see figure 7.6). Thus, the calculation parameters from table 7.1 will follow the gear Z2 specifications.

$$\Gamma = \frac{Fr}{Ta} \tag{7.1}$$

$$Fr = \frac{w^2 {R_p}^2}{gh} \tag{7.2}$$

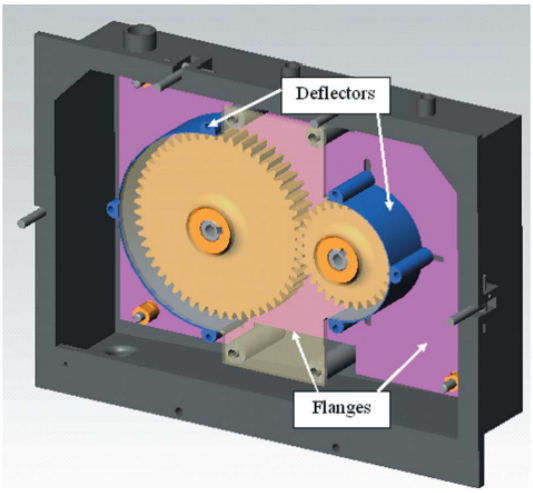

Figure 7.5: Housing layout with flange and deflectors [90]

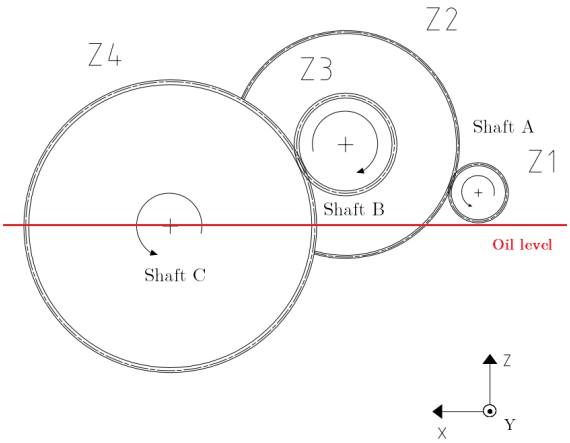

Figure 7.6: Transmission arrangement with the defined oil level

$$Ta = \frac{wJa^2}{\nu} \tag{7.3}$$

Table 7.1: Parameters necessary for the calculation of Γ

Pinion input speed (Z1) [rpm]	3500	14 000
Gearwheel speed (Z2) [rpm]	889,23	3556,83
Rotational speed (ω) [rad/s]	93,12	372,47
Pitch radius (R_p) [mm]	75,755	
Gravitational acceleration (g) [m s^{-2}]	9,81	
Submerged height (h) [mm]	21,7	
Oil kinematic viscosity (ν) [mm^2/s]	25,9 (@65 °C)	20,6 (@75 °C)

The Ja parameter represents the axial distance between the flanges and the gear and is the variable which must be iterated until the expected outcome is found.

Concluding results are in table 7.2, where a Ja value of 2 mm was selected, since it the value in agreement with the stipulated specifications. A value of 3 mm for the axial clearance would result in a Γ value smaller than 10 (for the road condition), consequently, the flanges would not operate at their maximum potential.

Table 7.2: Calculations results for Γ parameter

Input speed [rpm]	3500	14 000
Gearwheel speed (Z2) [rpm]	889,23	3556,83
Froude number (Fr)	233,76	3739,99
Taylor number (Ta)	14,38	72,32
Γ	16	52

7.3 Sealing

The reducer is not completely sealed, because of the input and an output shaft extension outside of the transmission, where the spline coupling is going to be done. Thus, there is a requirement for radial shaft seals in shaft A and C, to retain the oil inside the transmission.

The seal forms a barrier between the outside environment and the oil inside the transmission. In order to achieve maximum service life, a proper sealing solution is required to retain the lubricant and exclude contaminants.

For oil applications, SKF rotary shaft seals feature a wave lip, molded in a sinusoidal wave pattern onto a case with a metal outside diameter. A robust sealing system has a higher pump rate. SKF Wave seal has a better performance pumping the oil to the oil side (figure 7.7). Seals with a significant pump rate suppress undetectable flaws of the sealing system and reduce impacts of unmanageable operating parameters.

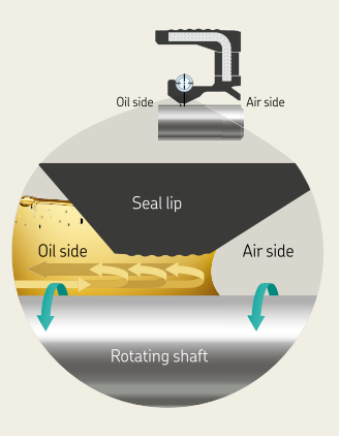

Figure 7.7: Pumping effect by the SKF Wave seal [91]

The major advantages of the SKF Wave seal [91] are:

- Two times more pump rate than standard seals;
- Handles shaft misalignment;
- Runs cooler with less drag;
- Reduces shaft wear;

- Reduces energy consumption.

Operating temperatures are an important factor when working with seals. The sealing efficiency decreases at low temperatures since the seals are more rigid and therefore, predisposed to damages. At higher temperatures, if there is insufficient lubrication, premature seal failure can also occur [91].

Acrylonitrile-butadiene rubber (nitrile rubber) (NBR) or Fluorocarbon rubber (FPM) are the available materials for the sealing solution required (table 7.3). Since the temperature should never exceed 100 °C, the preferred material is the NBR. If required, the FPM material could be used for operating temperatures up to 200 °C.

Table 7.3: Operating temperature of seal materials [91]

Material	Abbreviation	Operating temperature [°C]
Nitrile Rubber	NBR	-40 to 100
Fluorocarbon Rubber	FPM	-20 to 200

A further consideration must be that the seal operates properly at the maximum input speed. The seal has a limiting working speed, which is determined by its design and lip material, as well as shaft condition. It also has to be consider that no pressure differential across the seal is present and normal operation is followed.

In [91], a formulation is provided to access the circumferential speed (see equation 7.4.)

$$CS = \frac{shaft\ diameter\ (\text{mm}) \times shaft\ rotational\ speed\ (\text{rpm})}{19\,100}\ (\text{m/s}) \tag{7.4}$$

which for the most critical case, with 14 000 rpm in the input shaft, and for a shaft diameter of 20 mm, the result is 14,66 m/s.

Based on that, the chosen seals for the input shaft and output shaft are presented in the next tables (7.4 and 7.5). In the appendix F information from the SKF catalogue regarding the selected seals is provided.

Table 7.4: Input shaft radial seal characteristics

Parameter	Value
Designation	20x30x7 CRW1 R
Lip material	NBR
Operating temperature (max.) [°C]	100
Operating temperature, short period (max.) [°C]	120
Rotational speed (max.) [rpm]	17189
Shaft surface speed (max.) [m/s]	18

Table 7.5: Output shaft radial seal characteristics

Parameter	Value
Designation	35x47x7 CRW1 R
Lip material	NBR
Operating temperature (max.) [°C]	100
Operating temperature, short period (max.) [°C]	120
Rotational speed (max.) [rpm]	9822
Shaft surface speed (max.) [m/s]	18

Chapter 8

Thermal analysis

In the following chapter, a thermal analysis regarding power losses and heat dissipation is performed. Power losses in electric vehicle transmission are determinant, since they are directly related to the overall efficiency, a major feature and requirement in the industry. Heat dissipation, specially when components are immersed in oil bath, is determinant, so that the bulk temperature does not rise to incompatible values and leads to catastrophic damage in components and, subsequently, in the transmission itself.

8.1 Power losses

Power losses in a transmission are split in gears, bearings, seals and auxiliary losses (figure 8.1). Those losses can be divided in load and no-load losses. Housing design, operating conditions, lubricant density and viscosity, all play a role in no-load losses. When the splash (oil bath) lubrication method is employed, there is immersion of components in the transmission, which leads to greater losses. Parameters that have an impact on load losses are related to the contacting areas and are, for example, sliding velocity, friction coefficient and transmitted load [92].

The load losses of the gear meshes prevail over other losses at moderate load and medium speed. When working at high speeds and minimum loads, the no-load losses are dominant.

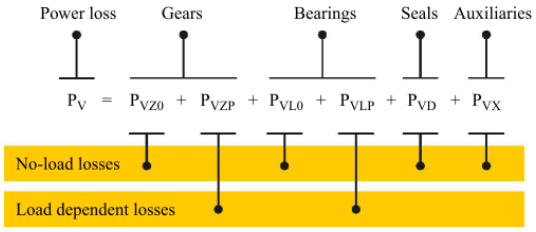

Figure 8.1: Composition of transmission power loss [92]

Special attention is going to be given to churning losses, since they are considerable in the splash lubricant method.

The no-load gear loss provided in the technical report ISO/TR 14179-2 [93] only takes into consideration the immersion depth and tooth width of the cylindrical gear pair, resulting in a basic calculation, which is not very objective. Thus, a model proposed in recent years that considers a large number of variables and with positive results across

a wide range of parameters (e.g. gear module, speed, lubricant viscosity), is going to be used in the ensuing churning loss assessment [63, 94, 95].

The churning torque (C_{ch}) is calculated according to:

$$C_{ch} = \frac{\rho\,\omega^2 S_m {R_p}^3\, C_m}{2} \tag{8.1}$$

where,

- ρ - oil density;
- ω - gear angular velocity;
- S_{m} - gear submerged surface;
- R_{p} - gear pitch radius;
- C_{m} - dimensionless parameter.

The immersed surface of the gear, S_{m} is split into the wet surface of the gear flank, S_{mf} and the wet surface of the teeth, S_{md}. Figure 8.2 presents how the angle θ is obtained for the calculations.

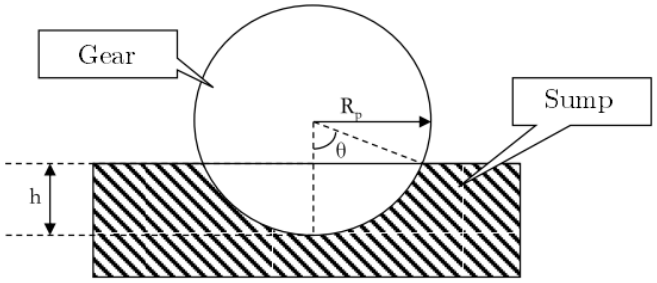

Figure 8.2: Partially submerged gear in oil bath

$$S_{mf} = {R_p}^2\,(2\theta - \sin(2\theta)) \tag{8.2}$$

Considering helical gears, S_{md} is calculated according to:

$$S_{md} = D_p b\theta + \frac{2bZ\theta H_t}{\pi \cos\alpha \cos\beta} \tag{8.3}$$

where,

- $\mathrm{D_p}$ - gear pitch diameter;
- b - gear face width;
- Z - number of gear teeth;
- H_{t} - tooth height;
- α_{n} - pressure angle;
- β - helix angle.

The dimensionless parameter, C_{m}, is dependant on the flow regime. Four regimes are proposed by [94] and two parameters (γ and Re_{c}) are necessary to adopt the correct regime.

The centrifugal acceleration, γ, is given by:

$$\gamma = \omega^2 (R_p b m_n)^{1/3} \tag{8.4}$$

where m_n is the gear normal module.

The critical Reynolds number, Re_c, is calculated according to:

$$Re_c = \frac{wbR_p}{\nu} \tag{8.5}$$

where ν is the oil kinematic viscosity.

The selected regime for the calculations, regarding the ensuing evaluations, follows the requirements of $\gamma < 750\ \mathrm{m\,s^{-2}}$ and $Re_c > 4000$ and is given by:

$$C_m = 0{,}1752 \left(\frac{h}{R_p}\right)^{0{,}45} \left(\frac{V_0}{{D_p}^3}\right)^{0{,}1} Fr^{-0{,}6} \left(\frac{b}{R_p}\right)^{0{,}21} \tag{8.6}$$

where h is the oil level defined in figure 8.2, and V_0 is the oil volume inside the housing (see figure 7.6).

In [63], the dimensionless parameter, C_m, for a regime characterized by $\gamma > 1250\ \mathrm{m\,s^{-2}}$ and $Re_c > 4000$, already considers the axial flanges effect on churning losses, therefore, it will be based on it that the churning losses from the first stage, at maximum speed, will be calculated. It is given by the equation:

$$C_m = 0{,}16 \left(\frac{h}{D_p}\right)^{-0{,}13} \left(\frac{V_0}{{D_p}^3}\right)^{-0{,}35} Fr^{-0{,}68} \left(\frac{b}{D_p}\right)^{0{,}85} \left(\frac{H_f}{D_p}\right)^{1{,}8} \left(\frac{Ja}{b}\right)^{0{,}26(D_p/H_f)} \tag{8.7}$$

where H_f is the flange height with a value of 190 mm, and Ja is the flange axial displacement that is 2 mm, as previously calculated.

The Froude number, Fr, is obtained according to:

$$Fr = \frac{w^2 R_p}{g} \tag{8.8}$$

Tables 8.1 and 8.2 have the required calculation parameters and the respective values.

Table 8.1: General calculation parameters

	1st stage	2nd stage
b [mm]	30	40
D_p [mm]	151,509	194,356
g [$\mathrm{m\,s^{-2}}$]	9,81	
h [mm]	21,7	97,2
H_t [mm]	2,049	3,265
m_n [mm]	0,8	1,25
R_p [mm]	75,755	97,178
V_0 [$\mathrm{m^3}$]	0,001	0,002
Z	185	151
α_n [°]	20	
β [°]	12	
θ [rad]	0,776	1,571
ρ [$\mathrm{kg\,m^{-3}}$]	870	

In table 8.3, a summary of the calculation results is presented, where the resultant churning torque, C_{ch} is derived.

Table 8.2: Calculations parameters that change with load

	Maximum torque		Maximum speed	
	1st stage	2nd stage	1st stage	2nd stage
ν [m^2/s]	0,0000285		0,0000180	
ω [rad/s]	93,12	31,45	372,47	125,80
n [rpm]	889,2	300,3	3556,8	1201,3

Table 8.3: Summary of calculation results for churning torque

	Maximum torque		Maximum speed	
	1st stage	2nd stage	1st stage	2nd stage
γ [m s^{-2}]	105,834	16,753	1693,26	268,05
Re_c	7425,536	4289,471	47027,13	27166,65
Fr	66,962	9,799	3739,99	156,77
C_m	0,005822	0,032468	0,00026	0,0062
C_{ch} [N m]	0,1223	0,8120	0,08622	2,4612

Since, as stated before, flanges are going to be used to reduce the churning losses, that decrease has to be taken into account.

In [63, 90], two formulations were proposed to account for the flanges contribution to reducing losses, if the flow regime does not follow the requirement $\gamma > 1250$ m s^{-2} and $Re_c > 4000$. The formulations rely only on the value of the critical Reynolds number, Re_c.

For $Re_c < 6000$:

$$\frac{Q}{Q_{ref}} = 2{,}17 \left(\frac{D_p}{H_f}\right)^{3/4} \left(\frac{Ja}{R_p}\right)^{0{,}383(D_p/H_f)} \tag{8.9}$$

For $Re_c > 9000$:

$$\frac{Q}{Q_{ref}} = 0{,}76 \left(\frac{D_p}{H_f}\right)^{0{,}48} \left(\frac{Ja}{\sqrt{m_n b}}\right)^{0{,}548(D_p/H_f)} \tag{8.10}$$

If Re_c is between 6000 and 9000, which is the case ($Re_c \approx 7426$ for the first stage at maximum torque), an interpolation between both formulations is required.

These formulations result in a ratio, Q/Q_{ref}, relating churning losses and reference churning losses.

The final no-load power loss is calculated, multiplying the churning torque with the rotational velocity of the gear wheel of the respective stage. The total no-load power loss is the sum of the losses of each stage, following the equation below.

$$P_{VZ0} = \sum_{i=1}^{stage} C_{ch} \frac{\pi n_i}{30} \tag{8.11}$$

The table 8.4 shows the resulting churning losses based on the previously mentioned calculations.

The value 6,10 of the first stage at maximum torque, present in table 8.4, has already been revised with a Q/Q_{ref} consideration of 53,55 % after interpolation.

Table 8.4: Churning losses for the right wheel transmission

	Maximum torque		Maximum speed	
	1st stage	2nd stage	1st stage	2nd stage
P_{VZ0} [W]	6,10	25,36	32,12	309,61
$\sum$	31,46		341,73	

The radial shaft seal losses (P_{VD}) are not considered, since the corresponding value is negligible compared with the remaining power losses. Rolling bearings power losses (P_{VL}) are the combined no-load and load dependent losses. No auxiliary losses are considered (P_{VX}).

A summary of the overall transmission power losses and the global power efficiency is present in table 8.5.

Table 8.5: Transmission power losses for the right wheel transmission

	Power loss [W]	
	Maximum torque	Maximum speed
First stage gear pair (Z1, Z2) [P_{VZP}]	144	108
Second stage gear pair (Z3, Z4) [P_{VZP}]	160	111
Shaft A rolling bearings [P_{VL}]	44,7	90,1
Shaft B rolling bearings [P_{VL}]	40,1	45,8
Shaft C rolling bearings [P_{VL}]	19,8	15,9
Churning losses [P_{VZ0}]	31,5	341,7
Seal losses [P_{VD}]	disregarded	disregarded
Total [P_{V}]	450,1	712,5
Global transmission efficiency [η]	97,0 %	95,3 %

Considering these results, it is clear that churning losses at maximum speed have a strong impact. Despite the use of flanges to reduce churning losses in the first stage, the significant immersion depth of gear Z4 in the oil bath has considerable churning losses associated.

The immersion depth was a consequence of the relative position of the shafts, which was a requirement to manage the loads for the preferential deep groove rolling bearings. One possible solution to reduce the strong churning losses, at the second stage, is to have two separated oil baths with different oil levels for each stage (figure 8.3).

8.2 Heat dissipation

The power losses calculated in the previous section must be balanced by the heat dissipation provided by the ventilated housing and the oil inside, which must transfer the heat from the contact meshing to the housing. This balance leads to an acceptable temperature in the transmission, resulting in a compliance with the estimated components and oil lifetime, as well as an effective overall performance [50].

According to the technical report ISO/TR 14179-2 [93], the power loss in the transmission must be balanced by the dissipated heat (Q) (equation 8.12), at an

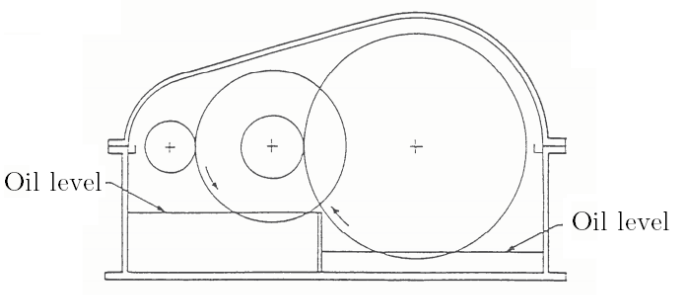

Figure 8.3: Splash lubrication method with two oil levels [64]

equilibrium temperature level (T_{oil}). The total heat dissipation can be divided in four components (equation 8.13): heat dissipation via the housing (Q_{ca}), via the foundation (Q_{fun}), via connected shafts and coupling (Q_{rot}) and, if injection lubrication is used, via the cooling oil flow, (ΔH_{oil}).

$$P_V = Q \tag{8.12}$$

$$Q = Q_{ca} + Q_{fun} + Q_{rot} + \Delta H_{oil} \tag{8.13}$$

There is no foundation in this specific project, so Q_{fun} will not be considered. Q_{rot}, due to the calculation complexity and resulting minimal heat dissipation is not formulated. Finally, since the considered method is splash lubrication, ΔH_{oil} is not regarded, (constant operating temperature).

The heat dissipation comes down to being only through the housing. Therefore, the following calculations are proposed:

$$Q_{ca} = kA_{ca}(T_{oil} - T_{\infty}) \tag{8.14}$$

where k, A_{ca}, T_{oil} and T_{∞} are, respectively: heat transmission coefficient, external housing area, oil temperature and ambient temperature.

In figure 8.4 some of the variables, which will be under discussion, are presented. The housing and fins geometry parameters were adapted from the technical report to the designed transmission.

The heat transmission coefficient (equation 8.15) consist of, respectively: the internal heat transfer between oil and housing, heat conduction through the housing wall and external heat transfer to the environment. The heat conduction through the housing wall is going to be neglected, since it should only be regarded in special cases, such as double-walled housings or housings with sound insulation.

$$\frac{1}{k} = \frac{1}{\alpha_{oil}}\frac{A_{ca}}{A_{oil}} + \frac{\delta_{wall}}{\lambda_{wall}}\frac{A_{ca}}{A_{oil}} + \frac{1}{\alpha_{ca}} \tag{8.15}$$

where α_{ca}, A_{oil} and α_{oil} represent air-side heat transfer coefficient, internal housing area, oil-side heat transfer coefficient, respectively.

The air-side heat transmission coefficient (α_{ca}) is split into a convection part (α_{con}) and a radiation part (α_{rad}).

$$\alpha_{ca} = \alpha_{con} + \alpha_{rad} \tag{8.16}$$

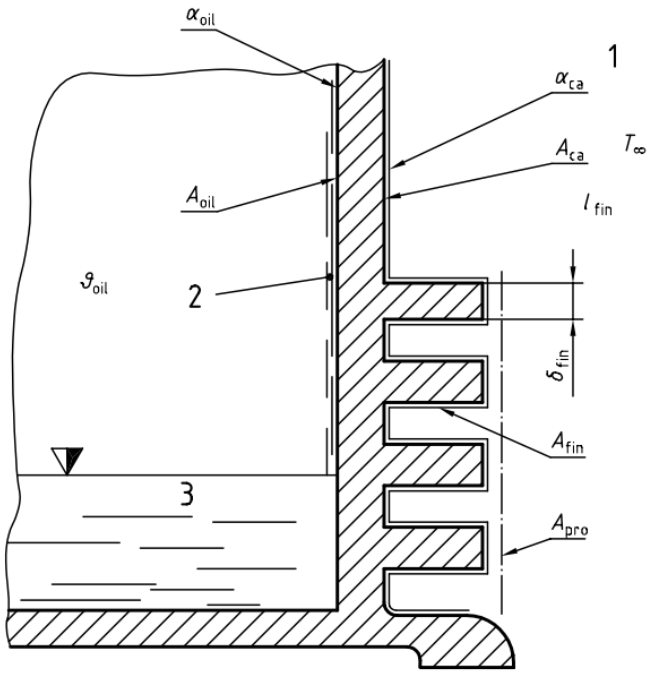

Figure 8.4: Housing with thermal finning (1 – Environment; 2 – Oil film; 3 – Oil sump) [93]

The radiation coefficient can be calculated by:

$$\alpha_{rad} = 0,23 \cdot 10^{-6}\, \epsilon \left(\frac{T_{wall} + T_{\infty}}{2} \right)^3 \tag{8.17}$$

where T_{wall} is the housing wall temperature and ε is the housing emission ratio.

The convection coefficient can be further split into free ($\alpha_{\text{K,free}}$) and forced ($\alpha_{\text{K,forced}}$) convection:

$$\alpha_{con} = \alpha_{K,free} \left(1 - \frac{A_{air}}{A_{ca}} \right) + \alpha_{K,forced} \frac{A_{air}}{A_{ca}} \eta^* \tag{8.18}$$

where A_{air} is the ventilated housing area and η^* follows the equation:

$$\eta^* = \frac{T_{wall} - T_{air}}{T_{wall} - T_{\infty}} \tag{8.19}$$

where T_{air} is the cooling air temperature.

The free convection coefficient (when $v_{\text{air}} < 1{,}5$ m/s) can be calculated from:

$$\alpha_{K,free} = 18 h_{ca}^{-0,1} \left(\frac{T_{wall} - T_{\infty}}{T_{\infty}} \right)^{0,3} \tag{8.20}$$

where h_{ca} is the overall height of the transmission housing.

Regarding forced convection ($v_{\text{air}} > 1{,}5$ m/s):

$$\alpha_{K,forced} = \frac{0,0086 (Re')^{0,64}}{l_x} \tag{8.21}$$

where l_{x} represents the flow length (path of flow filament along along the housing wall) and *Re*' is given by:

$$Re' = \sqrt{Re^2 + \frac{Gr}{2,5}} \tag{8.22}$$

where Re is the Reynolds number and Gr is the Grashoff number, given by equations 8.23 and 8.24, respectively.

$$Re = \frac{\nu_{air} l_x}{\nu_{air}} \tag{8.23}$$

$$Gr = \frac{g\, h_{ca}^3 (T_{wall} - T_\infty)}{T_\infty\, \nu_{air}^2} \tag{8.24}$$

with ν_{air} as the air kinematic viscosity, v_{air} as the air velocity and g as the gravitational acceleration.

Since the housing will have thermal finning, the following is valid:

For free and forced convection ($A_{\text{air}} \geqslant A_{\text{fin}}$)

$$\begin{aligned}\alpha_{ca} = \left(1 - \frac{A_{air}}{A_{ca}}\right)(\alpha_{K,free} + \alpha_{rad}) + \frac{A_{air} - A_{fin}}{A_{ca}}(\alpha_{K,forced}\,\eta^* + \alpha_{rad}) + \\ \frac{A_{fin}}{A_{ca}}\left(\alpha_{K,forced}\eta^* + \alpha_{rad}\frac{A_{pro}}{A_{fin}}\right)\eta_f\end{aligned} \tag{8.25}$$

where A_{fin} and A_{pro} are the total and projected fin area, respectively. The fin efficiency η_f is:

$$\eta_f = \frac{tanh(m l_{fin})}{m l_{fin}} \tag{8.26}$$

where l_{fin} is the depth of one fin and m is given by:

$$m = \sqrt{2\frac{\alpha_{con} + \alpha_{rad}\frac{A_{pro}}{A_{fin}}}{\delta_{fin}\,\lambda_{fin}}} \tag{8.27}$$

where δ_{fin} is the thickness of one fin and λ_{fin} is the fin thermal conductivity.

In table 8.6 the required parameters are defined. The following considerations were taken from the ISO/TR 14179-2:

- An emissivity ratio, ε, of 0,15 for an aluminium housing with oxide skin (in table 8 of the technical report);
- The air kinematic viscosity value, ν_{air}, is 15,6 $\cdot 10^{-6}$ m^2/s;
- The oil heat transfer coefficient, α_{oil}, has a reference value of 200 W m^{-2} K^{-1}.

The ventilated housing area, A_{air} is approximated by adding the external housing area, A_{ca}, to the total fin area A_{fin}.

Tables 8.6 and 8.7 present the necessary variables and their respective value to perform the heat dissipation calculations.

In table 8.8, the major heat dissipation results are presented and it can be concluded that when operating at maximum torque, the oil temperature is close to 65 °C, while at maximum speed, the expected value is around 75 °Cfor the specified power losses. This results are in line with the previously stated information, which referred that the transmission generally operates in the 60 – 90 °C temperature range.

Table 8.6: Parameters to perform thermal calculations

Parameter	Value
A_{air} [m^2]	0,271
A_{ca} [m^2]	0,247
A_{oil} [m^2]	0,221
A_{fin} [m^2]	2,376 $\cdot 10^{-2}$
A_{pro} [m^2]	8,910 $\cdot 10^{-3}$
h_{ca} [m]	0,250
l_{fin} [m]	6 $\cdot 10^{-3}$
l_{x} [m]	0,390
T_{air} [K]	293,15
T_{wall} [K]	328,15
T_{∞} [K]	288,15
α_{oil} [$\text{W m}^{-2} \text{K}^{-1}$]	200
δ_{fin}	5,5 $\cdot 10^{-2}$
ε	0,15
λ_{fin} [$\text{W m}^{-1} \text{K}^{-1}$]	237
ν_{air} [m^2/s]	15,6 $\cdot 10^{-6}$

Table 8.7: Variables which depend on load

Parameter	Maximum Torque	Maximum Speed
v_{air} [m/s]	5	10
T_{oil} [K]	338,15 (65 °C)	348,15 (75 °C)
$Twall$ [K]	328,15 (55 °C)	338,15 (65 °C)

Table 8.8: Heat dissipation results

	Maximum Torque	Maximum Speed
Re	12500	250000
$\alpha_{\text{K,forced}}$ [$\text{W m}^{-2} \text{K}^{-1}$]	40,34	62,84
$\alpha_{\text{K,free}}$ [$\text{W m}^{-2} \text{K}^{-1}$]	11,43	12,23
α_{con} [$\text{W m}^{-2} \text{K}^{-1}$]	37,61	60,86
α_{rad} [$\text{W m}^{-2} \text{K}^{-1}$]	1,01	1,06
k [$\text{W m}^{-1} \text{K}^{-1}$]	31,72	45,97
T_{oil} [°C]	65	75
Q [W]	425,85	700,21
P_{V} [W]	450,1	712,5

Chapter 9

Housing and Parts

Transmission housing supports all the gearbox components. Therefore, several considerations need to be accounted in the housing design phase, such as [35]:

- Secure the exact position of all components relative to each other under all operating conditions, in particular, shafts, gears, and rolling bearings;
- Withstand and absorb the applied forces and moments;
- Provide good heat dissipation (conduction, convection and radiation);
- Damp and isolate the generated noise;
- Easy to mount and remove;
- Rigid structure with the necessary strength;
- Low weight.

9.1 Housing

9.1.1 Material

Generally, aluminium or magnesium are the preferred choices for the housing material due to properties such as, low density and good thermal conduction [50]. Nowadays, the aim is to make hybrid metal-composite housings become a viable production option, since the most useful features of each material (e.g. strength, low density, thermal properties) can be meshed and placed at specific locations.

Automotive housing are generally made of die cast aluminium, which is a good trade-off between cost and weight. The magnesium alloys, have lower density resulting in reduced weight. However, sometimes it is necessary to add thicker ribs or walls to provide the required rigidity and strength, limiting the lower density advantage [35].

The selected material for this transmission housing is the cast aluminium alloy G-AlSi10Mg from the KISSsoft catalogue. It has overall good strength (R_m = 220 $\mathrm{N\,mm^{-2}}$) and thermal properties (α = 22·10^{-6}/K), as well as low density (ρ = 2750 $\mathrm{kg\,m^{-3}}$).

9.1.2 Design

The selected structure for the housing is a split housing with an end-loaded design, which is a common design for automotive transmissions [35]. As advantages, compared to the other designs presented in figure 9.1, it has a rigid housing, components are easier to fit and the fitting can be automated. As disadvantages, expensive production equipment is required and, there are critical bores in clamping operations.

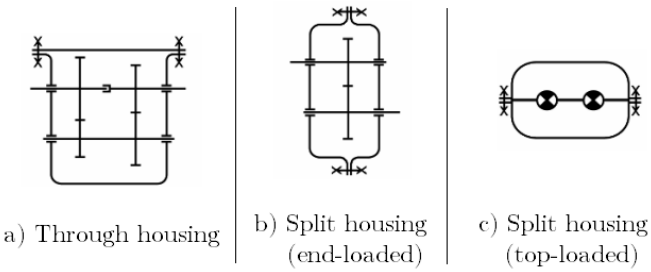

Figure 9.1: Types of housings [35]

The housing is designed with ribs in order to have thinner walls and the same rigidity and strength. The ribs also provide a way to decrease noise generation and must be arranged in a star shape from the bearing bores [35]. In the housing cover, the rolling bearing are mounted with an axial gap ($\approx$ 0,1 mm) to compensate for thermal expansions avoiding the generation of additional axial loads on the rolling bearings.

Figures 9.2 and 9.3 show the housing design, interior and exterior, respectively.

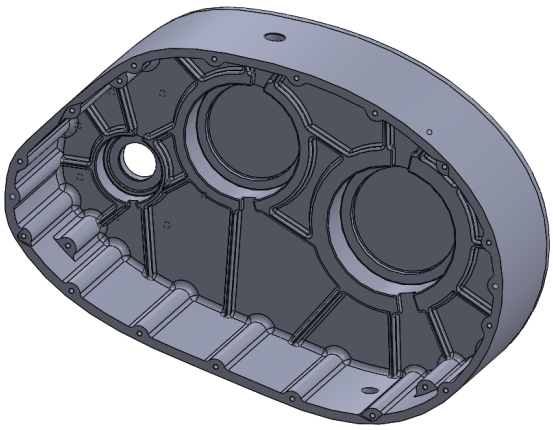

Figure 9.2: Housing interior

In figure 9.2, the ribs coming from the bearing bores are clearly visible. In each bearing bore, there are two recesses to promote the oil flow inside the transmission and facilitate the oil supply to the rolling bearings. These recesses have a rib on each side to maintain the rigidity of the overall structure.

In figure 9.3, the fins are disposed in a star shape and, apart from the fin effect they also act as ribs. Figure 9.4 shows the detail of the housing flange around the input shaft. This flange including seven threaded holes is prepared to receive a connection part between the electric motor and the housing.

Figure 9.5, shows the housing interior from another view, where interior projections

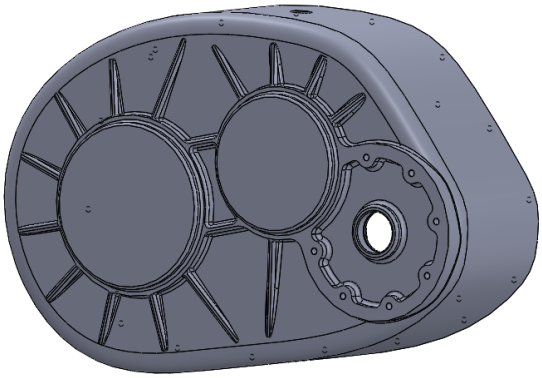

Figure 9.3: Housing exterior

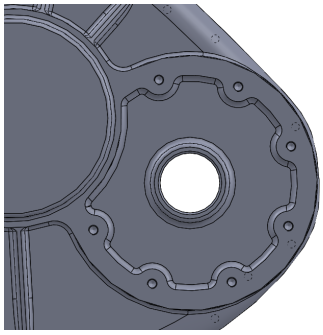

Figure 9.4: Housing exterior, detailed view of connection structure

are more visible. These protrusions contain the screws threaded holes used to afterwards connect the cover to the housing. The lower inside projections provide the support and the threaded holes where the internal flange will be fastened. On the left and right side, there are two projections where a rib ends, and where the two set pins will be inserted to accurately position the cover in relation to the housing.

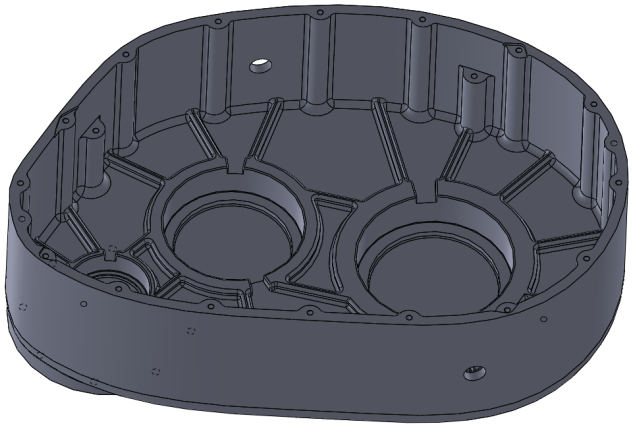

Figure 9.5: Housing interior (other view)

The cover has got the same design principles used for the housing, as can be seen in figures 9.6 and 9.7.

The housing and cover ribs have the same height across all length, but, in the cover,

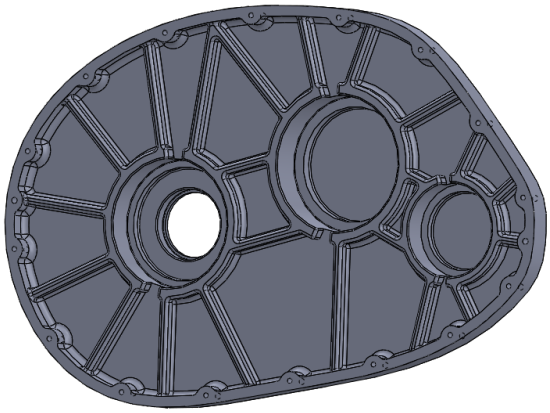

Figure 9.6: Cover interior

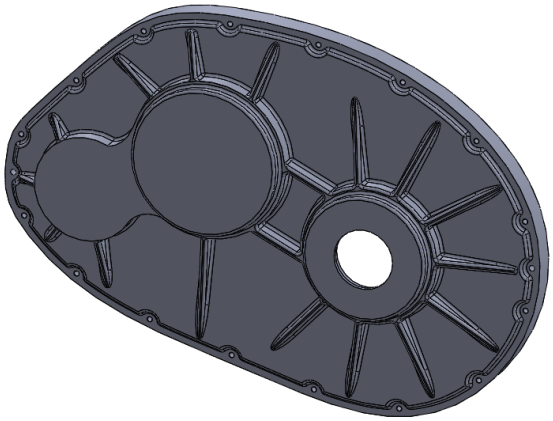

Figure 9.7: Cover exterior

the fins height decreases from the inside to the outside (see figure 9.8).

9.2 Parts

9.2.1 Flanges

The internal (figure 9.9) and external (figure 9.10) flanges are from the same material as the housing, aluminium. Since they are very thin sheets (1 mm), there is a corrugation through the entire flange in order to increase the flange rigidity. The minimum inside radius of the bending operation is 1,5 times the sheet thickness (figure 9.11), for an aluminium sheet, according to [96].

Besides the axial displacement between the flanges and the first stage gear pair, necessary to effectively reduce churning losses, the distance between the external flange and the bearings, as well as the distance between the internal flange and other components are also both taken into account.

9.2.2 Screws

A total of 20 screws are used. The 16 hexagon socket head cap screws (ISO 4762), which are conventionally used in the automotive industry are selected to tighten the cover, as

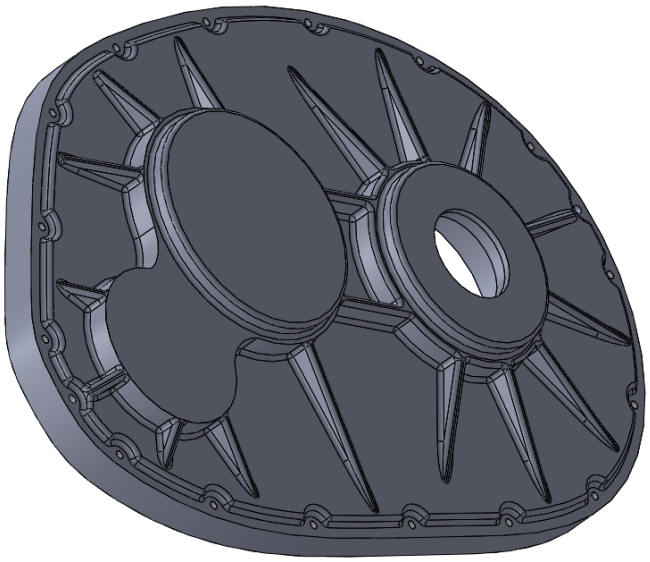

Figure 9.8: Cover exterior, detailed view of fins

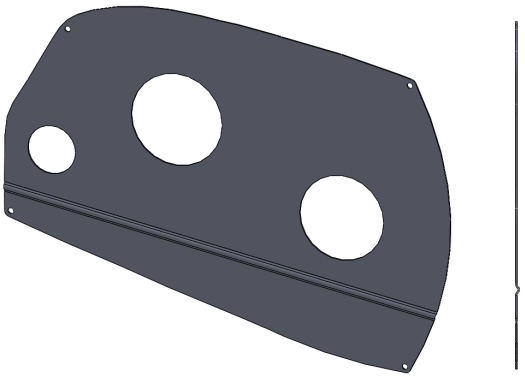

Figure 9.9: Interior flange

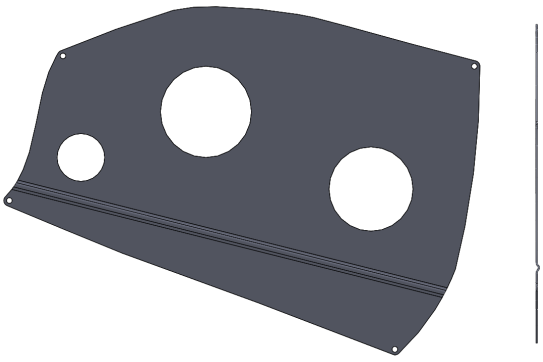

Figure 9.10: Exterior flange

well as the external flange to the housing. A M4 thread is the minimum thread generally employed and, in order to minimize the thickness of the housing wall, it is the preferential choice. The M4 thread has associated a 12.9 steel property class, providing good strength

Figure 9.11: Detail of flange sheet corrugation

properties. Finally, the screws have a 35 mm length to be in agreement with the total housing cover length, and to still have a considerable threaded length in the housing.

The 4 screws used to hold the internal flange are hexagon socket button head screws (ISO 7380). The same thread, M4, is also applied. All this screws have a 12.9 steel property class, and are employed in applications where the space is limited. The length of the button head screws is 16 mm, which is the maximum length for the considered M4 thread.

Therefore, the selected screws are:

- ISO 4762 - M4 x 35 - 12,9 (16 screws)
- ISO 7380 - M4 x 16 - 12,9 (4 screws)

9.2.3 Set pins

Two locating pins are necessary to precisely locate the cover in relation to the housing to get a fully working transmission without vulnerable areas from where the oil could easily leak.

In the automotive industry, spring-type straight pins (figure 9.12) are used for controlled, fine tolerance positioning of the work pieces. They are manufactured in steel (quenching) with a hardness between 550 and 650 HV.

The two selected pins are, according to the standard EN ISO 8752, designated as: Spring-Type Straight Pin - ISO 8752 - 4 x 30 - St.

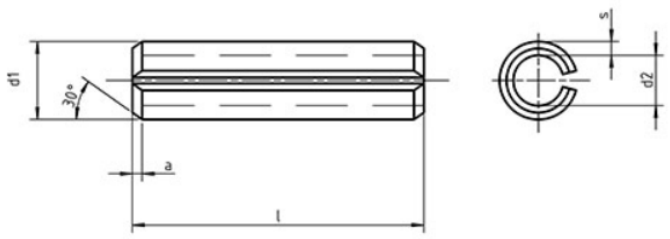

Figure 9.12: Spring-Type Straight Pin

9.2.4 Shaft spacer sleeves

The spacer sleeves are necessary to control the axial position of the gears in relation to other components, in this case, the rolling bearings. They are very important to maintain a correct gear positioning, so that the meshing between the gear pairs is exact. A common material for spacer sleeves is a medium carbon steel, such as the EN C45E, which is available from stock in bars and can be easily cut to the necessary requirements

Two spacer sleeves are employed in the transmission. One in shaft B to locate the gear Z2 and one in shaft C to accurately locate the gear Z4. The shaft C spacer sleeve has a length of 45 mm, so, if considered necessary, a hole may be drilled to facilitate oil flow.

The selected spacer sleeves dimensions (shaft diameter x thickness x length) are:

- Spacer sleeve shaft B - 42 x 5 - 3
- Spacer sleeve shaft C - 50 x 4 - 45

9.2.5 Retaining rings (circlips)

The retaining rings, or circlips, have the main task of reliably secure components in a shaft axial position, if the acting axial forces are not significant. One of the usual materials for retaining rings is the DIN C 75.

There are three retaining rings positioned in the three shafts, one on each. The purpose of these circlips is to hold in axial position the inner ring of the rolling bearings, guaranteeing its proper functioning while operating.

The circlip for bore, present in the housing wall, is required in order to keep the input radial shaft seal in place when its assembly takes place.

The selected retaining rings, according to the standards DIN 471 (shaft) and DIN 472 (bore), are:

- DIN 471 - 25 x 1,2 (Shaft A)
- DIN 471 - 40 x 1,75 (Shaft B)
- DIN 471 - 45 x 1,75 (Shaft C)
- DIN 472 - 32 x 1,2 (Housing bore)

9.2.6 Plugs

In transmissions where the splash lubrication method is applied, there is a requirement for both drain and fill plugs. Even though, nowadays the transmission fluid is usually not changed during the vehicle lifetime, it is wise to have these elements if, for some reason, an oil drain or refill is required. A magnetic drain plug is very effective at removing metallic particles from oil circulation within the transmission, leading to an increased lifetime of all components.

Since the housing walls, where the plugs are positioned, are not completely straight, a conical thread is a good solution to guarantee the transmission leakproofness. When fastening the plug, a threaded coating can be applied that generates a reinforced seal (figure 9.13).

The drain and fill conical plug (with a hexagon socket) have the same dimensions and follow the designation, DIN 906 - M18 x 1,5. The drain plug is a magnetic plug.

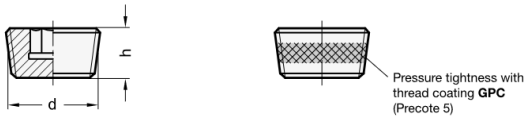

Figure 9.13: Conical thread plugs

9.2.7 Parts list

In table 9.1 the transmission parts list is presented.

Table 9.1: Transmission parts list

Item	Quantity	Material
Rolling Bearings	6	
Button head screws	4	Steel
Spring-type straight pins	2	Steel
Flanges	2	Aluminium
Gears	4	Steel 18CrNiMo7-6
Hexagon socket head cap screws	16	Steel
Housing	1	Aluminium
Cover	1	Aluminium
Plugs	2	
Radial shaft seals	2	
Retaining rings (shaft)	3	
Retaining ring (bore)	1	
Shafts	3	Steel 18CrNiMo7-6
Spacer sleeves	2	Steel EN C45E

Chapter 10

Assembly

The assembly of the transmission is the final step in the overall transmission design. Even though it is the concluding phase, in the previous design phases, such as gear pairs, shafts and housing design, it is necessary to have in mind if the assembly is appropriate, and simplifications are always welcomed.

The assembly steps which results in the final transmission arrangement are detailed in table 10.1

Table 10.1: Transmission assembly steps

Step	Figure	Comment
1	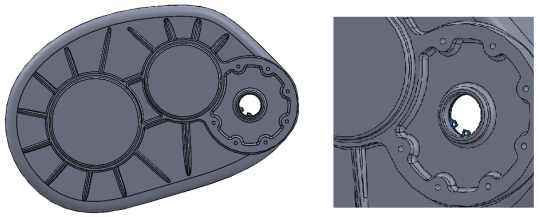	The retaining ring (circlip) is positioned in the housing bore, near the external flange connection.
2	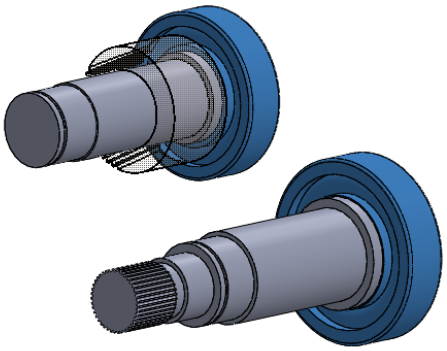	Two rolling bearings are mounted at the the shafts B and C right-ends, one rolling bearing in each shaft.

3	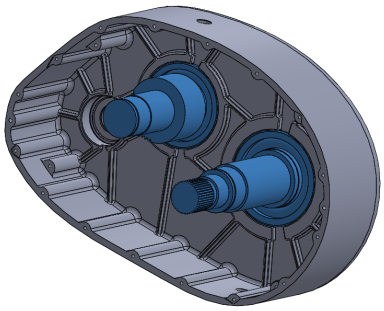	The shafts B and C, with the rolling bearings assembled, are inserted in the housing. The rolling bearings are positioned in the respective housing bores.
4	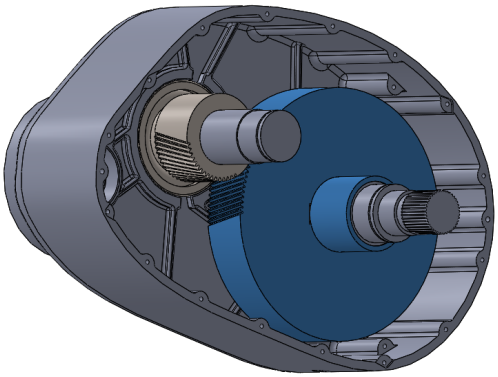	The key is fitted in the keyway of shaft C and the gear Z4 is mounted. To guarantee the correct position of the gear Z4 in relation to the pinion Z3 (from shaft B), ensuring a correct meshing, the spacer sleeve is installed.
5	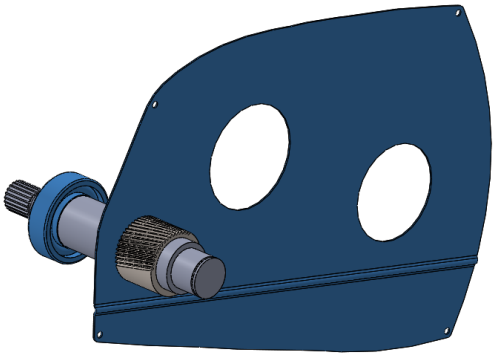	The internal flange is placed along the pinion shaft A, while the right-end rolling bearing is mounted in the shaft, assuring that the flange is located between the pinion Z1 and the right-end rolling bearing. Another solution was based on increasing the flange hole diameter so that the rolling bearing (mounted in the shaft) could freely pass through the flange. However, this diameter increase would lead to a weak zone in the flange, thus this solution was disregarded.

6	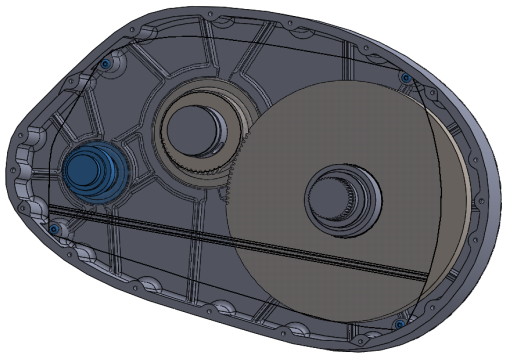	The pinion shaft A along with the rolling bearing, which is positioned in the respective housing bore, are placed inside the housing. The internal flange is now properly set by tightening the button head screws.
7	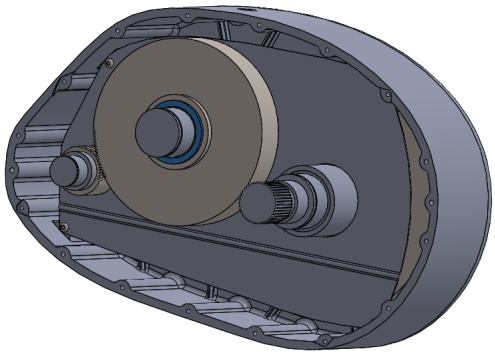	The key is fitted in the keyway of shaft B and the gear Z2 is mounted. A spacer sleeve is installed once more to ensure the correct positioning of the gear Z2 in relation to the pinion Z1 (from shaft A), so that the desired meshing is achieved.
8	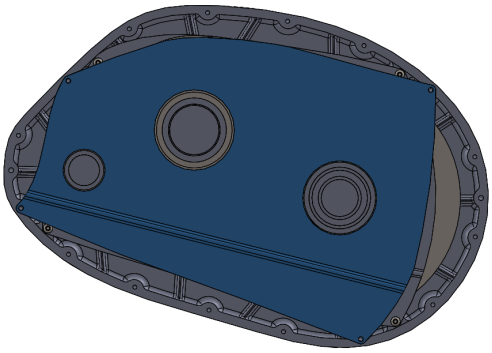	The external flange is located in the housing, being supported by the designed recesses. It will be fixed afterwards when the cover is fastened to the housing.
9	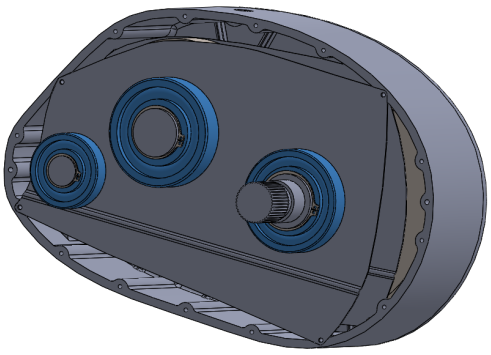	Three rolling bearings are mounted in the left-end of the three shafts, one rolling bearing in each shaft. Then, three retaining rings are assembled in the respective shafts grooves, to axially locate the inner ring of the rolling bearings.

10	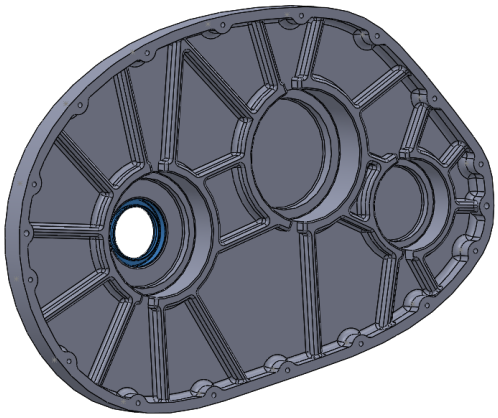	The output radial shaft seal is mounted with an interference fit in the cover bore.
11	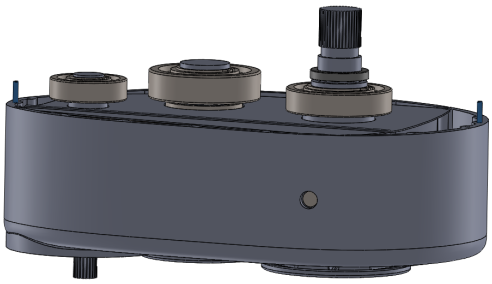	Two set pins are inserted in the housing holes, one on each end of the housing, in order to correctly position the cover in relation to the housing. To correctly mate the cover and housing surfaces, as well as to create a sealant layer, a anaerobic gasket maker is applied along the housing surface.
12	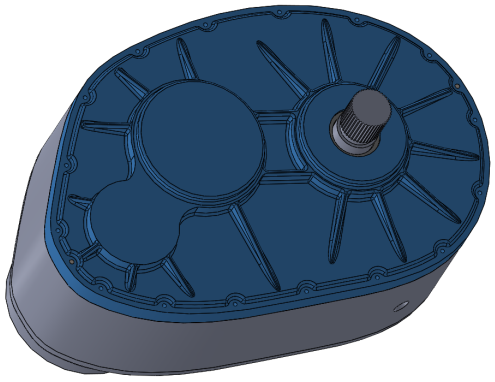	The cover is now accurately positioned in relation to the housing. Now, it is important to check if the input and output shafts rotate freely.

13	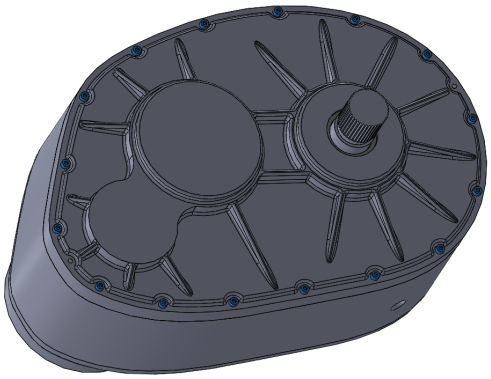	The 16 hexagon socket head cap screws are tightened, resulting in a compact and rigid connection between the cover and the housing. The external flange is also now accurately fastened in relation to the housing.
14	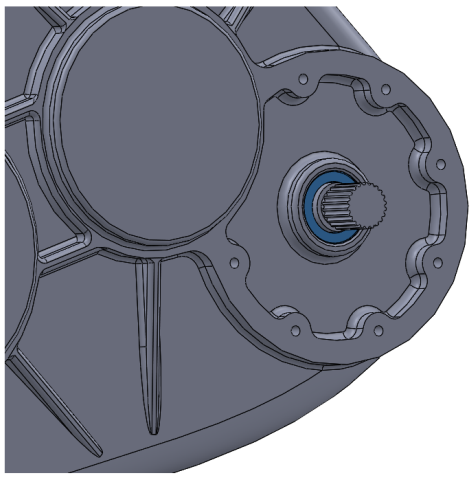	The input radial shaft seal is mounted in the housing bore and it is located axially by the retaining ring positioned in the first assembly step.
15	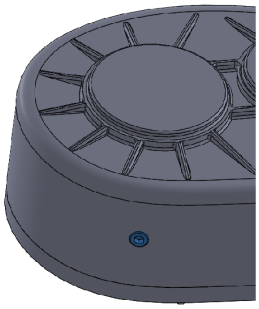 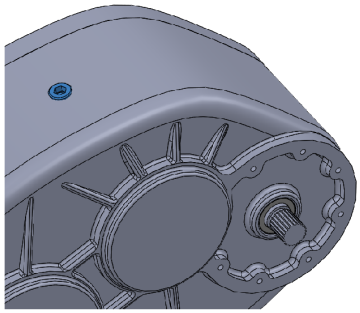	The drain plug is tightened at the bottom of the housing and, after filling the transmission with the required oil volume, the fill plug is tightened at the top to completely seal the transmission.

Chapter 11

Electronic differential

An increasing number of automotive companies, particularly regarding electric vehicles, are working in torque-vectoring solutions. These solutions have the main advantage of leaving the mechanical differential since it is no longer necessary, reducing the global powertrain weight. With two electric motors and two independent transmission, an electronic differential can be applied, which gathers vehicle operating information and transmits it to each electric motor. In turn, the electric vehicle will directly influence the input speed at the transmission, resulting in a suitable output transmission and, therefore vehicle speed.

There are two main situations when driving a vehicle, straight line cruise and steady state cornering. For the first situation, both electric motors provide the respective transmission with the same input torque and speed, leading to a same output left and right wheel speed, as well as torque. For steady state cornering, the outer wheel must rotate faster than the inner wheel, when turning. Consequently, the electric motors get different signals and the torque and speed provided to the transmissions are also different. A correct assessment of the cornering conditions, vehicle speed and load distribution in the vehicle is key to provide accurately information to the motors, so that the vehicle can corner smoothly [97, 98].

11.1 Critical cornering speed

Two situations are going to be considered in order to get the critical cornering vehicle speed at the minimum vehicle turning radius. The skidding situation and roll-over situation.

Considering the skidding situation:

The centripetal acceleration is:

$$a = \frac{v^2}{R} \tag{11.1}$$

where, v is the vehicle cornering speed and R is the turning radius.

The centripetal acceleration is governed by the horizontal static friction (f_{s}), which relates the road and the tires. Regarding Newton's Second Law, as speed increases, the acceleration strongly increases (proportional to the square of the speed). Static friction will also increase accordingly. However, the increase of static friction is not unlimited. When the speed reaches a certain value, the maximum static friction ($f_{\mathrm{s,max}}$) reaches a point where it cannot increase anymore. At this point, if the vehicle velocity continues to increase, it is insufficient to overcome the static friction sliding trend. In the critical state when skidding begins:

$$f_s = f_{s,max} = \mu_s mg = \frac{m{v_c}^2}{R} \tag{11.2}$$

where m is the vehicle mass and g is the gravitational acceleration.
Rearranging,

$$v_c = \sqrt{\mu_s Rg} \tag{11.3}$$

where v_c is the critical speed side-slip and μ_s is the static friction coefficient.

Regarding the vehicle roll-over situation, it generally occurs in large heavy-duty trucks or in vehicles with a high gravity center.

Taking the figure 11.1 as reference: R_A and R_B are the supportive ground forces of left and right wheels, respectively; F_A and F_B represent the friction force at the curve points; F_C is the centrifugal force and is equal to mv^2/R.

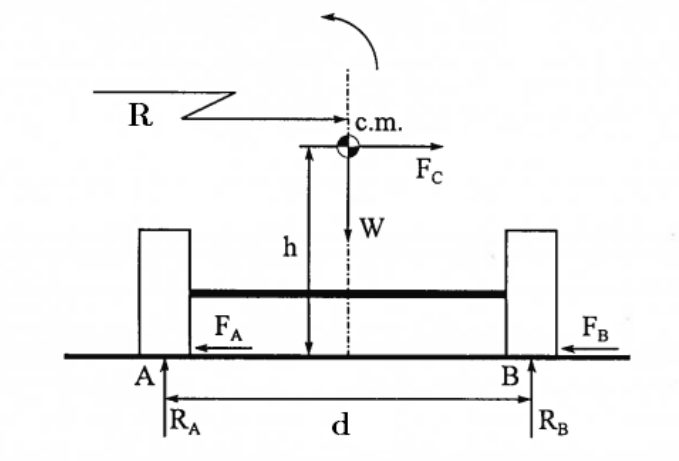

Figure 11.1: Free-body diagram of a vehicle turning left [64]

Obtained by torque balance at point B:

$$R_A d + \frac{mv^2}{R}h - mg\frac{d}{2} = 0 \tag{11.4}$$

where d is the distance between the left and right wheel.
In the stationary situation ($v = 0$), the above equation becomes:

$$R_A d - mg\frac{d}{2} = 0 \tag{11.5}$$

Simplified,

$$R_A = \frac{1}{2}mg \tag{11.6}$$

This implies that the load at the left and right wheels has the same value, each one supporting half the vehicle's weight. When the vehicle is turning left:

$$R_A = \frac{1}{2}mg - \frac{mv^2}{Rd}h \tag{11.7}$$

From the above equation 11.7 it can be assessed that the left wheel load, R_A decreases when the vehicle cornering speed increases and/or turning radius decreases. The critical

situation occurs when $R_A = 0$. Considering it is due to a critical cornering speed, v_c, if the speed is greater than it, the vehicle will roll-over. Therefore, the limit situation can be arranged as:

$$mg\frac{d}{2} = \frac{mv^2}{R}h \tag{11.8}$$

Rearranging the equation, one can obtain the critical cornering vehicle speed:

$$v_c = \sqrt{\frac{1}{2} \cdot g \cdot R \cdot \frac{d}{h}} \tag{11.9}$$

The table 11.1 presents the required variables to perform the calculations, as well as the final critical speed results. General passenger vehicles have, usually, a turning radius (R) between 7 and 9 m, the latter was selected.

Table 11.1: Calculation parameters and results

Parameter	Value
d [m]	1,4
h [m]	0,5
R [m]	9
μ_s	0,8
v_c (skidding) [km/h]	29,8
v_c (roll-over) [km/h]	40,0

From table 11.1, the maximum cornering speed occurs for skidding, as expected, and has a value of 8,28 m/s, or approximately 30 km/h.

Considering this critical vehicle speed, one can access what is the speed of the front left and right wheel. The electronic differential must make use of this information and actively provide the desired input to the electric motor in order to get the required output in the respective wheel.

11.2 Ackerman steering

The Ackerman steering geometry model (figure 11.2) is going to be followed to perform the forthcoming considerations:

The Ackerman steer angle (δ) is obtained by:

$$\delta = \frac{L}{R} - K\frac{v^2}{gR} \tag{11.10}$$

where L is the distance between the front and the rear wheel axles, K is a constant which considers the effect of weight distribution and tire cornering stiffness.

The factor K is considered zero in the initial analysis, resulting in a neutral steering condition.

The inner (equation 11.11) and outer (equation 11.12) steering angle of the front wheel are given by:

$$\delta_1 = \arctan\left[\frac{L\tan\delta}{L - ((P/2)\tan\delta)}\right] \tag{11.11}$$

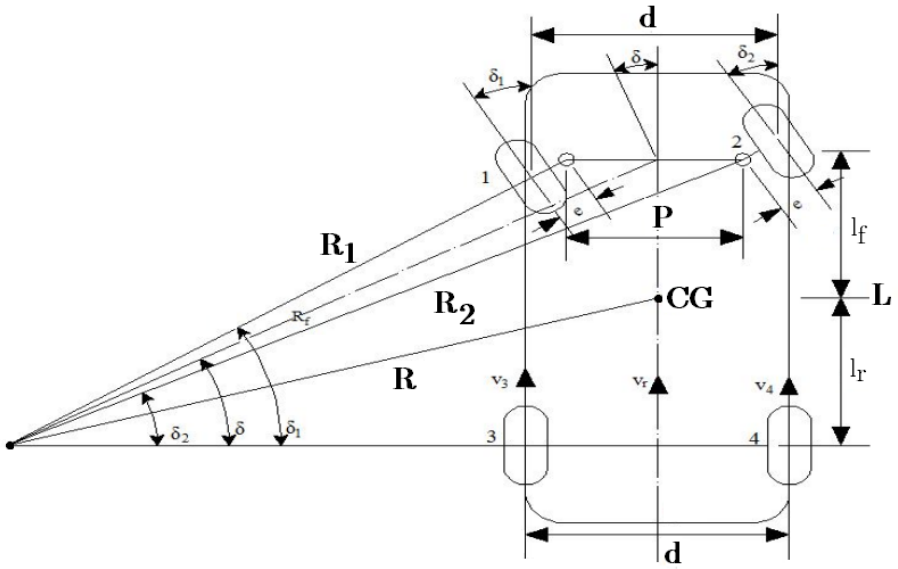

Figure 11.2: Ackerman model of cornering trajectory [99]

$$\delta_2 = \arctan\left[\frac{L\tan\delta}{L + ((P/2)\tan\delta)}\right] \tag{11.12}$$

where P is the distance between the left and right wheel kingpin.

The turning radii of the front left and right wheels is required to determine the respective wheel speeds. The inner wheel, left wheel in this case, turning radius, is given by:

$$R_1 = \frac{L}{\sin\delta_1} \tag{11.13}$$

The outer (right) wheel turning radius is:

$$R_2 = \frac{L}{\sin\delta_2} \tag{11.14}$$

Finally, the angular speed of the front wheels, left and right can be calculated according to equations 11.15 and 11.16, respectively.

$$\omega_1 = \frac{v\,R_1}{R\,r_t} \tag{11.15}$$

$$\omega_2 = \frac{v\,R_2}{R\,r_t} \tag{11.16}$$

where R is the vehicle turning radius (with respect to the center of gravity), and r_t is the tire radius.

Since the angular speed (ω) is expressed in rad/s, the following equations 11.17 and 11.18 are used to obtain the final wheel speeds in rotations per minute.

$$n_1 = \omega_1 \frac{60}{2\pi} \text{ (rpm)} \tag{11.17}$$

$$n_2 = \omega_2 \frac{60}{2\pi} \text{ (rpm)} \tag{11.18}$$

Finally, the rotational speed that the electric motor must provide at the transmission input is given by:

$$n_{1,motor} = n_1 * i_g \tag{11.19}$$

$$n_{2,motor} = n_2 * i_g \tag{11.20}$$

where i_g is the overall transmission ratio.

In table 11.2, the required parameters, which are constant across the following calculations, are summarised. The overall transmission ratio is given by multiplying the two transmission stages calculated before. The kingpin distance (P) also takes an approximate value, compared to the distance between the front left and right wheels (d).

Table 11.2: Summary of the required parameters

Parameter	Value
i_g [m]	11,65
L [m]	2,4
P [m]	1,3
r_t [m]	0,31

Table 11.3 contains a summary of the calculated results for the variables exposed above, taken into account a turning radius of 9 m and the previously calculated critical cornering speed of 8,28 m/s.

Table 11.3: Summary of the results for the critical cornering speed (R = 9 m; v=v_c = 29,8 km/h)

Parameter	Value
δ [rad]	0,2667
δ_1 [rad]	0,2869
δ_2 [rad]	0,2491
ω_1 [rpm]	240,386
ω_2 [rpm]	275,919
$\delta_{1,\text{motor}}$ [rpm]	2800,5
$\delta_{2,\text{motor}}$ [rpm]	3214,5

From the results presented above and as anticipated, the rotational speed of the inner wheel is smaller compared to the outside wheel speed. Accordingly, the inner steering angle is higher than the outer steering angle.

With the specified turning radius and vehicle speed conditions, the left (inner) front wheel has a speed of approximately 28 km/h and the right (outside) front wheel is taking the corner at 32 km/h, while the vehicle is cornering at around 30 km/h.

Figures 11.3 and 11.4 present two graphs that were plot in Matlab software. In the first a turning radius of 9 m is considered and in the second the turning radius is considered to

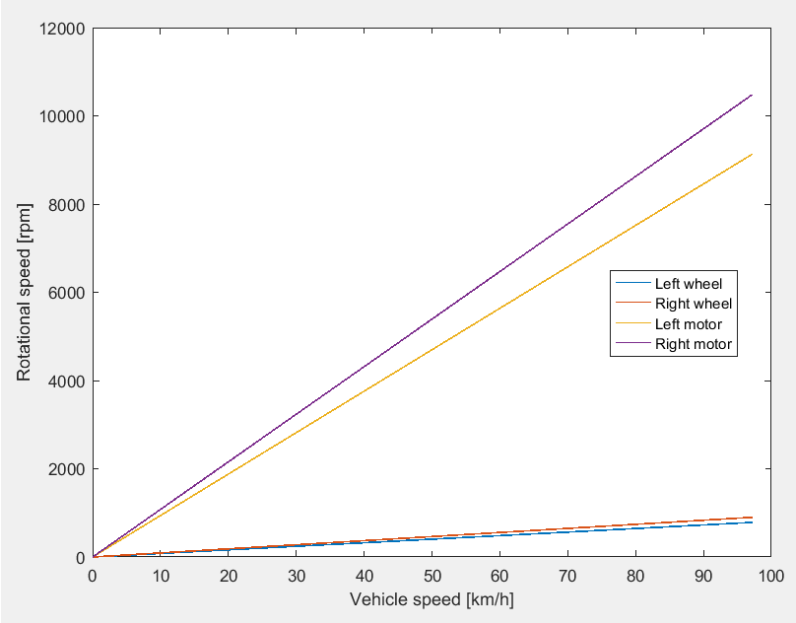

Figure 11.3: Rotational speed of wheel and motor over a vehicle speed range (R = 9 m)

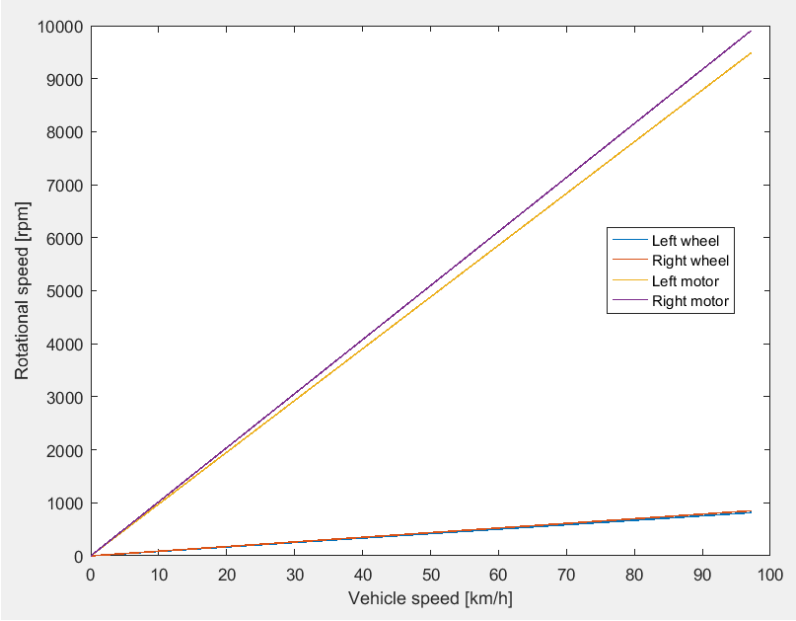

Figure 11.4: Rotational speed of wheel and motor over a vehicle speed range (R = 30 m)

be 30 m. From the graphs it can be concluded that, as the turning radius increases, the difference in the rotational speed of the left and right wheels decreases.

The electronic differential must also take into account the K gradient, which considers the weight distribution in the vehicle and the tire cornering stiffness [100]. This gradient is calculated according to:

$$K = \frac{W_f}{C_{\alpha f}} - \frac{W_r}{C_{\alpha r}} \tag{11.21}$$

where, W_{f} and W_{r} are, respectively, the front and rear vehicle loads. $C_{\alpha\,\mathrm{f}}$ and $C_{\alpha\,\mathrm{r}}$

are, respectively, the front and rear tire cornering stiffness.

In the following figure 11.5, the influence of the K gradient in vehicle steering is visible. A positive K gradient results in vehicle understeer, while a negative K gradient leads to the oversteer situation.

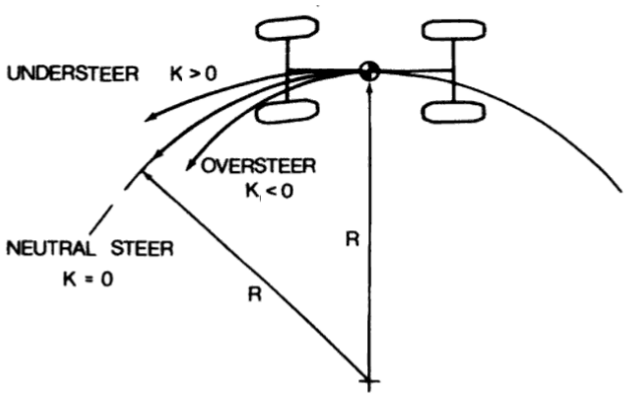

Figure 11.5: Influence of K gradient in steering [97]

The understeer situation is characteristic of vehicles with a front wheel drive (case considered in this thesis), since usually there is a larger load present in the front axle compared to the rear axle. On the other hand, oversteer is not very common, and it is harder to compensate from the driver side. The driver has to steer the wheel in the opposite direction of cornering unlike in the understeer case, where it must steer into the cornering direction [97].

The front tire cornering stiffness is given by:

$$C_{\alpha f} = \frac{W_f}{2} \cdot Factor \tag{11.22}$$

The factor in equation 11.22 represents the tire cornering stiffness $C_{\alpha\,\mathrm{f,r}}$ with respect to the load that the tire is subjected to. A value between 11 % to 19 % is usually employed, according to [98].

Table 11.4 presents the steering angles, together with the respective turning radius for both the understeer and oversteer conditions with a stipulated gradient value (K) of 0,1 and $-0{,}1$, respectively.

Table 11.4: Summary of the results for understeer and oversteer conditions

	Front-wheel drive	Rear-wheel drive
Parameter	**Understeer (K > 0)**	Oversteer (K < 0)
δ [rad]	**0,1890**	0,3443
δ_1 [rad]	**0,1991**	0,3781
δ_2 [rad]	**0,1799**	0,3159
R [rpm]	**9**	9
R_1 [rpm]	**12,14**	6,50
R_2 [rpm]	**13,41**	7,72

Looking at the results from the table 11.4, it can be concluded that both the understeer and oversteer validate the above stated concerns. When the K gradient is positive, the

calculated turning radii are both (for inner and outer wheel) above the alleged vehicle turning radius of 9 m. Conversely, for a negative K gradient, the inner and outer wheel turning radius are both lower than the expected turning radius, while when turning left, only the inner (left) wheel should have a turning radius lower than the vehicle turning radius.

Thereby, the electronic differential must also take into account the constant variation of the K gradient, in order to correctly provide the electric motors with the necessary information, so that they can compensate, accordingly, the required transmission input speed, resulting in a proper vehicle cornering management.

When the final vehicle design is complete, it can be found if the vehicle is significantly understeered and, the corresponding suspension tuning and weight optimization must be fulfilled to get a more desirable cornering performance, specially at high speeds where the instability increases possibly leading to life threatening situations.

Chapter 12

Conclusions and future work

12.1 Conclusions

In this thesis, the design of a high-speed gear transmission for a front-wheel drive electric vehicle was performed. The transmission is best suited for passenger vehicles where a urban drive cycle is expected. Two electric motors power two independent transmissions and, since there is no mechanical differential present, an electronic differential is necessary to provide the necessary torque and speed shifts between the output of both transmissions when the vehicle is cornering.

In chapter 2, the background research was an important step to get a better understanding of the current paradigm of the electric automotive industry. Despite the strong increase in electric vehicles (EV) sales, there is still a high price tag associated with them, in particular, due to battery costs and vehicle range, which is still very limited. The electric motors presently used are already at an advance stage regarding efficiency and the transmission arrangement in the EV industry is conventionally a fixed ratio single speed transmission.

The chapter 3 presented the main project characteristics where specifications for a small passenger vehicle (segment A and B) were drawn. A permanent magnet synchronous motor (PMSM) from the company Zytek Automotive was selected since it provided the necessary power and torque characteristics to fulfil the requirements which were further specified. Requirements such as a top speed of around 130 km/h, acceleration time from 0 to 100 km/h below 20 seconds and capacity to overcome a road slope of 30 %. An overall transmission ratio (≈ 12) was assessed and a suitable transmission overall arrangement, with two stages, was conceived.

In chapter 4 the focus was on gear design. Several parameters were specified according to the current industry developments and requirements. Small module helical gear pairs, which provide better efficiency and NVH behaviour were engineered making use of the capabilities of the KISSsoft software. Two main operating conditions were considered: maximum torque and maximum speed. These are extreme conditions at which the transmission has to operate for a certain period of time, so if the transmission properly works at these conditions, it will certainly correctly operate at normal conditions. It was concluded that when operating at maximum speed, the efficiency is greater but the noise generation increases. All gears comply with the demanded safeties regarding teeth root and flank strength. The stipulated safeties are probably overstated, but there is still a need for additional experimental data to validate this statement.

Afterwards, in chapter 5, the shafts were designed and the rolling bearings selected. Special attention was given to the shaft layout and the relative position between the three

shafts, which greatly influences the loads supported by the bearings. Deep groove ball bearings were preferred since they were a good solution with respect to withstanding axial and radial forces, as well as the considerable speed at the input shaft, when the vehicle is operating at maximum speed. The locating/non-locating arrangement was employed, due to the presence of axial forces. They are also very efficient and compact. At the end of the chapter, a shaft stress and deflection analysis was performed. The deflection at the first stage gear pair meshing zone brought concerns when the transmission is operating at maximum speed. In order to counteract this significant deflection, gear modifications were conceived in chapter 6.

In chapter 6, a gear modification sizing was performed to account for the shafts deflection and manufacturing tolerances. Theoretical flank modifications (e.g. crowning) and additional crowning as well as profile modifications, specifically, tip relief with a long profile modification (arc-like) were established, resulting in a more uniform load distribution, higher efficiency and smaller peak-to-peak transmission error, which is associated to noise generation.

The lubrication method and the sealing system were investigated in chapter 7. A splash lubrication method, due to economic factors was selected. However, the high speed associated with electric vehicle transmissions brings challenges regarding churning losses. The proposed solution was to employ two flanges, one on each side of the first stage cylindrical gear pair, reducing the teeth suction effect and effectively reducing churning losses. Lubricant and required radial shaft seals for the input and output shafts were selected based on requisites and industry available solutions.

Later, in chapter 8, the thermal analysis was explored. Power losses, more precisely, churning losses were calculated regarding the most appropriate models for the two operating conditions (maximum torque and maximum speed). The remaining power losses, for example, gear and rolling bearing power loss were obtained from the KISSsoft software calculations. After gathering the information regarding the power losses, from the heat dissipation analysis it was concluded that to ensure a proper transmission operation, the oil temperature inside the transmission is between 65 and 80 °C.

The chapter 9 regarded the housing design and other necessary components. A die cast aluminium housing with a split housing arrangement was designed, paying close attention to details, such as ribs to increase rigidity and strength while controlling the wall thickness. Some arrangement inside the housing was necessary to accommodate and tighten the flanges employed. Fins on the housing exterior to facilitate heat dissipation and that also act as ribs were added. Several parts, such as, set pins, screws and plugs were characterized and at the end of chapter a parts list table is presented.

The chapter 10 presents another important design phase regarding the transmission. The assembly of all the components must follow a specific order so that all elements are in their correct position and stable inside the housing and, to make sure that the input shaft and output shaft rotate properly, exhibiting that the transmission is operating correctly.

Some appreciations regarding the electronic differential are made in the chapter 11. The critical cornering speed is calculated for a vehicle turning at the minimum possible radius, the skidding and the roll-over situations were reviewed. Then, the Ackerman steering model was used to assess the individual speeds of the left and right wheel, when a vehicle is turning left, and the influence of the K gradient concerning under and oversteering. Since the front wheel drive vehicle is explored in this thesis, the understeer problem is more worrisome and should be further analysed.

Finally, the assembly drawing was made. All the transmission components are exposed and several details presented. The manufacturing drawings of the housing and cover, due

to the level of detail required and lack of available time, were not realized, but they are a crucial phase in the transmission design and manufacture.

12.2 Future Work

The electric vehicle transmission design, despite the alleged simplicity compared to internal combustion engine vehicle transmissions, still integrates a vast number of variables which form a network and influence each other. This makes the design an intricate project, constantly changing. Given that there is still a number of topics that could be considered, some future work which can be developed is presented below:

- Evaluate if a transmission with a mirror arrangement compared to the designed transmission also performs adequately or if additional changes are required for the left wheel transmission;
- Further developments in gears design may be performed considering the defined road profile. This would lead to less oversized gear with respect to the required safeties;
- A complete system model to analyse the housing response to vibration sources within the transmission to review the noise generation;
- Close evaluation of the gear modification sizing solutions, in particular, profile modifications which have a greater impact in the NVH gear behaviour. Choosing the best solutions, they could be assessed at different operating conditions;
- Testing of different shaft relative positioning, in order to further reduce churning losses, or implementing a housing solution where two oil distinct oil levels are present, one for the first stage and another for the second stage;
- Execute a housing structural design analysis to check for structural problems which could be improved;
- Perform practical experiments so that the obtained results could be validated, in particular, lubrication and thermal analysis to assess the influence of the inserted flanges;
- When all the vehicle parameters are defined, a torque vectoring model, which gather information from several sensors across the vehicle could be created and implemented in the dual motor vehicle.

References

[1] Jorge Martins and FP Brito. *Carros Elétricos*. Publindústria, 2011.

[2] Zifei Yang and Anup Bandivadekar. Light-duty vehicle greenhouse gas and fuel economy standards. Technical report, ICCT, 2017.

[3] Eurostat. Greenhouse gas emission statistics - emission inventories, 2017. Available: http://ec.europa.eu/eurostat/statistics-explained/index.php/Greenhouse_gas_emission_statistics_-_emission_inventories. Accessed: 01-03-2018.

[4] M. Nikowitz. *Advanced Hybrid and Electric Vehicles: System Optimization and Vehicle Integration*. Lecture Notes in Mobility. Springer International Publishing, 2016. ISBN 9783319263052.

[5] Clean Energy Ministerial. EV30@30, 2018. Available: http://www.cleanenergyministerial.org/Our-Work/CEM-Campaigns/EV30at30. Accessed: 25-02-2018.

[6] SM Knupfer, R Hensley, P Hertzke, P Schaufuss, N Laverty, and N Kramer. Electrifying insights: How automakers can drive electrified vehicle sales and profitability. *McKinsey & Company*, 2017.

[7] Rodrigo Garcia-Valle and João A Peças Lopes. *Electric vehicle integration into modern power networks*. Springer Science & Business Media, 2012.

[8] International Energy Agency. Global EV Outlook 2017, 2017. Available: https://www.iea.org/publications/freepublications/publication/global-ev-outlook-2017.html. Accessed: 12-02-2018.

[9] Fred Lambert. Electric cars reach new 52 % market share record in Norway thanks to Tesla's record deliveries, 2018. Available: https://electrek.co/2018/01/03/electric-car-market-share-norway-tesla-record-deliveries/. Accessed: 12-03-2018.

[10] Nissan Norway. Nye NISSAN LEAF, 2018. Available: https://www.nissan.no/biler/nye-biler/leaf.html. Accessed: 15-03-2018.

[11] Nissan Germany. Der neue NISSAN LEAF, 2018. Available: https://www.nissan.de/fahrzeuge/neuwagen/leaf.html. Accessed: 15-03-2018.

[12] Frankfurter Allgemeine. Diesel-Marktanteil fällt weiter, 2017. Available: http://www.faz.net/aktuell/wirtschaft/diesel-affaere/neuzulassungen-diesel-marktanteil-faellt-weiter-15182844.html. Accessed: 12-03-2018.

[13] Nationale Plattform Elektromobilität. Mit Elektromobilität nach vorn, 2017. Available: http://nationale-plattform-elektromobilitaet.de/. Accessed: 12-03-2018.

[14] Joel Maguire and Mitsuru Ishihara. BorgWarner Electrification, 2017.

[15] Thomas Hülshorst, Jürgen Ogrzewalla, and Christoph Bollig. FEV - Trends in Electrification, 2017. Available: https://autotechreview.com/events/transmission/Presentations_Transmission_tech_2017/FEV_BE_Electrification%20Trends_India_TransmissionTech_short.pdf. Accessed: 14-02-2018.

[16] Mehrdad Ehsani, Yimin Gao, Stefano Longo, and Kambiz Ebrahimi. *Modern electric, hybrid electric, and fuel cell vehicles*. CRC press, 2018.

[17] Christian Thiel, Johannes Schmidt, Arnold Van Zyl, and Erwin Schmid. Cost and well-to-wheel implications of the vehicle fleet CO_2 emission regulation in the European Union. *Transportation Research Part A: policy and practice*, 63:25–42, 2014.

[18] Emma Arfa Grunditz and Torbjörn Thiringer. Performance analysis of current bevs based on a comprehensive review of specifications. *IEEE Transactions on Transportation Electrification*, 2(3):270–289, 2016.

[19] Volkswagen Portugal. Vw up! e vw e-up!, 2018. Available: https://www.volkswagen.pt/pt/automoveis-novos/automovel-pequeno-vw-up.html. Accessed: 25-03-2018.

[20] Tom Denton. *Electric and Hybrid Vehicles*. Routledge, 2016.

[21] BorgWarner. BorgWarner's 48 Volt Technologies electrify vehicles for better efficiency, 2018. Available: https://www.borgwarner.com/news-media/press-releases/2017/09/12/borgwarner-s-48-volt-technologies-electrify-vehicles-for-better-efficiency. Accessed: 20-02-2018.

[22] Bosch. New hybrid battery from Bosch – 48 volts is a recipe for success, 2017. Available: http://www.bosch-presse.de/pressportal/de/en/new-hybrid-battery-from-bosch-%E2%80%93-48-volts-is-a-recipe-for-success-129984.html. Accessed: 22-02-2018.

[23] Continental. 48 Volt Technologies, 2017. Available: https://www.continental-automotive.com/en-gl/Landing-Pages/IAA/Electrification/48-Volt-Technologies. Accessed: 25-02-2018.

[24] Continental. Continental supplies the heart of the 48 Volt electrical system in the new Audi A8, 2018. Available: https://www.continental-corporation.com/en/press/press-releases/2018-01-15-audi-48-volt-119096. Accessed: 26-02-2018.

[25] Mauro Erriquez, Thomas Morel, Pierre-Yves Moulière, and Philip Schäfer. Trends in electric-vehicle design, 2017. Available: https://www.mckinsey.com/industries/automotive-and-assembly/our-insights/trends-in-electric-vehicle-design. Accessed: 15-02-2018.

[26] ING. Electric cars will take over, threatening European car industry, 2017. Available: https://www.ing.com/Newsroom/All-news/Electric-cars-will-take-over-threatening-European-car-industry.htm. Accessed: 20-02-2018.

[27] L. Guzzella and A. Sciarretta. *Vehicle Propulsion Systems: Introduction to Modeling and Optimization*. SpringerLink : Bücher. Springer Berlin Heidelberg, 2012. ISBN 9783642359132.

[28] Joaquim Carlos Novais de Freitas. Projeto e análise ao funcionamento de carros elétricos. Master's thesis, Universidade do Minho, 2012.

[29] Gwangmin Park, Seonghun Lee, Sungho Jin, and Sangshin Kwak. Integrated modeling and analysis of dynamics for electric vehicle powertrains. *Expert Systems with Applications*, 41(5):2595–2607, 2014.

[30] Amit Jha. Let's discuss motors in electric vehicles, 2016. Available: http://etn-demeter.eu/lets-discuss-motors-in-electric-vehicles. Accessed: 05-03-2018.

[31] ZVEI-German Electrical, Electronic Manufacturers Association, et al. Voltage classes for electric mobility. *Frankfurt am Main, Germany*, 2013.

[32] Nasser Hashemnia and Behzad Asaei. Comparative study of using different electric motors in the electric vehicles. In *18th International Conference on Electrical Machines, 2008. ICEM 2008.*, pages 1–5. IEEE, 2008.

[33] Nicola Bianchi. Synchronous reluctance and pm assisted reluctance motors. In *The Rediscovery of Synchronous Reluctance and Ferrite Permanent Magnet Motors*, pages 27–57. Springer, 2016.

[34] Thomas Finken, Matthias Felden, and Kay Hameyer. Comparison and design of different electrical machine types regarding their applicability in hybrid electrical vehicles. In *Electrical Machines, 2008. ICEM 2008. 18th International Conference on*, pages 1–5. IEEE, 2008.

[35] Harald Naunheimer, Bernd Bertsche, Joachim Ryborz, and Wolfgang Novak. *Automotive transmissions: Fundamentals, selection, design and application*. Springer Science & Business Media, 2010.

[36] Saphir Faid. A highly efficient two speed transmission for electric vehicles, 2015. Available: www.evs28.org/event_file/event_file/1/pfile/EVS28_Saphir_Faid.pdf.

[37] Jiageng Ruan, Paul Walker, and Nong Zhang. A comparative study energy consumption and costs of battery electric vehicle transmissions. *Applied Energy*, 165:119–134, 2016.

[38] Paul D Walker, Salisa Abdul Rahman, Bo Zhu, and Nong Zhang. Modelling, simulations, and optimisation of electric vehicles for analysis of transmission ratio selection. *Advances in Mechanical Engineering*, 5:340435, 2013.

[39] Jimmy King, Kevin Kristopher Andrew Moore, and Charissa Cadence Seid. Electric vehicle drivetrain final design review, 2017. Available: http://digitalcommons.calpoly.edu/mesp/395. Accessed: 26-02-2018.

[40] Jack Erjavec and Rob Thompson. *Automotive technology: a systems approach*. Cengage learning, 2014.

[41] Stephen Neil. Drivetrain systems explained: Difference between FWD, RWD, AWD and 4WD, 2017. Available: https://www.drivespark.com/off-beat/car-drivetrain-systems-explained-022723.html. Accessed: 12-03-2018.

[42] Tommaso Goggia, Aldo Sorniotti, Leonardo De Novellis, Antonella Ferrara, Patrick Gruber, Johan Theunissen, Dirk Steenbeke, Bernhard Knauder, and Josef Zehetner. Integral sliding mode for the torque-vectoring control of fully electric vehicles: Theoretical design and experimental assessment. *IEEE Transactions on Vehicular Technology*, 64(5):1701–1715, 2015.

[43] GETRAG. Single-speed eDRiVE for performance applications - 1eDT330, 2018. Available: http://www.getrag.com/en/products/edrive_1/1edt330/1edt330_1.html. Accessed: 08-03-2018.

[44] GKN. GKN to reveal world's most advanced electric driveline at Frankfurt Motor Show, 2017. Available: https://www.gkn.com/en/newsroom/news-releases/driveline/2017/gkn-to-reveal-worlds-most-advanced-electric-driveline-at-frankfurt-motor-show/. Accessed: 10-03-2018.

[45] A3PS. Electrically scalable axial-module, 2015. Available: http://www.a3ps.at/site/sites/default/files/Workshop_Lightweight/Wolfgang%20Pflug_Projekt%20ESKAM.pdf. Accessed: 01-03-2018.

[46] Queval Loic. ESKAM project - Electric Scalable Axle Module for e-Mobility, 2015. Available: https://www.researchgate.net/publication/278847071_ESKAM_Project_-_Electric_Scalable_Axle_Module_for_e-Mobility.

[47] Philipp Gwinner, Karsten Stahl, Steffen Rupp, and Alexander Strube. Innovative high-speed powertrain concept for highly efficient electric vehicles. *ATZ worldwide*, 119(3):66–71, 2017.

[48] Martin Sedlmair, Patrick Fischer, Thomas Lohner, Hermann Pflaum, and Karsten Stahl. Holistic investigations on the innovative high-speed powertrain Speed2E for electric vehicles, 12 2017. Available: https://www.researchgate.net/publication/322196986_Holistic_Investigations_on_the_Innovative_High-Speed_Powertrain_Speed2E_for_Electric_Vehicles. Accessed: 12-03-2018.

[49] A. von Entress Fürsteneck, Philipp Gwinner, M. Otto, and S. Flügel. Elektromechanischer antriebsstrang mit torque vectoring. *ATZ extra*, 2014.

[50] George Scott. Transmission design for very high input speeds,. 8th International CTI Symposium 2014, 2014. Drive System Design UK.

[51] Emma Grunditz. *Design and assessment of battery electric vehicle powertrain, with respect to performance, energy consumption and electric motor thermal capability*. Chalmers University of Technology, 2016.

[52] Zytek Automotive. Zytek twin 25kw, 2018. Available: http://www.zytekautomotive.co.uk/products/electric-engines/twin-25kw/. Accessed: 20-03-2018.

[53] Richard Budynas. *Shigley's Mechanical Engineering Design (McGraw-Hill Series in Mechanical Engineering)*. McGraw-Hill Higher Education, 2014. ISBN 9780077591670.

[54] Robert Norton. *Design of Machinery*. McGraw-Hill, 2011. ISBN 9780073529356.

[55] KHK gears. Gear technical reference – the role gears are playing, 2018. Available: https://khkgears.net/new/gear_knowledge/gear_technical_reference/index.html. Accessed: 26-04-2018.

[56] Stephen Radzevich and Darle Dudley. *Handbook Of Practical Gear Design*. CRC Press, 2009. ISBN 9781566762182. Available: https://www.amazon.com/Handbook-Of-Practical-Gear-Design/dp/B01CMYCRBG?SubscriptionId=0JYN1NVW651KCA56C102&tag=techkie-20&linkCode=xm2&camp=2025&creative=165953&creativeASIN=B01CMYCRBG.

[57] Alexander L. Kapelevich. *Direct Gear Design*. Taylor & Francis, 2013. Available: https://www.ebook.de/de/product/21178282/alexander_l_kapelevich_direct_gear_design.html.

[58] KISSsoft AG. Kisssoft (release 03/2017f), 2017. Available: http://www.kisssoft.ch.

[59] ISO 6336-6:2006. Calculation of load capacity of spur and helical gears – part 6: Calculation of service life under variable load. Technical report, ISO, 2006.

[60] DIN 3990-41. Calculation of load capacity of cylindrical gears; application standard for vehicle gears. Technical report, DIN, 1990.

[61] ISO 6336-1:2006. Calculation of load capacity of spur and helical gears – part 1: Basic principles, introduction and general influence factors. Technical report, ISO, 2006.

[62] United Nations. Regulation no. 101 - rev.3 - co2 emission/fuel consumption - e/ece/324 ece/trans/505/rev.2/add.100/rev.3. Technical report, UN, 2013.

[63] Adrien Neurouth. *Etude de la performance énergetique d'une transmission de puissance haute vitesse*. PhD thesis, Université de Lyon, 2016.

[64] Tiago Viegas Vidinha. Design of an ultra high-speed transmission for a 50 kW electric vehicle. Master's thesis, University of Porto, 2017.

[65] Bernd-Robert Höhn, Peter Oster, and Christo Braykoff. Size and material influence on the tooth root, pitting, scuffing and wear load carrying capacity of fine module gears. In *International Conference on Gears, Garching*, pages 1295–1307, 2010.

[66] Randy Stott. Cleaner steels provide gear design opportunities. Geartechnology Newsletter, November 2017.

[67] ISO 1328:1995. Cylindrical gears – iso system of accuracy – part 1: Definitions and allowable values of deviations relevant to corresponding flanks of gear teeth. Technical report, ISO, 1995.

[68] DIN 3961. Tolerances for cylindrical gear teeth; bases. Technical report, DIN, 1978.

[69] Nicolás Larburu Arrizabalaga. *Máquinas : prontuario*. Ediciones Paraninfo, S.A, 1994. ISBN 8428319685.

[70] DIN 4766-1. Surface roughnes associated with types of manufacturing methods - attainable arthmetical mean value of peak-to-valley height rz according to din 4768 part 1. Technical report, DIN, 1981.

[71] DIN 4766-2. Surface roughness associated with types of manufacturing method - attainable arithmetical mean value ra according to din 4768 part 1. Technical report, DIN, 1981.

[72] ISO/TR 10064-4:1998. Code of inspection practice – part 4: Recommendations relative to surface texture and tooth contact pattern checking. Technical report, ISO, 1998.

[73] DIN 780-1. Series of modules for gears; modules for spur gears. Technical report, DIN, 1977.

[74] Karl-Heinrich Grote and Erik K. Antonsson. *Springer Handbook of Mechanical Engineering (Springer Handbooks)*. Springer, 2009. ISBN 9783540491316. Available: https://www.amazon.com/Springer-Handbook-Mechanical-Engineering-Handbooks/dp/3540491317?SubscriptionId=0JYN1NVW651KCA56C102&tag=techkie-20&linkCode=xm2&camp=2025&creative=165953&creativeASIN=3540491317.

[75] DIN 509. Forms and dimensions of undercuts. Technical report, DIN, 1998.

[76] P. Orlov. *Fundamentals Of Machine Design - Part 2*. Central Books Ltd, 1982. ISBN 9780714718606.

[77] ISO/R 775. Cylindrical and 1/10 conical shaft ends. Technical report, ISO, 1969.

[78] J. Almacinha and J. S. Morais. *Texto de apoio à unidade curricular de Desenho de Construção Mecânica*. DEMEC - Faculdade de Engenharia da Universidade do Porto, 2015.

[79] P. Orlov. *Fundamentals Of Machine Design - Part 4*. MIR Publishers, 1977.

[80] DIN 5480-2. Involute splines based on reference diameters - part 2: Nominal and inspection dimensions. Technical report, DIN, 2015.

[81] P. Orlov. *Fundamentals Of Machine Design - Part 3*. Central Books Ltd, 1982.

[82] 6885-1. Drive type fastenings without taper action; parallel keys, keyways, deep pattern. Technical report, DIN, 1968.

[83] ISO 281:2007. Rolling bearings – dynamic load ratings and rating life. Technical report, ISO, 2007.

[84] SKF. *Rolling bearings catalogue*. SKF, 2018. Available: http://www.skf.com/group/knowledge-centre/media-library/index.html#tcm:12-121486.

[85] ISO 4406:2017. Hydraulic fluid power – fluids – method for coding the level of contamination by solid particles. Technical report, ISO, 2017.

[86] DIN 732. Rolling bearings - thermally safe operating speed - calculation and correction values. Technical report, DIN, 2010.

[87] DIN 743. Load calculation of shafts and axles. Technical report, DIN, 2012.

[88] V. B. Bhandari. *Design of Machine Elements*. India Professional, 2016. ISBN 9339221125.

[89] Adrien Neurouth, Christophe Changenet, Fabrice Ville, Philippe Velex, and Michel Octrue. Is splash lubrication compatible with efficient gear units for high-speed applications? *POWERTRANSMISSION*, 2015.

[90] Christophe Changenet and Philippe Velex. Housing influence on churning losses in geared transmissions. *Journal of Mechanical Design*, 130(6):062603, 2008.

[91] SKF. *CR Seals handbook*. SKF, 2018. Available: http://www.skf.com/group/products/seals/industrial-seals/cr-seals/index.html.

[92] Klaus Michaelis, Bernd-Robert Höhn, and Michael Hinterstoißer. Influence factors on gearbox power loss. *Industrial lubrication and tribology*, 63(1):46–55, 2011.

[93] ISO/TR 14179-2:2001. Gears – thermal capacity – part 2: Thermal load-carrying capacity. Technical report, ISO, 2001.

[94] Christophe Changenet, Gauthier Leprince, Fabrice Ville, and Philippe Velex. A note on flow regimes and churning loss modeling. *Journal of Mechanical Design*, 133(12): 121009, 2011.

[95] Christophe Changenet and Philippe Velex. A model for the prediction of churning losses in geared transmissions—preliminary results. *Journal of Mechanical Design*, 129(1):128–133, 2007.

[96] Jorge Rodrigues & Paulo Martins. *Tecnologia Mecanica - Tecnologia da Deformacao Plastica - Vol.2 - Aplicacoes Industriais*. Escolar Editora, 2010. ISBN 9725922808.

[97] J. Y. Wong. *Theory of Ground Vehicles*. Wiley, 2008. ISBN 0470170387.

[98] Thomas D. Gillespie. *Fundamentals of Vehicle Dynamics (Premiere Series Books)*. SAE International, 1992. ISBN 1560911999.

[99] Merve Yıldırım, Eyyüp Öksüztepe, Burak Tanyeri, and Hasan Kürüm. Design of electronic differential system for an electric vehicle with in-wheel motor. In *Power and Energy Conference at Illinois (PECI), 2016 IEEE*, pages 1–5. IEEE, 2016.

[100] Balasharmila Rao Munusamy and Joerg Dieter Weigl. Design of rear wheel torque vectoring for dual motor electric drive system. In *Ecological Vehicles and Renewable Energies (EVER), 2014 Ninth International Conference on Ecological Vehicles and Renewable Energies*, pages 1–20. IEEE, 2014.

Appendix A

Steel 18CrNiMo7-6

Specifications of the gear and shaft material, steel 18CrNiMo7-6 according to the standard EN 10084:2008, are presented in the next appendix.

Quality	**18CrNiMo7-6**
According to standards	**EN 10084: 2008**
Number	**1.6587**

GRUPPO LUCEFIN Lovin' Steel

Chemical composition

C%	**Si%** max	**Mn%**	**P%** max	**S%** max	**Cr%**	**Mo%**	**Ni%**	
0,15-0,21	0,40	0,50-0,90	0,025	0,035	1,50-1,80	0,25-0,35	1,40-1,70	Product deviations are allowed
± 0.02	+ 0.03	± 0.04	+ 0.005	+ 0.005	± 0.05	± 0.03	± 0.05	

Temperature °C

Hot-forming	**Normalizing +N**	**Core hardening**	Carburizing	**Hardening carburiz. surface**	**Tempering +T**	**Annealing +FP**
1150-900	860-925 air	830-870 oil or polymer	900-950 (HRC 60-63)	780-820 oil or polymer	150-200 air	900-1000 (HB 159-207)

Soft annealing +A	**Isothermal annealing +I**	**Spheroidized annealed +AC**	**End quench hardenability test**	**Pre-heating welding**		**Stress-relieving after welding**
				welding must be carried out on the annealed state and before carburizing		
660-700 air (HB max 229)	850-900 furnace cooling to 610 then air (HB 140-210)	1000-1100 furnace cooling to 650 then air (HB max 180)	860 water	250-350		furnace cooling
				Ac1	**Ac3**	**MS** * core ** carburizing surface
				745	825	400* 170**

Mechanical properties

Mechanical properties for **hot-formed** products according to Stalschlüssel 2010 standard, after hardening 850 °C oil + stress-relieving at 200°C

size mm		Testing at room temperature (longitudinal)					**Lucefin** experience quenching 850 °C water, tempering 200 °C air				
		R min	**Rp** 0.2	**A**%	**Kcu**	***HB***					
from	to	N/mm²	N/mm² min.	min.	J min.	*min*	**Ø**	**R**	**Rp** 0.2	**A**	**Kv** +20 °C
	16	1200				*359*	mm	N/mm²	N/mm²	%	J
16	40	1100				*331*					
40	100	900				*271*	30	1160	1010	12.2	48-46-52

18CrNiMo7-6 **1.6587** Stalschlüssel 2010. Material: casehardened, quenched and tempered

size mm		**R**	**Rp** 0.2	**A**%	**C%**	Kv	HB
from	to	N/mm²	N/mm² min	min	min	J min	
	11	1180-1420	835	7	30	44	354-406
12	30	1080-1320	785	8	35	44	327-384
31	63	980-1270	685	8	35		295-373

EN 10084: 2008 **Jominy test HRC**

mm distance from quenched end

mm	**1.5**	**3**	**5**	**7**	**9**	**11**	**13**	**15**	**20**	**25**	**30**	**35**	**40**	**45**	grades
min	40	40	39	38	37	36	35	34	32	31	30	29	29		**H** = normal
max	48	48	48	48	47	47	46	46	44	43	42	41	41		
min	43	43	42	41	40	40	39	38	36	35	34	33	33		**HH** restricted scatter bands
max	48	48	48	48	47	47	46	46	44	43	42	41	41		
min	40	40	39	38	37	36	35	34	32	31	30	29	29		**HL** restricted scatter bands
max	45	45	45	45	44	43	42	42	40	39	38	37	37		

Thermal Expansion	$10^{-6} \cdot K^{-1}$ ►		11.1	12.1	12.9	13.5	13.9
Mod. of Elasticity long.	GPa	210					
Specific Heat Capacity	J/(Kg•K)	460					
Thermal Conductivity	W/(m•K)	38					
Density	Kg/dm³	7.85					
Specific Electric Resistivity	Ohm•mm²/m	0.18					
Electrical Conductivity	Siemens•m/mm²	5.55					
°C		**20**	**100**	**200**	**300**	**400**	**500**

The symbol ► indicates temperature between 20 °C and 100 °C, 20 °C and 200 °C …

18CrNiMo7-6 1.6587

Table of tempering values obtained at room temperature on rounds Ø 11 mm after quenching at 850 °C in water

HB		400	393	384	363	319	258	213
HRC		43	42.5	41.5	39	34	26	
R	N/mm^2	1390	1360	1320	1230	1050	860	700
Rp 0.2	N/mm^2	1230	1210	1170	1080	940	791	560
A	%	12	12	12	13	15	18	20
C	%	52	53	54	55	58	65	68
Kv	J	44	60	50	40	80	140	160
Tempering at **°C**		**100**	**200**	**300**	**400**	**500**	**600**	**700**

EUROPE EN	**ITALY** UNI	**CHINA** GB	**GERMANY** DIN	**FRANCE** AFNOR	**U.K.** B.S.	**RUSSIA** GOST	**USA** AISI/SAE
18CrNiMo7-6	18CrNiMo7-6		17CrNiMo6	18CND6	822M17 ~		4820 ~

Classification of steel grades according to minimum tensile strength as a function of diameter after hardening and tempering at 200 ° C (EN 10084)

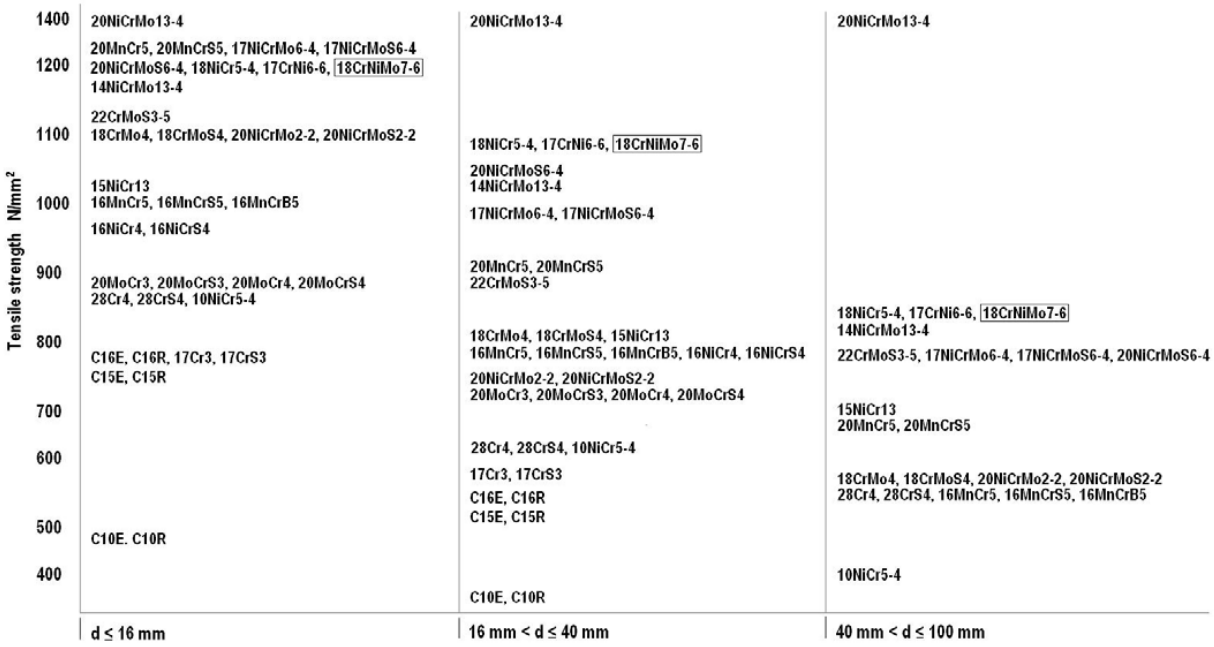

Appendix B

Lubricant - Castrol ATF Dex II Multivehicle

Specifications of the selected lubricant, Castrol ATF Dex II Multivehicle, are specified in the following appendix.

Product Data

Castrol ATF Dex II Multivehicle

Automatic Transmission Fluid

Description

Castrol ATF Dex II Multivehicle is an Automatic Transmission Fluid which may be used in automatic transmissions and power steering units of many types of vehicle where Dexron IID or Mercon performance is required.It is also approved for use in many european heavy duty automatic transmissions and Mercedes Benz manual transmissions.

Advantages

- Multiple approvals provide wide ranging use.
- Ensures efficient operation of power steering units under all conditions.
- High thermal stability protects against deposits and oil thickening prolonging the life of components and lubricant.
- Enhanced friction characteristics and wear protection maintain effective operation of equipment.
- Effective seal compatibility reduces the risk of leakages

Typical Characteristics

Name	Method	Units	ATF Dex II Multivehicle
Density @ 20°C, Relative	ASTM D4052	g/ml	0.870
Colour	Visual	-	red
Viscosity, Kinematic 100°C	ASTM D445	mm²/s	7.5
Pour Point	ASTM D97	°C	-42
Viscosity, Brookfield @ -40°C	ASTM D2983	mPa.s (cP)	<50.000
Viscosity, Kinematic 40°C	ASTM D445	mm²/s	39
Viscosity Index	ASTM D2270	None	163

Appendix C

Cylindrical gear pairs KISSsoft report

In this appendix the reports from the KISSsoft software, for the cylindrical gear pairs at the operating conditions of maximum torque and maximum speed, are sequentially presented as follows:

- First stage cylindrical gear pair at maximum torque (GearZ1Z2Torque);
- Second stage cylindrical gear pair at maximum torque (GearZ3Z4Torque);
- First stage cylindrical gear pair at maximum speed (GearZ1Z2Speed);
- Second stage cylindrical gear pair at maximum speed (GearZ3Z4Speed).

KISSsoft Release 03/2017 F

KISSsoft University license - Universidade do Porto

File

Name : GearZ1Z2Torque

Changed by: Carlos Rodrigues on: 02.07.2018 at: 23:48:26

CALCULATION OF A HELICAL GEAR PAIR

Drawing or article number:
Gear 1: 0.000.0
Gear 2: 0.000.0

Calculation method ISO 6336:2006 Method B

		------- GEAR 1	-------- GEAR 2 --
Power (kW)	[P]	25.656	
Speed (1/min)	[n]	3500.0	889.2
Torque (Nm)	[T]	70.0	275.5
Application factor	[KA]	1.25	
Required service life (h)	[H]	5000.00	
Gear driving (+) / driven (-)		+	-

Working flank gear 1: Right flank
Sense of rotation gear 1 clockwise

1. TOOTH GEOMETRY AND MATERIAL

(geometry calculation according to ISO 21771:2007, DIN ISO 21771)

		------- GEAR 1	-------- GEAR 2 --
Center distance (mm)	[a]	95.000	
Center distance tolerance	ISO 286:2010 Measure js7		
Normal module (mm)	[mn]	0.8000	
Pressure angle at normal section (°)	[alfn]	20.0000	
Helix angle at reference circle (°)	[beta]	12.0000	
Number of teeth	[z]	47	185
Facewidth (mm)	[b]	30.00	30.00
Hand of gear		left	right
Accuracy grade	[Q-ISO 1328:1995]	5	5
Inner diameter (mm)	[di]	0.00	42.00
Inner diameter of gear rim (mm)	[dbi]	0.00	132.92

Material
Gear 1: 18CrNiMo7-6, Case-carburized steel, case-hardened
ISO 6336-5 Figure 9/10 (MQ), Core hardness >=30HRC
Gear 2: 18CrNiMo7-6, Case-carburized steel, case-hardened
ISO 6336-5 Figure 9/10 (MQ), Core hardness >=30HRC

		------- GEAR 1	-------- GEAR 2 --
Surface hardness		HRC 61	HRC 61
Material quality according to ISO 6336:2006 Normal (Life factors ZNT and YNT >=0.85)			
Fatigue strength. tooth root stress (N/mm²)	[σFlim]	500.00	500.00
Fatigue strength for Hertzian pressure (N/mm²)	[σHlim]	1500.00	1500.00
Tensile strength (N/mm²)	[σB]	1200.00	1200.00
Yield point (N/mm²)	[σS]	850.00	850.00
Young's modulus (N/mm²)	[E]	206000	206000
Poisson's ratio	[v]	0.300	0.300
Roughness average value DS, flank (µm)	[RAH]	0.30	0.30
Roughness average value DS, root (µm)	[RAF]	1.00	1.00

Mean roughness height, Rz, flank (µm)	[RZH]	2.00	2.00
Mean roughness height, Rz, root (µm)	[RZF]	6.00	6.00

Gear reference profile 1 :
Reference profile (Own input)

Dedendum coefficient	[hfP*]	1.400
Root radius factor	[rhofP*]	0.393 (rhofPmax*=0.394)
Addendum coefficient	[haP*]	1.150
Tip radius factor	[rhoaP*]	0.000
Protuberance height coefficient	[hprP*]	0.000
Protuberance angle	[alfprP]	0.000
Tip form height coefficient	[hFaP*]	0.000
Ramp angle	[alfKP]	0.000

not topping

Gear reference profile 2 :
Reference profile (Own input)

Dedendum coefficient	[hfP*]	1.400
Root radius factor	[rhofP*]	0.393 (rhofPmax*=0.394)
Addendum coefficient	[haP*]	1.150
Tip radius factor	[rhoaP*]	0.000
Protuberance height coefficient	[hprP*]	0.000
Protuberance angle	[alfprP]	0.000
Tip form height coefficient	[hFaP*]	0.000
Ramp angle	[alfKP]	0.000

not topping

Summary of reference profile gears:

Dedendum reference profile	[hfP*]	1.400	1.400
Tooth root radius Refer. profile	[rofP*]	0.393	0.393
Addendum Reference profile	[haP*]	1.150	1.150
Protuberance height coefficient	[hprP*]	0.000	0.000
Protuberance angle (°)	[alfprP]	0.000	0.000
Tip form height coefficient	[hFaP*]	0.000	0.000
Ramp angle (°)	[alfKP]	0.000	0.000

Type of profile modification:for high load capacity gearboxe

Tip relief (µm)	[Ca]	3.0	3.0

Lubrication type		Oil bath lubrication
Type of oil (Own input)		Castrol ATF Dex II Multivehicle
Lubricant base		Mineral-oil base
Kinem. viscosity oil at 40 °C (mm²/s)	[nu40]	39.00
Kinem. viscosity oil at 100 °C (mm²/s)	[nu100]	7.50
Specific density at 15 °C (kg/dm³)	[roOil]	0.870
Oil temperature (°C)	[TS]	65.000

		------- GEAR 1 --------	GEAR 2 --
Overall transmission ratio	[itot]	-3.936	
Gear ratio	[u]	3.936	
Transverse module (mm)	[mt]	0.818	
Pressure angle at pitch circle (°)	[alft]	20.410	
Working transverse pressure angle (°)	[alfwt]	20.615	
	[alfwt.e/i]	20.643 /	20.587
Working pressure angle at normal section (°)	[alfwn]	20.200	
Helix angle at operating pitch circle (°)	[betaw]	12.016	

KISSSOFT
Calculation programs for machine design

Base helix angle (°)	[betab]	11.267	
Reference center distance (mm)	[ad]	94.873	
Sum of profile shift coefficients	[Summexi]	0.1593	
Profile shift coefficient	[x]	0.0907	0.0685
Tooth thickness (Arc) (module) (module)	[sn*]	1.6369	1.6207
Tip alteration (mm)	[k*mn]	0.009	0.009
Reference diameter (mm)	[d]	38.440	151.306
Base diameter (mm)	[db]	36.027	141.807
Tip diameter (mm)	[da]	40.444	153.275
(mm)	[da.e/i]	40.444 / 40.434	153.275 / 153.265
Tip diameter allowances (mm)	[Ada.e/i]	0.000 / -0.010	0.000 / -0.010
Tip form diameter (mm)	[dFa]	40.444	153.275
(mm)	[dFa.e/i]	40.444 / 40.434	153.275 / 153.265
Active tip diameter (mm)	[dNa]	40.444	153.275
Active tip diameter (mm)	[dNa.e/i]	40.444 / 40.434	153.275 / 153.265
Operating pitch diameter (mm)	[dw]	38.491	151.509
(mm)	[dw.e/i]	38.498 / 38.484	151.537 / 151.481
Root diameter (mm)	[df]	36.345	149.176
Generating Profile shift coefficient	[xE.e/i]	0.0152/ -0.0707	-0.0689/ -0.2062
Manufactured root diameter with xE (mm)	[df.e/i]	36.224 / 36.087	148.956 / 148.736
Theoretical tip clearance (mm)	[c]	0.190	0.190
Effective tip clearance (mm)	[c.e/i]	0.432 / 0.282	0.342 / 0.233
Active root diameter (mm)	[dNf]	37.068	149.877
(mm)	[dNf.e/i]	37.098 / 37.045	149.916 / 149.845
Root form diameter (mm)	[dFf]	37.036	149.661
(mm)	[dFf.e/i]	36.957 / 36.871	149.461 / 149.263
Reserve (dNf-dFf)/2 (mm)	[cF.e/i]	0.113 / 0.044	0.327 / 0.192
Addendum (mm)	[ha=mn*(haP*+x+k)]	1.002	0.984
(mm)	[ha.e/i]	1.002 / 0.997	0.984 / 0.979
Dedendum (mm)	[hf=mn*(hfP*-x)]	1.047	1.065
(mm)	[hf.e/i]	1.108 / 1.177	1.175 / 1.285
Roll angle at dFa (°)	[xsi_dFa.e/i]	29.230 / 29.195	23.504 / 23.493
Roll angle to dNa (°)	[xsi_dNa.e/i]	29.230 / 29.195	23.504 / 23.493
Roll angle to dNf (°)	[xsi_dNf.e/i]	14.075 / 13.717	19.652 / 19.562
Roll angle at dFf (°)	[xsi_dFf.e/i]	13.102 / 12.476	19.076 / 18.822
Tooth height (mm)	[h]	2.049	2.049
Virtual gear no. of teeth	[zn]	49.957	196.639
Normal tooth thickness at tip circle (mm)	[san]	0.485	0.555
(mm)	[san.e/i]	0.443 / 0.386	0.478 / 0.393
Normal tooth thickness on tip form circle (mm)	[sFan]	0.485	0.555
(mm)	[sFan.e/i]	0.443 / 0.386	0.478 / 0.393
Normal space width at root circle (mm)	[efn]	0.603	0.476
(mm)	[efn.e/i]	0.628 / 0.662	0.485 / 0.494
Max. sliding velocity at tip (m/s)	[vga]	1.109	1.110
Specific sliding at the tip	[zetaa]	0.329	0.410
Specific sliding at the root	[zetaf]	-0.694	-0.491
Mean specific sliding	[zetam]	0.370	
Sliding factor on tip	[Kga]	0.157	0.157
Sliding factor on root	[Kgf]	-0.157	-0.157
Pitch on reference circle (mm)	[pt]	2.569	
Base pitch (mm)	[pbt]	2.408	
Transverse pitch on contact-path (mm)	[pet]	2.408	
Lead height (mm)	[pz]	568.145	2236.313
Axial pitch (mm)	[px]	12.088	
Length of path of contact (mm)	[ga, e/i]	4.828 (4.877 / 4.754)	
Length T1-A, T2-A (mm)	[T1A, T2A]	4.362(4.312/ 4.425)	29.086(29.086/ 29.073)

Length T1-B (mm)	[T1B, T2B]	4.374(	4.374/	6.771)	29.074(	29.025/	26.727)
Length T1-C (mm)	[T1C, T2C]	6.776(	6.766/	6.786)	26.672(	26.632/	26.711)
Length T1-D (mm)	[T1D, T2D]	9.178(	9.129/	6.833)	24.270(	24.270/	26.664)
Length T1-E (mm)	[T1E, T2E]	9.190(	9.190/	9.179)	24.258(	24.208/	24.319)
Length T1-T2 (mm)	[T1T2]			33.448 (	33.398 /	33.498)	
Diameter of single contact point B (mm)	[d-B]	37.073(	37.073/	38.488)	153.266(	153.229/	151.547)
Diameter of single contact point D (mm)	[d-D]	40.434(	40.389/	38.532)	149.884(	149.884/	151.503)
Addendum contact ratio	[eps]	1.002(	1.006/	0.994)	1.002(	1.019/	0.980)
Minimal length of contact line (mm)	[Lmin]			61.295			

Transverse contact ratio	[eps_a]		2.005	
Transverse contact ratio with allowances	[eps_a.e/m/i]	2.025 /	2.000 /	1.974
Overlap ratio	[eps_b]		2.482	
Total contact ratio	[eps_g]		4.486	
Total contact ratio with allowances	[eps_g.e/m/i]	4.507 /	4.481 /	4.456

2. FACTORS OF GENERAL INFLUENCE

		------- GEAR 1 --------	GEAR 2 --
Nominal circum. force at pitch circle (N)	[Ft]	3642.0	
Axial force (N)	[Fa]	774.1	
Radial force (N)	[Fr]	1355.2	
Normal force (N)	[Fnorm]	3962.4	
Nominal circumferential force per mm (N/mm)	[w]	121.40	
Only as information: Forces at operating pitch circle:			
Nominal circumferential force (N)	[Ftw]	3637.2	
Axial force (N)	[Faw]	774.1	
Radial force (N)	[Frw]	1368.2	
Circumferential speed reference circle (m/s)	[v]	7.04	
Circumferential speed operating pitch circle (m/s)	[v(dw)]	7.05	

Running-in value (µm)	[yp]	0.4	
Running-in value (µm)	[yf]	0.4	
Correction coefficient	[CM]	0.800	
Gear body coefficient	[CR, bs/b, sr/mn]	0.962	(0.250, 9.885)
Basic rack factor	[CBS]	0.900	
Material coefficient	[E/Est]	1.000	
Singular tooth stiffness (N/mm/µm)	[c']	13.357	
Meshing stiffness (N/mm/µm)	[cgalf]	23.422	
Meshing stiffness (N/mm/µm)	[cgbet]	19.909	
Reduced mass (kg/mm)	[mRed]	0.00484	
Resonance speed (min-1)	[nE1]	14141	
Resonance ratio (-)	[N]	0.248	
Subcritical range			
Running-in value (µm)	[ya]	0.4	

KHb calculated according to ISO 6336-1: 2006, Annex E (takes into account K_A*K_V)
Shaft data shaft1ststage.W10
Shaft data shaft2ndstage.W10
Torque (0: -, 1: <I, 2: <II, 3: <from shaft calculation) -1 3
KHb is determined as biggest value out of following variants
(axis deviation error fma and meshing error fHb):
fma/fHb (µm): -0.0/ -8.8; 3: -0.0/ 8.8; 4: 0.0/ -8.8; 5: 0.0/ 8.8
(For intermediate results refer to file: KHbeta_calc12.tmp)

Dynamic factor	[KV]	1.057
Face load factor - flank	[KHb]	1.330

- Tooth root	[KFb]	1.302	
- Scuffing	[KBb]	1.330	
Transverse load factor - flank	[KHa]	1.030	
- Tooth root	[KFa]	1.030	
- Scuffing	[KBa]	1.030	
Helical load factor scuffing	[Kbg]	1.300	
Number of load cycles (in mio.)	[NL]	1050.000	266.757

3. TOOTH ROOT STRENGTH

Calculation of Tooth form coefficients according method: B

		GEAR 1	GEAR 2
Calculated with manufacturing profile shift	[xE.e]	0.0152	-0.0689
Tooth form factor	[YF]	1.11	1.15
Stress correction factor	[YS]	2.09	2.24
Working angle (°)	[alfFen]	18.11	19.71
Bending moment arm (mm)	[hF]	0.73	0.87
Tooth thickness at root (mm)	[sFn]	1.79	1.91
Tooth root radius (mm)	[roF]	0.45	0.38

(hF* = 0.913/ 1.089 sFn* = 2.235/ 2.388 roF* = 0.559/ 0.470)
(den (mm) =
39.947/ 157.444 dsFn(mm) = 36.571/ 149.288 alfsFn(°) = 30.00/ 30.00 qs = 1.997/ 2.543)

Helix angle factor	[Ybet]		0.900	
Deep tooth factor	[YDT]		1.000	
Gear rim factor	[YB]	1.00		1.00
Effective facewidth (mm)	[beff]	30.00		30.00
Nominal stress at tooth root (N/mm²)	[sigF0]	317.40		351.97
Tooth root stress (N/mm²)	[sigF]	562.68		623.97
Permissible bending stress at root of Test-gear				
Notch sensitivity factor	[YdrelT]	0.995		1.000
Surface factor	[YRrelT]	1.031		1.031
size factor (Tooth root)	[YX]	1.000		1.000
Finite life factor	[YNT]	0.889		0.914
[YdrelT*YRrelT*YX*YNT]		0.913		0.943
Alternating bending factor (mean stress influence coefficient)	[YM]		1.000	1.000
Stress correction factor	[Yst]		2.00	
Yst*sigFlim (N/mm²)	[sigFE]	1000.00		1000.00
Permissible tooth root stress (N/mm²)	[sigFP=sigFG/SFmin]	651.86		673.61
Limit strength tooth root (N/mm²)	[sigFG]	912.60		943.06
Required safety	[SFmin]	1.40		1.40
Safety for tooth root stress	[SF=sigFG/sigF]	1.62		1.51
Transmittable power (kW)	[kWRating]	29.72		27.70

4. SAFETY AGAINST PITTING (TOOTH FLANK)

		GEAR 1	GEAR 2
Zone factor	[ZH]		2.436
Elasticity factor (√N/mm²)	[ZE]		189.812

Contact ratio factor	[Zeps]	0.706	
Helix angle factor	[Zbet]	1.011	
Effective facewidth (mm)	[beff]	30.00	
Nominal contact stress (N/mm²)	[sigH0]	657.25	
Contact stress at operating pitch circle (N/mm²)	[sigHw]	884.29	
Single tooth contact factor	[ZB,ZD]	1.00	1.00
Contact stress (N/mm²)	[sigHB, sigHD]	884.29	884.29
Lubrication coefficient at NL	[ZL]	0.927	0.927
Speed coefficient at NL	[ZV]	0.991	0.991
Roughness coefficient at NL	[ZR]	1.016	1.016
Material pairing coefficient at NL	[ZW]	1.000	1.000
Finite life factor	[ZNT]	0.911	0.950
	[ZL*ZV*ZR*ZNT]	0.850	0.886
Limited pitting is permitted:	No		
Size factor (flank)	[ZX]	1.000	1.000
Permissible contact stress (N/mm²)	[sigHP=sigHG/SHmin]	1158.62	1208.36
Pitting stress limit (N/mm²)	[sigHG]	1274.48	1329.19
Required safety	[SHmin]	1.10	1.10
Safety factor for contact stress at operating pitch circle			
	[SHw]	1.44	1.50
Safety for stress at single tooth contact	[SHBD=sigHG/sigHBD]	1.44	1.50
(Safety regarding transmittable torque)	[(SHBD)^2]	2.08	2.26
Transmittable power (kW)	[kWRating]	44.04	47.91

4b. MICROPITTING ACCORDING TO ISO/TR 15144-1:2014

Calculation did not run. (Lubricant: Load stage micropitting test is unknown.)

5. SCUFFING LOAD CAPACITY

Calculation method according to ISO TR 13989:2000

Lubrication coefficient (for lubrication type)	[XS]	1.000	
Scuffing test and load stage	[FZGtest]	FZG - Test A / 8.3 / 90 (ISO 14635 - 1)	12
Multiple meshing factor	[Xmp]	1.000	
Relative structure coefficient (Scuffing)	[XWrelT]	1.000	
Thermal contact factor (N/mm/s^.5/K)	[BM]	13.780	13.780
Relevant tip relief (µm)	[Ca]	3.00	3.00
Optimal tip relief (µm)	[Ceff]	6.48	
Ca taken as optimal in the calculation (0=no, 1=yes)		1	1
Effective facewidth (mm)	[beff]	30.000	
Applicable circumferential force/facewidth (N/mm)	[wBt]	219.765	
Kbg = 1.300, wBt*Kbg = 285.694			
Angle factor (ε1:1.002, ε2:1.002)	[Xalfbet]	0.982	
Flash temperature-criteria			
Lubricant factor	[XL]	0.875	
Tooth mass temperature (°C) (theMi = theoil + XS*0.47*Xmp*theflm)	[theMi]	67.41	
Average flash temperature (°C)	[theflm]	5.12	
Scuffing temperature (°C)	[theS]	363.63	
Coordinate gamma (point of highest temp.)	[Gamma]	-0.205	

KISSSOFT
Calculation programs for machine design

[Gamma.A]=-0.356 [Gamma.E]=0.356		
Highest contact temp. (°C)	[theB]	75.96
Flash factor (°K*N^-.75*s^.5*m^-.5*mm)	[XM]	50.058
Approach factor	[XJ]	1.000
Load sharing factor	[XGam]	0.565
Dynamic viscosity (mPa*s)	[etaM]	14.32 (65.0 °C)
Coefficient of friction	[mym]	0.052
Required safety	[SBmin]	2.000
Safety factor for scuffing (flash temperature)	[SB]	27.250
Integral temperature-criteria		
Lubricant factor	[XL]	1.000
Tooth mass temperature (°C)	[theMC]	67.47
(theMC = theoil + XS*0.70*theflaint)		
Mean flash temperature (°C)	[theflaint]	3.52
Integral scuffing temperature (°C)	[theSint]	366.33
Flash factor (°K*N^-.75*s^.5*m^-.5*mm)	[XM]	50.058
Running-in factor (well run in)	[XE]	1.000
Contact ratio factor	[Xeps]	0.220
Dynamic viscosity (mPa*s)	[etaOil]	14.32 (65.0 °C)
Mean coefficient of friction	[mym]	0.067
Geometry factor	[XBE]	0.161
Meshing factor	[XQ]	1.000
Tip relief factor	[XCa]	1.954
Integral tooth flank temperature (°C)	[theint]	72.75
Required safety	[SSmin]	1.800
Safety factor for scuffing (intg.-temp.)	[SSint]	5.035
Safety referring to transmittable torque	[SSL]	38.865

6. MEASUREMENTS FOR TOOTH THICKNESS

		------- Gear 1	------ Gear 2 --		
Tooth thickness deviation		DIN 3967 d26		DIN 3967 d26	
Tooth thickness allowance (normal section) (mm)	[As.e/i]	-0.044 /	-0.094	-0.080 /	-0.160
Number of teeth spanned	[k]	6.000		22.000	
Base tangent length (no backlash) (mm)	[Wk]	13.600		53.022	
Actual base tangent length ('span') (mm)	[Wk.e/i]	13.559 /	13.512	52.947 /	52.872
(mm)	[ΔWk.e/i]	-0.041 /	-0.088	-0.075 /	-0.150
Diameter of measuring circle (mm)	[dMWk.m]	38.394		151.003	
Theoretical diameter of ball/pin (mm)	[DM]	1.364		1.343	
Effective diameter of ball/pin (mm)	[DMeff]	1.400		1.400	
Radial single-ball measurement backlash free (mm)	[MrK]	20.289		76.722	
Radial single-ball measurement (mm)	[MrK.e/i]	20.235 /	20.172	76.615 /	76.507
Diameter of measuring circle (mm)	[dMMr.m]	38.502		151.240	
Diametral measurement over two balls without clearance (mm)	[MdK]	40.556		153.439	
Diametral two ball measure (mm)	[MdK.e/i]	40.448 /	40.323	153.225 /	153.009
Diametral measurement over pins without clearance (mm)	[MdR]	40.578		153.444	
Measurement over pins according to DIN 3960 (mm)	[MdR.e/i]	40.470 /	40.345	153.230 /	153.015
Measurement over 2 pins (free) according to AGMA 2002 (mm)	[dk2f.e/i]	40.447 /	40.322	153.225 /	153.009
Measurement over 2 pins (transverse) according to AGMA 2002 (mm)	[dk2t.e/i]	40.491 /	40.366	153.236 /	153.020
Measurement over 3 pins (axial) according to AGMA 2002 (mm)	[dk3A.e/i]	40.470 /	40.345	153.230 /	153.015

Chordal tooth thickness (no backlash) (mm)	[sc]	1.309	1.297
Actual chordal tooth thickness (mm)	[sc.e/i]	1.265 / 1.215	1.217 / 1.137
Reference chordal height from da.m (mm)	[ha]	1.010	0.984
Tooth thickness (Arc) (mm)	[sn]	1.309	1.297
(mm)	[sn.e/i]	1.265 / 1.215	1.217 / 1.137
Backlash free center distance (mm)	[aControl.e/i]	94.830 / 94.650	
Backlash free center distance, allowances (mm)	[jta]	-0.170 / -0.350	
dNf.i with aControl (mm)	[dNf0.i]	36.646	149.237
Reserve (dNf0.i-dFf.e)/2 (mm)	[cF0.i]	-0.155	-0.112
Tip clearance (mm)	[c0.i(aControl)]	-0.050	-0.100
Center distance allowances (mm)	[Aa.e/i]	0.018 / -0.018	
Circumferential backlash from Aa (mm)	[jtw_Aa.e/i]	0.013 / -0.013	
Radial clearance (mm)	[jrw]	0.368 / 0.152	
Circumferential backlash (transverse section) (mm)	[jtw]	0.273 / 0.114	
Normal backlash (mm)	[jnw]	0.251 / 0.105	
Torsional angle at entry with fixed output:			
Entire torsional angle (°)	[j.tSys]	0.8133/ 0.3387	

7. GEAR ACCURACY

		------- GEAR 1	-------- GEAR 2 --
According to ISO 1328-1:1995, ISO 1328-2:1997			
Accuracy grade	[Q]	5	5
Single pitch deviation (µm)	[fptT]	5.00	6.00
Base circle pitch deviation (µm)	[fpbT]	4.70	5.60
Sector pitch deviation over k/8 pitches (µm)	[Fpk/8T]	8.00	13.00
Profile form deviation (µm)	[ffaT]	4.00	5.50
Profile slope deviation (µm)	[fHaT]	3.30	4.40
Total profile deviation (µm)	[FaT]	5.00	7.00
Helix form deviation (µm)	[ffbT]	6.00	6.50
Helix slope deviation (µm)	[fHbT]	6.00	6.50
Total helix deviation (µm)	[FbT]	8.00	9.00
Total cumulative pitch deviation (µm)	[FpT]	14.00	24.00
Runout (µm)	[FrT]	11.00	20.00
Single flank composite, total (µm)	[FisT]	20.00	31.00
Single flank composite, tooth-to-tooth (µm)	[fisT]	6.00	7.00
Radial composite, total (µm)	[FidT]	14.00	22.00
Radial composite, tooth-to-tooth (µm)	[fidT]	2.70	2.80

8. ADDITIONAL DATA

Maximal possible center distance (eps_a=1.0)	[aMAX]	95.879	
Mass (kg)	[m]	0.272	3.894
Total mass (kg)	[m]	4.166	
Moment of inertia (system with reference to the drive):			
calculation without consideration of the exact tooth shape			
single gears ((da+df)/2...di) (kg*m²)	[TraeghMom]	5.012e-005	0.01199
System ((da+df)/2...di) (kg*m²)	[TraeghMom]	0.0008239	
Torsional stiffness on input for stopped output:			
Torsional stiffness (MNm/rad)	[cr]	0.194	
Torsion when subjected to nominal torque (°)	[delcr]	0.021	
Mean coeff. of friction (acc. Niemann)	[mum]	0.065	

Wear sliding coef. by Niemann	[zetw]	0.741	
Gear power loss (kW)	[PVZ]	0.144	
(Meshing efficiency (%)	[etaz]	99.440)	
Sound pressure level (according to Masuda)	[dB(A)]	69.6	

Indications for the manufacturing by wire cutting:

Deviation from theoretical tooth trace (µm)	[WireErr]	263.8		67.2
Permissible deviation (µm)	[Fb/2]	4.0		4.5

9. MODIFICATIONS AND TOOTH FORM DEFINITION

Profile and tooth trace modifications for gear 1

Symmetric (both flanks)

- Crowning Cb = 6.000µm (rcrown=18750mm)
- Helix angle modification, parallel CHb = -1.509µm

Positive modification increases the left hand helix angle and decreases the right hand helix angle (ISO 21771)

CHb=-1.509µm -> β.eff=11.9971°-left

- Tip relief, arc-like Caa = 3.000µm LCa = 1.147*mn dCa = 39.644mm

Profile and tooth trace modifications for gear 2

Symmetric (both flanks)

- Crowning Cb = 0.430µm (rcrown=261839mm)
- Helix angle modification, parallel CHb = -1.509µm

Positive modification increases the left hand helix angle and decreases the right hand helix angle (ISO 21771)

CHb=-1.509µm -> β.eff=12.0029°-right

- Tip relief, arc-like Caa = 3.000µm LCa = 1.339*mn dCa = 152.475mm

Tip relief verification

Diameter (mm)	[dcheck]	40.418	153.249
Tip relief left/right (µm)	[Ca L/R]	2.8 / 2.8	2.8 / 2.8

Data for the tooth form calculation :

Calculation of Gear 1

Tooth form, Gear 1, Step 1: Automatic (final machining)

haP*= 1.277, hfP*= 1.400, rofP*= 0.393

Calculation of Gear 2

Tooth form, Gear 2, Step 1: Automatic (final machining)

haP*= 1.365, hfP*= 1.400, rofP*= 0.393

10. SERVICE LIFE, DAMAGE, LOAD DISTRIBUTION

Required safety for tooth root	[SFmin]	1.40
Required safety for tooth flank	[SHmin]	1.10

Service life (calculated with required safeties):

System service life (h)	[Hatt]	>	1000000

Tooth root service life (h)	[HFatt]	1e+006	1e+006
Tooth flank service life (h)	[HHatt]	1e+006	1e+006

Note: The entry 1e+006 h means that the Service life > 1,000,000 h.

Damage calculated on the basis of the required service life [H] (5000.0 h)

F1%	F2%	H1%	H2%
0.00	0.00	0.00	0.00

Calculation of the factors required to define reliability R(t) according to B. Bertsche with Weibull distribution:
R(t) = 100 * Exp(-((t*fac - t0)/(T - t0))^b) %; t (h)

Gear		fac	b	t0	T	R(H)%
1	Tooth root	210000	1.7	9.654e+029	1.484e+030	100.00
1	Tooth flank	210000	1.3	9.014e+029	4.295e+030	100.00
2	Tooth root	53351	1.7	9.654e+029	1.484e+030	100.00
2	Tooth flank	53351	1.3	9.014e+029	4.295e+030	100.00

Reliability of the configuration for required service life (%) 100.00 (Bertsche)

Load distribution (ISO6336-1, Annex E)

$K_{H\beta}$	w_m (N/mm)	w_I (N/mm)	w_{II} (N/mm)	w_{max} (N/mm)	σ_{Hm} (N/mm^2)	σ_{HI} (N/mm^2)	σ_{HII} (N/mm^2)	σ_{Hmax} (N/mm^2)
1.330	171.2	199.2	175.4	227.6	755.5	815.0	764.8	871.2

Index m, I, II stand for: Middle of facewidth, Side I and Side II

REMARKS:

- Specifications with [.e/i] imply: Maximum [e] and Minimal value [i] with consideration of all tolerances
  Specifications with [.m] imply: Mean value within tolerance
- For the backlash tolerance, the center distance tolerances and the tooth thickness deviation are taken into account. Shown is the maximal and the minimal backlash corresponding the largest resp. the smallest allowances
  The calculation is done for the operating pitch circle.
- Calculation of Zbet according Corrigendum 1 ISO 6336-2:2008 with Zbet = 1/(COS(beta)^0.5)
- Details of calculation method:
  cg according to method B
  KV according to method B
- The logarithmically interpolated value taken from the values for the fatigue strength and the static strength, based on the number of load cycles, is used for coefficients ZL, ZV, ZR, ZW, ZX, YdrelT, YRrelT and YX..

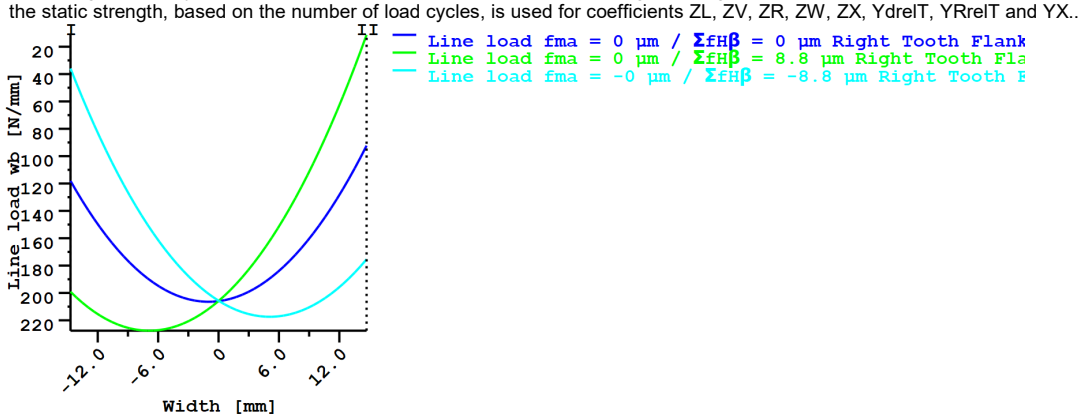

Working flank: Right Tooth Flank

at nominal load
fma = 0 µm / ΣfHβ = 0 µm:
wbmax = 206.4556 N/mm wbm = 171.1747 N/mm KHbeta = 1.2061
fma = 0 µm / ΣfHβ = 8.8 µm:
wbmax = 227.5839 N/mm wbm = 171.1747 N/mm KHbeta = 1.3295
fma = 0 µm / ΣfHβ = -8.8 µm:
wbmax = 0.0000 N/mm wbm = 0.0000 N/mm KHbeta = 0.0000
fma = -0 µm / ΣfHβ = 8.8 µm:
wbmax = 0.0000 N/mm wbm = 0.0000 N/mm KHbeta = 0.0000
fma = -0 µm / ΣfHβ = -8.8 µm:
wbmax = 217.4232 N/mm wbm = 171.1747 N/mm KHbeta = 1.2702

wbm = Kv * KA * Kγ * (Ft/b) / cos(αwt)

Figure: Load distribution

End of Report lines: 549

KISSsoft Release 03/2017 F

KISSsoft University license - Universidade do Porto

File

Name : GearZ3Z4Torque

Changed by: Carlos Rodrigues on: 02.07.2018 at: 23:53:10

CALCULATION OF A HELICAL GEAR PAIR

Drawing or article number:
Gear 1: Z3
Gear 2: Z4

Calculation method ISO 6336:2006 Method B

		------- GEAR 1	-------- GEAR 2 --
Power (kW)	[P]	25.657	
Speed (1/min)	[n]	889.2	300.3
Torque (Nm)	[T]	275.5	815.8
Application factor	[KA]	1.25	
Required service life (h)	[H]	5000.00	
Gear driving (+) / driven (-)		+	-

Working flank gear 1: Right flank
Sense of rotation gear 1 clockwise

1. TOOTH GEOMETRY AND MATERIAL

(geometry calculation according to ISO 21771:2007, DIN ISO 21771)

		------- GEAR 1	-------- GEAR 2 --
Center distance (mm)	[a]	130.000	
Center distance tolerance	ISO 286:2010 Measure js7		
Normal module (mm)	[mn]	1.2500	
Pressure angle at normal section (°)	[alfn]	20.0000	
Helix angle at reference circle (°)	[beta]	12.0000	
Number of teeth	[z]	51	151
Facewidth (mm)	[b]	40.00	40.00
Hand of gear		right	left
Accuracy grade	[Q-ISO 1328:1995]	6	6
Inner diameter (mm)	[di]	0.00	50.00
Inner diameter of gear rim (mm)	[dbi]	0.00	177.47

Material
Gear 1: 18CrNiMo7-6, Case-carburized steel, case-hardened
ISO 6336-5 Figure 9/10 (MQ), Core hardness >=30HRC
Gear 2: 18CrNiMo7-6, Case-carburized steel, case-hardened
ISO 6336-5 Figure 9/10 (MQ), Core hardness >=30HRC

		------- GEAR 1	-------- GEAR 2 --
Surface hardness		HRC 61	HRC 61
Material quality according to ISO 6336:2006 Normal (Life factors ZNT and YNT >=0.85)			
Fatigue strength. tooth root stress (N/mm²)	[σFlim]	500.00	500.00
Fatigue strength for Hertzian pressure (N/mm²)	[σHlim]	1500.00	1500.00
Tensile strength (N/mm²)	[σB]	1200.00	1200.00
Yield point (N/mm²)	[σS]	850.00	850.00
Young's modulus (N/mm²)	[E]	206000	206000
Poisson's ratio	[v]	0.300	0.300
Roughness average value DS, flank (µm)	[RAH]	0.50	0.50

Roughness average value DS, root (µm)	[RAF]	1.00	1.00
Mean roughness height, Rz, flank (µm)	[RZH]	3.00	3.00
Mean roughness height, Rz, root (µm)	[RZF]	6.00	6.00

Gear reference profile 1 :
Reference profile (Own input)

Dedendum coefficient	[hfP*]	1.431
Root radius factor	[rhofP*]	0.377 (rhofPmax*=0.378)
Addendum coefficient	[haP*]	1.181
Tip radius factor	[rhoaP*]	0.000
Protuberance height coefficient	[hprP*]	0.000
Protuberance angle	[alfprP]	0.000
Tip form height coefficient	[hFaP*]	0.000
Ramp angle	[alfKP]	0.000

not topping

Gear reference profile 2 :
Reference profile (Own input)

Dedendum coefficient	[hfP*]	1.431
Root radius factor	[rhofP*]	0.377 (rhofPmax*=0.378)
Addendum coefficient	[haP*]	1.181
Tip radius factor	[rhoaP*]	0.000
Protuberance height coefficient	[hprP*]	0.000
Protuberance angle	[alfprP]	0.000
Tip form height coefficient	[hFaP*]	0.000
Ramp angle	[alfKP]	0.000

not topping

Summary of reference profile gears:

Dedendum reference profile	[hfP*]	1.431	1.431
Tooth root radius Refer. profile	[rofP*]	0.377	0.377
Addendum Reference profile	[haP*]	1.181	1.181
Protuberance height coefficient	[hprP*]	0.000	0.000
Protuberance angle (°)	[alfprP]	0.000	0.000
Tip form height coefficient	[hFaP*]	0.000	0.000
Ramp angle (°)	[alfKP]	0.000	0.000

Type of profile modification: none (only running-in)

Tip relief (µm)	[Ca]	2.0	2.0

Lubrication type		Oil bath lubrication
Type of oil (Own input)		Castrol ATF Dex II Multivehicle
Lubricant base		Mineral-oil base
Kinem. viscosity oil at 40 °C (mm²/s)	[nu40]	39.00
Kinem. viscosity oil at 100 °C (mm²/s)	[nu100]	7.50
Specific density at 15 °C (kg/dm³)	[roOil]	0.870
Oil temperature (°C)	[TS]	65.000

		------- GEAR 1 --------	GEAR 2 --
Overall transmission ratio	[itot]		-2.961
Gear ratio	[u]		2.961
Transverse module (mm)	[mt]		1.278
Pressure angle at pitch circle (°)	[alft]		20.410
Working transverse pressure angle (°)	[alfwt]		21.484
	[alfwt.e/i]	21.507 /	21.462
Working pressure angle at normal section (°)	[alfwn]		21.050

Helix angle at operating pitch circle (°)	[betaw]	12.084	
Base helix angle (°)	[betab]	11.267	
Reference center distance (mm)	[ad]	129.071	
Sum of profile shift coefficients	[Summexi]	0.7625	
Profile shift coefficient	[x]	0.3715	0.3910
Tooth thickness (Arc) (module) (module)	[sn*]	1.8412	1.8554
Tip alteration (mm)	[k*mn]	0.000	0.000
Reference diameter (mm)	[d]	65.174	192.967
Base diameter (mm)	[db]	61.083	180.852
Tip diameter (mm)	[da]	69.055	196.897
(mm)	[da.e/i]	69.055 / 69.045	196.897 / 196.887
Tip diameter allowances (mm)	[Ada.e/i]	0.000 / -0.010	0.000 / -0.010
Tip form diameter (mm)	[dFa]	69.055	196.897
(mm)	[dFa.e/i]	69.055 / 69.045	196.897 / 196.887
Active tip diameter (mm)	[dNa]	69.055	196.897
Active tip diameter (mm)	[dNa.e/i]	69.055 / 69.045	196.897 / 196.887
Operating pitch diameter (mm)	[dw]	65.644	194.356
(mm)	[dw.e/i]	65.654 / 65.633	194.386 / 194.327
Root diameter (mm)	[df]	62.525	190.367
Generating Profile shift coefficient	[xE.e/i]	0.3056/ 0.2396	0.3031/ 0.2151
Manufactured root diameter with xE (mm)	[df.e/i]	62.361 / 62.196	190.147 / 189.927
Theoretical tip clearance (mm)	[c]	0.289	0.289
Effective tip clearance (mm)	[c.e/i]	0.534 / 0.379	0.479 / 0.351
Active root diameter (mm)	[dNf]	63.505	191.515
(mm)	[dNf.e/i]	63.542 / 63.475	191.558 / 191.479
Root form diameter (mm)	[dFf]	63.381	191.061
(mm)	[dFf.e/i]	63.256 / 63.135	190.859 / 190.658
Reserve (dNf-dFf)/2 (mm)	[cF.e/i]	0.204 / 0.110	0.450 / 0.310
Addendum (mm)	[ha=mn*(haP*+x+k)]	1.941	1.965
(mm)	[ha.e/i]	1.941 / 1.936	1.965 / 1.960
Dedendum (mm)	[hf=mn*(hfP*-x)]	1.324	1.300
(mm)	[hf.e/i]	1.407 / 1.489	1.410 / 1.520
Roll angle at dFa (°)	[xsi_dFa.e/i]	30.215 / 30.195	24.664 / 24.656
Roll angle to dNa (°)	[xsi_dNa.e/i]	30.215 / 30.195	24.664 / 24.656
Roll angle to dNf (°)	[xsi_dNf.e/i]	16.422 / 16.193	20.004 / 19.928
Roll angle at dFf (°)	[xsi_dFf.e/i]	15.420 / 14.977	19.322 / 19.122
Tooth height (mm)	[h]	3.265	3.265
Virtual gear no. of teeth	[zn]	54.209	160.500
Normal tooth thickness at tip circle (mm)	[san]	0.668	0.806
(mm)	[san.e/i]	0.610 / 0.541	0.728 / 0.643
Normal tooth thickness on tip form circle (mm)	[sFan]	0.668	0.806
(mm)	[sFan.e/i]	0.610 / 0.541	0.728 / 0.643
Normal space width at root circle (mm)	[efn]	0.797	0.701
(mm)	[efn.e/i]	0.818 / 0.842	0.708 / 0.717
Max. sliding velocity at tip (m/s)	[vga]	0.509	0.415
Specific sliding at the tip	[zetaa]	0.339	0.339
Specific sliding at the root	[zetaf]	-0.514	-0.514
Mean specific sliding	[zetam]	0.339	
Sliding factor on tip	[Kga]	0.166	0.136
Sliding factor on root	[Kgf]	-0.136	-0.166
Pitch on reference circle (mm)	[pt]	4.015	
Base pitch (mm)	[pbt]	3.763	
Transverse pitch on contact-path (mm)	[pet]	3.763	
Lead height (mm)	[pz]	963.277	2852.055
Axial pitch (mm)	[px]	18.888	
Length of path of contact (mm)	[ga, e/i]	7.419 (7.474 / 7.341)	

Length T1-A, T2-A (mm)	[T1A, T2A]	8.686(	8.632/	8.754)	38.926(	38.926/	38.913)
Length T1-B (mm)	[T1B, T2B]	12.343(	12.343/	12.332)	35.269(	35.214/	35.334)
Length T1-C (mm)	[T1C, T2C]	12.021(	12.007/	12.035)	35.591(	35.550/	35.632)
Length T1-D (mm)	[T1D, T2D]	12.449(	12.394/	12.516)	35.163(	35.163/	35.150)
Length T1-E (mm)	[T1E, T2E]	16.106(	16.106/	16.095)	31.506(	31.452/	31.571)
Length T1-T2 (mm)	[T1T2]			47.612 (	47.557 /	47.667)	
Diameter of single contact point B (mm)	[d-B]	65.882(	65.882/	65.874)	194.121(	194.082/	194.169)
Diameter of single contact point D (mm)	[d-D]	65.962(	65.921/	66.013)	194.044(	194.044/	194.035)
Addendum contact ratio	[eps]	1.086(	1.089/	1.079)	0.886(	0.897/	0.872)
Minimal length of contact line (mm)	[Lmin]			79.945			

Transverse contact ratio	[eps_a]		1.972	
Transverse contact ratio with allowances	[eps_a.e/m/i]	1.986 /	1.969 /	1.951
Overlap ratio	[eps_b]		2.118	
Total contact ratio	[eps_g]		4.090	
Total contact ratio with allowances	[eps_g.e/m/i]	4.104 /	4.087 /	4.069

2. FACTORS OF GENERAL INFLUENCE

		------- GEAR 1	-------- GEAR 2 --	
Nominal circum. force at pitch circle (N)	[Ft]		8455.1	
Axial force (N)	[Fa]		1797.2	
Radial force (N)	[Fr]		3146.2	
Normal force (N)	[Fnorm]		9198.8	
Nominal circumferential force per mm (N/mm)	[w]		211.38	
Only as information: Forces at operating pitch circle:				
Nominal circumferential force (N)	[Ftw]		8394.7	
Axial force (N)	[Faw]		1797.2	
Radial force (N)	[Frw]		3304.1	
Circumferential speed reference circle (m/s)	[v]		3.03	
Circumferential speed operating pitch circle (m/s)	[v(dw)]		3.06	
Running-in value (µm)	[yp]		0.6	
Running-in value (µm)	[yf]		0.6	
Correction coefficient	[CM]		0.800	
Gear body coefficient	[CR, bs/b, sr/mn]		0.898	(0.250, 4.983)
Basic rack factor	[CBS]		0.885	
Material coefficient	[E/Est]		1.000	
Singular tooth stiffness (N/mm/µm)	[c']		12.887	
Meshing stiffness (N/mm/µm)	[cgalf]		22.280	
Meshing stiffness (N/mm/µm)	[cgbet]		18.938	
Reduced mass (kg/mm)	[mRed]		0.01382	
Resonance speed (min-1)	[nE1]		7518	
Resonance ratio (-)	[N]		0.118	
Subcritical range				
Running-in value (µm)	[ya]		0.6	
Bearing distance l of pinion shaft (mm)	[l]		80.000	
Distance s of pinion shaft (mm)	[s]		8.000	
Outside diameter of pinion shaft (mm)	[dsh]		40.000	
Load in accordance with Figure 13, ISO 6336-1:2006	[-]	4		
0:a), 1:b), 2:c), 3:d), 4:e)				
Coefficient K' according to Figure 13, ISO 6336-1:2006	[K']	-1.00		
Without support effect				
Tooth trace deviation (active) (µm)	[Fby]		3.83	
from deformation of shaft (µm)	[fsh*B1]		1.55	
(fsh (µm) = 1.55, B1= 1.00, fHb5 (µm) = 6.50)				

Tooth without tooth trace modification
Position of Contact pattern: favorable

from production tolerances (µm) (B2= 1.00)	[fma*B2]	12.38	
Tooth trace deviation, theoretical (µm)	[Fbx]	4.50	
Running-in value (µm)	[yb]	0.67	
Dynamic factor	[KV]	1.024	
Face load factor - flank	[KHb]	1.134	
- Tooth root	[KFb]	1.122	
- Scuffing	[KBb]	1.134	
Transverse load factor - flank	[KHa]	1.164	
- Tooth root	[KFa]	1.164	
- Scuffing	[KBa]	1.164	
Helical load factor scuffing	[Kbg]	1.300	
Number of load cycles (in mio.)	[NL]	266.769	90.101

3. TOOTH ROOT STRENGTH

Calculation of Tooth form coefficients according method: B

		------- GEAR 1	-------- GEAR 2 --
Calculated with manufacturing profile shift	[xE.e]	0.3056	0.3031
Tooth form factor	[YF]	1.02	1.10
Stress correction factor	[YS]	2.34	2.39
Working angle (°)	[alfFen]	19.83	20.28
Bending moment arm (mm)	[hF]	1.16	1.36
Tooth thickness at root (mm)	[sFn]	2.93	3.04
Tooth root radius (mm)	[roF]	0.59	0.53

(hF* = 0.930/ 1.088 sFn* = 2.345/ 2.436 roF* = 0.474/ 0.423)
(den (mm) =
68.437/201.674 dsFn(mm) = 62.846/190.628 alfsFn(°) = 30.00/ 30.00 qs = 2.472/ 2.881)

Helix angle factor	[Ybet]		0.900	
Deep tooth factor	[YDT]		1.000	
Gear rim factor	[YB]	1.00		1.00
Effective facewidth (mm)	[beff]	40.00		40.00
Nominal stress at tooth root (N/mm²)	[sigF0]	361.89		400.02
Tooth root stress (N/mm²)	[sigF]	605.05		668.80
Permissible bending stress at root of Test-gear				
Notch sensitivity factor	[YdrelT]	1.000		1.003
Surface factor	[YRrelT]	1.031		1.031
size factor (Tooth root)	[YX]	1.000		1.000
Finite life factor	[YNT]	0.914		0.934
	[YdrelT*YRrelT*YX*YNT]	0.942		0.967
Alternating bending factor (mean stress influence coefficient)	[YM]	1.000		1.000
Stress correction factor	[Yst]		2.00	
Yst*sigFlim (N/mm²)	[sigFE]	1000.00		1000.00
Permissible tooth root stress (N/mm²)	[sigFP=sigFG/SFmin]	673.16		690.54
Limit strength tooth root (N/mm²)	[sigFG]	942.43		966.76
Required safety	[SFmin]	1.40		1.40
Safety for tooth root stress	[SF=sigFG/sigF]	1.56		1.45

Transmittable power (kW)	[kWRating]	28.55	26.49

4. SAFETY AGAINST PITTING (TOOTH FLANK)

		GEAR 1	GEAR 2
Zone factor	[ZH]	2.382	
Elasticity factor (√N/mm²)	[ZE]	189.812	
Contact ratio factor	[Zeps]	0.712	
Helix angle factor	[Zbet]	1.011	
Effective facewidth (mm)	[beff]	40.00	
Nominal contact stress (N/mm²)	[sigH0]	678.09	
Contact stress at operating pitch circle (N/mm²)	[sigHw]	881.49	
Single tooth contact factor	[ZB,ZD]	1.00	1.00
Contact stress (N/mm²)	[sigHB, sigHD]	881.49	881.49
Lubrication coefficient at NL	[ZL]	0.927	0.927
Speed coefficient at NL	[ZV]	0.972	0.972
Roughness coefficient at NL	[ZR]	0.997	0.997
Material pairing coefficient at NL	[ZW]	1.000	1.000
Finite life factor	[ZNT]	0.950	0.982
	[ZL*ZV*ZR*ZNT]	0.853	0.882
Limited pitting is permitted:	No		
Size factor (flank)	[ZX]	1.000	1.000
Permissible contact stress (N/mm²)	[sigHP=sigHG/SHmin]	1163.01	1202.38
Pitting stress limit (N/mm²)	[sigHG]	1279.31	1322.62
Required safety	[SHmin]	1.10	1.10
Safety factor for contact stress at operating pitch circle			
	[SHw]	1.45	1.50
Safety for stress at single tooth contact	[SHBD=sigHG/sigHBD]	1.45	1.50
(Safety regarding transmittable torque)	[(SHBD)^2]	2.11	2.25
Transmittable power (kW)	[kWRating]	44.66	47.74

4b. MICROPITTING ACCORDING TO ISO/TR 15144-1:2014

Calculation did not run. (Lubricant: Load stage micropitting test is unknown.)

5. SCUFFING LOAD CAPACITY

Calculation method according to ISO TR 13989:2000

Lubrication coefficient (for lubrication type)	[XS]	1.000	
Scuffing test and load stage	[FZGtest]	FZG - Test A / 8.3 / 90 (ISO 14635 - 1)	12
Multiple meshing factor	[Xmp]	1.000	
Relative structure coefficient (Scuffing)	[XWrelT]	1.000	
Thermal contact factor (N/mm/s^.5/K)	[BM]	13.780	13.780
Relevant tip relief (µm)	[Ca]	2.00	2.00
Optimal tip relief (µm)	[Ceff]	11.86	
Ca taken as optimal in the calculation (0=no, 1=yes)		0	0
Effective facewidth (mm)	[beff]	40.000	
Applicable circumferential force/facewidth (N/mm)	[wBt]	357.208	

Kbg = 1.300, wBt*Kbg = 464.370

Angle factor	[Xalfbet]	0.995
(ε1:1.086, ε2:0.886)		
Flash temperature-criteria		
Lubricant factor	[XL]	0.875
Tooth mass temperature (°C)	[theMi]	68.38
(theMi = theoil + XS*0.47*Xmp*theflm)		
Average flash temperature (°C)	[theflm]	7.19
Scuffing temperature (°C)	[theS]	363.63
Coordinate gamma (point of highest temp.)	[Gamma]	0.340
[Gamma.A]=-0.277 [Gamma.E]=0.340		
Highest contact temp. (°C)	[theB]	85.91
Flash factor (°K*N^-.75*s^.5*m^-.5*mm)	[XM]	50.058
Approach factor	[XJ]	1.000
Load sharing factor	[XGam]	0.659
Dynamic viscosity (mPa*s)	[etaM]	14.32 (65.0 °C)
Coefficient of friction	[mym]	0.069
Required safety	[SBmin]	2.000
Safety factor for scuffing (flash temperature)	[SB]	14.281
Integral temperature-criteria		
Lubricant factor	[XL]	1.000
Tooth mass temperature (°C)	[theMC]	68.78
(theMC = theoil + XS*0.70*theflaint)		
Mean flash temperature (°C)	[theflaint]	5.41
Integral scuffing temperature (°C)	[theSint]	366.33
Flash factor (°K*N^-.75*s^.5*m^-.5*mm)	[XM]	50.058
Running-in factor (well run in)	[XE]	1.000
Contact ratio factor	[Xeps]	0.211
Dynamic viscosity (mPa*s)	[etaOil]	14.32 (65.0 °C)
Mean coefficient of friction	[mym]	0.078
Geometry factor	[XBE]	0.161
Meshing factor	[XQ]	1.000
Tip relief factor	[XCa]	1.259
Integral tooth flank temperature (°C)	[theint]	76.89
Required safety	[SSmin]	1.800
Safety factor for scuffing (intg.-temp.)	[SSint]	4.764
Safety referring to transmittable torque	[SSL]	25.335

6. MEASUREMENTS FOR TOOTH THICKNESS

		------- Gear 1 ------	Gear 2 --
Tooth thickness deviation		DIN 3967 d26	DIN 3967 d26
Tooth thickness allowance (normal section) (mm)	[As.e/i]	-0.060 / -0.120	-0.080 / -0.160
Number of teeth spanned	[k]	7.000	19.000
Base tangent length (no backlash) (mm)	[Wk]	25.255	71.418
Actual base tangent length ('span') (mm)	[Wk.e/i]	25.198 / 25.142	71.343 / 71.268
(mm)	[ΔWk.e/i]	-0.056 / -0.113	-0.075 / -0.150
Diameter of measuring circle (mm)	[dMWk.m]	65.882	193.902
Theoretical diameter of ball/pin (mm)	[DM]	2.191	2.124
Effective diameter of ball/pin (mm)	[DMeff]	2.500	2.500
Radial single-ball measurement backlash free (mm)	[MrK]	35.101	99.112
Radial single-ball measurement (mm)	[MrK.e/i]	35.034 / 34.967	99.011 / 98.910
Diameter of measuring circle (mm)	[dMMr.m]	66.495	194.505

Diametral measurement over two balls without clearance (mm)	[MdK]	70.170	198.213
Diametral two ball measure (mm)	[MdK.e/i]	70.037 / 69.902	198.012 / 197.809
Diametral measurement over pins without clearance (mm)	[MdR]	70.202	198.223
Measurement over pins according to DIN 3960 (mm)	[MdR.e/i]	70.069 / 69.933	198.022 / 197.820
Measurement over 2 pins (free) according to AGMA 2002 (mm)	[dk2f.e/i]	70.035 / 69.900	198.011 / 197.809
Measurement over 2 pins (transverse) according to AGMA 2002 (mm)	[dk2t.e/i]	70.100 / 69.965	198.033 / 197.830
Measurement over 3 pins (axial) according to AGMA 2002 (mm)	[dk3A.e/i]	70.069 / 69.933	198.022 / 197.820

Chordal tooth thickness (no backlash) (mm)	[sc]	2.301	2.319
Actual chordal tooth thickness (mm)	[sc.e/i]	2.241 / 2.181	2.239 / 2.159
Reference chordal height from da.m (mm)	[ha]	1.958	1.969
Tooth thickness (Arc) (mm)	[sn]	2.302	2.319
(mm)	[sn.e/i]	2.242 / 2.182	2.239 / 2.159

Backlash free center distance (mm)	[aControl.e/i]	129.816 /129.630
Backlash free center distance, allowances (mm)	[jta]	-0.184 / -0.370
dNf.i with aControl (mm)	[dNf0.i]	62.978 190.854
Reserve (dNf0.i-dFf.e)/2 (mm)	[cF0.i]	-0.139 -0.002
Tip clearance (mm)	[c0.i(aControl)]	0.029 0.002
Center distance allowances (mm)	[Aa.e/i]	0.020 / -0.020

Circumferential backlash from Aa (mm)	[jtw_Aa.e/i]	0.016 / -0.016
Radial clearance (mm)	[jrw]	0.390 / 0.164
Circumferential backlash (transverse section) (mm)	[jtw]	0.304 / 0.128
Normal backlash (mm)	[jnw]	0.279 / 0.118
Torsional angle at entry with fixed output:		
Entire torsional angle (°)	[j.tSys]	0.5308/ 0.2242

7. GEAR ACCURACY

		------- GEAR 1	------- GEAR 2 --
According to ISO 1328-1:1995, ISO 1328-2:1997			
Accuracy grade	[Q]	6	6
Single pitch deviation (µm)	[fptT]	7.50	8.50
Base circle pitch deviation (µm)	[fpbT]	7.00	8.00
Sector pitch deviation over k/8 pitches (µm)	[Fpk/8T]	13.00	18.00
Profile form deviation (µm)	[ffaT]	6.50	7.50
Profile slope deviation (µm)	[fHaT]	5.50	6.00
Total profile deviation (µm)	[FaT]	8.50	10.00
Helix form deviation (µm)	[ffbT]	8.50	9.00
Helix slope deviation (µm)	[fHbT]	8.50	9.00
Total helix deviation (µm)	[FbT]	12.00	13.00
Total cumulative pitch deviation (µm)	[FpT]	26.00	35.00
Runout (µm)	[FrT]	21.00	28.00
Single flank composite, total (µm)	[FisT]	35.00	44.00
Single flank composite, tooth-to-tooth (µm)	[fisT]	9.00	9.50
Radial composite, total (µm)	[FidT]	27.00	34.00
Radial composite, tooth-to-tooth (µm)	[fidT]	6.50	6.50

Axis alignment tolerances (recommendation acc. to ISO TR 10064-3:1996, Quality)		6)
Maximum value for deviation error of axis (µm)	[fSigbet]	13.00 (Fb= 13.00)
Maximum value for inclination error of axes (µm)	[fSigdel]	26.00

8. ADDITIONAL DATA

Maximal possible center distance (eps_a=1.0)	[aMAX]		131.383	
Mass (kg)	[m]		1.065	8.608
Total mass (kg)	[m]		9.673	
Moment of inertia (system with reference to the drive):				
calculation without consideration of the exact tooth shape				
single gears ((da+df)/2...di) (kg*m²)	[TraeghMom]	0.0005761		0.04303
System ((da+df)/2...di) (kg*m²)	[TraeghMom]		0.005485	
Torsional stiffness on input for stopped output:				
Torsional stiffness (MNm/rad)	[cr]		0.702	
Torsion when subjected to nominal torque (°)	[delcr]		0.023	
Mean coeff. of friction (acc. Niemann)	[mum]		0.075	
Wear sliding coef. by Niemann	[zetw]		0.669	
Gear power loss (kW)	[PVZ]		0.160	
(Meshing efficiency (%)	[etaz]		99.375)	
Sound pressure level (according to Masuda)	[dB(A)]		68.4	

Indications for the manufacturing by wire cutting:			
Deviation from theoretical tooth trace (µm)	[WireErr]	276.9	93.6
Permissible deviation (µm)	[Fb/2]	6.0	6.5

9. MODIFICATIONS AND TOOTH FORM DEFINITION

Data for the tooth form calculation :
Data not available.

10. SERVICE LIFE, DAMAGE

Required safety for tooth root	[SFmin]		1.40
Required safety for tooth flank	[SHmin]		1.10

Service life (calculated with required safeties):

System service life (h)	[Hatt]		24693
Tooth root service life (h)	[HFatt]	1e+006	2.469e+004
Tooth flank service life (h)	[HHatt]	1e+006	1e+006

Note: The entry 1e+006 h means that the Service life > 1,000,000 h.

Damage calculated on the basis of the required service life [H] (5000.0 h)

F1%	F2%	H1%	H2%
0.00	20.25	0.00	0.00

Damage calculated on basis of system service life [Hatt] (24693.0 h)

F1%	F2%	H1%	H2%
0.00	100.00	0.00	0.00

Calculation of the factors required to define reliability R(t) according to B. Bertsche with Weibull distribution:
R(t) = 100 * Exp(-((t*fac - t0)/(T - t0))^b) %; t (h)

Gear		fac	b	t0	T	R(H)%
1	Tooth root	53354	1.7	9.654e+029	1.484e+030	100.00

1	Tooth flank	53354	1.3	9.014e+029	4.295e+030	100.00
2	Tooth root	18020	1.7	4.296e+008	6.602e+008	100.00
2	Tooth flank	18020	1.3	9.014e+029	4.295e+030	100.00

Reliability of the configuration for required service life (%) 100.00 (Bertsche)

REMARKS:

- Specifications with [.e/i] imply: Maximum [e] and Minimal value [i] with consideration of all tolerances
  Specifications with [.m] imply: Mean value within tolerance
- For the backlash tolerance, the center distance tolerances and the tooth thickness deviation are taken into account. Shown is the maximal and the minimal backlash corresponding the largest resp. the smallest allowances
  The calculation is done for the operating pitch circle.
- Calculation of Zbet according Corrigendum 1 ISO 6336-2:2008 with Zbet = 1/(COS(beta)^0.5)
- Details of calculation method:
  cg according to method B
  KV according to method B
  KHb, KFb according method C
  fma following equation (64), fsh following (57/58), Fbx following (52/53/57)
  KHa, KFa according to method B
- The logarithmically interpolated value taken from the values for the fatigue strength and the static strength, based on the number of load cycles, is used for coefficients ZL, ZV, ZR, ZW, ZX, YdrelT, YRrelT and YX..

End of Report lines: 534

KISSsoft Release 03/2017 F

KISSsoft University license - Universidade do Porto

File

Name : GearZ1Z2Speed

Changed by: Carlos Rodrigues on: 02.07.2018 at: 23:50:17

Important hint: At least one warning has occurred during the calculation:

1-> The circumferential speed is very high (28.1780 m/s)!
You have to take adequate action to
guarantee proper lubrication.

CALCULATION OF A HELICAL GEAR PAIR

Drawing or article number:
Gear 1: Z1
Gear 2: Z2

Calculation method ISO 6336:2006 Method B

		------- GEAR 1	-------- GEAR 2 --
Power (kW)	[P]	25.000	
Speed (1/min)	[n]	14000.0	3556.8
Torque (Nm)	[T]	17.1	67.1
Application factor	[KA]	1.25	
Required service life (h)	[H]	5000.00	
Gear driving (+) / driven (-)		+	-

Working flank gear 1: Right flank
Sense of rotation gear 1 clockwise

1. TOOTH GEOMETRY AND MATERIAL

(geometry calculation according to ISO 21771:2007, DIN ISO 21771)

		------- GEAR 1	-------- GEAR 2 --
Center distance (mm)	[a]	95.000	
Center distance tolerance	ISO 286:2010 Measure js7		
Normal module (mm)	[mn]	0.8000	
Pressure angle at normal section (°)	[alfn]	20.0000	
Helix angle at reference circle (°)	[beta]	12.0000	
Number of teeth	[z]	47	185
Facewidth (mm)	[b]	30.00	30.00
Hand of gear		left	right
Accuracy grade	[Q-ISO 1328:1995]	5	5
Inner diameter (mm)	[di]	0.00	42.00
Inner diameter of gear rim (mm)	[dbi]	0.00	132.92

Material
Gear 1: 18CrNiMo7-6, Case-carburized steel, case-hardened
ISO 6336-5 Figure 9/10 (MQ), Core hardness >=30HRC
Gear 2: 18CrNiMo7-6, Case-carburized steel, case-hardened
ISO 6336-5 Figure 9/10 (MQ), Core hardness >=30HRC

		------- GEAR 1	-------- GEAR 2 --
Surface hardness		HRC 61	HRC 61
Material quality according to ISO 6336:2006 Normal (Life factors ZNT and YNT >=0.85)			
Fatigue strength. tooth root stress (N/mm²)	[σFlim]	500.00	500.00
Fatigue strength for Hertzian pressure (N/mm²)	[σHlim]	1500.00	1500.00

Tensile strength (N/mm²)	[σB]	1200.00	1200.00
Yield point (N/mm²)	[σS]	850.00	850.00
Young's modulus (N/mm²)	[E]	206000	206000
Poisson's ratio	[v]	0.300	0.300
Roughness average value DS, flank (µm)	[RAH]	0.30	0.30
Roughness average value DS, root (µm)	[RAF]	1.00	1.00
Mean roughness height, Rz, flank (µm)	[RZH]	2.00	2.00
Mean roughness height, Rz, root (µm)	[RZF]	6.00	6.00

Gear reference profile 1 :
Reference profile (Own input)

Dedendum coefficient	[hfP*]	1.400
Root radius factor	[rhofP*]	0.393 (rhofPmax*=0.394)
Addendum coefficient	[haP*]	1.150
Tip radius factor	[rhoaP*]	0.000
Protuberance height coefficient	[hprP*]	0.000
Protuberance angle	[alfprP]	0.000
Tip form height coefficient	[hFaP*]	0.000
Ramp angle	[alfKP]	0.000

not topping

Gear reference profile 2 :
Reference profile (Own input)

Dedendum coefficient	[hfP*]	1.400
Root radius factor	[rhofP*]	0.393 (rhofPmax*=0.394)
Addendum coefficient	[haP*]	1.150
Tip radius factor	[rhoaP*]	0.000
Protuberance height coefficient	[hprP*]	0.000
Protuberance angle	[alfprP]	0.000
Tip form height coefficient	[hFaP*]	0.000
Ramp angle	[alfKP]	0.000

not topping

Summary of reference profile gears:

Dedendum reference profile	[hfP*]	1.400	1.400
Tooth root radius Refer. profile	[rofP*]	0.393	0.393
Addendum Reference profile	[haP*]	1.150	1.150
Protuberance height coefficient	[hprP*]	0.000	0.000
Protuberance angle (°)	[alfprP]	0.000	0.000
Tip form height coefficient	[hFaP*]	0.000	0.000
Ramp angle (°)	[alfKP]	0.000	0.000

Type of profile modification:for high load capacity gearboxe

Tip relief (µm)	[Ca]	3.0	3.0

Lubrication type		Oil bath lubrication
Type of oil (Own input)		Castrol ATF Dex II Multivehicle
Lubricant base		Mineral-oil base
Kinem. viscosity oil at 40 °C (mm²/s)	[nu40]	39.00
Kinem. viscosity oil at 100 °C (mm²/s)	[nu100]	7.50
Specific density at 15 °C (kg/dm³)	[roOil]	0.870
Oil temperature (°C)	[TS]	75.000

		------- GEAR 1 --------	GEAR 2 --
Overall transmission ratio	[itot]		-3.936
Gear ratio	[u]		3.936

Transverse module (mm)	[mt]	0.818	
Pressure angle at pitch circle (°)	[alft]	20.410	
Working transverse pressure angle (°)	[alfwt]	20.615	
	[alfwt.e/i]	20.643 / 20.587	
Working pressure angle at normal section (°)	[alfwn]	20.200	
Helix angle at operating pitch circle (°)	[betaw]	12.016	
Base helix angle (°)	[betab]	11.267	
Reference center distance (mm)	[ad]	94.873	
Sum of profile shift coefficients	[Summexi]	0.1593	
Profile shift coefficient	[x]	0.0907	0.0685
Tooth thickness (Arc) (module) (module)	[sn*]	1.6369	1.6207
Tip alteration (mm)	[k*mn]	0.009	0.009
Reference diameter (mm)	[d]	38.440	151.306
Base diameter (mm)	[db]	36.027	141.807
Tip diameter (mm)	[da]	40.444	153.275
(mm)	[da.e/i]	40.444 / 40.434	153.275 / 153.265
Tip diameter allowances (mm)	[Ada.e/i]	0.000 / -0.010	0.000 / -0.010
Tip form diameter (mm)	[dFa]	40.444	153.275
(mm)	[dFa.e/i]	40.444 / 40.434	153.275 / 153.265
Active tip diameter (mm)	[dNa]	40.444	153.275
Active tip diameter (mm)	[dNa.e/i]	40.444 / 40.434	153.275 / 153.265
Operating pitch diameter (mm)	[dw]	38.491	151.509
(mm)	[dw.e/i]	38.498 / 38.484	151.537 / 151.481
Root diameter (mm)	[df]	36.345	149.176
Generating Profile shift coefficient	[xE.e/i]	0.0152/ -0.0707	-0.0689/ -0.2062
Manufactured root diameter with xE (mm)	[df.e/i]	36.224 / 36.087	148.956 / 148.736
Theoretical tip clearance (mm)	[c]	0.190	0.190
Effective tip clearance (mm)	[c.e/i]	0.432 / 0.282	0.342 / 0.233
Active root diameter (mm)	[dNf]	37.068	149.877
(mm)	[dNf.e/i]	37.098 / 37.045	149.916 / 149.845
Root form diameter (mm)	[dFf]	37.036	149.661
(mm)	[dFf.e/i]	36.957 / 36.871	149.461 / 149.263
Reserve (dNf-dFf)/2 (mm)	[cF.e/i]	0.113 / 0.044	0.327 / 0.192
Addendum (mm)	[ha=mn*(haP*+x+k)]	1.002	0.984
(mm)	[ha.e/i]	1.002 / 0.997	0.984 / 0.979
Dedendum (mm)	[hf=mn*(hfP*-x)]	1.047	1.065
(mm)	[hf.e/i]	1.108 / 1.177	1.175 / 1.285
Roll angle at dFa (°)	[xsi_dFa.e/i]	29.230 / 29.195	23.504 / 23.493
Roll angle to dNa (°)	[xsi_dNa.e/i]	29.230 / 29.195	23.504 / 23.493
Roll angle to dNf (°)	[xsi_dNf.e/i]	14.075 / 13.717	19.652 / 19.562
Roll angle at dFf (°)	[xsi_dFf.e/i]	13.102 / 12.476	19.076 / 18.822
Tooth height (mm)	[h]	2.049	2.049
Virtual gear no. of teeth	[zn]	49.957	196.639
Normal tooth thickness at tip circle (mm)	[san]	0.485	0.555
(mm)	[san.e/i]	0.443 / 0.386	0.478 / 0.393
Normal tooth thickness on tip form circle (mm)	[sFan]	0.485	0.555
(mm)	[sFan.e/i]	0.443 / 0.386	0.478 / 0.393
Normal space width at root circle (mm)	[efn]	0.603	0.476
(mm)	[efn.e/i]	0.628 / 0.662	0.485 / 0.494
Max. sliding velocity at tip (m/s)	[vga]	4.438	4.438
Specific sliding at the tip	[zetaa]	0.329	0.410
Specific sliding at the root	[zetaf]	-0.694	-0.491
Mean specific sliding	[zetam]	0.370	
Sliding factor on tip	[Kga]	0.157	0.157
Sliding factor on root	[Kgf]	-0.157	-0.157
Pitch on reference circle (mm)	[pt]	2.569	

Base pitch (mm)	[pbt]			2.408				
Transverse pitch on contact-path (mm)	[pet]			2.408				
Lead height (mm)	[pz]		568.145			2236.313		
Axial pitch (mm)	[px]			12.088				
Length of path of contact (mm)	[ga, e/i]		4.828 (	4.877 /	4.754)			
Length T1-A, T2-A (mm)	[T1A, T2A]	4.362(	4.312/	4.425)	29.086(	29.086/	29.073)	
Length T1-B (mm)	[T1B, T2B]	4.374(	4.374/	6.771)	29.074(	29.025/	26.727)	
Length T1-C (mm)	[T1C, T2C]	6.776(	6.766/	6.786)	26.672(	26.632/	26.711)	
Length T1-D (mm)	[T1D, T2D]	9.178(	9.129/	6.833)	24.270(	24.270/	26.664)	
Length T1-E (mm)	[T1E, T2E]	9.190(	9.190/	9.179)	24.258(	24.208/	24.319)	
Length T1-T2 (mm)	[T1T2]		33.448 (	33.398 /	33.498)			
Diameter of single contact point B (mm)	[d-B]	37.073(	37.073/	38.488)	153.266(	153.229/	151.547)	
Diameter of single contact point D (mm)	[d-D]	40.434(	40.389/	38.532)	149.884(	149.884/	151.503)	
Addendum contact ratio	[eps]	1.002(	1.006/	0.994)	1.002(	1.019/	0.980)	
Minimal length of contact line (mm)	[Lmin]			61.295				

Transverse contact ratio	[eps_a]		2.005	
Transverse contact ratio with allowances	[eps_a.e/m/i]	2.025 /	2.000 /	1.974
Overlap ratio	[eps_b]		2.482	
Total contact ratio	[eps_g]		4.486	
Total contact ratio with allowances	[eps_g.e/m/i]	4.507 /	4.481 /	4.456

2. FACTORS OF GENERAL INFLUENCE

		------- GEAR 1	-------- GEAR 2 --	
Nominal circum. force at pitch circle (N)	[Ft]		887.2	
Axial force (N)	[Fa]		188.6	
Radial force (N)	[Fr]		330.1	
Normal force (N)	[Fnorm]		965.2	
Nominal circumferential force per mm (N/mm)	[w]		29.57	
Only as information: Forces at operating pitch circle:				
Nominal circumferential force (N)	[Ftw]		886.0	
Axial force (N)	[Faw]		188.6	
Radial force (N)	[Frw]		333.3	
Circumferential speed reference circle (m/s)	[v]		28.18	
Circumferential speed operating pitch circle (m/s)	[v(dw)]		28.22	
Running-in value (µm)	[yp]		0.4	
Running-in value (µm)	[yf]		0.4	
Correction coefficient	[CM]		0.800	
Gear body coefficient	[CR, bs/b, sr/mn]		0.962	(0.250, 9.885)
Basic rack factor	[CBS]		0.900	
Material coefficient	[E/Est]		1.000	
Singular tooth stiffness (N/mm/µm)	[c']		10.415	
Meshing stiffness (N/mm/µm)	[cgalf]		18.263	
Meshing stiffness (N/mm/µm)	[cgbet]		15.524	
Reduced mass (kg/mm)	[mRed]		0.00484	
Resonance speed (min-1)	[nE1]		12487	
Resonance ratio (-)	[N]		1.121	
Range of the main resonance!				
Running-in value (µm)	[ya]		0.4	
KHb calculated according to ISO 6336-1: 2006, Annex E (takes into account K_A*K_V)				
Shaft data	shaft1ststage-14000rpm.W10			
Shaft data	shaft2ndstage-3500rpm.W10			
Torque (0: -, 1: <I, 2: <II, 3: <from shaft calculation)		-1	3	
KHb is determined as biggest value out of following variants				
(axis deviation error fma and meshing error fHb):				

fma/fHb (µm): -0.0/ -8.8; 3: -0.0/ 8.8; 4: 0.0/ -8.8; 5: 0.0/ 8.8
(For intermediate results refer to file: KHbeta_calc12.tmp)

Dynamic factor	[KV]	1.680	
Face load factor - flank	[KHb]	1.603	
- Tooth root	[KFb]	1.548	
- Scuffing	[KBb]	1.603	
Transverse load factor - flank	[KHa]	1.118	
- Tooth root	[KFa]	1.118	
- Scuffing	[KBa]	1.118	
Helical load factor scuffing	[Kbg]	1.300	
Number of load cycles (in mio.)	[NL]	4200.000	1067.027

3. TOOTH ROOT STRENGTH

Calculation of Tooth form coefficients according method: B

		------- GEAR 1 --------	GEAR 2 --
Calculated with manufacturing profile shift	[xE.e]	0.0152	-0.0689
Tooth form factor	[YF]	1.11	1.15
Stress correction factor	[YS]	2.09	2.24
Working angle (°)	[alfFen]	18.11	19.71
Bending moment arm (mm)	[hF]	0.73	0.87
Tooth thickness at root (mm)	[sFn]	1.79	1.91
Tooth root radius (mm)	[roF]	0.45	0.38

(hF* = 0.913/ 1.089 sFn* = 2.235/ 2.388 roF* = 0.559/ 0.470)
(den (mm) =
39.947/ 157.444 dsFn(mm) = 36.571/ 149.288 alfsFn(°) = 30.00/ 30.00 qs = 1.997/ 2.543)

Helix angle factor	[Ybet]		0.900	
Deep tooth factor	[YDT]		1.000	
Gear rim factor	[YB]	1.00		1.00
Effective facewidth (mm)	[beff]	30.00		30.00
Nominal stress at tooth root (N/mm²)	[sigF0]	77.32		85.74
Tooth root stress (N/mm²)	[sigF]	280.95		311.56
Permissible bending stress at root of Test-gear				
Notch sensitivity factor	[YdrelT]	0.995		1.000
Surface factor	[YRrelT]	1.031		1.031
size factor (Tooth root)	[YX]	1.000		1.000
Finite life factor	[YNT]	0.865		0.889
	[YdrelT*YRrelT*YX*YNT]	0.888		0.917
Alternating bending factor (mean stress influence coefficient)	[YM]		1.000	1.000
Stress correction factor	[Yst]		2.00	
Yst*sigFlim (N/mm²)	[sigFE]	1000.00		1000.00
Permissible tooth root stress (N/mm²)	[sigFP=sigFG/SFmin]	634.00		655.16
Limit strength tooth root (N/mm²)	[sigFG]	887.60		917.22
Required safety	[SFmin]	1.40		1.40
Safety for tooth root stress	[SF=sigFG/sigF]	3.16		2.94
Transmittable power (kW)	[kWRating]	56.42		52.57

KISSSOFT
Calculation programs for machine design

4. SAFETY AGAINST PITTING (TOOTH FLANK)

		------- GEAR 1	-------- GEAR 2 --
Zone factor	[ZH]	2.436	
Elasticity factor (√N/mm²)	[ZE]	189.812	
Contact ratio factor	[Zeps]	0.706	
Helix angle factor	[Zbet]	1.011	
Effective facewidth (mm)	[beff]	30.00	
Nominal contact stress (N/mm²)	[sigH0]	324.39	
Contact stress at operating pitch circle (N/mm²)	[sigHw]	629.16	
Single tooth contact factor	[ZB,ZD]	1.00	1.00
Contact stress (N/mm²)	[sigHB, sigHD]	629.16	629.16
Lubrication coefficient at NL	[ZL]	0.927	0.927
Speed coefficient at NL	[ZV]	1.031	1.031
Roughness coefficient at NL	[ZR]	1.016	1.016
Material pairing coefficient at NL	[ZW]	1.000	1.000
Finite life factor	[ZNT]	0.873	0.910
	[ZL*ZV*ZR*ZNT]	0.847	0.884
Limited pitting is permitted:	No		
Size factor (flank)	[ZX]	1.000	1.000
Permissible contact stress (N/mm²)	[sigHP=sigHG/SHmin]	1155.30	1204.89
Pitting stress limit (N/mm²)	[sigHG]	1270.83	1325.38
Required safety	[SHmin]	1.10	1.10
Safety factor for contact stress at operating pitch circle			
	[SHw]	2.02	2.11
Safety for stress at single tooth contact	[SHBD=sigHG/sigHBD]	2.02	2.11
(Safety regarding transmittable torque)	[(SHBD)^2]	4.08	4.44
Transmittable power (kW)	[kWRating]	84.30	91.69

4b. MICROPITTING ACCORDING TO ISO/TR 15144-1:2014

Calculation did not run. (Lubricant: Load stage micropitting test is unknown.)

5. SCUFFING LOAD CAPACITY

Calculation method according to ISO TR 13989:2000

Lubrication coefficient (for lubrication type)	[XS]	1.000	
Scuffing test and load stage	[FZGtest]	FZG - Test A / 8.3 / 90 (ISO 14635 - 1)	12
Multiple meshing factor	[Xmp]	1.000	
Relative structure coefficient (Scuffing)	[XWrelT]	1.000	
Thermal contact factor (N/mm/s^.5/K)	[BM]	13.780	13.780
Relevant tip relief (µm)	[Ca]	3.00	3.00
Optimal tip relief (µm)	[Ceff]	2.02	
Ca taken as optimal in the calculation (0=no, 1=yes)		1	1
Effective facewidth (mm)	[beff]	30.000	
Applicable circumferential force/facewidth (N/mm)	[wBt]	111.246	
Kbg = 1.300, wBt*Kbg = 144.619			
Angle factor	[Xalfbet]	0.982	
(ε1:1.002, ε2:1.002)			

Flash temperature-criteria

Lubricant factor	[XL]	0.888
Tooth mass temperature (°C)	[theMi]	76.94
(theMi = theoil + XS*0.47*Xmp*theflm)		
Average flash temperature (°C)	[theflm]	4.12
Scuffing temperature (°C)	[theS]	467.95
Contact time (µsec)	[tc]	12.42
theS increased because of short contact time by (°C)		100.38
Coordinate gamma (point of highest temp.)	[Gamma]	-0.205
[Gamma.A]=-0.356 [Gamma.E]=0.356		
Highest contact temp. (°C)	[theB]	83.82
Flash factor (°K*N^-.75*s^.5*m^-.5*mm)	[XM]	50.058
Approach factor	[XJ]	1.000
Load sharing factor	[XGam]	0.565
Dynamic viscosity (mPa*s)	[etaM]	10.86 (75.0 °C)
Coefficient of friction	[mym]	0.035
Required safety	[SBmin]	2.000
Safety factor for scuffing (flash temperature)	[SB]	44.550

Integral temperature-criteria		
Lubricant factor	[XL]	1.000
Tooth mass temperature (°C)	[theMC]	76.99
(theMC = theoil + XS*0.70*theflaint)		
Mean flash temperature (°C)	[theflaint]	2.84
Integral scuffing temperature (°C)	[theSint]	366.33
Flash factor (°K*N^-.75*s^.5*m^-.5*mm)	[XM]	50.058
Running-in factor (well run in)	[XE]	1.000
Contact ratio factor	[Xeps]	0.220
Dynamic viscosity (mPa*s)	[etaOil]	10.86 (75.0 °C)
Mean coefficient of friction	[mym]	0.045
Geometry factor	[XBE]	0.161
Meshing factor	[XQ]	1.000
Tip relief factor	[XCa]	1.954
Integral tooth flank temperature (°C)	[theint]	81.24
Required safety	[SSmin]	1.800
Safety factor for scuffing (intg.-temp.)	[SSint]	4.509
Safety referring to transmittable torque	[SSL]	46.685

6. MEASUREMENTS FOR TOOTH THICKNESS

		------- Gear 1	------ Gear 2 --
Tooth thickness deviation		DIN 3967 d26	DIN 3967 d26
Tooth thickness allowance (normal section) (mm)	[As.e/i]	-0.044 / -0.094	-0.080 / -0.160
Number of teeth spanned	[k]	6.000	22.000
Base tangent length (no backlash) (mm)	[Wk]	13.600	53.022
Actual base tangent length ('span') (mm)	[Wk.e/i]	13.559 / 13.512	52.947 / 52.872
(mm)	[ΔWk.e/i]	-0.041 / -0.088	-0.075 / -0.150
Diameter of measuring circle (mm)	[dMWk.m]	38.394	151.003
Theoretical diameter of ball/pin (mm)	[DM]	1.364	1.343
Effective diameter of ball/pin (mm)	[DMeff]	1.400	1.400
Radial single-ball measurement backlash free (mm)	[MrK]	20.289	76.722
Radial single-ball measurement (mm)	[MrK.e/i]	20.235 / 20.172	76.615 / 76.507
Diameter of measuring circle (mm)	[dMMr.m]	38.502	151.240
Diametral measurement over two balls without clearance (mm)	[MdK]	40.556	153.439
Diametral two ball measure (mm)	[MdK.e/i]	40.448 / 40.323	153.225 / 153.009

Diametral measurement over pins without clearance (mm)	[MdR]	40.578	153.444
Measurement over pins according to DIN 3960 (mm)	[MdR.e/i]	40.470 / 40.345	153.230 / 153.015
Measurement over 2 pins (free) according to AGMA 2002 (mm)	[dk2f.e/i]	40.447 / 40.322	153.225 / 153.009
Measurement over 2 pins (transverse) according to AGMA 2002 (mm)	[dk2t.e/i]	40.491 / 40.366	153.236 / 153.020
Measurement over 3 pins (axial) according to AGMA 2002 (mm)	[dk3A.e/i]	40.470 / 40.345	153.230 / 153.015
Chordal tooth thickness (no backlash) (mm)	[sc]	1.309	1.297
Actual chordal tooth thickness (mm)	[sc.e/i]	1.265 / 1.215	1.217 / 1.137
Reference chordal height from da.m (mm)	[ha]	1.010	0.984
Tooth thickness (Arc) (mm)	[sn]	1.309	1.297
(mm)	[sn.e/i]	1.265 / 1.215	1.217 / 1.137
Backlash free center distance (mm)	[aControl.e/i]	94.830 / 94.650	
Backlash free center distance, allowances (mm)	[jta]	-0.170 / -0.350	
dNf.i with aControl (mm)	[dNf0.i]	36.646	149.237
Reserve (dNf0.i-dFf.e)/2 (mm)	[cF0.i]	-0.155	-0.112
Tip clearance (mm)	[c0.i(aControl)]	-0.050	-0.100
Center distance allowances (mm)	[Aa.e/i]	0.018 / -0.018	
Circumferential backlash from Aa (mm)	[jtw_Aa.e/i]	0.013 / -0.013	
Radial clearance (mm)	[jrw]	0.368 / 0.152	
Circumferential backlash (transverse section) (mm)	[jtw]	0.273 / 0.114	
Normal backlash (mm)	[jnw]	0.251 / 0.105	
Torsional angle at entry with fixed output:			
Entire torsional angle (°)	[j.tSys]	0.8133/ 0.3387	

7. GEAR ACCURACY

		------- GEAR 1	------- GEAR 2 --
According to ISO 1328-1:1995, ISO 1328-2:1997			
Accuracy grade	[Q]	5	5
Single pitch deviation (µm)	[fptT]	5.00	6.00
Base circle pitch deviation (µm)	[fpbT]	4.70	5.60
Sector pitch deviation over k/8 pitches (µm)	[Fpk/8T]	8.00	13.00
Profile form deviation (µm)	[ffaT]	4.00	5.50
Profile slope deviation (µm)	[fHaT]	3.30	4.40
Total profile deviation (µm)	[FaT]	5.00	7.00
Helix form deviation (µm)	[ffbT]	6.00	6.50
Helix slope deviation (µm)	[fHbT]	6.00	6.50
Total helix deviation (µm)	[FbT]	8.00	9.00
Total cumulative pitch deviation (µm)	[FpT]	14.00	24.00
Runout (µm)	[FrT]	11.00	20.00
Single flank composite, total (µm)	[FisT]	20.00	31.00
Single flank composite, tooth-to-tooth (µm)	[fisT]	6.00	7.00
Radial composite, total (µm)	[FidT]	14.00	22.00
Radial composite, tooth-to-tooth (µm)	[fidT]	2.70	2.80

8. ADDITIONAL DATA

Maximal possible center distance (eps_a=1.0)	[aMAX]	95.879	
Mass (kg)	[m]	0.272	3.894
Total mass (kg)	[m]	4.166	

Moment of inertia (system with reference to the drive):
calculation without consideration of the exact tooth shape

single gears ((da+df)/2...di) (kg*m²)	[TraeghMom]	5.012e-005		0.01199
System ((da+df)/2...di) (kg*m²)	[TraeghMom]		0.0008239	

Torsional stiffness on input for stopped output:

Torsional stiffness (MNm/rad)	[cr]	0.151
Torsion when subjected to nominal torque (°)	[delcr]	0.006
Mean coeff. of friction (acc. Niemann)	[mum]	0.050
Wear sliding coef. by Niemann	[zetw]	0.741
Gear power loss (kW)	[PVZ]	0.108
(Meshing efficiency (%)	[etaz]	99.569)
Sound pressure level (according to Masuda)	[dB(A)]	80.5

Indications for the manufacturing by wire cutting:

Deviation from theoretical tooth trace (µm)	[WireErr]	263.8		67.2
Permissible deviation (µm)	[Fb/2]		4.0	4.5

9. MODIFICATIONS AND TOOTH FORM DEFINITION

Profile and tooth trace modifications for gear 1

Symmetric (both flanks)

- Crowning Cb = 6.000µm (rcrown=18750mm)
- Helix angle modification, parallel CHb = -1.509µm

Positive modification increases the left hand helix angle and decreases the right hand helix angle (ISO 21771)
CHb=-1.509µm -> β.eff=11.9971°-left

- Tip relief, arc-like Caa = 3.000µm LCa = 1.147*mn dCa = 39.644mm

Profile and tooth trace modifications for gear 2

Symmetric (both flanks)

- Crowning Cb = 0.430µm (rcrown=261811mm)
- Helix angle modification, parallel CHb = -1.509µm

Positive modification increases the left hand helix angle and decreases the right hand helix angle (ISO 21771)
CHb=-1.509µm -> β.eff=12.0029°-right

- Tip relief, arc-like Caa = 3.000µm LCa = 1.339*mn dCa = 152.475mm

Tip relief verification

Diameter (mm)	[dcheck]	40.418		153.249	
Tip relief left/right (µm)	[Ca L/R]	2.8 /	2.8	2.8 /	2.8

Data for the tooth form calculation :

Calculation of Gear 1
Tooth form, Gear 1, Step 1: Automatic (final machining)
haP*= 1.277, hfP*= 1.400, rofP*= 0.393

Calculation of Gear 2
Tooth form, Gear 2, Step 1: Automatic (final machining)
haP*= 1.365, hfP*= 1.400, rofP*= 0.393

10. SERVICE LIFE, DAMAGE, LOAD DISTRIBUTION

Required safety for tooth root [SFmin] 1.40

KISSSOFT
Calculation programs for machine design

Required safety for tooth flank [SHmin] 1.10

Service life (calculated with required safeties):
System service life (h) [Hatt] > 1000000

Tooth root service life (h) [HFatt] 1e+006 1e+006
Tooth flank service life (h) [HHatt] 1e+006 1e+006
Note: The entry 1e+006 h means that the Service life > 1,000,000 h.

Damage calculated on the basis of the required service life [H] (5000.0 h)

F1%	F2%	H1%	H2%
0.00	0.00	0.00	0.00

Calculation of the factors required to define reliability R(t) according to B. Bertsche with Weibull distribution:
R(t) = 100 * Exp(-((t*fac - t0)/(T - t0))^b) %; t (h)

Gear		fac	b	t0	T	R(H)%
1	Tooth root	840000	1.7	9.654e+029	1.484e+030	100.00
1	Tooth flank	840000	1.3	9.014e+029	4.295e+030	100.00
2	Tooth root	213405	1.7	9.654e+029	1.484e+030	100.00
2	Tooth flank	213405	1.3	9.014e+029	4.295e+030	100.00

Reliability of the configuration for required service life (%) 100.00 (Bertsche)

Load distribution (ISO6336-1, Annex E)

$K_{H\beta}$	w_m (N/mm)	w_I (N/mm)	w_{II} (N/mm)	w_{max} (N/mm)	σ_{Hm} (N/mm^2)	σ_{HI} (N/mm^2)	σ_{HII} (N/mm^2)	σ_{Hmax} (N/mm^2)
1.603	66.3	59.7	77.0	106.2	470.1	446.4	506.8	595.1

Index m, I, II stand for: Middle of facewidth, Side I and Side II

REMARKS:
- Specifications with [.e/i] imply: Maximum [e] and Minimal value [i] with consideration of all tolerances
  Specifications with [.m] imply: Mean value within tolerance
- For the backlash tolerance, the center distance tolerances and the tooth thickness deviation are taken into account. Shown is the maximal and the minimal backlash corresponding the largest resp. the smallest allowances
  The calculation is done for the operating pitch circle.
- Calculation of Zbet according Corrigendum 1 ISO 6336-2:2008 with Zbet = 1/(COS(beta)^0.5)
- Details of calculation method:
  cg according to method B
  KV according to method B
- The logarithmically interpolated value taken from the values for the fatigue strength and the static strength, based on the number of load cycles, is used for coefficients ZL, ZV, ZR, ZW, ZX, YdrelT, YRrelT and YX..

End of Report lines: 551

KISSsoft Release 03/2017 F

KISSsoft University license - Universidade do Porto

File

Name : GearZ3Z4Speed

Changed by: Carlos Rodrigues on: 02.07.2018 at: 23:55:42

CALCULATION OF A HELICAL GEAR PAIR

Drawing or article number:
Gear 1: Z3
Gear 2: Z4

Calculation method ISO 6336:2006 Method B

		------- GEAR 1	-------- GEAR 2 --
Power (kW)	[P]	25.000	
Speed (1/min)	[n]	3556.8	1201.3
Torque (Nm)	[T]	67.1	198.7
Application factor	[KA]	1.25	
Required service life (h)	[H]	5000.00	
Gear driving (+) / driven (-)		+	-

Working flank gear 1: Right flank
Sense of rotation gear 1 clockwise

1. TOOTH GEOMETRY AND MATERIAL

(geometry calculation according to ISO 21771:2007, DIN ISO 21771)

		------- GEAR 1	-------- GEAR 2 --
Center distance (mm)	[a]	130.000	
Center distance tolerance	ISO 286:2010 Measure js7		
Normal module (mm)	[mn]	1.2500	
Pressure angle at normal section (°)	[alfn]	20.0000	
Helix angle at reference circle (°)	[beta]	12.0000	
Number of teeth	[z]	51	151
Facewidth (mm)	[b]	40.00	40.00
Hand of gear		right	left
Accuracy grade	[Q-ISO 1328:1995]	6	6
Inner diameter (mm)	[di]	0.00	50.00
Inner diameter of gear rim (mm)	[dbi]	0.00	177.47

Material
Gear 1: 18CrNiMo7-6, Case-carburized steel, case-hardened
ISO 6336-5 Figure 9/10 (MQ), Core hardness >=30HRC
Gear 2: 18CrNiMo7-6, Case-carburized steel, case-hardened
ISO 6336-5 Figure 9/10 (MQ), Core hardness >=30HRC

		------- GEAR 1	-------- GEAR 2 --
Surface hardness		HRC 61	HRC 61
Material quality according to ISO 6336:2006 Normal (Life factors ZNT and YNT >=0.85)			
Fatigue strength. tooth root stress (N/mm²)	[σFlim]	500.00	500.00
Fatigue strength for Hertzian pressure (N/mm²)	[σHlim]	1500.00	1500.00
Tensile strength (N/mm²)	[σB]	1200.00	1200.00
Yield point (N/mm²)	[σS]	850.00	850.00
Young's modulus (N/mm²)	[E]	206000	206000
Poisson's ratio	[v]	0.300	0.300
Roughness average value DS, flank (µm)	[RAH]	0.50	0.50

Roughness average value DS, root (µm)	[RAF]	1.00	1.00
Mean roughness height, Rz, flank (µm)	[RZH]	3.00	3.00
Mean roughness height, Rz, root (µm)	[RZF]	6.00	6.00

Gear reference profile 1 :
Reference profile (Own input)

Dedendum coefficient	[hfP*]	1.431
Root radius factor	[rhofP*]	0.377 (rhofPmax*=0.378)
Addendum coefficient	[haP*]	1.181
Tip radius factor	[rhoaP*]	0.000
Protuberance height coefficient	[hprP*]	0.000
Protuberance angle	[alfprP]	0.000
Tip form height coefficient	[hFaP*]	0.000
Ramp angle	[alfKP]	0.000

not topping

Gear reference profile 2 :
Reference profile (Own input)

Dedendum coefficient	[hfP*]	1.431
Root radius factor	[rhofP*]	0.377 (rhofPmax*=0.378)
Addendum coefficient	[haP*]	1.181
Tip radius factor	[rhoaP*]	0.000
Protuberance height coefficient	[hprP*]	0.000
Protuberance angle	[alfprP]	0.000
Tip form height coefficient	[hFaP*]	0.000
Ramp angle	[alfKP]	0.000

not topping

Summary of reference profile gears:

Dedendum reference profile	[hfP*]	1.431	1.431
Tooth root radius Refer. profile	[rofP*]	0.377	0.377
Addendum Reference profile	[haP*]	1.181	1.181
Protuberance height coefficient	[hprP*]	0.000	0.000
Protuberance angle (°)	[alfprP]	0.000	0.000
Tip form height coefficient	[hFaP*]	0.000	0.000
Ramp angle (°)	[alfKP]	0.000	0.000

Type of profile modification: none (only running-in)

Tip relief (µm)	[Ca]	2.0	2.0

Lubrication type		Oil bath lubrication
Type of oil (Own input)		Castrol ATF Dex II Multivehicle
Lubricant base		Mineral-oil base
Kinem. viscosity oil at 40 °C (mm²/s)	[nu40]	39.00
Kinem. viscosity oil at 100 °C (mm²/s)	[nu100]	7.50
Specific density at 15 °C (kg/dm³)	[roOil]	0.870
Oil temperature (°C)	[TS]	75.000

		------- GEAR 1 --------	GEAR 2 --
Overall transmission ratio	[itot]		-2.961
Gear ratio	[u]		2.961
Transverse module (mm)	[mt]		1.278
Pressure angle at pitch circle (°)	[alft]		20.410
Working transverse pressure angle (°)	[alfwt]		21.484
	[alfwt.e/i]	21.507 /	21.462
Working pressure angle at normal section (°)	[alfwn]		21.050

Helix angle at operating pitch circle (°)	[betaw]	12.084	
Base helix angle (°)	[betab]	11.267	
Reference center distance (mm)	[ad]	129.071	
Sum of profile shift coefficients	[Summexi]	0.7625	
Profile shift coefficient	[x]	0.3715	0.3910
Tooth thickness (Arc) (module) (module)	[sn*]	1.8412	1.8554
Tip alteration (mm)	[k*mn]	0.000	0.000
Reference diameter (mm)	[d]	65.174	192.967
Base diameter (mm)	[db]	61.083	180.852
Tip diameter (mm)	[da]	69.055	196.897
(mm)	[da.e/i]	69.055 / 69.045	196.897 / 196.887
Tip diameter allowances (mm)	[Ada.e/i]	0.000 / -0.010	0.000 / -0.010
Tip form diameter (mm)	[dFa]	69.055	196.897
(mm)	[dFa.e/i]	69.055 / 69.045	196.897 / 196.887
Active tip diameter (mm)	[dNa]	69.055	196.897
Active tip diameter (mm)	[dNa.e/i]	69.055 / 69.045	196.897 / 196.887
Operating pitch diameter (mm)	[dw]	65.644	194.356
(mm)	[dw.e/i]	65.654 / 65.633	194.386 / 194.327
Root diameter (mm)	[df]	62.525	190.367
Generating Profile shift coefficient	[xE.e/i]	0.3056/ 0.2396	0.3031/ 0.2151
Manufactured root diameter with xE (mm)	[df.e/i]	62.361 / 62.196	190.147 / 189.927
Theoretical tip clearance (mm)	[c]	0.289	0.289
Effective tip clearance (mm)	[c.e/i]	0.534 / 0.379	0.479 / 0.351
Active root diameter (mm)	[dNf]	63.505	191.515
(mm)	[dNf.e/i]	63.542 / 63.475	191.558 / 191.479
Root form diameter (mm)	[dFf]	63.381	191.061
(mm)	[dFf.e/i]	63.256 / 63.135	190.859 / 190.658
Reserve (dNf-dFf)/2 (mm)	[cF.e/i]	0.204 / 0.110	0.450 / 0.310
Addendum (mm)	[ha=mn*(haP*+x+k)]	1.941	1.965
(mm)	[ha.e/i]	1.941 / 1.936	1.965 / 1.960
Dedendum (mm)	[hf=mn*(hfP*-x)]	1.324	1.300
(mm)	[hf.e/i]	1.407 / 1.489	1.410 / 1.520
Roll angle at dFa (°)	[xsi_dFa.e/i]	30.215 / 30.195	24.664 / 24.656
Roll angle to dNa (°)	[xsi_dNa.e/i]	30.215 / 30.195	24.664 / 24.656
Roll angle to dNf (°)	[xsi_dNf.e/i]	16.422 / 16.193	20.004 / 19.928
Roll angle at dFf (°)	[xsi_dFf.e/i]	15.420 / 14.977	19.322 / 19.122
Tooth height (mm)	[h]	3.265	3.265
Virtual gear no. of teeth	[zn]	54.209	160.500
Normal tooth thickness at tip circle (mm)	[san]	0.668	0.806
(mm)	[san.e/i]	0.610 / 0.541	0.728 / 0.643
Normal tooth thickness on tip form circle (mm)	[sFan]	0.668	0.806
(mm)	[sFan.e/i]	0.610 / 0.541	0.728 / 0.643
Normal space width at root circle (mm)	[efn]	0.797	0.701
(mm)	[efn.e/i]	0.818 / 0.842	0.708 / 0.717
Max. sliding velocity at tip (m/s)	[vga]	2.035	1.661
Specific sliding at the tip	[zetaa]	0.339	0.339
Specific sliding at the root	[zetaf]	-0.514	-0.514
Mean specific sliding	[zetam]	0.339	
Sliding factor on tip	[Kga]	0.166	0.136
Sliding factor on root	[Kgf]	-0.136	-0.166
Pitch on reference circle (mm)	[pt]	4.015	
Base pitch (mm)	[pbt]	3.763	
Transverse pitch on contact-path (mm)	[pet]	3.763	
Lead height (mm)	[pz]	963.277	2852.055
Axial pitch (mm)	[px]	18.888	
Length of path of contact (mm)	[ga, e/i]	7.419 (7.474 / 7.341)	

Length T1-A, T2-A (mm)	[T1A, T2A]	8.686(	8.632/	8.754)	38.926(	38.926/	38.913)
Length T1-B (mm)	[T1B, T2B]	12.343(	12.343/	12.332)	35.269(	35.214/	35.334)
Length T1-C (mm)	[T1C, T2C]	12.021(	12.007/	12.035)	35.591(	35.550/	35.632)
Length T1-D (mm)	[T1D, T2D]	12.449(	12.394/	12.516)	35.163(	35.163/	35.150)
Length T1-E (mm)	[T1E, T2E]	16.106(	16.106/	16.095)	31.506(	31.452/	31.571)
Length T1-T2 (mm)	[T1T2]			47.612 (	47.557 /	47.667)	
Diameter of single contact point B (mm)	[d-B]	65.882(	65.882/	65.874)	194.121(	194.082/	194.169)
Diameter of single contact point D (mm)	[d-D]	65.962(	65.921/	66.013)	194.044(	194.044/	194.035)
Addendum contact ratio	[eps]	1.086(	1.089/	1.079)	0.886(	0.897/	0.872)
Minimal length of contact line (mm)	[Lmin]			79.945			

Transverse contact ratio	[eps_a]		1.972	
Transverse contact ratio with allowances	[eps_a.e/m/i]	1.986 /	1.969 /	1.951
Overlap ratio	[eps_b]		2.118	
Total contact ratio	[eps_g]		4.090	
Total contact ratio with allowances	[eps_g.e/m/i]	4.104 /	4.087 /	4.069

2. FACTORS OF GENERAL INFLUENCE

		------- GEAR 1	-------- GEAR 2 --	
Nominal circum. force at pitch circle (N)	[Ft]		2059.7	
Axial force (N)	[Fa]		437.8	
Radial force (N)	[Fr]		766.4	
Normal force (N)	[Fnorm]		2240.9	
Nominal circumferential force per mm (N/mm)	[w]		51.49	
Only as information: Forces at operating pitch circle:				
Nominal circumferential force (N)	[Ftw]		2045.0	
Axial force (N)	[Faw]		437.8	
Radial force (N)	[Frw]		804.9	
Circumferential speed reference circle (m/s)	[v]		12.14	
Circumferential speed operating pitch circle (m/s)	[v(dw)]		12.23	
Running-in value (µm)	[yp]		0.6	
Running-in value (µm)	[yf]		0.6	
Correction coefficient	[CM]		0.800	
Gear body coefficient	[CR, bs/b, sr/mn]		0.898	(0.250, 4.983)
Basic rack factor	[CBS]		0.885	
Material coefficient	[E/Est]		1.000	
Singular tooth stiffness (N/mm/µm)	[c']		11.543	
Meshing stiffness (N/mm/µm)	[cgalf]		19.956	
Meshing stiffness (N/mm/µm)	[cgbet]		16.962	
Reduced mass (kg/mm)	[mRed]		0.01382	
Resonance speed (min-1)	[nE1]		7116	
Resonance ratio (-)	[N]		0.500	
Subcritical range				
Running-in value (µm)	[ya]		0.6	
Bearing distance l of pinion shaft (mm)	[l]		80.000	
Distance s of pinion shaft (mm)	[s]		8.000	
Outside diameter of pinion shaft (mm)	[dsh]		40.000	
Load in accordance with Figure 13, ISO 6336-1:2006	[-]	4		
0:a), 1:b), 2:c), 3:d), 4:e)				
Coefficient K' according to Figure 13, ISO 6336-1:2006	[K']	-1.00		
Without support effect				
Tooth trace deviation (active) (µm)	[Fby]		4.97	
from deformation of shaft (µm)	[fsh*B1]		0.49	
(fsh (µm) = 0.49, B1= 1.00, fHb5 (µm) = 6.50)				

Tooth without tooth trace modification			
Position of Contact pattern: favorable			
from production tolerances (µm)	[fma*B2]	12.38	
(B2= 1.00)			
Tooth trace deviation, theoretical (µm)	[Fbx]	5.85	
Running-in value (µm)	[yb]	0.88	
Dynamic factor	[KV]	1.325	
Face load factor - flank	[KHb]	1.495	
- Tooth root	[KFb]	1.444	
- Scuffing	[KBb]	1.495	
Transverse load factor - flank	[KHa]	1.470	
- Tooth root	[KFa]	1.470	
- Scuffing	[KBa]	1.470	
Helical load factor scuffing	[Kbg]	1.300	
Number of load cycles (in mio.)	[NL]	1067.040	360.391

3. TOOTH ROOT STRENGTH

Calculation of Tooth form coefficients according method: B

		------- GEAR 1	-------- GEAR 2 --
Calculated with manufacturing profile shift	[xE.e]	0.3056	0.3031
Tooth form factor	[YF]	1.02	1.10
Stress correction factor	[YS]	2.34	2.39
Working angle (°)	[alfFen]	19.83	20.28
Bending moment arm (mm)	[hF]	1.16	1.36
Tooth thickness at root (mm)	[sFn]	2.93	3.04
Tooth root radius (mm)	[roF]	0.59	0.53

(hF* = 0.930/ 1.088 sFn* = 2.345/ 2.436 roF* = 0.474/ 0.423)
(den (mm) =
68.437/201.674 dsFn(mm) = 62.846/190.628 alfsFn(°) = 30.00/ 30.00 qs = 2.472/ 2.881)

Helix angle factor	[Ybet]		0.900	
Deep tooth factor	[YDT]		1.000	
Gear rim factor	[YB]	1.00		1.00
Effective facewidth (mm)	[beff]	40.00		40.00
Nominal stress at tooth root (N/mm²)	[sigF0]	88.16		97.45
Tooth root stress (N/mm²)	[sigF]	309.89		342.54
Permissible bending stress at root of Test-gear				
Notch sensitivity factor	[YdrelT]	1.000		1.003
Surface factor	[YRrelT]	1.031		1.031
size factor (Tooth root)	[YX]	1.000		1.000
Finite life factor	[YNT]	0.889		0.909
[YdrelT*YRrelT*YX*YNT]		0.917		0.940
Alternating bending factor (mean stress influence coefficient)	[YM]		1.000	1.000
Stress correction factor	[Yst]		2.00	
Yst*sigFlim (N/mm²)	[sigFE]	1000.00		1000.00
Permissible tooth root stress (N/mm²)	[sigFP=sigFG/SFmin]	654.72		671.63
Limit strength tooth root (N/mm²)	[sigFG]	916.61		940.28
Required safety	[SFmin]	1.40		1.40
Safety for tooth root stress	[SF=sigFG/sigF]	2.96		2.74

Transmittable power (kW)	[kWRating]	52.82	49.02

4. SAFETY AGAINST PITTING (TOOTH FLANK)

		GEAR 1	GEAR 2
Zone factor	[ZH]	2.382	
Elasticity factor (√N/mm²)	[ZE]	189.812	
Contact ratio factor	[Zeps]	0.712	
Helix angle factor	[Zbet]	1.011	
Effective facewidth (mm)	[beff]	40.00	
Nominal contact stress (N/mm²)	[sigH0]	334.68	
Contact stress at operating pitch circle (N/mm²)	[sigHw]	638.31	
Single tooth contact factor	[ZB,ZD]	1.00	1.00
Contact stress (N/mm²)	[sigHB, sigHD]	638.31	638.31
Lubrication coefficient at NL	[ZL]	0.927	0.927
Speed coefficient at NL	[ZV]	1.006	1.006
Roughness coefficient at NL	[ZR]	0.997	0.997
Material pairing coefficient at NL	[ZW]	1.000	1.000
Finite life factor	[ZNT]	0.910	0.941
	[ZL*ZV*ZR*ZNT]	0.846	0.875
Limited pitting is permitted:	No		
Size factor (flank)	[ZX]	1.000	1.000
Permissible contact stress (N/mm²)	[sigHP=sigHG/SHmin]	1153.55	1192.61
Pitting stress limit (N/mm²)	[sigHG]	1268.91	1311.87
Required safety	[SHmin]	1.10	1.10
Safety factor for contact stress at operating pitch circle			
	[SHw]	1.99	2.06
Safety for stress at single tooth contact	[SHBD=sigHG/sigHBD]	1.99	2.06
(Safety regarding transmittable torque)	[(SHBD)^2]	3.95	4.22
Transmittable power (kW)	[kWRating]	81.65	87.27

4b. MICROPITTING ACCORDING TO ISO/TR 15144-1:2014

Calculation did not run. (Lubricant: Load stage micropitting test is unknown.)

5. SCUFFING LOAD CAPACITY

Calculation method according to ISO TR 13989:2000

Lubrication coefficient (for lubrication type)	[XS]	1.000	
Scuffing test and load stage	[FZGtest]	FZG - Test A / 8.3 / 90 (ISO 14635 - 1)	12
Multiple meshing factor	[Xmp]	1.000	
Relative structure coefficient (Scuffing)	[XWrelT]	1.000	
Thermal contact factor (N/mm/s^.5/K)	[BM]	13.780	13.780
Relevant tip relief (µm)	[Ca]	2.00	2.00
Optimal tip relief (µm)	[Ceff]	3.23	
Ca taken as optimal in the calculation (0=no, 1=yes)		0	0
Effective facewidth (mm)	[beff]	40.000	
Applicable circumferential force/facewidth (N/mm)	[wBt]	187.305	

Kbg = 1.300, wBt*Kbg = 243.497

Angle factor	[Xalfbet]	0.995
(ε1:1.086, ε2:0.886)		
Flash temperature-criteria		
Lubricant factor	[XL]	0.888
Tooth mass temperature (°C)	[theMi]	77.81
(theMi = theoil + XS*0.47*Xmp*theflm)		
Average flash temperature (°C)	[theflm]	5.97
Scuffing temperature (°C)	[theS]	367.57
Coordinate gamma (point of highest temp.)	[Gamma]	0.340
[Gamma.A]=-0.277 [Gamma.E]=0.340		
Highest contact temp. (°C)	[theB]	92.40
Flash factor (°K*N^-.75*s^.5*m^-.5*mm)	[XM]	50.058
Approach factor	[XJ]	1.000
Load sharing factor	[XGam]	0.659
Dynamic viscosity (mPa*s)	[etaM]	10.86 (75.0 °C)
Coefficient of friction	[mym]	0.047
Required safety	[SBmin]	2.000
Safety factor for scuffing (flash temperature)	[SB]	16.819
Integral temperature-criteria		
Lubricant factor	[XL]	1.000
Tooth mass temperature (°C)	[theMC]	77.31
(theMC = theoil + XS*0.70*theflaint)		
Mean flash temperature (°C)	[theflaint]	3.30
Integral scuffing temperature (°C)	[theSint]	366.33
Flash factor (°K*N^-.75*s^.5*m^-.5*mm)	[XM]	50.058
Running-in factor (well run in)	[XE]	1.000
Contact ratio factor	[Xeps]	0.211
Dynamic viscosity (mPa*s)	[etaOil]	10.86 (75.0 °C)
Mean coefficient of friction	[mym]	0.053
Geometry factor	[XBE]	0.161
Meshing factor	[XQ]	1.000
Tip relief factor	[XCa]	1.714
Integral tooth flank temperature (°C)	[theint]	82.27
Required safety	[SSmin]	1.800
Safety factor for scuffing (intg.-temp.)	[SSint]	4.453
Safety referring to transmittable torque	[SSL]	40.078

6. MEASUREMENTS FOR TOOTH THICKNESS

		------- Gear 1 ------	Gear 2 --
Tooth thickness deviation		DIN 3967 d26	DIN 3967 d26
Tooth thickness allowance (normal section) (mm)	[As.e/i]	-0.060 / -0.120	-0.080 / -0.160
Number of teeth spanned	[k]	7.000	19.000
Base tangent length (no backlash) (mm)	[Wk]	25.255	71.418
Actual base tangent length ('span') (mm)	[Wk.e/i]	25.198 / 25.142	71.343 / 71.268
(mm)	[ΔWk.e/i]	-0.056 / -0.113	-0.075 / -0.150
Diameter of measuring circle (mm)	[dMWk.m]	65.882	193.902
Theoretical diameter of ball/pin (mm)	[DM]	2.191	2.124
Effective diameter of ball/pin (mm)	[DMeff]	2.500	2.500
Radial single-ball measurement backlash free (mm)	[MrK]	35.101	99.112
Radial single-ball measurement (mm)	[MrK.e/i]	35.034 / 34.967	99.011 / 98.910
Diameter of measuring circle (mm)	[dMMr.m]	66.495	194.505

Diametral measurement over two balls without clearance (mm)	[MdK]		70.170		198.213
Diametral two ball measure (mm)	[MdK.e/i]	70.037 /	69.902	198.012 /	197.809
Diametral measurement over pins without clearance (mm)	[MdR]		70.202		198.223
Measurement over pins according to DIN 3960 (mm)	[MdR.e/i]	70.069 /	69.933	198.022 /	197.820
Measurement over 2 pins (free) according to AGMA 2002 (mm)					
	[dk2f.e/i]	70.035 /	69.900	198.011 /	197.809
Measurement over 2 pins (transverse) according to AGMA 2002 (mm)					
	[dk2t.e/i]	70.100 /	69.965	198.033 /	197.830
Measurement over 3 pins (axial) according to AGMA 2002 (mm)					
	[dk3A.e/i]	70.069 /	69.933	198.022 /	197.820
Chordal tooth thickness (no backlash) (mm)	[sc]		2.301		2.319
Actual chordal tooth thickness (mm)	[sc.e/i]	2.241 /	2.181	2.239 /	2.159
Reference chordal height from da.m (mm)	[ha]		1.958		1.969
Tooth thickness (Arc) (mm)	[sn]		2.302		2.319
(mm)	[sn.e/i]	2.242 /	2.182	2.239 /	2.159
Backlash free center distance (mm)	[aControl.e/i]		129.816	/129.630	
Backlash free center distance, allowances (mm)	[jta]		-0.184 /	-0.370	
dNf.i with aControl (mm)	[dNf0.i]		62.978		190.854
Reserve (dNf0.i-dFf.e)/2 (mm)	[cF0.i]		-0.139		-0.002
Tip clearance (mm)	[c0.i(aControl)]		0.029		0.002
Center distance allowances (mm)	[Aa.e/i]		0.020 /	-0.020	
Circumferential backlash from Aa (mm)	[jtw_Aa.e/i]		0.016 /	-0.016	
Radial clearance (mm)	[jrw]		0.390 /	0.164	
Circumferential backlash (transverse section) (mm)	[jtw]		0.304 /	0.128	
Normal backlash (mm)	[jnw]		0.279 /	0.118	
Torsional angle at entry with fixed output:					
Entire torsional angle (°)	[j.tSys]			0.5308/ 0.2242	

7. GEAR ACCURACY

		------- GEAR 1	------- GEAR 2 --
According to ISO 1328-1:1995, ISO 1328-2:1997			
Accuracy grade	[Q]	6	6
Single pitch deviation (µm)	[fptT]	7.50	8.50
Base circle pitch deviation (µm)	[fpbT]	7.00	8.00
Sector pitch deviation over k/8 pitches (µm)	[Fpk/8T]	13.00	18.00
Profile form deviation (µm)	[ffaT]	6.50	7.50
Profile slope deviation (µm)	[fHaT]	5.50	6.00
Total profile deviation (µm)	[FaT]	8.50	10.00
Helix form deviation (µm)	[ffbT]	8.50	9.00
Helix slope deviation (µm)	[fHbT]	8.50	9.00
Total helix deviation (µm)	[FbT]	12.00	13.00
Total cumulative pitch deviation (µm)	[FpT]	26.00	35.00
Runout (µm)	[FrT]	21.00	28.00
Single flank composite, total (µm)	[FisT]	35.00	44.00
Single flank composite, tooth-to-tooth (µm)	[fisT]	9.00	9.50
Radial composite, total (µm)	[FidT]	27.00	34.00
Radial composite, tooth-to-tooth (µm)	[fidT]	6.50	6.50

Axis alignment tolerances (recommendation acc. to ISO TR 10064-3:1996, Quality)		6)
Maximum value for deviation error of axis (µm)	[fSigbet]	13.00 (Fb= 13.00)
Maximum value for inclination error of axes (µm)	[fSigdel]	26.00

8. ADDITIONAL DATA

Maximal possible center distance (eps_a=1.0)	[aMAX]	131.383	
Mass (kg)	[m]	1.065	8.608
Total mass (kg)	[m]	9.673	
Moment of inertia (system with reference to the drive):			
calculation without consideration of the exact tooth shape			
single gears ((da+df)/2...di) (kg*m²)	[TraeghMom]	0.0005761	0.04303
System ((da+df)/2...di) (kg*m²)	[TraeghMom]	0.005485	
Torsional stiffness on input for stopped output:			
Torsional stiffness (MNm/rad)	[cr]	0.628	
Torsion when subjected to nominal torque (°)	[delcr]	0.006	
Mean coeff. of friction (acc. Niemann)	[mum]	0.053	
Wear sliding coef. by Niemann	[zetw]	0.669	
Gear power loss (kW)	[PVZ]	0.111	
(Meshing efficiency (%)	[etaz]	99.558)	
Sound pressure level (according to Masuda)	[dB(A)]	73.4	

Indications for the manufacturing by wire cutting:			
Deviation from theoretical tooth trace (µm)	[WireErr]	276.9	93.6
Permissible deviation (µm)	[Fb/2]	6.0	6.5

9. MODIFICATIONS AND TOOTH FORM DEFINITION

Data for the tooth form calculation :
Data not available.

10. SERVICE LIFE, DAMAGE

Required safety for tooth root	[SFmin]	1.40
Required safety for tooth flank	[SHmin]	1.10

Service life (calculated with required safeties):

System service life (h)	[Hatt]	>	1000000

Tooth root service life (h)	[HFatt]	1e+006	1e+006
Tooth flank service life (h)	[HHatt]	1e+006	1e+006

Note: The entry 1e+006 h means that the Service life > 1,000,000 h.

Damage calculated on the basis of the required service life [H] (5000.0 h)

F1%	F2%	H1%	H2%
0.00	0.00	0.00	0.00

Calculation of the factors required to define reliability R(t) according to B. Bertsche with Weibull distribution:
R(t) = 100 * Exp(-((t*fac - t0)/(T - t0))^b) %; t (h)

Gear		fac	b	t0	T	R(H)%
1	Tooth root	213408	1.7	9.654e+029	1.484e+030	100.00
1	Tooth flank	213408	1.3	9.014e+029	4.295e+030	100.00
2	Tooth root	72078	1.7	9.654e+029	1.484e+030	100.00
2	Tooth flank	72078	1.3	9.014e+029	4.295e+030	100.00

Reliability of the configuration for required service life (%) 100.00 (Bertsche)

REMARKS:

- Specifications with [.e/i] imply: Maximum [e] and Minimal value [i] with consideration of all tolerances
  Specifications with [.m] imply: Mean value within tolerance
- For the backlash tolerance, the center distance tolerances and the tooth thickness deviation are taken into account. Shown is the maximal and the minimal backlash corresponding the largest resp. the smallest allowances
  The calculation is done for the operating pitch circle.
- Calculation of Zbet according Corrigendum 1 ISO 6336-2:2008 with Zbet = 1/(COS(beta)^0.5)
- Details of calculation method:
  cg according to method B
  KV according to method B
  KHb, KFb according method C
  fma following equation (64), fsh following (57/58), Fbx following (52/53/57)
  KHa, KFa according to method B
- The logarithmically interpolated value taken from the values for the fatigue strength and the static strength, based on the number of load cycles, is used for coefficients ZL, ZV, ZR, ZW, ZX, YdrelT, YRrelT and YX..

End of Report lines: 531

Appendix D

Shaft calculation KISSsoft report

In this appendix the reports from the KISSsoft software, for the shaft calculations, where specific information regarding shafts, bearings and their thermally safe operating speed, again at the operating conditions of maximum torque and maximum speed, are sequentially presented as follows:

- Shaft A operating at maximum torque (shaftATorque);
- Shaft B operating at maximum torque (shaftBTorque);
- Shaft C operating at maximum torque (shaftCTorque);
- Shaft A operating at maximum speed (shaftASpeed);
- Shaft B operating at maximum speed (shaftBSpeed);
- Shaft C operating at maximum speed (shaftCSpeed).

KISSsoft Release 03/2017 F

KISSsoft University license - Universidade do Porto

File

Name : shaftATorque

Changed by: Carlos Rodrigues on: 02.07.2018 at: 14:26:34

Analysis of shafts, axle and beams

Input data

Coordinate system shaft: see picture W-002

Label		Shaft 1
Drawing		
Initial position (mm)		0.000
Length (mm)		163.900
Speed (1/min)		3500.00
Sense of rotation: clockwise		
Material		18CrNiMo7-6
Young's modulus (N/mm²)		206000.000
Poisson's ratio nu		0.300
Density (kg/m³)		7830.000
Coefficient of thermal expansion	(10^-6/K)	11.500
Temperature (°C)		65.000
Weight of shaft (kg)		0.799
(Notice: Weight stands for the shaft only without considering the gears)		
Weight of shaft, including additional masses (kg)		0.839
Mass moment of inertia (kg*mm²)		100.120
Momentum of mass GD2 (Nm²)		0.004
Position in space (°)		0.000
Gears mounted with stiffness according to ISO		
Consider deformations due to shearing		
Shear correction coefficient		1.100
Contact angle of rolling bearings is considered		
Tolerance field: Mean value		
Housing material		G-AlSi10Mg
Coefficient of thermal expansion	(10^-6/K)	22.000
Temperature of housing (°C)		55.000
Thermal housing reference point (mm)		0.000
Reference temperature (°C)		20.000

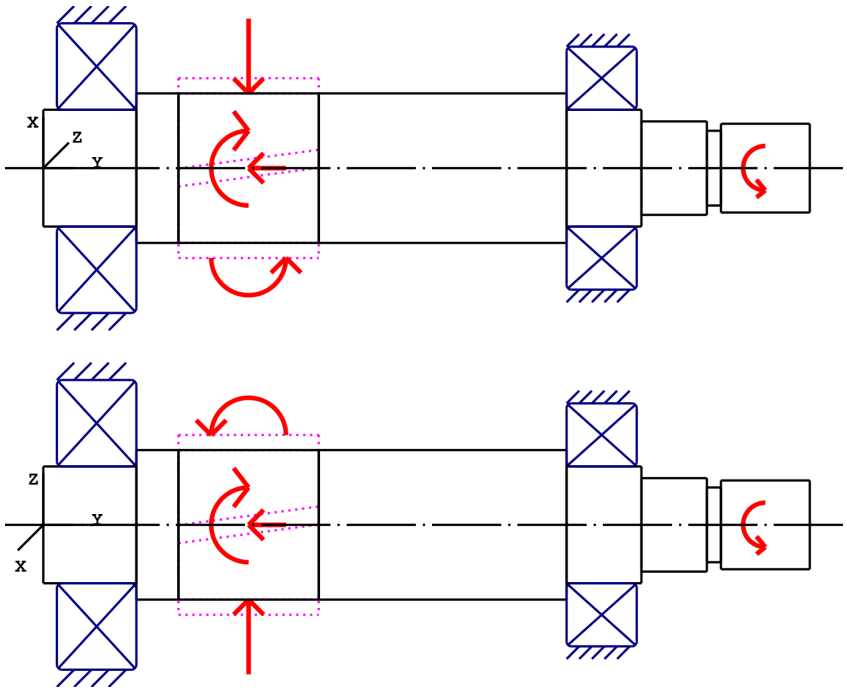

Figure: Load applications

Shaft definition (Shaft 1)

Outer contour

Cylinder (Cylinder)			0.000mm ... 19.900mm
Diameter (mm)	[d]	25.0000	
Length (mm)	[l]	19.9000	
Surface roughness (µm)	[Rz]	4.8000	

Relief groove right (Relief groove right)
r=0.80 (mm), t=0.30 (mm), l=2.50 (mm), Rz=8.0, Turned (Ra=3.2µm/125µin)
Form E (DIN 509), Series 1, with the usual stressing

Chamfer left (Chamfer left)
l=0.50 (mm), alpha=45.00 (°)

Square groove (Square groove)
b=1.30 (mm), t=0.55 (mm), r=0.10 (mm), Rz=8.0, Turned (Ra=3.2µm/125µin)

Cylinder (Cylinder)			19.900mm ... 111.900mm
Diameter (mm)	[d]	32.0000	
Length (mm)	[l]	92.0000	
Surface roughness (µm)	[Rz]	4.8000	

Cylinder (Cylinder)			111.900mm ... 127.900mm
Diameter (mm)	[d]	25.0000	
Length (mm)	[l]	16.0000	

Surface roughness (µm)	[Rz]	4.8000

Relief groove left (Relief groove left)
r=0.80 (mm), t=0.30 (mm), l=2.50 (mm), Rz=8.0, Turned (Ra=3.2µm/125µin)
Form E (DIN 509), Series 1, with the usual stressing

Chamfer right (Chamfer right)
l=0.50 (mm), alpha=45.00 (°)

Cylinder (Cylinder)			127.900mm ...	141.900mm
Diameter (mm)	[d]	20.0000		
Length (mm)	[l]	14.0000		
Surface roughness (µm)	[Rz]	8.0000		

Chamfer right (Chamfer right)
l=0.50 (mm), alpha=45.00 (°)

Radius left (Radius left)
r=0.10 (mm), Rz=8.0, Turned (Ra=3.2µm/125µin)

Cylinder (Cylinder)			141.900mm ...	144.900mm
Diameter (mm)	[d]	16.0000		
Length (mm)	[l]	3.0000		
Surface roughness (µm)	[Rz]	8.0000		

Radius left (Radius left)
r=0.10 (mm), Rz=8.0, Turned (Ra=3.2µm/125µin)

Cylinder (Cylinder)			144.900mm ...	163.900mm
Diameter (mm)	[d]	19.0000		
Length (mm)	[l]	19.0000		
Surface roughness (µm)	[Rz]	8.0000		

Chamfer right (Chamfer right)
l=0.50 (mm), alpha=45.00 (°)

Spline (Spline) 135.400mm ... 154.400mm
da=18.84 (mm), df=17.16 (mm), z=22, mn=0.80 (mm), l=19.00 (mm), Rz=8.0, Turned (Ra=3.2µm/125µin)

Forces

Type of force element		**Cylindrical gear**
Label in the model		Cylindrical gear
Position on shaft (mm)	[y_{local}]	43.9000
Position in global system (mm)	[y_{global}]	43.9000
Operating pitch diameter (mm)		38.4914
Helix angle (°)		12.0156 left
Working pressure angle at normal section (°)		20.2001
Position of contact (°)		20.0000
Length of load application (mm)		30.0000
Power (kW)		25.6563 driving (output)
Torque (Nm)		-70.0000
Axial force (N)		-774.1393

Shearing force X (N)		-2529.6762
Shearing force Z (N)		2949.8772
Bending moment X (Nm)		5.0957
Bending moment Z (Nm)		-14.0003

Type of force element		**Coupling**
Label in the model		Coupling
Position on shaft (mm)	[y_{local}]	154.4000
Position in global system (mm)	[y_{global}]	154.4000
Effective diameter (mm)		20.0000
Radial force factor (-)		0.0000
Direction of the radial force (°)		0.0000
Axial force factor (-)		0.0000
Length of load application (mm)		19.0000
Power (kW)		25.6563 driven (input)
Torque (Nm)		70.0000
Axial force (N)		0.0000
Shearing force X (N)		0.0000
Shearing force Z (N)		0.0000
Bending moment X (Nm)		0.0000
Bending moment Z (Nm)		0.0000
Mass (kg)		0.0000
Mass moment of inertia Jp (kg*m²)		0.0000
Mass moment of inertia Jxx (kg*m²)		0.0000
Mass moment of inertia Jzz (kg*m²)		0.0000
Eccentricity (mm)		0.0000

Bearing

Label in the model		Rolling bearing
Bearing type		SKF 6205 ETN9
Bearing type		Deep groove ball bearing (single row)

Bearing position (mm)	[y_{lokal}]	119.400
Bearing position (mm)	[y_{global}]	119.400
Attachment of external ring		Fixed bearing
Inner diameter (mm)	[d]	25.000
External diameter (mm)	[D]	52.000
Width (mm)	[b]	15.000
Corner radius (mm)	[r]	1.000
Basic static load rating (kN)	[C_0]	9.300
Basic dynamic load rating (kN)	[C]	17.800
Fatigue load rating (kN)	[C_u]	0.400
Values for approximated geometry:		
Basic dynamic load rating (kN)	[C_{theo}]	0.000
Basic static load rating (kN)	[C_{0theo}]	0.000

Label in the model		Rolling bearing
Bearing type		SKF 6305 ETN9
Bearing type		Deep groove ball bearing (single row)

Bearing position (mm)	[y_{lokal}]	11.400
Bearing position (mm)	[y_{global}]	11.400
Attachment of external ring		Free bearing
Inner diameter (mm)	[d]	25.000
External diameter (mm)	[D]	62.000

Width (mm)	[b]	17.000
Corner radius (mm)	[r]	1.100
Basic static load rating (kN)	[C_0]	13.400
Basic dynamic load rating (kN)	[C]	26.000
Fatigue load rating (kN)	[C_u]	0.570
Values for approximated geometry:		
Basic dynamic load rating (kN)	[C_{theo}]	0.000
Basic static load rating (kN)	[C_{0theo}]	0.000

Shaft 'Shaft 1': Cylindrical gear 'Cylindrical gear' (y= 43.9000 (mm)) is taken into account as component of the shaft.
EI (y= 28.9000 (mm)): 10603.2019 (Nm²), EI (y= 58.9000 (mm)): 10603.2019 (Nm²), m (yS= 43.9000 (mm)): 0.0403 (kg)
Jp: 0.0000 (kg*m²), Jxx: 0.0000 (kg*m²), Jzz: 0.0000 (kg*m²)

Results

Shaft

Maximum deflection (µm)	13.764
Position of the maximum (mm)	58.900
Mass center of gravity (mm)	72.807
Total axial load (N)	-774.139
Torsion under torque (°)	0.159

Bearing

Probability of failure	[n]	10.00	%
Axial clearance	[u_A]	10.00	µm
Lubricant	Castrol ATF Dex II Multivehicle		
Lubricant with additive, effect on bearing lifetime confirmed in tests.			
Oil lubrication, off-line/no filtration, ISO4406 -/15/12			
Lubricant - service temperature	[T_B]	65.00	°C
Limit for factor aISO	[a_{ISOmax}]	50.00	
Oil level	[h_{oil}]	0.00	mm
Oil bath lubrication			

Rolling bearings, classical calculation (contact angle considered)

Shaft 'Shaft 1' Rolling bearing 'Rolling bearing'

Position (Y-coordinate)	[y]	119.40	mm
Dynamic equivalent load	[P]	1.83	kN
Equivalent load	[P_0]	1.12	kN
Life modification factor for reliability	[a_1]	1.000	
Life modification factor	[a_{ISO}]	1.064	
Nominal bearing service life	[L_{nh}]	4382.87	h
Modified bearing service life	[L_{nmh}]	4665.27	h
Operating viscosity	[v]	16.74	mm²/s
Static safety factor	[S_0]	8.27	
Bearing reaction force	[Fx]	0.632	kN

Bearing reaction force	[Fy]	0.776	kN
Bearing reaction force	[Fz]	-0.930	kN
Bearing reaction force	[Fr]	1.125	kN (-55.82°)
Oil level	[H]	0.000	mm
Rolling moment of friction	[M_{rr}]	0.039	Nm
Sliding moment of friction	[M_{sl}]	0.024	Nm
Moment of friction, seals	[M_{seal}]	0.000	Nm
Moment of friction for seals determined according to SKF main catalog 10000/1 EN:2013			
Moment of friction flow losses	[M_{drag}]	0.000	Nm
Torque of friction	[M_{loss}]	0.063	Nm
Power loss	[P_{loss}]	23.242	W
The moment of friction is calculated according to the details in SKF Catalog 2013.			
The calculation is always performed with a coefficient for additives in the lubricant μbl=0.15.			
Displacement of bearing	[u_x]	-3.512	μm
Displacement of bearing	[u_y]	81.938	μm
Displacement of bearing	[u_z]	5.170	μm
Displacement of bearing	[u_r]	6.250	μm (124.18°)
Misalignment of bearing	[r_x]	-0.134	mrad (-0.46')
Misalignment of bearing	[r_y]	0.715	mrad (2.46')
Misalignment of bearing	[r_z]	-0.109	mrad (-0.38')
Misalignment of bearing	[r_r]	0.173	mrad (0.59')

Shaft 'Shaft 1' Rolling bearing 'Rolling bearing'

Position (Y-coordinate)	[y]	11.40	mm
Dynamic equivalent load	[P]	2.77	kN
Equivalent load	[P_0]	2.77	kN
Life modification factor for reliability	[a_1]	1.000	
Life modification factor	[a_{ISO}]	1.172	
Nominal bearing service life	[L_{nh}]	3958.85	h
Modified bearing service life	[L_{nmh}]	4638.99	h
Operating viscosity	[v]	16.74	mm²/s
Static safety factor	[S_0]	4.85	
Bearing reaction force	[Fx]	1.898	kN
Bearing reaction force	[Fy]	0.000	kN
Bearing reaction force	[Fz]	-2.011	kN
Bearing reaction force	[Fr]	2.765	kN (-46.66°)
Bearing reaction moment	[Mx]	0.00	Nm
Bearing reaction moment	[My]	0.00	Nm
Bearing reaction moment	[Mz]	-0.00	Nm
Bearing reaction moment	[Mr]	0.00	Nm (-49.4°)
Oil level	[H]	0.000	mm
Rolling moment of friction	[M_{rr}]	0.029	Nm
Sliding moment of friction	[M_{sl}]	0.029	Nm
Moment of friction, seals	[M_{seal}]	0.000	Nm
Moment of friction for seals determined according to SKF main catalog 10000/1 EN:2013			
Moment of friction flow losses	[M_{drag}]	0.000	Nm
Torque of friction	[M_{loss}]	0.058	Nm
Power loss	[P_{loss}]	21.421	W
The moment of friction is calculated according to the details in SKF Catalog 2013.			
The calculation is always performed with a coefficient for additives in the lubricant μbl=0.15.			
Displacement of bearing	[u_x]	-4.317	μm
Displacement of bearing	[u_y]	25.685	μm
Displacement of bearing	[u_z]	4.520	μm
Displacement of bearing	[u_r]	6.250	μm (133.69°)
Misalignment of bearing	[r_x]	0.174	mrad (0.6')
Misalignment of bearing	[r_y]	0.000	mrad (0')

Misalignment of bearing	[r_Z]	0.121	mrad	(0.42')
Misalignment of bearing	[r_r]	0.212	mrad	(0.73')

Damage (%) [Lreq] (5000.000)

Bin no	B1	B2
1	107.17	107.78
Σ	107.17	107.78

Utilization (%) [Lreq] (5000.000)

B1	B2
102.34	102.53

Note: Utilization = (Lreq/Lh)^(1/k)
Ball bearing: k = 3, roller bearing: k = 10/3

B1: Rolling bearing
B2: Rolling bearing

Shaft '

Shaft 1', Dokumentationspunkt Meshing gear point

Y position (mm)	[y]	43.90
Equivalent stress (N/mm²)	[sigV]	25.91

	X	Y	Z	R
Displacement (mm)	-0.0081	0.0425	0.0100	0.0129
Rotation (mrad)	0.0873	0.0219	0.0440	0.0978
Force (kN)	-0.6329	0.3871	0.5385	0.8310
Torque (Nm)	-56.8896	35.0000	-45.1902	72.6538

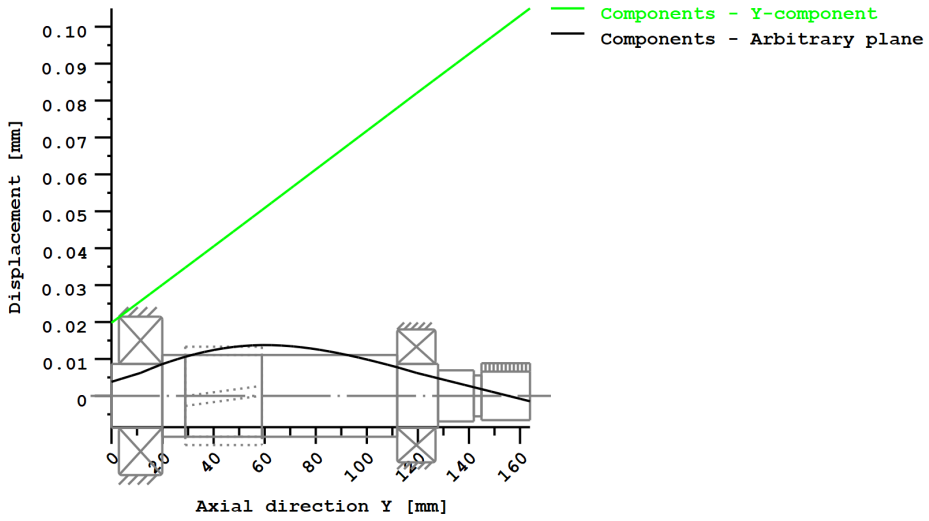

Figure: Deformation (bending etc.) (Arbitrary plane 128.0156261 121)

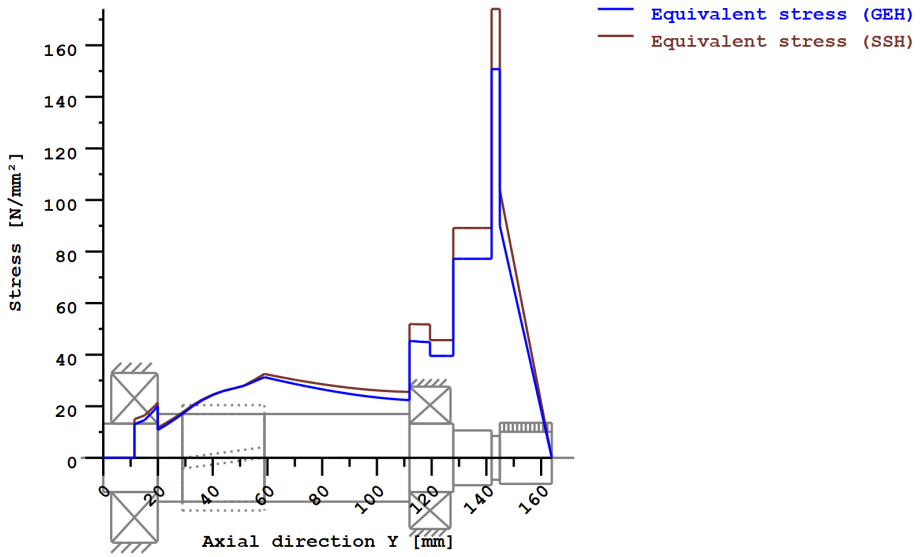

Nominal stresses, without taking into account stress concentrations
GEH(von Mises): sigV = ((sigB+sigZ,D)^2 + 3*(tauT+tauS)^2)^1/2
SSH(Tresca): sigV = ((sigB-sigZ,D)^2 + 4*(tauT+tauS)^2)^1/2

Figure: Equivalent stress

Eigenfrequencies/Critical speeds

1. Eigenfrequency:	0.00 Hz, Critical speed:	0.00 1/min	Rigid body rotation Y 'Shaft 1'
2. Eigenfrequency:	4559.70 Hz, Critical speed:	273581.98 1/min	Bending XY 'Shaft 1', Bending YZ 'Shaft 1'
3. Eigenfrequency:	7336.79 Hz, Critical speed:	440207.17 1/min	Bending XY 'Shaft 1', Bending YZ 'Shaft 1'
4. Eigenfrequency:	10674.69 Hz, Critical speed:	640481.54 1/min	Axial 'Shaft 1'
5. Eigenfrequency:	13739.13 Hz, Critical speed:	824347.98 1/min	Torsion 'Shaft 1'

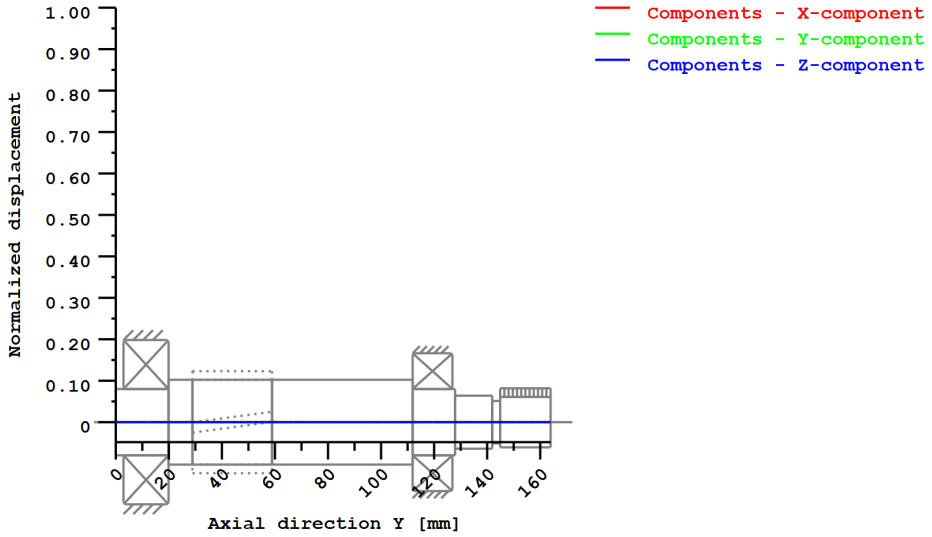

Figure: Eigenfrequencies (Normalized rotation) (Eigenfrequency: 1. (0 Hz))

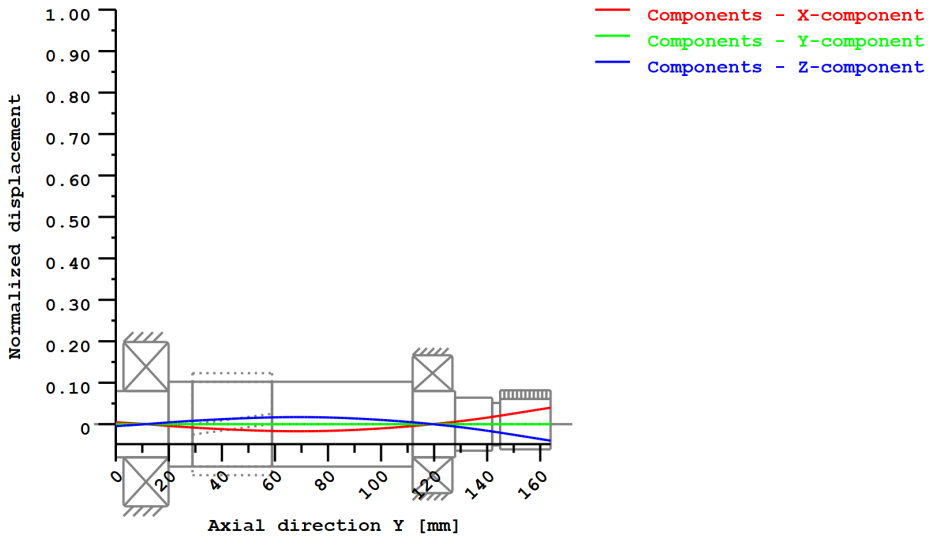

Figure: Eigenfrequencies (Normalized rotation) (Eigenfrequency: 2. (4559.7 Hz))

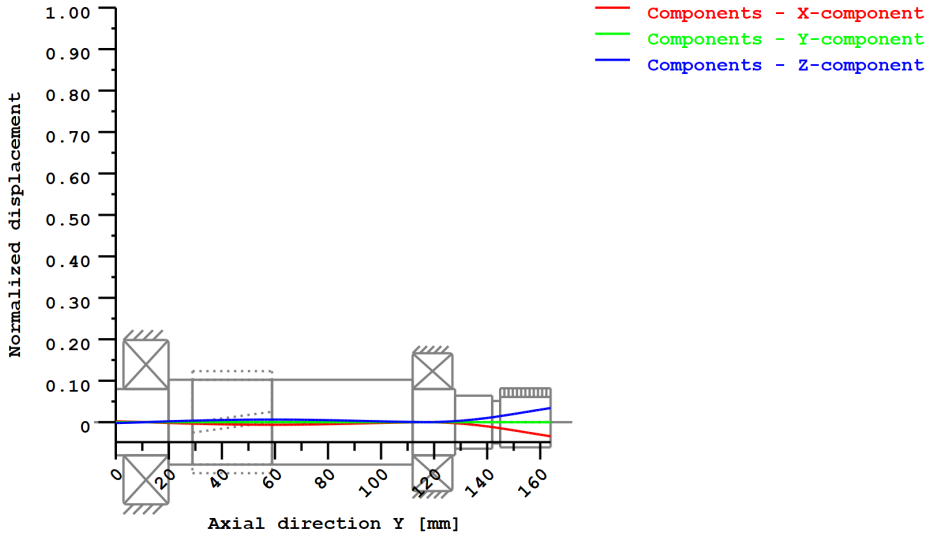

Figure: Eigenfrequencies (Normalized rotation) (Eigenfrequency: 3. (7336.79 Hz))

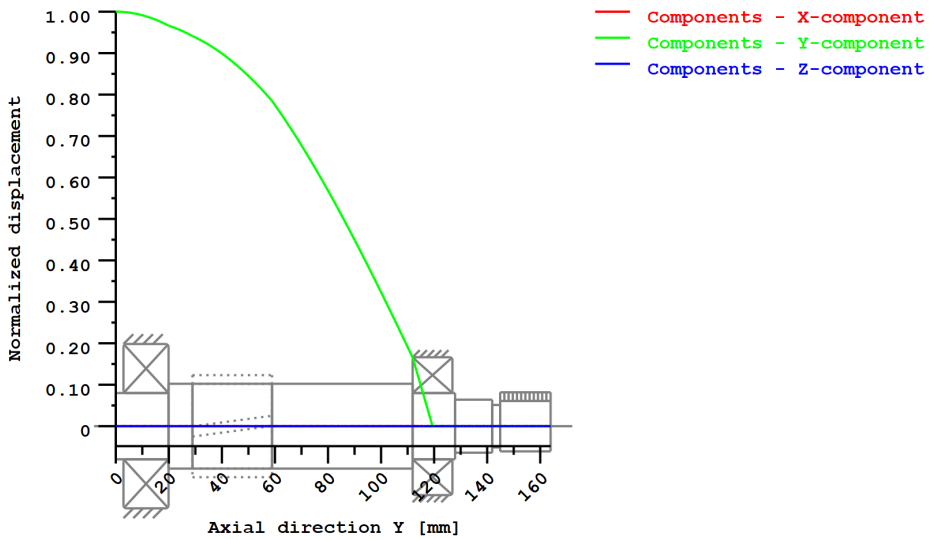

Figure: Eigenfrequencies (Normalized rotation) (Eigenfrequency: 4. (10674.69 Hz))

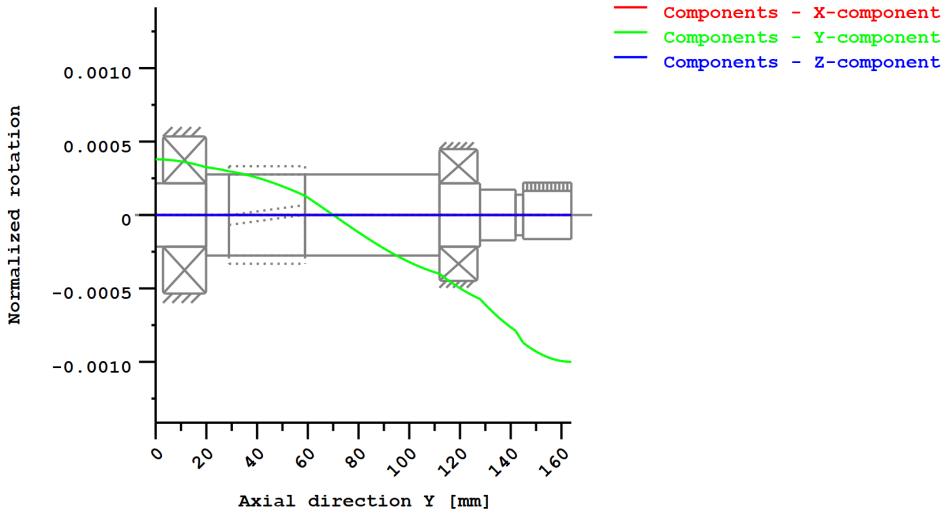

Figure: Eigenfrequencies (Normalized displacement) (Eigenfrequency: 5. (13739.13 Hz))

Strength calculation according to DIN 743:2012
with finite life fatigue strength according to FKM standard and FVA draft

Summary

Shaft 1

Material	18CrNiMo7-6
Material type	Case-carburized steel
Material treatment	case-hardened
Surface treatment	No

Calculation of finite life fatigue strength and static strength

Calculation for load case 2 (σav/σmv = const)

Cross section	Position (Y-Coord) (mm)	
A-A Shoulder	141.90	Shoulder
B-B Spline	144.91	Spline
C-C Shoulder	127.90	Shoulder

Results:

Cross section	Kfb	Kfs	K2d	SD	SS	SA
A-A Shoulder	2.06	0.85	0.95	4.15	3.02	6.09
B-B Spline	1.00	1.00	0.94	5.67	3.73	19.19
C-C Shoulder	2.25	0.85	0.93	7.62	5.91	11.09

Required safeties: 1.20 1.20 1.20

Abbreviations:
Kfb: Notch factor bending
Kfσ: Surface factor
K2d: size factor bending
SD: Safety endurance limit
SS: Safety against yield point
SA: Safety against incipient crack

Service life and damage

System service life (h) [Hatt] 1000000.00

Damage to system (%) [D] 0.00

Damage (%) [H] (5000.0 h)

Calculation of reliability R(t) using a Weibull distribution; t in (h):

R(t) = 100 * Exp(-((t*fac - t0)/(T - t0))^b) %

Welle	fac	b	t0	T
1	210000	1.5	1.915e+011	4.061e+011

Damage to cross sections (%) [D]
A-A Shoulder: 0.00
B-B Spline: 0.00

KISSSOFT
Calculation programs for machine design

C-C Shoulder: 0.00

Utilization (%) [Smin/S]

Cross section	Static	Endurance
A-A Shoulder	39.689	28.913
B-B Spline	32.155	21.148
C-C Shoulder	20.321	15.749

Maximum utilization (%) [A] 39.689

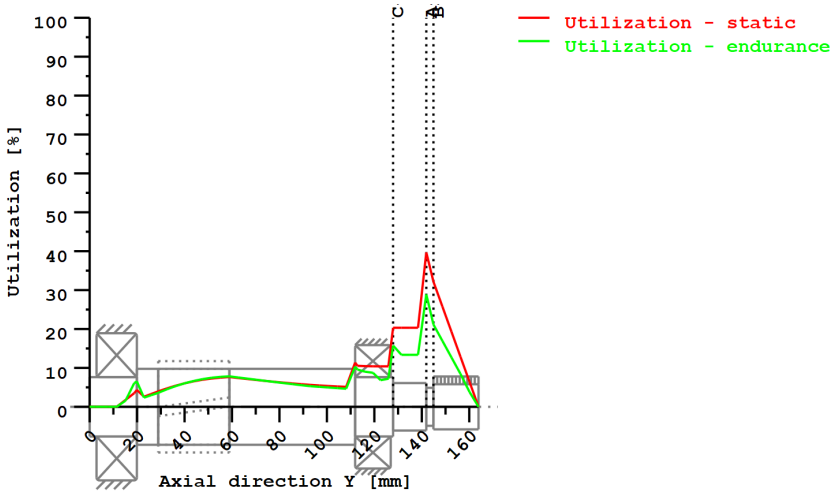

Utilization = Smin/S (%)

Figure: Strength

Calculation details

General statements

Label	Shaft 1		
Drawing			
Length (mm)		[l]	163.90
Speed (1/min)		[n]	3500.00
Material	18CrNiMo7-6		
Material type	Case-carburized steel		
Material treatment	case-hardened		
Surface treatment	No		

	Tension/Compression	Bending	Torsion	Shearing
Load factor static calculation	1.700	1.700	1.700	1.700
Load factor endurance limit	1.000	1.000	1.000	1.000

Reference diameter material (mm)	[dB]	16.00
σB according to DIN 743 (at dB) (N/mm²)	[σB]	1200.00
σS according to DIN 743 (at dB) (N/mm²)	[σS]	850.00
[σzdW] (bei dB) (N/mm²)		480.00
[σbW] (bei dB) (N/mm²)		600.00
[τtW] (bei dB) (N/mm²)		360.00
Thickness of raw material (mm)	[dWerkst]	35.00
Material data calculated according DIN743/3 with K1(d)		
Material strength calculated from size of raw material		
Geometric size factor K1d calculated from raw material diameter		
[σBeff] (N/mm²)		1093.94
[σSeff] (N/mm²)		774.87
[σbF] (N/mm²)		774.87
[τtF] (N/mm²)		447.37
[σBRand] (N/mm²)		2300.00
[σzdW] (N/mm²)		437.57

KISSSOFT
Calculation programs for machine design

[σbW] (N/mm²)		546.97
[τtW] (N/mm²)		328.18

Fatigue strength for single stage use

Required life time	[H]	5000.00
Number of load cycles (Mio)	[NL]	1050.000

Data of S-N curve (Woehler line) analog to FKM standard:

[kσ, kτ]	15	25
[kDσ, kDτ]	0	0
[NDσ, NDτ]	1e+006	1e+006
[NDσII, NDτII]	0	0

Calculation for load case 2 (σ.av/σ.mv = const)

Cross section 'A-A Shoulder' **Shoulder**

Comment	Y= 141.90mm			
Position (Y-Coordinate) (mm)		[y]		141.900
External diameter (mm)		[da]		16.000
Inner diameter (mm)		[di]		0.000
Notch effect			Shoulder	
[D, r, t] (mm)	20.000	0.100	2.000	
Mean roughness (µm)		[Rz]		8.000

		Tension/Compression	Bending	Torsion	Shearing
Load: (N) (Nm)					
Mean value	[Fzdm, Mbm, Tm, Fqm]	0.000	0.000	35.000	0.000
Amplitude	[Fzda, Mba, Ta, Fqa]	0.000	0.005	35.000	0.460
Maximum value	[Fzdmax, Mbmax, Tmax, Fqmax]	0.000	0.009	119.000	0.782
Cross section, moment of resistance: (mm²)					
[A, Wb, Wt, A]		201.062	402.124	804.248	201.062

Stresses: (N/mm²)				
[σzdm, σbm, τm, τqm] (N/mm²)	0.000	0.000	43.519	0.000
[σzda, σba, τa, τqa] (N/mm²)	0.000	0.013	43.519	0.003
[σzdmax,σbmax,τmax,τqmax] (N/mm²)	0.000	0.022	147.964	0.005

Technological size influence	[K1(σB)]	0.912	
	[K1(σS)]	0.912	

		Tension/Compression	Bending	Torsion
Stress concentration factor	[a]	4.631	4.081	2.551
References stress slope	[G']	24.156	24.156	11.500
Notch sensitivity factor	[n]	1.981	1.981	1.677
Notch effect coefficient	[ß]	2.338	2.060	1.522
Geometrical size influence	[K2(d)]	1.000	0.949	0.949
Influence coefficient surface roughness	[KF]	0.853	0.853	0.916
Surface stabilization factor	[KV]	1.000	1.133	1.133
Total influence coefficient	[K]	2.510	2.066	1.496

Present safety for endurance limit:				
Equivalent mean stress (N/mm²)	[σmV]		75.377	
Equivalent mean stress (N/mm²)	[τmV]		43.519	
Fatigue limit of part (N/mm²)	[σWK]	174.339	264.684	219.446
Influence coefficient of mean stress sensitivity.	[ψσK]	0.087	0.138	0.111
Permissible amplitude (N/mm²)	[σADK]	0.010	0.134	197.435
Permissible amplitude (N/mm²)	[σANK]	0.010	0.134	197.435
Effective Miner sum	[DM]	0.300	0.300	0.300
Load spectrum factor	[fKoll]	1.000	1.000	1.000
Safety against fatigue	[S]		4.150	
Required safety against fatigue	[Smin]		1.200	
Result (%)	[S/Smin]		345.9	

Present safety for proof against exceed of yield point:				
Static notch sensitivity factor	[K2F]	1.000	1.000	1.000
Increase coefficient	[γF]	1.000	1.000	1.000
Yield stress of part (N/mm²)	[σFK]	774.871	774.871	447.372
Safety yield stress	[S]		3.024	
Required safety	[Smin]		1.200	

Result (%)	[S/Smin]	252.0

Present safety
for proof of avoiding incipient crack on hard surface layers:

Safety against incipient crack	[S]	6.092
Required safety	[Smin]	1.200
Result (%)	[S/Smin]	507.6

Cross section 'B-B Spline' Spline

Comment	Y= 144.90...163.90mm				
Position (Y-Coordinate) (mm)		[y]		144.910	
External diameter (mm)		[da]		19.000	
Inner diameter (mm)		[di]		0.000	
Notch effect			Spline		
ISO 4156:2005, DIN 5480:2005					
[da, df, z, mn] (mm)	18.840	17.160	22	0.800	
Mean roughness (µm)		[Rz]		8.000	

		Tension/Compression	Bending	Torsion	Shearing
Load: (N) (Nm)					
Mean value	[Fzdm, Mbm, Tm, Fqm]	0.000	0.000	34.982	0.000
Amplitude	[Fzda, Mba, Ta, Fqa]	0.000	0.004	34.982	0.414
Maximum value	[Fzdmax, Mbmax, Tmax, Fqmax]	0.000	0.007	118.937	0.703
Cross section, moment of resistance: (mm²)					
[A, Wb, Wt, A]		231.273	496.080	992.160	231.273

Stresses: (N/mm²)					
[σzdm, σbm, τm, τqm] (N/mm²)		0.000	0.000	35.258	0.000
[σzda, σba, τa, τqa] (N/mm²)		0.000	0.008	35.258	0.002
[σzdmax,σbmax,τmax,τqmax] (N/mm²)		0.000	0.013	119.877	0.004
Technological size influence	[K1(σB)]	0.912			
	[K1(σS)]	0.912			

		Tension/Compression	Bending	Torsion
Notch effect coefficient	[ß(dB)]	1.000	1.000	1.000
[dB] (mm) = 29.0				
Geometrical size influence	[K3(d)]	1.000	1.000	1.000
Geometrical size influence	[K3(dB)]	1.000	1.000	1.000
Notch effect coefficient	[ß]	1.000	1.000	1.000
Geometrical size influence	[K2(d)]	1.000	0.938	0.938
Influence coefficient surface roughness	[KF]	1.000	1.000	1.000
Roughness factor is included into the notch effect coefficient				
Surface stabilization factor	[KV]	1.000	1.000	1.000
Total influence coefficient	[K]	1.000	1.066	1.066

Present safety for endurance limit:

Equivalent mean stress (N/mm²)	[σmV]		61.069	
Equivalent mean stress (N/mm²)	[τmV]		35.258	
Fatigue limit of part (N/mm²)	[σWK]	437.574	513.025	307.815
Influence coefficient of mean stress sensitivity.				
	[ψσK]	0.250	0.306	0.164
Permissible amplitude (N/mm²)	[σADK]	0.013	0.100	223.686
Permissible amplitude (N/mm²)	[σANK]	0.013	0.100	223.686
Effective Miner sum	[DM]	0.300	0.300	0.300
Load spectrum factor	[fKoll]	1.000	1.000	1.000
Safety against fatigue	[S]		5.674	
Required safety against fatigue	[Smin]		1.200	
Result (%)	[S/Smin]		472.9	

Present safety
for proof against exceed of yield point:

Static notch sensitivity factor	[K2F]	1.000	1.000	1.000
Increase coefficient	[γF]	1.000	1.000	1.000
Yield stress of part (N/mm²)	[σFK]	774.871	774.871	447.372
Safety yield stress	[S]		3.732	
Required safety	[Smin]		1.200	
Result (%)	[S/Smin]		311.0	

KISSSOFT
Calculation programs for machine design

Present safety
for proof of avoiding incipient crack on hard surface layers:

Safety against incipient crack	[S]	19.185
Required safety	[Smin]	1.200
Result (%)	[S/Smin]	1598.8

Cross section 'C-C Shoulder' **Shoulder**

Comment	Y= 127.90mm			
Position (Y-Coordinate) (mm)		[y]		127.900
External diameter (mm)		[da]		20.000
Inner diameter (mm)		[di]		0.000
Notch effect			Shoulder	
[D, r, t] (mm)	25.000	0.100	2.500	
Mean roughness (µm)		[Rz]		8.000

		Tension/Compression	Bending	Torsion	Shearing
Load: (N) (Nm)					
Mean value	[Fzdm, Mbm, Tm, Fqm]	0.000	0.000	35.000	0.000
Amplitude	[Fzda, Mba, Ta, Fqa]	0.000	0.014	35.000	0.798
Maximum value	[Fzdmax, Mbmax, Tmax, Fqmax]	0.000	0.024	119.000	1.356
Cross section, moment of resistance: (mm²)					
[A, Wb, Wt, A]		314.159	785.398	1570.796	314.159
Stresses: (N/mm²)					
[σzdm, σbm, τm, τqm] (N/mm²)		0.000	0.000	22.282	0.000
[σzda, σba, τa, τqa] (N/mm²)		0.000	0.018	22.282	0.003
[σzdmax,σbmax,τmax,τqmax] (N/mm²)		0.000	0.030	75.758	0.006
Technological size influence	[K1(σB)]	0.912			
	[K1(σS)]	0.912			

		Tension/Compression	Bending	Torsion
Stress concentration factor	[a]	5.065	4.451	2.738
References stress slope	[G']	24.045	24.045	11.500
Notch sensitivity factor	[n]	1.978	1.978	1.677
Notch effect coefficient	[ß]	2.560	2.250	1.633
Geometrical size influence	[K2(d)]	1.000	0.935	0.935
Influence coefficient surface roughness	[KF]	0.853	0.853	0.916
Surface stabilization factor	[KV]	1.000	1.133	1.133
Total influence coefficient	[K]	2.732	2.276	1.623

Present safety for endurance limit:

Equivalent mean stress (N/mm²)	[σmV]		38.593	
Equivalent mean stress (N/mm²)	[τmV]		22.282	
Fatigue limit of part (N/mm²)	[σWK]	160.155	240.349	202.199
Influence coefficient of mean stress sensitivity.	[ψσK]	0.079	0.123	0.102
Permissible amplitude (N/mm²)	[σADK]	0.020	0.359	183.513
Permissible amplitude (N/mm²)	[σANK]	0.020	0.359	183.513
Effective Miner sum	[DM]	0.300	0.300	0.300
Load spectrum factor	[fKoll]	1.000	1.000	1.000
Safety against fatigue	[S]		7.619	
Required safety against fatigue	[Smin]		1.200	
Result (%)	[S/Smin]		634.9	

Present safety
for proof against exceed of yield point:

Static notch sensitivity factor	[K2F]	1.000	1.000	1.000
Increase coefficient	[γF]	1.000	1.000	1.000
Yield stress of part (N/mm²)	[σFK]	774.871	774.871	447.372
Safety yield stress	[S]		5.905	
Required safety	[Smin]		1.200	
Result (%)	[S/Smin]		492.1	

Present safety
for proof of avoiding incipient crack on hard surface layers:

Safety against incipient crack	[S]	11.085

Required safety	[Smin]	1.200
Result (%)	[S/Smin]	923.8

Remarks:
- The shearing force is not considered in the analysis specified in DIN 743.
- Cross section with interference fit:
  The notching factor for the light fit case is no longer defined in DIN 743.
  The values are imported from the FKM-Guideline..

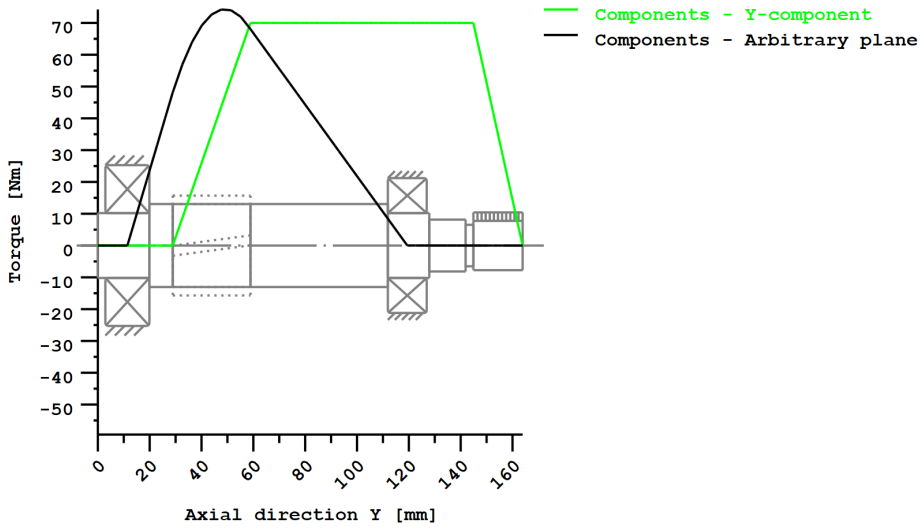

Figure: Moment diagram (Arbitrary plane 127.5363808 121)

End of Report lines: 705

KISSsoft Release 03/2017 F

KISSsoft University license - Universidade do Porto

File

Name : shaftATorque

Changed by: Carlos Rodrigues on: 02.07.2018 at: 23:24:21

THERMALLY SAFE OPERATING SPEED CALCULATION

(according to DIN ISO 15312 and DIN 732)

Lubricant	Castrol ATF Dex II Multivehicle		
Lubrication type:			
Oil-groove lubrication			
Mean bearing temperature	$[T_m]$	75.000	°C
Temperature of bearing environment	$[T_u]$	65.000	°C
Lubricant - service temperature	$[T_B]$	65.000	°C
Lubricant temperature - Reference conditions	$[T_{ref}]$	70.000	°C

Shaft 'Shaft 1', Rolling bearing 'Rolling bearing':

Thermal nominal speed according to DIN ISO 15312:

Type of support	Deep groove ball bearing (single row)		
Bearing number	SKF 6205 ETN9		
Design series	62		
Speed	$[n]$	3500.000	1/min
Coefficient	$[f_{0r}]$	2.000	
(Depends upon type of design and lubrication at reference conditions)			
Coefficient	$[f_{1r}]$	0.000200	
(Depends upon type of design and load at reference conditions)			
Heat sink reference surface	$[A_s]$	3628.540	mm²
Reference load	$[P_{1r}]$	0.465	kN
Bearing mean diameter	$[d_m]$	38.500	mm
Bearing-specific reference heat flow density	$[q_r]$	16.000	kW/m²
kinematic viscosity (for reference conditions)	$[v_r]$	12.000	mm²/s
Thermal nominal speed	$[n_{\theta r}]$	15140.793	1/min

Thermally safe operating speed according to DIN 732:

Coefficient	$[f_0]$	2.000	
(Depends upon type of design and lubrication)			
Coefficient	$[f_1]$	0.000313	
(Depends upon type of design and load)			
Temperature difference	$[\Delta\theta=\theta_o-\theta_i]$	10.000	°C
Lubricant Oil-volume	$[V_L]$	0.300	l/min
Heat flow (dissipated by the lubricant)	$[\Phi_L]$	0.086	kW
Heat flow (dissipated by the bearing support surface)	$[\Phi_S]$	0.011	kW
Total heat flow	$[\Phi]$	0.097	kW
Dynamic equivalent load	$[P_1]$	2447.072	N
kinematic viscosity at service temperature	$[v]$	16.738	mm²/s
Lubricant film parameter	$[K_L]$	0.749	
Charge parameter	$[K_P]$	0.483	
Speed ratio	$[f_n]$	0.864	
Thermally safe operating speed	$[n_\theta]$	13085.549	1/min

Shaft 'Shaft 1', Rolling bearing 'Rolling bearing':

Thermal nominal speed according to DIN ISO 15312:

Type of support		Deep groove ball bearing (single row)		
Bearing number		SKF 6305 ETN9		
Design series		63		
Speed	[n]	3500.000	1/min	
Coefficient	[f_{0r}]		2.300	
(Depends upon type of design and lubrication at reference conditions)				
Coefficient	[f_{1r}]		0.000200	
(Depends upon type of design and load at reference conditions)				
Heat sink reference surface	[A_S]		4646.416	mm²
Reference load	[P_{1r}]		0.670	kN
Bearing mean diameter	[d_m]		43.500	mm
Bearing-specific reference heat flow density	[q_r]		16.000	kW/m²
kinematic viscosity (for reference conditions)	[v_r]		12.000	mm²/s
Thermal nominal speed	[$n_{\theta r}$]		12963.076	1/min

Thermally safe operating speed according to DIN 732:

Coefficient	[f_0]	2.300	
(Depends upon type of design and lubrication)			
Coefficient	[f_1]	0.000409	
(Depends upon type of design and load)			
Temperature difference	[$\Delta\theta=\theta_o-\theta_i$]	10.000	°C
Lubricant Oil-volume	[V_L]	0.300	l/min
Heat flow (dissipated by the lubricant)	[Φ_L]	0.086	kW
Heat flow (dissipated by the bearing support surface)	[Φ_S]	0.014	kW
Total heat flow	[Φ]	0.100	kW
Dynamic equivalent load	[P_1]	2765.099	N
kinematic viscosity at service temperature	[v]	16.738	mm²/s
Lubricant film parameter	[K_L]	0.929	
Charge parameter	[K_P]	0.668	
Speed ratio	[f_n]	0.710	
Thermally safe operating speed	[n_θ]	9209.607	1/min

The reference conditions for calculating the thermal nominal speed are taken from the DIN ISO 15312 standard.

End of Report lines: 96

KISSsoft Release 03/2017 F

KISSsoft University license - Universidade do Porto

File

Name : shaftBTorque

Changed by: Carlos Rodrigues on: 02.07.2018 at: 14:52:22

Analysis of shafts, axle and beams

Input data

Coordinate system shaft: see picture W-002

Label		Shaft 1
Drawing		
Initial position (mm)		0.000
Length (mm)		145.550
Speed (1/min)		889.23
Sense of rotation: counter clockwise		
Material		18CrNiMo7-6
Young's modulus (N/mm²)		206000.000
Poisson's ratio nu		0.300
Density (kg/m³)		7830.000
Coefficient of thermal expansion	(10^-6/K)	11.500
Temperature (°C)		65.000
Weight of shaft (kg)		1.552
(Notice: Weight stands for the shaft only without considering the gears)		
Weight of shaft, including additional masses (kg)		3.233
Mass moment of inertia (kg*mm²)		2451.291
Momentum of mass GD2 (Nm²)		0.096
Position in space (°)		0.000
Gears mounted with stiffness according to ISO		
Consider deformations due to shearing		
Shear correction coefficient		1.100
Contact angle of rolling bearings is considered		
Tolerance field: Mean value		
Housing material		G-AlSi10Mg
Coefficient of thermal expansion	(10^-6/K)	22.000
Temperature of housing (°C)		55.000
Thermal housing reference point (mm)		0.000
Reference temperature (°C)		20.000

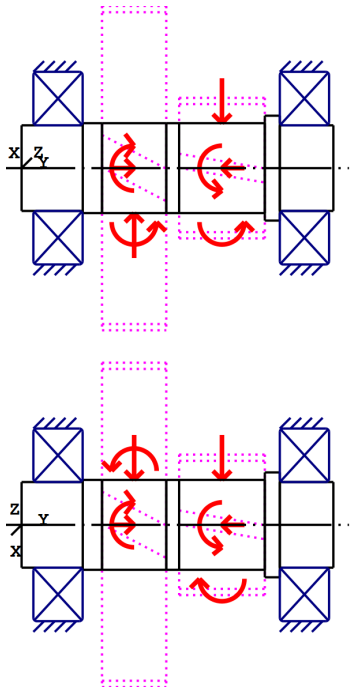

Figure: Load applications

Shaft definition (Shaft 1)

Outer contour

Cylinder (Cylinder)			0.000mm ... 28.550mm
Diameter (mm)	[d]	40.0000	
Length (mm)	[l]	28.5500	
Surface roughness (µm)	[Rz]	4.8000	

Relief groove right (Relief groove right)
r=0.80 (mm), t=0.30 (mm), l=2.50 (mm), Rz=8.0, Turned (Ra=3.2µm/125µin)
Form E (DIN 509), Series 1, with the usual stressing

Chamfer left (Chamfer left)
l=0.80 (mm), alpha=45.00 (°)

Square groove (Square groove)
b=1.85 (mm), t=1.25 (mm), r=0.20 (mm), Rz=8.0, Turned (Ra=3.2µm/125µin)

Cylinder (Cylinder)			28.550mm ... 113.550mm
Diameter (mm)	[d]	42.0000	
Length (mm)	[l]	85.0000	
Surface roughness (µm)	[Rz]	4.8000	

Key way (Key way) 38.550mm ... 66.550mm
l=28.00 (mm), i=1, Rz=8.0, Turned (Ra=3.2µm/125µin)

Radius right (Radius right)

r=0.10 (mm), Rz=8.0, Turned (Ra=3.2µm/125µin)

Cylinder (Cylinder)			113.550mm ...	120.550mm
Diameter (mm)	[d]	49.0000		
Length (mm)	[l]	7.0000		
Surface roughness (µm)	[Rz]	8.0000		

Cylinder (Cylinder)			120.550mm ...	145.550mm
Diameter (mm)	[d]	40.0000		
Length (mm)	[l]	25.0000		
Surface roughness (µm)	[Rz]	4.8000		

Relief groove left (Relief groove left)
r=0.80 (mm), t=0.30 (mm), l=2.50 (mm), Rz=8.0, Turned (Ra=3.2µm/125µin)
Form E (DIN 509), Series 1, with the usual stressing

Chamfer right (Chamfer right)
l=0.80 (mm), alpha=45.00 (°)

Forces

Type of force element		**Cylindrical gear**
Label in the model		Cylindrical gear
Position on shaft (mm)	[y_{local}]	52.5500
Position in global system (mm)	[y_{global}]	52.5500
Operating pitch diameter (mm)		151.5086
Helix angle (°)		12.0156 right
Working pressure angle at normal section (°)		20.2001
Position of contact (°)		200.0000
Length of load application (mm)		30.0000
Power (kW)		25.6563 driven (input)
Torque (Nm)		-275.5193
Axial force (N)		774.1037
Shearing force X (N)		2529.5601
Shearing force Z (N)		-2949.7418
Bending moment X (Nm)		20.0566
Bending moment Z (Nm)		-55.1052

Type of force element		**Cylindrical gear**
Label in the model		Cylindrical gear
Position on shaft (mm)	[y_{local}]	93.5500
Position in global system (mm)	[y_{global}]	93.5500
Operating pitch diameter (mm)		65.6436
Helix angle (°)		12.0839 right
Working pressure angle at normal section (°)		21.0503
Position of contact (°)		-25.0000
Length of load application (mm)		40.0000
Power (kW)		25.6572 driving (output)
Torque (Nm)		275.5286
Axial force (N)		-1797.1958
Shearing force X (N)		-6542.2743
Shearing force Z (N)		-6211.8000
Bending moment X (Nm)		-24.9291
Bending moment Z (Nm)		-53.4605

Bearing

Label in the model		Rolling bearing
Bearing type		SKF 6308
Bearing type		Deep groove ball bearing (single row)
		SKF Explorer
Bearing position (mm)	[y_{lokal}]	17.000
Bearing position (mm)	[y_{global}]	17.000
Attachment of external ring		Free bearing
Inner diameter (mm)	[d]	40.000
External diameter (mm)	[D]	90.000
Width (mm)	[b]	23.000
Corner radius (mm)	[r]	1.500
Basic static load rating (kN)	[C_0]	24.000
Basic dynamic load rating (kN)	[C]	42.300
Fatigue load rating (kN)	[C_u]	1.000
Values for approximated geometry:		
Basic dynamic load rating (kN)	[C_{theo}]	0.000
Basic static load rating (kN)	[C_{0theo}]	0.000

Label in the model		Rolling bearing
Bearing type		SKF 6308
Bearing type		Deep groove ball bearing (single row)
		SKF Explorer
Bearing position (mm)	[y_{lokal}]	132.050
Bearing position (mm)	[y_{global}]	132.050
Attachment of external ring		Fixed bearing
Inner diameter (mm)	[d]	40.000
External diameter (mm)	[D]	90.000
Width (mm)	[b]	23.000
Corner radius (mm)	[r]	1.500
Basic static load rating (kN)	[C_0]	24.000
Basic dynamic load rating (kN)	[C]	42.300
Fatigue load rating (kN)	[C_u]	1.000
Values for approximated geometry:		
Basic dynamic load rating (kN)	[C_{theo}]	0.000
Basic static load rating (kN)	[C_{0theo}]	0.000

Shaft 'Shaft 1': Cylindrical gear 'Cylindrical gear' (y= 52.5500 (mm)) is taken into account as component of the shaft.
EI (y= 37.5500 (mm)): 31465.4742 (Nm²), EI (y= 67.5500 (mm)): 31465.4742 (Nm²), m (yS= 52.5500 (mm)): 1.4016 (kg)
Jp: 0.0019 (kg*m²), Jxx: 0.0011 (kg*m²), Jzz: 0.0011 (kg*m²)

Shaft 'Shaft 1': Cylindrical gear 'Cylindrical gear' (y= 93.5500 (mm)) is taken into account as component of the shaft.
EI (y= 73.5500 (mm)): 31465.4742 (Nm²), EI (y= 113.5500 (mm)): 31465.4742 (Nm²), m (yS= 93.5500 (mm)): 0.2786 (kg)
Jp: 0.0002 (kg*m²), Jxx: 0.0001 (kg*m²), Jzz: 0.0001 (kg*m²)

Results

KISSSOFT
Calculation programs for machine design

Shaft

Maximum deflection (µm)	10.661
Position of the maximum (mm)	80.217
Mass center of gravity (mm)	73.663
Total axial load (N)	-1023.092
Torsion under torque (°)	0.009

Bearing

Probability of failure	[n]	10.00	%
Axial clearance	[u_A]	10.00	µm
Lubricant	Castrol ATF Dex II Multivehicle		
Lubricant with additive, effect on bearing lifetime confirmed in tests.			
Oil lubrication, off-line/no filtration, ISO4406 -/15/12			
Lubricant - service temperature	[T_B]	65.00	°C
Limit for factor aISO	[a_{ISOmax}]	50.00	
Oil level	[h_{oil}]	-54.94	mm
Oil bath lubrication			

Rolling bearings, classical calculation (contact angle considered)

Shaft 'Shaft 1' Rolling bearing 'Rolling bearing'

Position (Y-coordinate)	[y]	17.00	mm
Dynamic equivalent load	[P]	4.32	kN
Equivalent load	[P_0]	4.32	kN
Life modification factor for reliability[a_1]		1.000	
Life modification factor	[a_{ISO}]	0.798	
Nominal bearing service life	[L_{nh}]	17579.34	h
Modified bearing service life	[L_{nmh}]	14028.21	h
Operating viscosity	[v]	17.13	mm²/s
Static safety factor	[S_0]	5.55	
Bearing reaction force	[Fx]	1.385	kN
Bearing reaction force	[Fy]	0.000	kN
Bearing reaction force	[Fz]	4.093	kN
Bearing reaction force	[Fr]	4.321	kN (71.3°)
Bearing reaction moment	[Mx]	0.00	Nm
Bearing reaction moment	[My]	-0.00	Nm
Bearing reaction moment	[Mz]	-0.00	Nm
Bearing reaction moment	[Mr]	0.00	Nm (-90°)
Oil level	[H]	0.000	mm
Rolling moment of friction	[M_{rr}]	0.038	Nm
Sliding moment of friction	[M_{sl}]	0.088	Nm
Moment of friction, seals	[M_{seal}]	0.000	Nm
Moment of friction for seals determined according to SKF main catalog 10000/1 EN:2013			
Moment of friction flow losses	[M_{drag}]	0.000	Nm
Torque of friction	[M_{loss}]	0.126	Nm
Power loss	[P_{loss}]	11.737	W
The moment of friction is calculated according to the details in SKF Catalog 2013.			
The calculation is always performed with a coefficient for additives in the lubricant µbl=0.15.			
Displacement of bearing	[u_x]	-2.097	µm
Displacement of bearing	[u_y]	32.088	µm
Displacement of bearing	[u_z]	-6.152	µm

Displacement of bearing	[u_r]	6.500	µm (-108.82°)
Misalignment of bearing	[r_x]	-0.068	mrad (-0.23')
Misalignment of bearing	[r_y]	0.000	mrad (0')
Misalignment of bearing	[r_z]	0.035	mrad (0.12')
Misalignment of bearing	[r_r]	0.076	mrad (0.26')

Shaft 'Shaft 1' Rolling bearing 'Rolling bearing'

Position (Y-coordinate)	[y]	132.05	mm
Dynamic equivalent load	[P]	5.74	kN
Equivalent load	[P_0]	5.74	kN
Life modification factor for reliability[a_1]		1.000	
Life modification factor	[a_{ISO}]	0.649	
Nominal bearing service life	[L_{nh}]	7516.00	h
Modified bearing service life	[L_{nmh}]	4874.69	h
Operating viscosity	[v]	17.13	mm²/s
Static safety factor	[S_0]	4.18	
Bearing reaction force	[Fx]	2.627	kN
Bearing reaction force	[Fy]	1.028	kN
Bearing reaction force	[Fz]	5.099	kN
Bearing reaction force	[Fr]	5.736	kN (62.74°)
Oil level	[H]	0.000	mm
Rolling moment of friction	[M_{rr}]	0.074	Nm
Sliding moment of friction	[M_{sl}]	0.230	Nm
Moment of friction, seals	[M_{seal}]	0.000	Nm

Moment of friction for seals determined according to SKF main catalog 10000/1 EN:2013

Moment of friction flow losses	[M_{drag}]	0.000	Nm
Torque of friction	[M_{loss}]	0.304	Nm
Power loss	[P_{loss}]	28.318	W

The moment of friction is calculated according to the details in SKF Catalog 2013.
The calculation is always performed with a coefficient for additives in the lubricant µbl=0.15.

Displacement of bearing	[u_x]	-2.994	µm
Displacement of bearing	[u_y]	91.679	µm
Displacement of bearing	[u_z]	-5.769	µm
Displacement of bearing	[u_r]	6.500	µm (-117.43°)
Misalignment of bearing	[r_x]	0.082	mrad (0.28')
Misalignment of bearing	[r_y]	0.159	mrad (0.55')
Misalignment of bearing	[r_z]	-0.039	mrad (-0.13')
Misalignment of bearing	[r_r]	0.091	mrad (0.31')

Damage (%) [Lreq] (5000.000)

Bin no	B1	B2
1	35.64	102.57
Σ	35.64	102.57

Utilization (%) [Lreq] (5000.000)

B1	B2
70.90	100.85

Note: Utilization = (Lreq/Lh)^(1/k)
Ball bearing: k = 3, roller bearing: k = 10/3

B1: Rolling bearing
B2: Rolling bearing

Shaft '

Shaft 1', Dokumentationspunkt Meshing point Z2

Y position (mm)	[y]	52.55
Equivalent stress (N/mm²)	[sigV]	28.82

	X	Y	Z	R
Displacement (mm)	-0.0035	0.0505	-0.0089	0.0095
Rotation (mrad)	-0.0368	0.0015	0.0249	0.0444
Force (kN)	-2.6505	-0.3826	-2.6069	3.7177
Torque (Nm)	124.2267	137.7690	-31.1811	128.0802

Shaft '

Shaft 1', Dokumentationspunkt Meshing point Z3

Y position (mm)	[y]	93.55
Equivalent stress (N/mm²)	[sigV]	31.81

	X	Y	Z	R
Displacement (mm)	-0.0046	0.0717	-0.0094	0.0104
Rotation (mrad)	0.0298	0.1377	-0.0095	0.0313
Force (kN)	-0.6442	0.1290	1.9865	2.0883
Torque (Nm)	152.6450	137.7643	-95.1577	179.8764

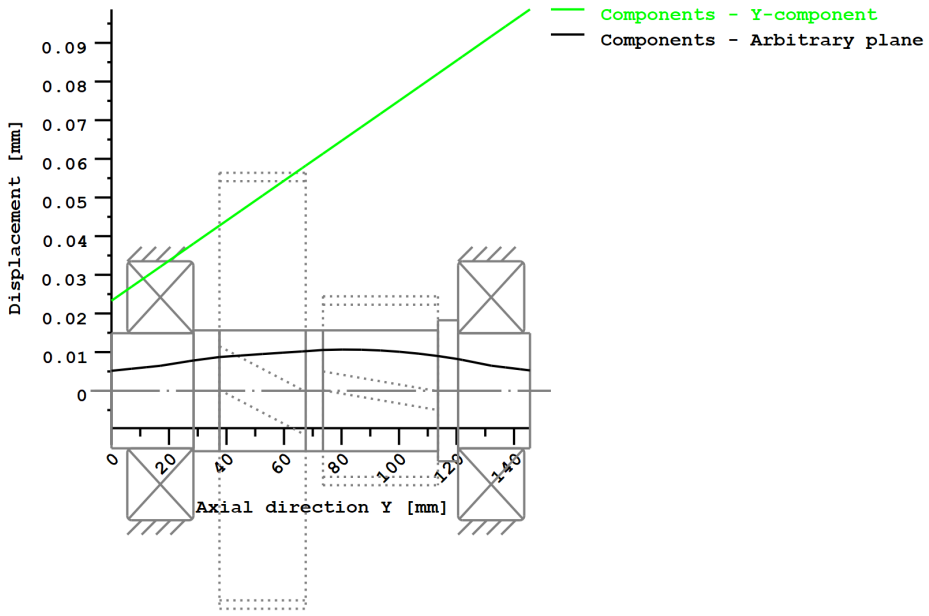

Figure: Deformation (bending etc.) (Arbitrary plane 245.1563514 121)

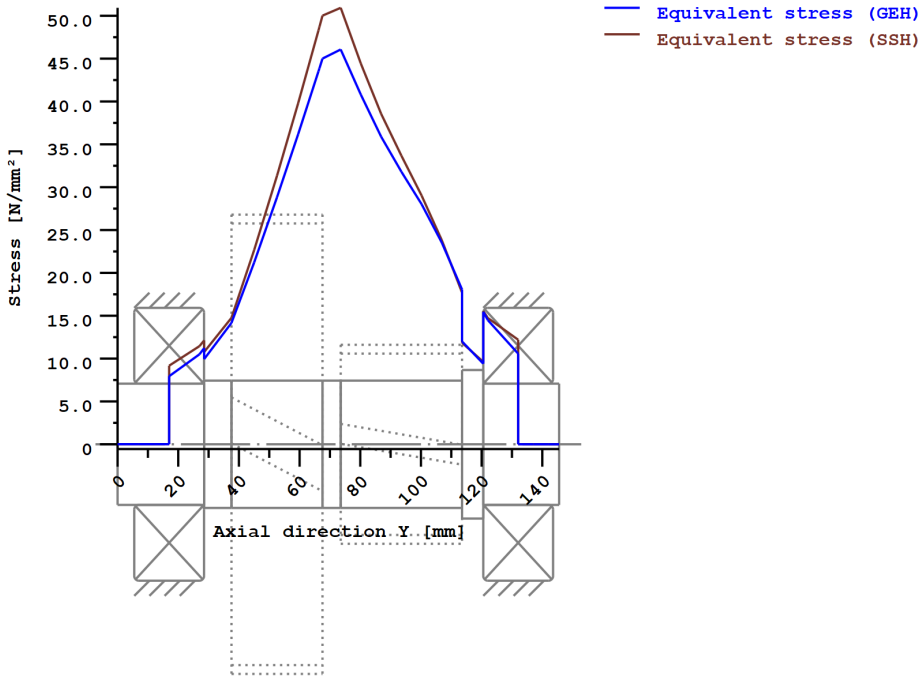

Nominal stresses, without taking into account stress concentrations
GEH(von Mises): sigV = ((sigB+sigZ,D)^2 + 3*(tauT+tauS)^2)^1/2
SSH(Tresca): sigV = ((sigB-sigZ,D)^2 + 4*(tauT+tauS)^2)^1/2

Figure: Equivalent stress

Eigenfrequencies/Critical speeds

1. Eigenfrequency:	0.00 Hz, Critical speed:	0.00 1/min	Rigid body rotation Y 'Shaft 1'
2. Eigenfrequency:	5020.52 Hz, Critical speed:	301231.06 1/min	Bending YZ 'Shaft 1', Bending XY 'Shaft 1'
3. Eigenfrequency:	7620.02 Hz, Critical speed:	457200.98 1/min	Bending XY 'Shaft 1'
4. Eigenfrequency:	12077.69 Hz, Critical speed:	724661.44 1/min	Bending XY 'Shaft 1'
5. Eigenfrequency:	12150.11 Hz, Critical speed:	729006.89 1/min	Torsion 'Shaft 1'

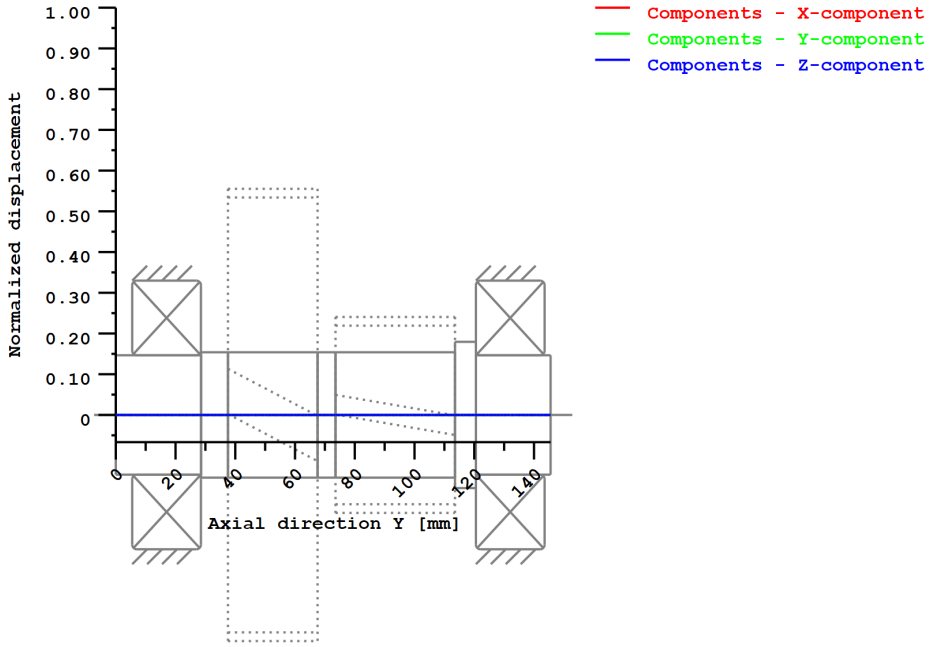

Figure: Eigenfrequencies (Normalized rotation) (Eigenfrequency: 1. (0 Hz))

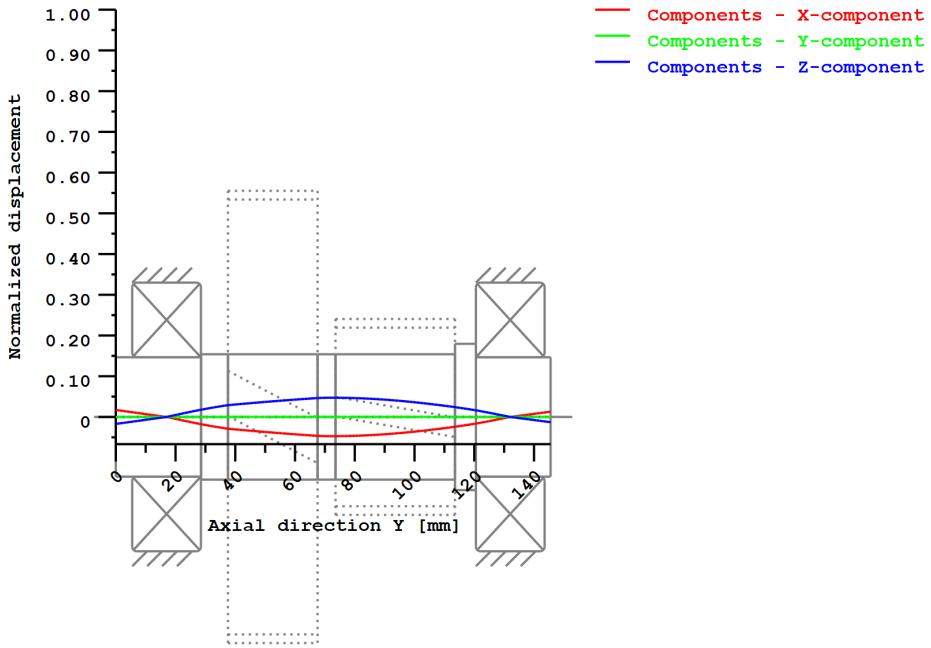

Figure: Eigenfrequencies (Normalized rotation) (Eigenfrequency: 2. (5020.52 Hz))

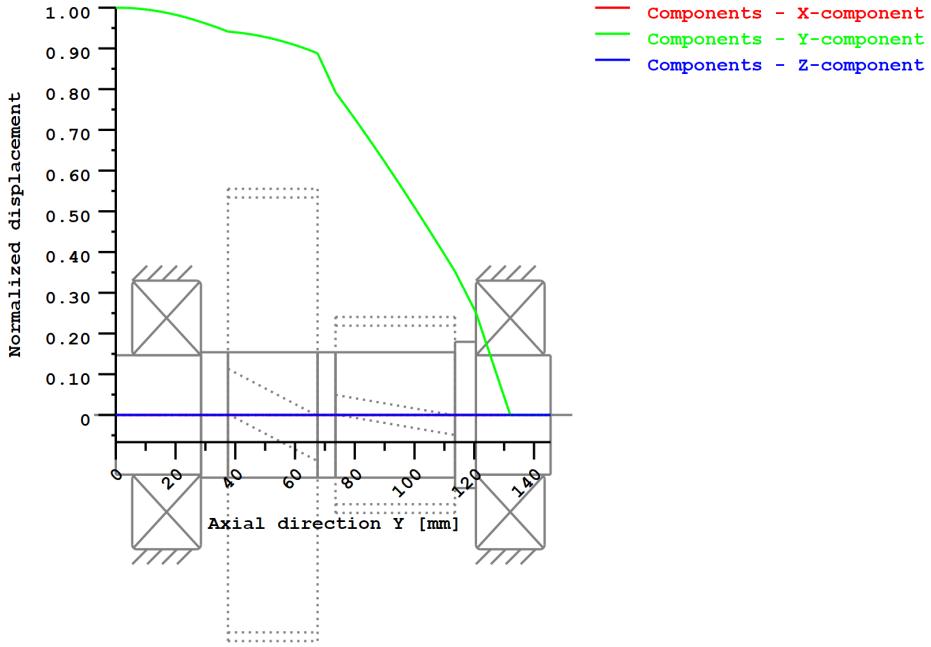

Figure: Eigenfrequencies (Normalized rotation) (Eigenfrequency: 3. (7620.02 Hz))

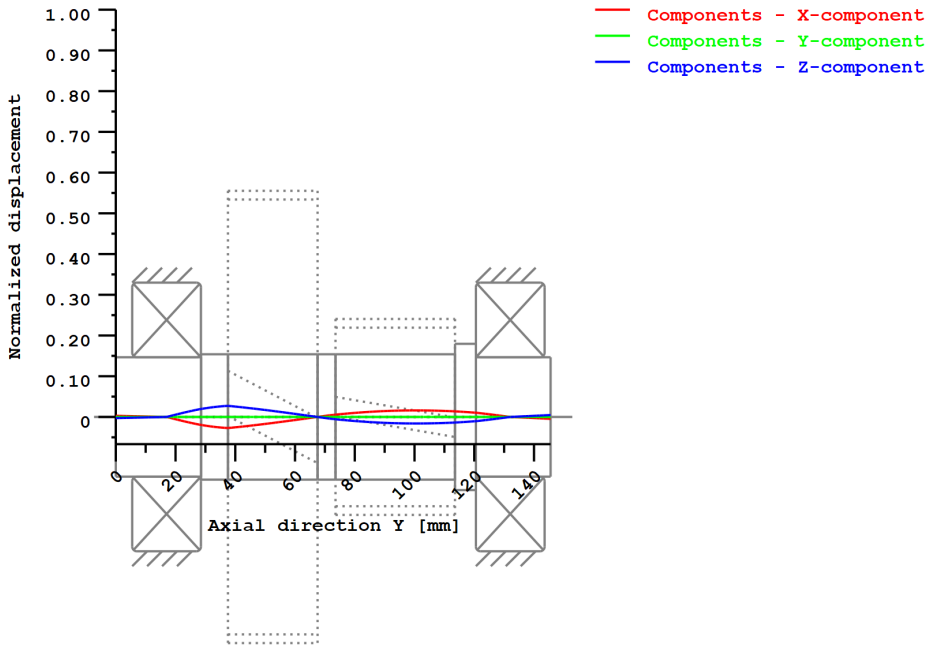

Figure: Eigenfrequencies (Normalized rotation) (Eigenfrequency: 4. (12077.69 Hz))

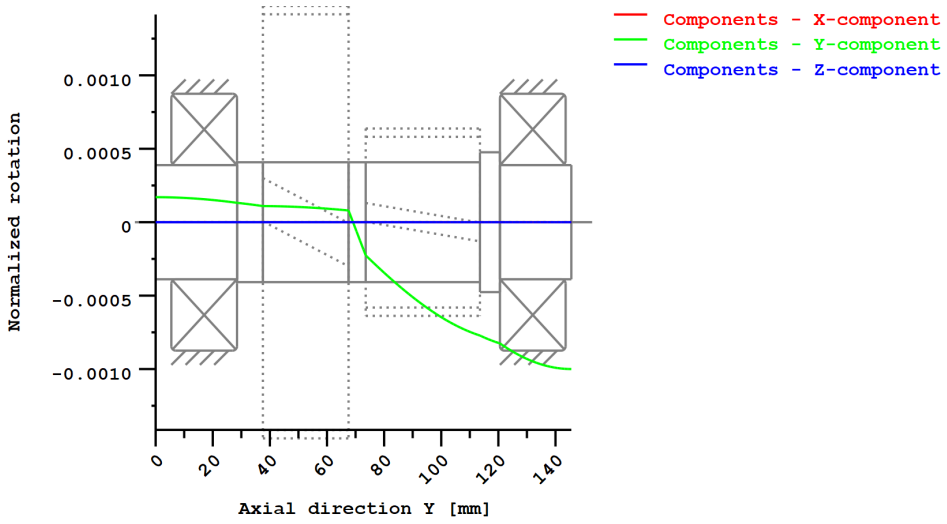

Figure: Eigenfrequencies (Normalized displacement) (Eigenfrequency: 5. (12150.11 Hz))

Strength calculation according to DIN 743:2012
with finite life fatigue strength according to FKM standard and FVA draft

Summary

Shaft 1

Material	18CrNiMo7-6
Material type	Case-carburized steel
Material treatment	case-hardened
Surface treatment	No

Calculation of finite life fatigue strength and static strength

Calculation for load case 2 (σav/σmv = const)

Cross section	Position (Y-Coord) (mm)	
A-A Key way	66.54	Key
B-B Smooth shaft	73.55	Smooth shaft
C-C Shoulder	113.55	Shoulder

Results:

Cross section	Kfb	Kfs	K2d	SD	SS	SA
A-A Key way	3.05	1.00	0.88	5.59	11.60	17.71
B-B Smooth shaft	1.00	0.89	0.88	10.37	10.96	40.71
C-C Shoulder	2.88	0.86	0.88	10.46	28.43	15.44
Required safeties:				1.20	1.20	1.20

Abbreviations:
Kfb: Notch factor bending
Kfσ: Surface factor
K2d: size factor bending
SD: Safety endurance limit
SS: Safety against yield point
SA: Safety against incipient crack

Service life and damage

System service life (h)	[Hatt]	1000000.00
Damage to system (%)	[D]	0.00
Damage (%)	[H] (5000.0 h)	

Calculation of reliability R(t) using a Weibull distribution; t in (h):

R(t) = 100 * Exp(-((t*fac - t0)/(T - t0))^b) %

Welle	fac	b	t0	T
1	53354	1.5	4.865e+010	1.032e+011

Damage to cross sections (%)	[D]
A-A Key way:	0.00
B-B Smooth shaft:	0.00

KISSSOFT
Calculation programs for machine design

C-C Shoulder: 0.00

Utilization (%) [Smin/S]

Cross section	Static	Endurance
A-A Key way	10.345	21.448
B-B Smooth shaft	10.947	11.569
C-C Shoulder	7.771	11.477
Maximum utilization (%)	[A]	21.448

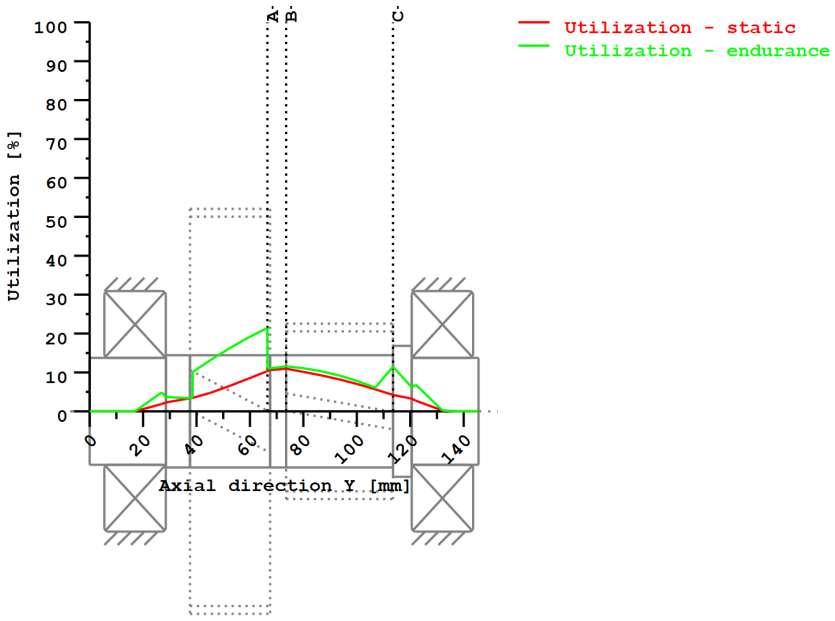

Utilization = Smin/S (%)

Figure: Strength

Calculation details

General statements

Label	Shaft 1		
Drawing			
Length (mm)		[l]	145.55
Speed (1/min)		[n]	889.23

Material	18CrNiMo7-6
Material type	Case-carburized steel
Material treatment	case-hardened
Surface treatment	No

	Tension/Compression	Bending	Torsion	Shearing
Load factor static calculation	1.700	1.700	1.700	1.700
Load factor endurance limit	1.000	1.000	1.000	1.000

Reference diameter material (mm)	[dB]	16.00
σB according to DIN 743 (at dB) (N/mm²)	[σB]	1200.00
σS according to DIN 743 (at dB) (N/mm²)	[σS]	850.00
[σzdW] (bei dB) (N/mm²)		480.00
[σbW] (bei dB) (N/mm²)		600.00
[τtW] (bei dB) (N/mm²)		360.00
Thickness of raw material (mm)	[dWerkst]	50.00
Material data calculated according DIN743/3 with K1(d)		
Material strength calculated from size of raw material		
Geometric size factor K1d calculated from raw material diameter		
[σBeff] (N/mm²)		1045.61
[σSeff] (N/mm²)		740.64
[σbF] (N/mm²)		740.64
[τtF] (N/mm²)		427.61
[σBRand] (N/mm²)		2300.00
[σzdW] (N/mm²)		418.24

[σbW] (N/mm²)		522.80
[τtW] (N/mm²)		313.68

Fatigue strength for single stage use

Required life time	[H]	5000.00
Number of load cycles (Mio)	[NL]	266.769

Data of S-N curve (Woehler line) analog to FKM standard:

[kσ, kτ]	15	25
[kDσ, kDτ]	0	0
[NDσ, NDτ]	1e+006	1e+006
[NDσII, NDτII]	0	0

Calculation for load case 2 (σ.av/σ.mv = const)

Cross section 'A-A Key way' Key

Comment	Y= 38.55... 66.55mm	
Position (Y-Coordinate) (mm)	[y]	66.540
External diameter (mm)	[da]	42.000
Inner diameter (mm)	[di]	0.000
Notch effect		Key
Number of keys	[n]	1

Groove with manufactured with end milling cutter

Standard:	DIN 6885.1:1968 Default	
[b, t] (mm)	12.000	5.100
Mean roughness (µm)	[Rz]	8.000

		Tension/Compression	Bending	Torsion	Shearing
Load: (N) (Nm)					
Mean value	[Fzdm, Mbm, Tm, Fqm]	-371.8	0.0	133.1	0.0
Amplitude	[Fzda, Mba, Ta, Fqa]	371.8	150.4	133.1	4020.8
Maximum value	[Fzdmax, Mbmax, Tmax, Fqmax]	-1264.1	255.7	452.6	6835.3
Cross section, moment of resistance: (mm²)					
[A, Wb, Wt, A]		1385.4	7273.6	14547.1	1385.4

Stresses: (N/mm²)

[σzdm, σbm, τm, τqm] (N/mm²)	-0.268	0.000	9.151	0.000
[σzda, σba, τa, τqa] (N/mm²)	0.268	20.676	9.151	3.870
[σzdmax,σbmax,τmax,τqmax] (N/mm²)	-0.912	35.149	31.115	6.578

Technological size influence	[K1(σB)]	0.871		
	[K1(σS)]	0.871		

		Tension/Compression	Bending	Torsion
Notch effect coefficient	[ß(dB)]	3.046	3.046	1.846
[dB] (mm) = 40.0				
Geometrical size influence	[K3(d)]	0.944	0.944	0.969
Geometrical size influence	[K3(dB)]	0.946	0.946	0.970
Notch effect coefficient	[ß]	3.051	3.051	1.847
Geometrical size influence	[K2(d)]	1.000	0.885	0.885
Influence coefficient surface roughness	[KF]	1.000	1.000	1.000
Roughness factor is included into the notch effect coefficient				
Surface stabilization factor	[KV]	1.000	1.000	1.000
Total influence coefficient	[K]	3.051	3.447	2.087

Present safety for endurance limit:

Equivalent mean stress (N/mm²)	[σmV]		15.848
Equivalent mean stress (N/mm²)	[τmV]		9.150

Fatigue limit of part (N/mm²)	[σWK]	137.098	151.662	150.279
Influence coefficient of mean stress sensitivity.				
	[ψσK]	0.070	0.078	0.077
Permissible amplitude (N/mm²)	[σADK]	12.332	143.086	139.481
Permissible amplitude (N/mm²)	[σANK]	12.332	143.086	139.481
Effective Miner sum	[DM]	0.300	0.300	0.300
Load spectrum factor	[fKoll]	1.000	1.000	1.000
Safety against fatigue	[S]		5.595	
Required safety against fatigue	[Smin]		1.200	
Result (%)	[S/Smin]		466.2	

Present safety
for proof against exceed of yield point:

Static notch sensitivity factor	[K2F]	1.000	1.000	1.000
Increase coefficient	[γF]	1.000	1.000	1.000
Yield stress of part (N/mm²)	[σFK]	740.638	740.638	427.608
Safety yield stress	[S]		11.600	
Required safety	[Smin]		1.200	
Result (%)	[S/Smin]		966.7	

Present safety
for proof of avoiding incipient crack on hard surface layers:

Safety against incipient crack	[S]	17.709
Required safety	[Smin]	1.200
Result (%)	[S/Smin]	1475.7

Cross section 'B-B Smooth shaft' Smooth shaft

Comment		
Position (Y-Coordinate) (mm)	[y]	73.550
External diameter (mm)	[da]	42.000
Inner diameter (mm)	[di]	0.000
Notch effect		Smooth shaft
Mean roughness (µm)	[Rz]	4.800

	Tension/Compression	Bending	Torsion	Shearing	
Load: (N) (Nm)					
Mean value [Fzdm, Mbm, Tm, Fqm]	-384.8	0.0	137.8	0.0	
Amplitude [Fzda, Mba, Ta, Fqa]	384.8	167.2	137.8	4073.1	
Maximum value [Fzdmax, Mbmax, Tmax, Fqmax]	-1308.4	284.3	468.4		6924.3
Cross section, moment of resistance: (mm²)					
[A, Wb, Wt, A]	1385.4	7273.6	14547.1	1385.4	

Stresses: (N/mm²)				
[σzdm, σbm, τm, τqm] (N/mm²)	-0.278	0.000	9.470	0.000
[σzda, σba, τa, τqa] (N/mm²)	0.278	22.992	9.470	3.920
[σzdmax,σbmax,τmax,τqmax] (N/mm²)	-0.944	39.086	32.199	6.664

Technological size influence	[K1(σB)]	0.871	
	[K1(σS)]	0.871	

	Tension/Compression	Bending	Torsion
Notch effect coefficient	[ß]	1.000	1.000	1.000
Geometrical size influence	[K2(d)]	1.000	0.885	0.885
Influence coefficient surface roughness	[KF]	0.892	0.892	0.938
Surface stabilization factor	[KV]	1.000	1.033	1.033
Total influence coefficient	[K]	1.121	1.210	1.157

Present safety for endurance limit:

Equivalent mean stress (N/mm²)	[σmV]	16.401
Equivalent mean stress (N/mm²)	[τmV]	9.469

Fatigue limit of part (N/mm²)	[σWK]	373.215	431.973	271.029
Influence coefficient of mean stress sensitivity.	[ψσK]	0.217	0.260	0.149
Permissible amplitude (N/mm²)	[σADK]	12.334	364.317	213.819
Permissible amplitude (N/mm²)	[σANK]	12.334	364.317	213.819
Effective Miner sum	[DM]	0.300	0.300	0.300
Load spectrum factor	[fKoll]	1.000	1.000	1.000
Safety against fatigue	[S]		10.373	
Required safety against fatigue	[Smin]		1.200	
Result (%)	[S/Smin]		864.4	

Present safety
for proof against exceed of yield point:

Static notch sensitivity factor	[K2F]	1.000	1.000	1.000
Increase coefficient	[γF]	1.000	1.000	1.000
Yield stress of part (N/mm²)	[σFK]	740.638	740.638	427.608
Safety yield stress	[S]		10.962	
Required safety	[Smin]		1.200	
Result (%)	[S/Smin]		913.5	

Present safety

KISSSOFT
Calculation programs for machine design

for proof of avoiding incipient crack on hard surface layers:

Safety against incipient crack	[S]	40.713
Required safety	[Smin]	1.200
Result (%)	[S/Smin]	3392.7

Cross section 'C-C Shoulder' **Shoulder**

Comment	Y= 113.55mm			
Position (Y-Coordinate) (mm)		[y]		113.550
External diameter (mm)		[da]		42.000
Inner diameter (mm)		[di]		0.000
Notch effect			Shoulder	
[D, r, t] (mm)	49.000	0.100	3.500	
Mean roughness (µm)		[Rz]		8.000

	Tension/Compression	Bending	Torsion	Shearing
Load: (N) (Nm)				
Mean value [Fzdm, Mbm, Tm, Fqm]	513.8	0.0	0.0	0.0
Amplitude [Fzda, Mba, Ta, Fqa]	513.8	106.1	0.0	5733.1
Maximum value [Fzdmax, Mbmax, Tmax, Fqmax]	1746.9	180.3	0.0	9746.3
Cross section, moment of resistance: (mm²)				
[A, Wb, Wt, A]	1385.4	7273.6	14547.1	1385.4

Stresses: (N/mm²)				
[σzdm, σbm, τm, τqm] (N/mm²)	0.371	0.000	0.000	0.000
[σzda, σba, τa, τqa] (N/mm²)	0.371	14.584	0.000	5.518
[σzdmax,σbmax,τmax,τqmax] (N/mm²)	1.261	24.792	0.000	9.380

Technological size influence	[K1(σB)]	0.871	
	[K1(σS)]	0.871	

	Tension/Compression	Bending	Torsion
Stress concentration factor [a]	6.381	5.683	3.299
References stress slope [G']	23.896	23.896	11.500
Notch sensitivity factor [n]	1.975	1.975	1.677
Notch effect coefficient [ß]	3.230	2.877	1.968
Geometrical size influence [K2(d)]	1.000	0.885	0.885
Influence coefficient surface roughness [KF]	0.857	0.857	0.918
Surface stabilization factor [KV]	1.000	1.033	1.033
Total influence coefficient [K]	3.397	3.307	2.238

Present safety for endurance limit:			
Equivalent mean stress (N/mm²)	[σmV]	0.371	
Equivalent mean stress (N/mm²)	[τmV]	0.214	
Fatigue limit of part (N/mm²)	[σWK]	123.135	158.089	140.148
Influence coefficient of mean stress sensitivity.				
	[ψσK]	0.063	0.082	0.072
Permissible amplitude (N/mm²)	[σADK]	115.884	157.761	1.988
Permissible amplitude (N/mm²)	[σANK]	115.884	157.761	1.988
Effective Miner sum	[DM]	0.300	0.300	0.300
Load spectrum factor	[fKoll]	1.000	1.000	1.000
Safety against fatigue	[S]		10.456	
Required safety against fatigue	[Smin]		1.200	
Result (%)	[S/Smin]		871.3	

Present safety				
for proof against exceed of yield point:				
Static notch sensitivity factor	[K2F]	1.000	1.000	1.000
Increase coefficient	[γF]	1.000	1.000	1.000
Yield stress of part (N/mm²)	[σFK]	740.638	740.638	427.608
Safety yield stress	[S]		28.428	
Required safety	[Smin]		1.200	
Result (%)	[S/Smin]		1286.9	

Present safety			
for proof of avoiding incipient crack on hard surface layers:			
Safety against incipient crack	[S]	15.443	
Required safety	[Smin]	1.200	
Result (%)	[S/Smin]	1286.9	

Remarks:
- The shearing force is not considered in the analysis specified in DIN 743.
- Cross section with interference fit:
  The notching factor for the light fit case is no longer defined in DIN 743.
  The values are imported from the FKM-Guideline..

End of Report lines: 694

KISSsoft Release 03/2017 F

KISSsoft University license - Universidade do Porto

File

Name : shaftBTorque

Changed by: Carlos Rodrigues on: 02.07.2018 at: 14:53:14

THERMALLY SAFE OPERATING SPEED CALCULATION

(according to DIN ISO 15312 and DIN 732)

Lubricant	Castrol ATF Dex II Multivehicle		
Lubrication type:			
Oil-groove lubrication			
Mean bearing temperature	$[T_m]$	75.000	°C
Temperature of bearing environment	$[T_u]$	65.000	°C
Lubricant - service temperature	$[T_B]$	65.000	°C
Lubricant temperature - Reference conditions	$[T_{ref}]$	70.000	°C

Shaft 'Shaft 1', Rolling bearing 'Rolling bearing':

Thermal nominal speed according to DIN ISO 15312:

Type of support	Deep groove ball bearing (single row)		
Bearing number	SKF 6308		
Design series	63		
Speed	$[n]$	889.230	1/min
Coefficient	$[f_{0r}]$	2.300	
(Depends upon type of design and lubrication at reference conditions)			
Coefficient	$[f_{1r}]$	0.000200	
(Depends upon type of design and load at reference conditions)			
Heat sink reference surface	$[A_S]$	9393.362	mm²
Reference load	$[P_{1r}]$	1.200	kN
Bearing mean diameter	$[d_m]$	65.000	mm
Bearing-specific reference heat flow density	$[q_r]$	16.000	kW/m²
kinematic viscosity (for reference conditions)	$[v_r]$	12.000	mm²/s
Thermal nominal speed	$[n_{\theta r}]$	9597.697	1/min

Thermally safe operating speed according to DIN 732:

Coefficient	$[f_0]$	2.300	
(Depends upon type of design and lubrication)			
Coefficient	$[f_1]$	0.000382	
(Depends upon type of design and load)			
Temperature difference	$[\Delta\theta=\theta_o-\theta_i]$	10.000	°C
Lubricant Oil-volume	$[V_L]$	0.300	l/min
Heat flow (dissipated by the lubricant)	$[\Phi_L]$	0.086	kW
Heat flow (dissipated by the bearing support surface)	$[\Phi_S]$	0.029	kW
Total heat flow	$[\Phi]$	0.115	kW
Dynamic equivalent load	$[P_1]$	4321.333	N
kinematic viscosity at service temperature	$[v]$	17.134	mm²/s
Lubricant film parameter	$[K_L]$	1.662	
Charge parameter	$[K_P]$	0.940	
Speed ratio	$[f_n]$	0.505	
Thermally safe operating speed	$[n_\theta]$	4850.399	1/min

Shaft 'Shaft 1', Rolling bearing 'Rolling bearing':

Thermal nominal speed according to DIN ISO 15312:

Type of support		Deep groove ball bearing (single row)		
Bearing number		SKF 6308		
Design series		63		
Speed	[n]	889.230	1/min	
Coefficient	[f_{0r}]		2.300	
(Depends upon type of design and lubrication at reference conditions)				
Coefficient	[f_{1r}]		0.000200	
(Depends upon type of design and load at reference conditions)				
Heat sink reference surface	[A_S]		9393.362	mm²
Reference load	[P_{1r}]		1.200	kN
Bearing mean diameter	[d_m]		65.000	mm
Bearing-specific reference heat flow density	[q_r]		16.000	kW/m²
kinematic viscosity (for reference conditions)	[v_r]		12.000	mm²/s
Thermal nominal speed	[$n_{\theta r}$]		9597.697	1/min

Thermally safe operating speed according to DIN 732:

Coefficient	[f_0]	2.300	
(Depends upon type of design and lubrication)			
Coefficient	[f_1]	0.000440	
(Depends upon type of design and load)			
Temperature difference	[$\Delta\theta=\theta_o-\theta_i$]	10.000	°C
Lubricant Oil-volume	[V_L]	0.300	l/min
Heat flow (dissipated by the lubricant)	[Φ_L]	0.086	kW
Heat flow (dissipated by the bearing support surface)	[Φ_S]	0.029	kW
Total heat flow	[Φ]	0.115	kW
Dynamic equivalent load	[P_1]	5736.183	N
kinematic viscosity at service temperature	[v]	17.134	mm²/s
Lubricant film parameter	[K_L]	1.662	
Charge parameter	[K_P]	1.438	
Speed ratio	[f_n]	0.425	
Thermally safe operating speed	[n_θ]	4077.147	1/min

The reference conditions for calculating the thermal nominal speed are taken from the DIN ISO 15312 standard.

End of Report lines: 96

KISSsoft Release 03/2017 F

KISSsoft University license - Universidade do Porto

File

Name : shaftCTorque

Changed by: Carlos Rodrigues on: 02.07.2018 at: 23:34:24

Analysis of shafts, axle and beams

Input data

Coordinate system shaft: see picture W-002

Label		Shaft 1
Drawing		
Initial position (mm)		0.000
Length (mm)		201.550
Speed (1/min)		300.31
Sense of rotation: clockwise		
Material		18CrNiMo7-6
Young's modulus (N/mm²)		206000.000
Poisson's ratio nu		0.300
Density (kg/m³)		7830.000
Coefficient of thermal expansion	(10^-6/K)	11.500
Temperature (°C)		65.000
Weight of shaft (kg)		2.509
(Notice: Weight stands for the shaft only without considering the gears)		
Weight of shaft, including additional masses (kg)		5.566
Mass moment of inertia (kg*mm²)		7357.325
Momentum of mass GD2 (Nm²)		0.289
Position in space (°)		0.000
Gears mounted with stiffness according to ISO		
Consider deformations due to shearing		
Shear correction coefficient		1.100
Contact angle of rolling bearings is considered		
Tolerance field: Mean value		
Housing material		G-AlSi10Mg
Coefficient of thermal expansion	(10^-6/K)	22.000
Temperature of housing (°C)		55.000
Thermal housing reference point (mm)		0.000
Reference temperature (°C)		20.000

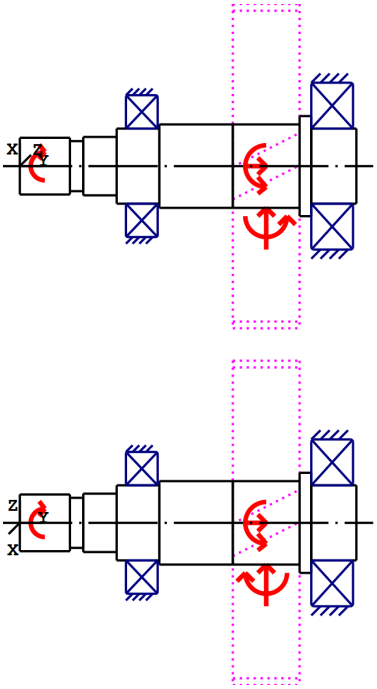

Figure: Load applications

Shaft definition (Shaft 1)

Outer contour

Cylinder (Cylinder)			0.000mm ... 30.000mm
Diameter (mm)	[d]	34.0000	
Length (mm)	[l]	30.0000	
Surface roughness (µm)	[Rz]	8.0000	

Spline (Spline) -15.000mm ... 15.000mm
da=33.84 (mm), df=32.16 (mm), z=41, mn=0.80 (mm), l=30.00 (mm), Rz=8.0, Turned (Ra=3.2µm/125µin)

Chamfer left (Chamfer left)
l=0.80 (mm), alpha=45.00 (°)

Cylinder (Cylinder)			30.000mm ... 38.000mm
Diameter (mm)	[d]	30.0000	
Length (mm)	[l]	8.0000	
Surface roughness (µm)	[Rz]	8.0000	

Radius right (Radius right)
r=0.10 (mm), Rz=8.0, Turned (Ra=3.2µm/125µin)

Radius left (Radius left)
r=0.10 (mm), Rz=8.0, Turned (Ra=3.2µm/125µin)

Cylinder (Cylinder) 38.000mm ... 58.000mm

Diameter (mm)	[d]	35.0000
Length (mm)	[l]	20.0000
Surface roughness (µm)	[Rz]	4.8000

Chamfer left (Chamfer left)
l=0.80 (mm), alpha=45.00 (°)

Radius right (Radius right)
r=0.10 (mm), Rz=8.0, Turned (Ra=3.2µm/125µin)

Cylinder (Cylinder) 58.000mm ... 83.550mm

Diameter (mm)	[d]	45.0000
Length (mm)	[l]	25.5500
Surface roughness (µm)	[Rz]	8.0000

Chamfer left (Chamfer left)
l=0.80 (mm), alpha=45.00 (°)

Square groove (Square groove)
b=1.75 (mm), t=1.25 (mm), r=0.20 (mm), Rz=57.0, Turned (Ra=3.2µm/125µin)

Relief groove right (Relief groove right)
r=0.80 (mm), t=0.30 (mm), l=2.50 (mm), Rz=8.0, Turned (Ra=3.2µm/125µin)
Form E (DIN 509), Series 1, with the usual stressing

Cylinder (Cylinder) 83.550mm ... 167.550mm

Diameter (mm)	[d]	50.0000
Length (mm)	[l]	84.0000
Surface roughness (µm)	[Rz]	4.8000

Key way (Key way) 129.550mm ... 165.550mm
l=36.00 (mm), i=1, Rz=8.0, Turned (Ra=3.2µm/125µin)

Radius right (Radius right)
r=0.10 (mm), Rz=8.0, Turned (Ra=3.2µm/125µin)

Cylinder (Cylinder) 167.550mm ... 174.550mm

Diameter (mm)	[d]	60.0000
Length (mm)	[l]	7.0000
Surface roughness (µm)	[Rz]	8.0000

Cylinder (Cylinder) 174.550mm ... 201.550mm

Diameter (mm)	[d]	45.0000
Length (mm)	[l]	27.0000
Surface roughness (µm)	[Rz]	4.8000

Relief groove left (Relief groove left)
r=0.80 (mm), t=0.30 (mm), l=2.50 (mm), Rz=8.0, Turned (Ra=3.2µm/125µin)
Form E (DIN 509), Series 1, with the usual stressing

Chamfer right (Chamfer right)
l=0.80 (mm), alpha=45.00 (°)

Forces

Type of force element		**Cylindrical gear**
Label in the model		Cylindrical gear
Position on shaft (mm)	[y_{local}]	147.5500
Position in global system (mm)	[y_{global}]	147.5500
Operating pitch diameter (mm)		194.3564
Helix angle (°)		12.0839 left
Working pressure angle at normal section (°)		21.0503
Position of contact (°)		160.0000
Length of load application (mm)		40.0000
Power (kW)		25.6572 driven (input)
Torque (Nm)		815.8513
Axial force (N)		1797.3512
Shearing force X (N)		5976.5016
Shearing force Z (N)		6758.9433
Bending moment X (Nm)		-59.7384
Bending moment Z (Nm)		-164.1299

Type of force element		**Coupling**
Label in the model		Coupling
Position on shaft (mm)	[y_{local}]	15.0000
Position in global system (mm)	[y_{global}]	15.0000
Effective diameter (mm)		40.0000
Radial force factor (-)		0.0000
Direction of the radial force (°)		0.0000
Axial force factor (-)		0.0000
Length of load application (mm)		30.0000
Power (kW)		25.6572 driving (output)
Torque (Nm)		-815.8509
Axial force (N)		0.0000
Shearing force X (N)		0.0000
Shearing force Z (N)		0.0000
Bending moment X (Nm)		0.0000
Bending moment Z (Nm)		0.0000
Mass (kg)		0.0000
Mass moment of inertia Jp (kg*m²)		0.0000
Mass moment of inertia Jxx (kg*m²)		0.0000
Mass moment of inertia Jzz (kg*m²)		0.0000
Eccentricity (mm)		0.0000

Bearing

Label in the model		Rolling bearing
Bearing type		SKF 6209
Bearing type		Deep groove ball bearing (single row) SKF Explorer
Bearing position (mm)	[y_{lokal}]	73.050
Bearing position (mm)	[y_{global}]	73.050
Attachment of external ring		Free bearing
Inner diameter (mm)	[d]	45.000
External diameter (mm)	[D]	85.000
Width (mm)	[b]	19.000
Corner radius (mm)	[r]	1.100
Basic static load rating (kN)	[C_0]	21.600
Basic dynamic load rating (kN)	[C]	35.100

Fatigue load rating (kN)	[C_u]	0.915
Values for approximated geometry:		
Basic dynamic load rating (kN)	[C_{theo}]	0.000
Basic static load rating (kN)	[C_{0theo}]	0.000

Label in the model		Rolling bearing
Bearing type		SKF 6309
Bearing type		Deep groove ball bearing (single row)
		SKF Explorer
Bearing position (mm)	[y_{lokal}]	187.050
Bearing position (mm)	[y_{global}]	187.050
Attachment of external ring		Fixed bearing
Inner diameter (mm)	[d]	45.000
External diameter (mm)	[D]	100.000
Width (mm)	[b]	25.000
Corner radius (mm)	[r]	1.500
Basic static load rating (kN)	[C_0]	31.500
Basic dynamic load rating (kN)	[C]	55.300
Fatigue load rating (kN)	[C_u]	1.300
Values for approximated geometry:		
Basic dynamic load rating (kN)	[C_{theo}]	0.000
Basic static load rating (kN)	[C_{0theo}]	0.000

Shaft 'Shaft 1': Cylindrical gear 'Cylindrical gear' (y= 147.5500 (mm)) is taken into account as component of the shaft.
EI (y= 127.5500 (mm)): 63200.0085 (Nm²), EI (y= 167.5500 (mm)): 63200.0085 (Nm²), m (yS= 147.5500 (mm)): 3.0570 (kg)
Jp: 0.0067 (kg*m²), Jxx: 0.0037 (kg*m²), Jzz: 0.0037 (kg*m²)

Results

Shaft

Maximum deflection (µm)	9.154
Position of the maximum (mm)	127.550
Mass center of gravity (mm)	114.120
Total axial load (N)	1797.351
Torsion under torque (°)	0.287

Bearing

Probability of failure	[n]	10.00	%
Axial clearance	[u_A]	10.00	µm
Lubricant	Castrol ATF Dex II Multivehicle		
Lubricant with additive, effect on bearing lifetime confirmed in tests.			
Oil lubrication, off-line/no filtration, ISO4406 -/15/12			
Lubricant - service temperature	[T_B]	65.00	°C
Limit for factor aISO	[a_{ISOmax}]	50.00	
Oil level	[h_{oil}]	0.00	mm
Oil bath lubrication			

Rolling bearings, classical calculation (contact angle considered)

Shaft 'Shaft 1' Rolling bearing 'Rolling bearing'

Position (Y-coordinate)	[y]	73.05	mm
Dynamic equivalent load	[P]	2.91	kN
Equivalent load	[P_0]	2.91	kN
Life modification factor for reliability[a_1]		1.000	
Life modification factor	[a_{ISO}]	0.201	
Nominal bearing service life	[L_{nh}]	97484.51	h
Modified bearing service life	[L_{nmh}]	19570.00	h
Operating viscosity	[v]	17.13	mm²/s
Static safety factor	[S_0]	7.43	
Bearing reaction force	[Fx]	-0.631	kN
Bearing reaction force	[Fy]	0.000	kN
Bearing reaction force	[Fz]	-2.840	kN
Bearing reaction force	[Fr]	2.909	kN (-102.53°)
Bearing reaction moment	[Mx]	-0.00	Nm
Bearing reaction moment	[My]	-0.00	Nm
Bearing reaction moment	[Mz]	-0.00	Nm
Bearing reaction moment	[Mr]	0.00	Nm (-179.56°)
Oil level	[H]	0.000	mm
Rolling moment of friction	[M_{rr}]	0.017	Nm
Sliding moment of friction	[M_{sl}]	0.082	Nm
Moment of friction, seals	[M_{seal}]	0.000	Nm
Moment of friction for seals determined according to SKF main catalog 10000/1 EN:2013			
Moment of friction flow losses	[M_{drag}]	0.000	Nm
Torque of friction	[M_{loss}]	0.099	Nm
Power loss	[P_{loss}]	3.122	W
The moment of friction is calculated according to the details in SKF Catalog 2013.			
The calculation is always performed with a coefficient for additives in the lubricant μbl=0.15.			
Displacement of bearing	[u_x]	1.791	μm
Displacement of bearing	[u_y]	95.139	μm
Displacement of bearing	[u_z]	7.025	μm
Displacement of bearing	[u_r]	7.250	μm (75.69°)
Misalignment of bearing	[r_x]	0.017	mrad (0.06')
Misalignment of bearing	[r_y]	3.996	mrad (13.74')
Misalignment of bearing	[r_z]	-0.055	mrad (-0.19')
Misalignment of bearing	[r_r]	0.058	mrad (0.2')

Shaft 'Shaft 1' Rolling bearing 'Rolling bearing'

Position (Y-coordinate)	[y]	187.05	mm
Dynamic equivalent load	[P]	6.60	kN
Equivalent load	[P_0]	6.60	kN
Life modification factor for reliability[a_1]		1.000	
Life modification factor	[a_{ISO}]	0.189	
Nominal bearing service life	[L_{nh}]	32703.57	h
Modified bearing service life	[L_{nmh}]	6192.45	h
Operating viscosity	[v]	17.13	mm²/s
Static safety factor	[S_0]	4.78	
Bearing reaction force	[Fx]	-5.345	kN
Bearing reaction force	[Fy]	-1.797	kN
Bearing reaction force	[Fz]	-3.865	kN
Bearing reaction force	[Fr]	6.596	kN (-144.13°)
Bearing reaction moment	[Mx]	0.00	Nm

Bearing reaction moment	[My]	0.00	Nm
Bearing reaction moment	[Mz]	-0.00	Nm
Bearing reaction moment	[Mr]	0.00	Nm (-51.28°)
Oil level	[H]	0.000	mm
Rolling moment of friction	[M_{rr}]	0.059	Nm
Sliding moment of friction	[M_{sl}]	0.471	Nm
Moment of friction, seals	[M_{seal}]	0.000	Nm
Moment of friction for seals determined according to SKF main catalog 10000/1 EN:2013			
Moment of friction flow losses	[M_{drag}]	0.000	Nm
Torque of friction	[M_{loss}]	0.530	Nm
Power loss	[P_{loss}]	16.664	W
The moment of friction is calculated according to the details in SKF Catalog 2013.			
The calculation is always performed with a coefficient for additives in the lubricant μbl=0.15.			
Displacement of bearing	[u_x]	6.067	μm
Displacement of bearing	[u_y]	154.029	μm
Displacement of bearing	[u_z]	3.970	μm
Displacement of bearing	[u_r]	7.250	μm (33.2°)
Misalignment of bearing	[r_x]	-0.064	mrad (-0.22')
Misalignment of bearing	[r_y]	5.013	mrad (17.23')
Misalignment of bearing	[r_z]	-0.024	mrad (-0.08')
Misalignment of bearing	[r_r]	0.069	mrad (0.24')

Damage (%) [Lreq] (5000.000)

Bin no	B1	B2
1	25.55	80.74
Σ	25.55	80.74

Utilization (%) [Lreq] (5000.000)

B1	B2
63.45	93.12

Note: Utilization = (Lreq/Lh)^(1/k)
Ball bearing: k = 3, roller bearing: k = 10/3

B1: Rolling bearing
B2: Rolling bearing

Shaft '

Shaft 1', Dokumentationspunkt Documentation point

Y position (mm)	[y]	147.55
Equivalent stress (N/mm²)	[sigV]	35.02

	X	Y	Z	R
Displacement (mm)	0.0055	0.1337	0.0068	0.0088
Rotation (mrad)	-0.0527	5.0101	-0.0395	0.0658
Force (kN)	-2.3572	-0.8987	-0.5079	2.4113
Torque (Nm)	-149.0735	407.9256	99.1971	179.0613

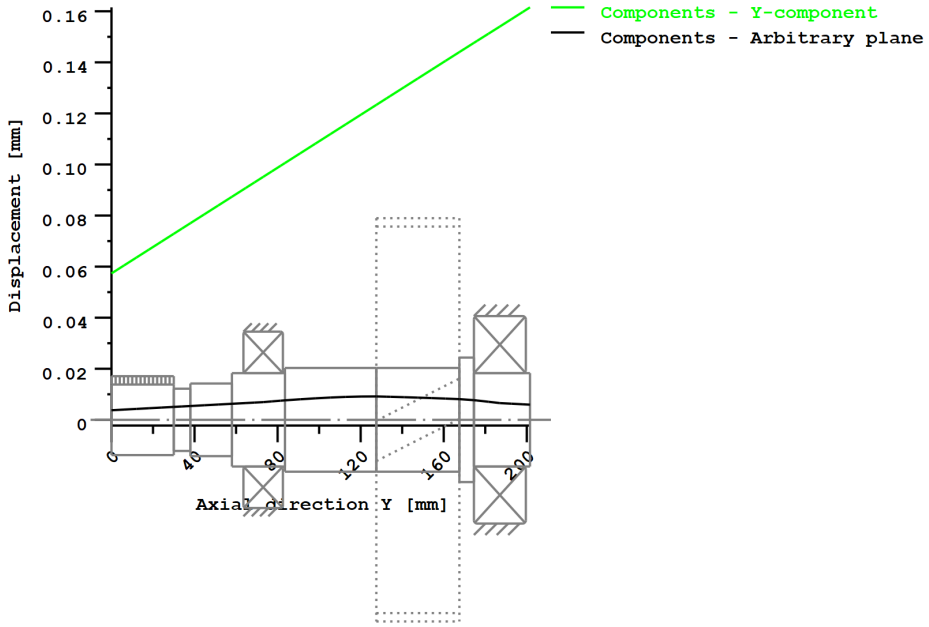

Figure: Deformation (bending etc.) (Arbitrary plane 58.5927984 121)

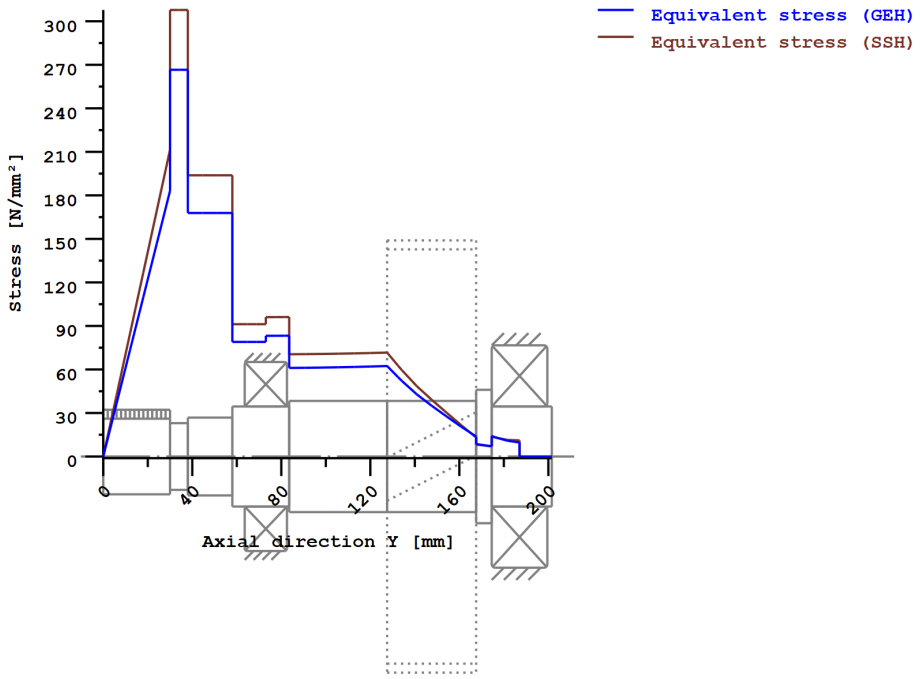

Nominal stresses, without taking into account stress concentrations
GEH(von Mises): sigV = ((sigB+sigZ,D)^2 + 3*(tauT+tauS)^2)^1/2
SSH(Tresca): sigV = ((sigB-sigZ,D)^2 + 4*(tauT+tauS)^2)^1/2

Figure: Equivalent stress

KISSSOFT
Calculation programs for machine design

Eigenfrequencies/Critical speeds

1. Eigenfrequency:	0.00 Hz, Critical speed:	0.00 1/min	Rigid body rotation Y 'Shaft 1'
2. Eigenfrequency:	3691.31 Hz, Critical speed:	221478.39 1/min	Bending XY 'Shaft 1', Bending YZ 'Shaft 1'
3. Eigenfrequency:	5194.18 Hz, Critical speed:	311650.85 1/min	Bending XY 'Shaft 1', Bending YZ 'Shaft 1'
4. Eigenfrequency:	8439.39 Hz, Critical speed:	506363.47 1/min	Bending XY 'Shaft 1'
5. Eigenfrequency:	9325.02 Hz, Critical speed:	559501.01 1/min	Torsion 'Shaft 1'

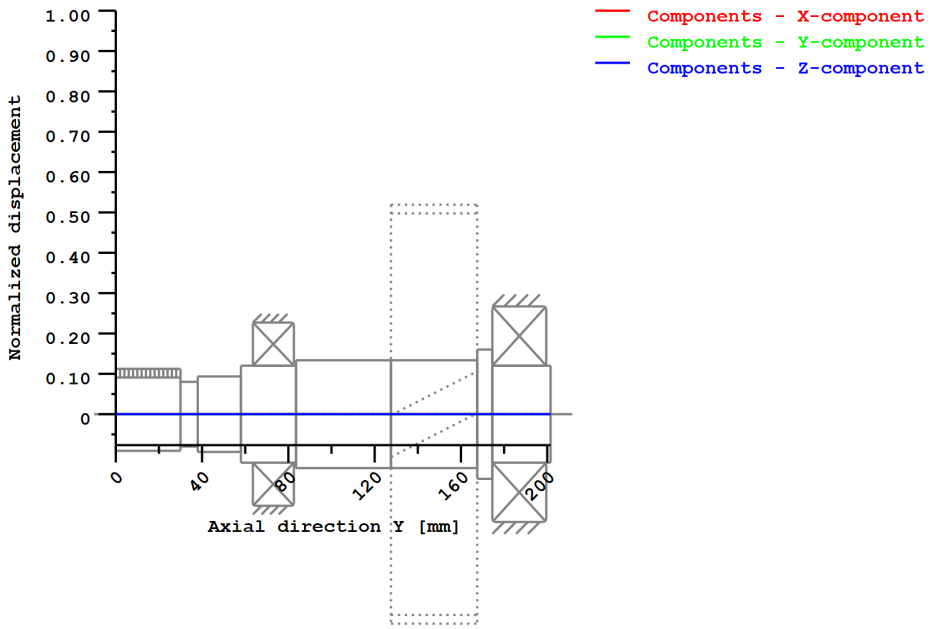

Figure: Eigenfrequencies (Normalized rotation) (Eigenfrequency: 1. (0 Hz))

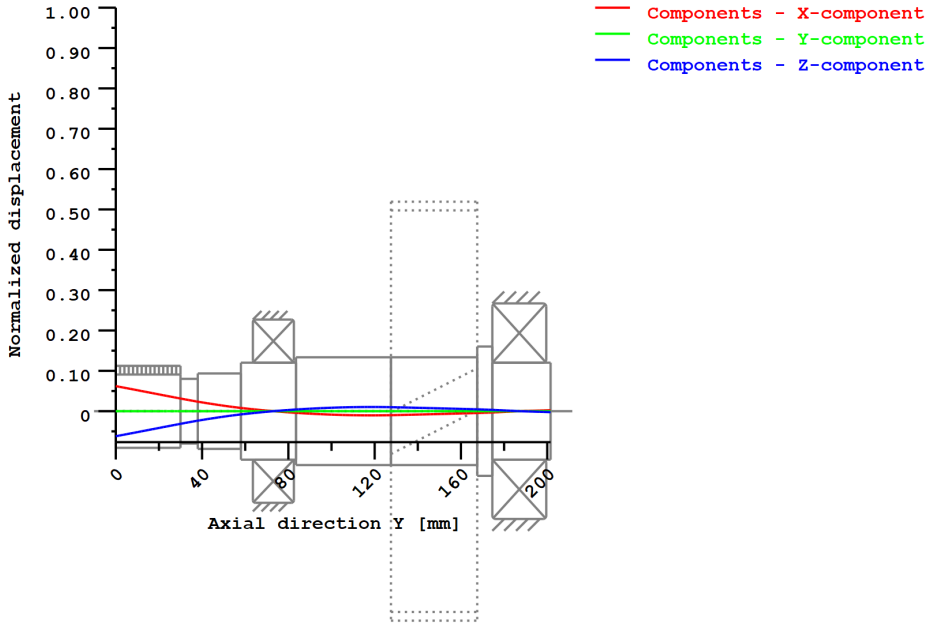

Figure: Eigenfrequencies (Normalized rotation) (Eigenfrequency: 2. (3691.31 Hz))

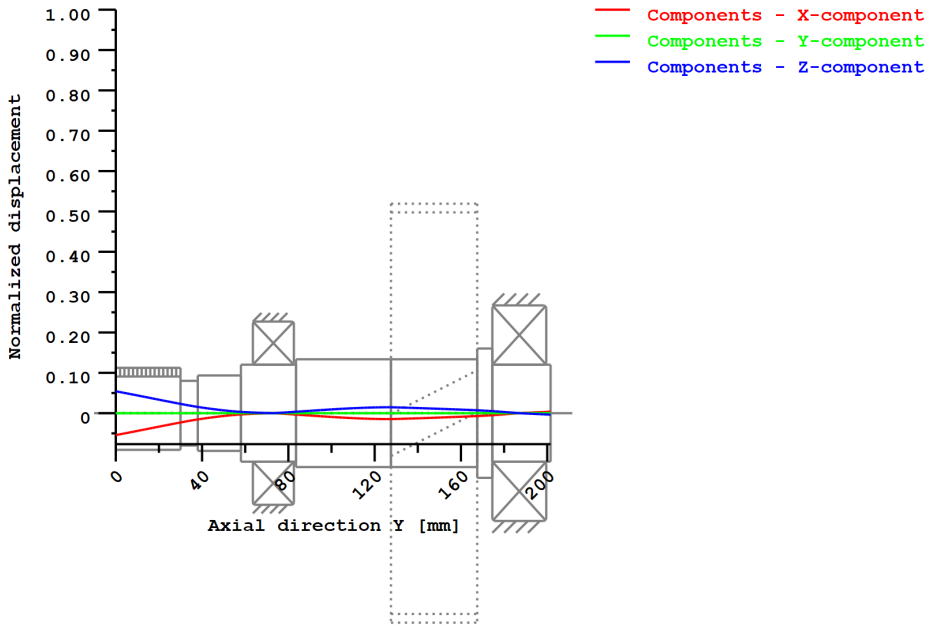

Figure: Eigenfrequencies (Normalized rotation) (Eigenfrequency: 3. (5194.18 Hz))

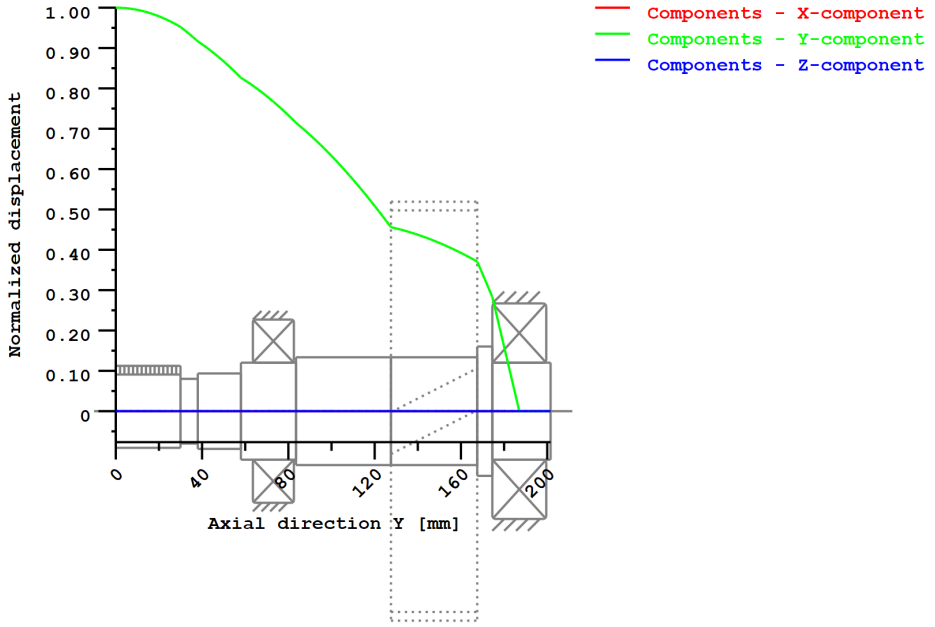

Figure: Eigenfrequencies (Normalized rotation) (Eigenfrequency: 4. (8439.39 Hz))

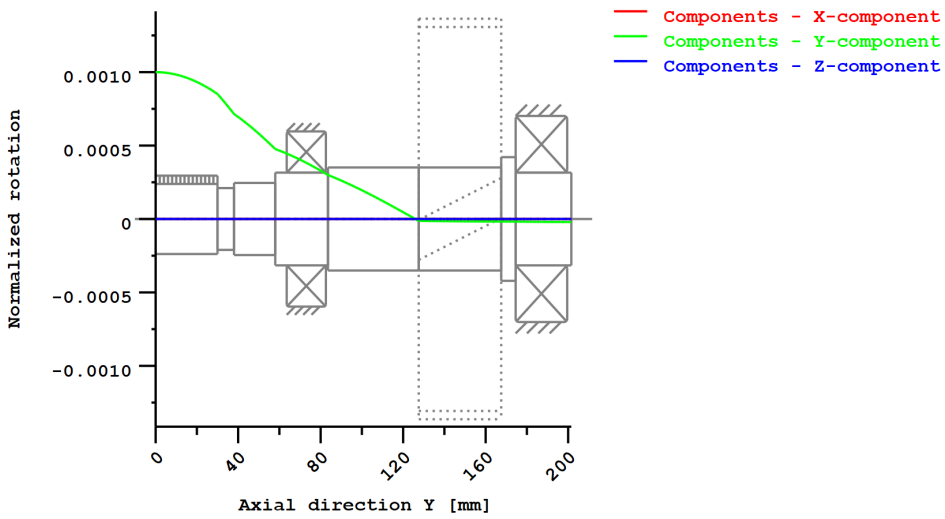

Figure: Eigenfrequencies (Normalized displacement) (Eigenfrequency: 5. (9325.02 Hz))

Strength calculation according to DIN 743:2012
with finite life fatigue strength according to FKM standard and FVA draft

Summary

Shaft 1

Material	18CrNiMo7-6
Material type	Case-carburized steel
Material treatment	case-hardened
Surface treatment	No

Calculation of finite life fatigue strength and static strength

Calculation for load case 2 (σav/σmv = const)

Cross section	Position (Y-Coord) (mm)	
A-A Shoulder	38.00	Shoulder
B-B Shoulder	30.00	Shoulder
C-C Smooth shaft	34.00	Smooth shaft
D-D Shoulder	58.00	Shoulder

Results:

Cross section	Kfb	Kfs	K2d	SD	SS	SA
A-A Shoulder	2.50	0.86	0.91	1.71	1.58	2.99
B-B Shoulder	2.41	0.86	0.91	1.76	1.58	3.11
C-C Smooth shaft	1.00	0.86	0.91	2.40	1.58	8.79
D-D Shoulder	2.87	0.86	0.90	2.41	2.51	4.14
Required safeties:				1.20	1.20	1.20

Abbreviations:
Kfb: Notch factor bending
Kfσ: Surface factor
K2d: size factor bending
SD: Safety endurance limit
SS: Safety against yield point
SA: Safety against incipient crack

Service life and damage

System service life (h)	[Hatt]	1000000.00
Damage to system (%)	[D]	0.00
Damage (%)	[H] (5000.0 h)	

Calculation of reliability R(t) using a Weibull distribution; t in (h):

R(t) = 100 * Exp(-((t*fac - t0)/(T - t0))^b) %

Welle	fac	b	t0	T
1	18019	1.5	1.643e+010	3.484e+010

Damage to cross sections (%) [D]

A-A Shoulder:	0.00
B-B Shoulder:	0.00
C-C Smooth shaft:	0.00
D-D Shoulder:	0.00

Utilization (%) [Smin/S]

Cross section	Static	Endurance
A-A Shoulder	76.002	70.204
B-B Shoulder	76.002	68.025
C-C Smooth shaft	76.002	50.077
D-D Shoulder	47.861	49.798

Maximum utilization (%)	[A]	76.002

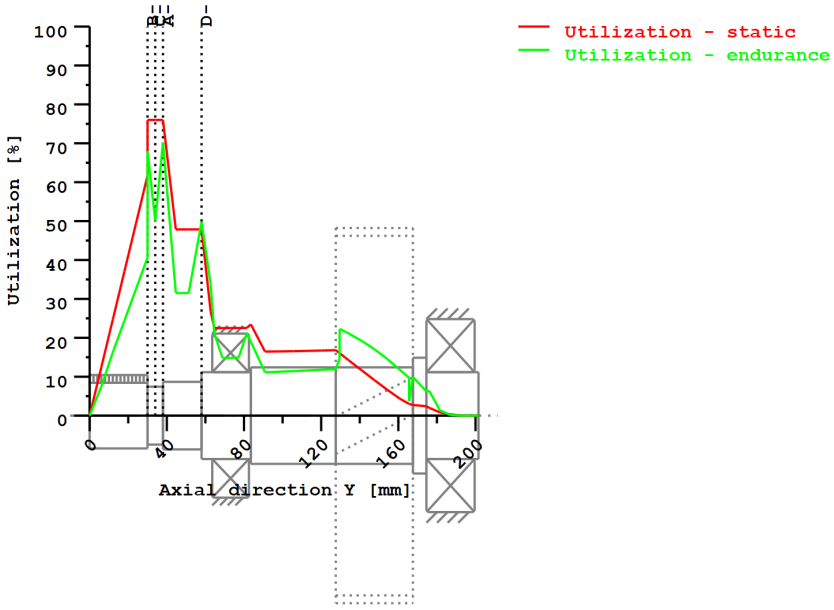

Utilization = Smin/S (%)

Figure: Strength

Calculation details

General statements

Label	Shaft 1		
Drawing			
Length (mm)	[l]	201.55	
Speed (1/min)	[n]	300.31	

Material	18CrNiMo7-6
Material type	Case-carburized steel
Material treatment	case-hardened
Surface treatment	No

	Tension/Compression	Bending	Torsion	Shearing
Load factor static calculation	1.700	1.700	1.700	1.700
Load factor endurance limit	1.000	1.000	1.000	1.000

Reference diameter material (mm)	[dB]	16.00
σB according to DIN 743 (at dB) (N/mm²)	[σB]	1200.00
σS according to DIN 743 (at dB) (N/mm²)	[σS]	850.00
[σzdW] (bei dB) (N/mm²)		480.00
[σbW] (bei dB) (N/mm²)		600.00
[τtW] (bei dB) (N/mm²)		360.00
Thickness of raw material (mm)	[dWerkst]	65.00
Material data calculated according DIN743/3 with K1(d)		
Material strength calculated from size of raw material		
Geometric size factor K1d calculated from raw material diameter		
[σBeff] (N/mm²)		1010.06
[σSeff] (N/mm²)		715.46
[σbF] (N/mm²)		715.46
[τtF] (N/mm²)		413.07
[σBRand] (N/mm²)		2300.00
[σzdW] (N/mm²)		404.02

KISSSOFT
Calculation programs for machine design

[σbW] (N/mm²)		505.03
[τtW] (N/mm²)		303.02

Fatigue strength for single stage use

Required life time	[H]	5000.00
Number of load cycles (Mio)	[NL]	90.093

Data of S-N curve (Woehler line) analog to FKM standard:

[kσ, kτ]	15	25
[kDσ, kDτ]	0	0
[NDσ, NDτ]	1e+006	1e+006
[NDσII, NDτII]	0	0

Calculation for load case 2 (σ.av/σ.mv = const)

Cross section 'A-A Shoulder' **Shoulder**

Comment	Y= 38.00mm			
Position (Y-Coordinate) (mm)		[y]		38.000
External diameter (mm)		[da]		30.000
Inner diameter (mm)		[di]		0.000
Notch effect			Shoulder	
[D, r, t] (mm)	35.000	0.100	2.500	
Mean roughness (µm)		[Rz]		8.000

		Tension/Compression	Bending	Torsion	Shearing	
Load: (N) (Nm)						
Mean value	[Fzdm, Mbm, Tm, Fqm]	0.0	0.0	407.9	0.0	
Amplitude	[Fzda, Mba, Ta, Fqa]	0.0	0.0	407.9	2.5	
Maximum value	[Fzdmax, Mbmax, Tmax, Fqmax]	0.0	0.1	1386.9		4.3
Cross section, moment of resistance: (mm²)						
[A, Wb, Wt, A]		706.9	2650.7	5301.4	706.9	

Stresses: (N/mm²)				
[σzdm, σbm, τm, τqm] (N/mm²)	0.000	0.000	76.946	0.000
[σzda, σba, τa, τqa] (N/mm²)	0.000	0.019	76.946	0.005
[σzdmax,σbmax,τmax,τqmax] (N/mm²)	0.000	0.032	261.617	0.008

Technological size influence	[K1(σB)]	0.842	
	[K1(σS)]	0.842	

		Tension/Compression	Bending	Torsion
Stress concentration factor	[a]	5.543	4.953	2.940
References stress slope	[G']	24.045	24.045	11.500
Notch sensitivity factor	[n]	1.978	1.978	1.677
Notch effect coefficient	[ß]	2.802	2.504	1.753
Geometrical size influence	[K2(d)]	1.000	0.907	0.907
Influence coefficient surface roughness	[KF]	0.860	0.860	0.920
Surface stabilization factor	[KV]	1.000	1.000	1.000
Total influence coefficient	[K]	2.964	2.921	2.020
Present safety for endurance limit:				
Equivalent mean stress (N/mm²)	[σmV]		133.275	
Equivalent mean stress (N/mm²)	[τmV]		76.946	
Fatigue limit of part (N/mm²)	[σWK]	136.294	172.877	150.034
Influence coefficient of mean stress sensitivity.	[ψσK]	0.072	0.094	0.080
Permissible amplitude (N/mm²)	[σADK]	0.005	0.101	138.891
Permissible amplitude (N/mm²)	[σANK]	0.005	0.101	138.891
Effective Miner sum	[DM]	0.300	0.300	0.300
Load spectrum factor	[fKoll]	1.000	1.000	1.000
Safety against fatigue	[S]		1.709	
Required safety against fatigue	[Smin]		1.200	
Result (%)	[S/Smin]		142.4	
Present safety for proof against exceed of yield point:				
Static notch sensitivity factor	[K2F]	1.000	1.000	1.000
Increase coefficient	[γF]	1.000	1.000	1.000
Yield stress of part (N/mm²)	[σFK]	715.457	715.457	413.069
Safety yield stress	[S]		1.579	
Required safety	[Smin]		1.200	

Result (%)	[S/Smin]	131.6

Present safety
for proof of avoiding incipient crack on hard surface layers:

Safety against incipient crack	[S]	2.990
Required safety	[Smin]	1.200
Result (%)	[S/Smin]	249.2

Cross section 'B-B Shoulder' **Shoulder**

Comment	Y= 30.00mm			
Position (Y-Coordinate) (mm)		[y]		30.000
External diameter (mm)		[da]		30.000
Inner diameter (mm)		[di]		0.000
Notch effect			Shoulder	
[D, r, t] (mm)	34.000	0.100	2.000	
Mean roughness (µm)		[Rz]		8.000

		Tension/Compression	Bending	Torsion	Shearing
Load: (N) (Nm)					
Mean value	[Fzdm, Mbm, Tm, Fqm]	0.0	0.0	407.9	0.0
Amplitude	[Fzda, Mba, Ta, Fqa]	0.0	0.0	407.9	2.1
Maximum value	[Fzdmax, Mbmax, Tmax, Fqmax]	0.0	0.1	1386.9	3.6
Cross section, moment of resistance: (mm²)					
[A, Wb, Wt, A]		706.9	2650.7	5301.4	706.9

Stresses: (N/mm²)					
[σzdm, σbm, τm, τqm] (N/mm²)		0.000	0.000	76.946	0.000
[σzda, σba, τa, τqa] (N/mm²)		0.000	0.012	76.946	0.004
[σzdmax,σbmax,τmax,τqmax] (N/mm²)		0.000	0.020	261.617	0.007
Technological size influence	[K1(σB)]	0.842			
	[K1(σS)]	0.842			

		Tension/Compression	Bending	Torsion
Stress concentration factor	[a]	5.278	4.774	2.824
References stress slope	[G']	24.156	24.156	11.500
Notch sensitivity factor	[n]	1.981	1.981	1.677
Notch effect coefficient	[ß]	2.665	2.410	1.684
Geometrical size influence	[K2(d)]	1.000	0.907	0.907
Influence coefficient surface roughness	[KF]	0.860	0.860	0.920
Surface stabilization factor	[KV]	1.000	1.000	1.000
Total influence coefficient	[K]	2.827	2.819	1.944

Present safety for endurance limit:

Equivalent mean stress (N/mm²)	[σmV]		133.275	
Equivalent mean stress (N/mm²)	[τmV]		76.946	
Fatigue limit of part (N/mm²)	[σWK]	142.910	179.175	155.913
Influence coefficient of mean stress sensitivity.	[ψσK]	0.076	0.097	0.084
Permissible amplitude (N/mm²)	[σADK]	0.005	0.064	143.880
Permissible amplitude (N/mm²)	[σANK]	0.005	0.064	143.880
Effective Miner sum	[DM]	0.300	0.300	0.300
Load spectrum factor	[fKoll]	1.000	1.000	1.000
Safety against fatigue	[S]		1.764	
Required safety against fatigue	[Smin]		1.200	
Result (%)	[S/Smin]		147.0	

Present safety
for proof against exceed of yield point:

Static notch sensitivity factor	[K2F]	1.000	1.000	1.000
Increase coefficient	[γF]	1.000	1.000	1.000
Yield stress of part (N/mm²)	[σFK]	715.457	715.457	413.069
Safety yield stress	[S]		1.579	
Required safety	[Smin]		1.200	
Result (%)	[S/Smin]		131.6	

Present safety
for proof of avoiding incipient crack on hard surface layers:

KISSSOFT
Calculation programs for machine design

Safety against incipient crack	[S]	3.113
Required safety	[Smin]	1.200
Result (%)	[S/Smin]	259.4

Cross section 'C-C Smooth shaft' Smooth shaft

Comment		
Position (Y-Coordinate) (mm)	[y]	34.000
External diameter (mm)	[da]	30.000
Inner diameter (mm)	[di]	0.000
Notch effect		Smooth shaft
Mean roughness (µm)	[Rz]	8.000

	Tension/Compression	Bending	Torsion	Shearing
Load: (N) (Nm)				
Mean value [Fzdm, Mbm, Tm, Fqm]	0.0	0.0	407.9	0.0
Amplitude [Fzda, Mba, Ta, Fqa]	0.0	0.0	407.9	2.3
Maximum value [Fzdmax, Mbmax, Tmax, Fqmax]	0.0	0.1	1386.9	3.9
Cross section, moment of resistance: (mm²)				
[A, Wb, Wt, A]	706.9	2650.7	5301.4	706.9

Stresses: (N/mm²)					
[σzdm, σbm, τm, τqm] (N/mm²)		0.000	0.000	76.946	0.000
[σzda, σba, τa, τqa] (N/mm²)		0.000	0.015	76.946	0.004
[σzdmax,σbmax,τmax,τqmax] (N/mm²)		0.000	0.026	261.617	0.007
Technological size influence	[K1(σB)]	0.842			
	[K1(σS)]	0.842			

		Tension/Compression	Bending	Torsion
Notch effect coefficient	[ß]	1.000	1.000	1.000
Geometrical size influence	[K2(d)]	1.000	0.907	0.907
Influence coefficient surface roughness	[KF]	0.860	0.860	0.920
Surface stabilization factor	[KV]	1.000	1.000	1.000
Total influence coefficient	[K]	1.162	1.264	1.189
Present safety for endurance limit:				
Equivalent mean stress (N/mm²)	[σmV]		133.275	
Equivalent mean stress (N/mm²)	[τmV]		76.946	
Fatigue limit of part (N/mm²)	[σWK]	347.567	399.414	254.774
Influence coefficient of mean stress sensitivity.				
	[ψσK]	0.208	0.246	0.144
Permissible amplitude (N/mm²)	[σADK]	0.005	0.082	206.535
Permissible amplitude (N/mm²)	[σANK]	0.005	0.082	206.535
Effective Miner sum	[DM]	0.300	0.300	0.300
Load spectrum factor	[fKoll]	1.000	1.000	1.000
Safety against fatigue	[S]		2.396	
Required safety against fatigue	[Smin]		1.200	
Result (%)	[S/Smin]		199.7	
Present safety for proof against exceed of yield point:				
Static notch sensitivity factor	[K2F]	1.000	1.000	1.000
Increase coefficient	[γF]	1.000	1.000	1.000
Yield stress of part (N/mm²)	[σFK]	715.457	715.457	413.069
Safety yield stress	[S]		1.579	
Required safety	[Smin]		1.200	
Result (%)	[S/Smin]		131.6	
Present safety for proof of avoiding incipient crack on hard surface layers:				
Safety against incipient crack	[S]		8.791	
Required safety	[Smin]		1.200	
Result (%)	[S/Smin]		732.6	

Cross section 'D-D Shoulder' Shoulder

Comment	Y= 58.00mm			
Position (Y-Coordinate) (mm)		[y]	58.000	
External diameter (mm)		[da]	35.000	
Inner diameter (mm)		[di]	0.000	
Notch effect			Shoulder	
[D, r, t] (mm)	45.000	0.100	5.000	
Mean roughness (µm)		[Rz]	8.000	

	Tension/Compression	Bending	Torsion	Shearing
Load: (N) (Nm)				
Mean value [Fzdm, Mbm, Tm, Fqm]	0.0	0.0	407.9	0.0
Amplitude [Fzda, Mba, Ta, Fqa]	0.0	0.1	407.9	4.0
Maximum value [Fzdmax, Mbmax, Tmax, Fqmax]		0.0	0.2	1386.9	6.8
Cross section, moment of resistance: (mm²)				
[A, Wb, Wt, A]	962.1	4209.2	8418.5	962.1	

Stresses: (N/mm²)				
[σzdm, σbm, τm, τqm] (N/mm²)	0.000	0.000	48.456	0.000
[σzda, σba, τa, τqa] (N/mm²)	0.000	0.027	48.456	0.006
[σzdmax,σbmax,τmax,τqmax] (N/mm²)	0.000	0.047	164.750	0.009

Technological size influence	[K1(σB)]	0.842	
	[K1(σS)]	0.842	

		Tension/Compression	Bending	Torsion
Stress concentration factor	[a]	6.536	5.666	3.369
References stress slope	[G']	23.759	23.759	11.500
Notch sensitivity factor	[n]	1.973	1.973	1.677
Notch effect coefficient	[ß]	3.313	2.873	2.010
Geometrical size influence	[K2(d)]	1.000	0.897	0.897
Influence coefficient surface roughness	[KF]	0.860	0.860	0.920
Surface stabilization factor	[KV]	1.000	1.000	1.000
Total influence coefficient	[K]	3.476	3.364	2.327
Present safety for endurance limit:				
Equivalent mean stress (N/mm²)	[σmV]		83.928	
Equivalent mean stress (N/mm²)	[τmV]		48.456	
Fatigue limit of part (N/mm²)	[σWK]	116.236	150.113	130.198
Influence coefficient of mean stress sensitivity.				
	[ψσK]	0.061	0.080	0.069
Permissible amplitude (N/mm²)	[σADK]	0.009	0.233	121.807
Permissible amplitude (N/mm²)	[σANK]	0.009	0.233	121.807
Effective Miner sum	[DM]	0.300	0.300	0.300
Load spectrum factor	[fKoll]	1.000	1.000	1.000
Safety against fatigue	[S]		2.410	
Required safety against fatigue	[Smin]		1.200	
Result (%)	[S/Smin]		200.8	
Present safety for proof against exceed of yield point:				
Static notch sensitivity factor	[K2F]	1.000	1.000	1.000
Increase coefficient	[γF]	1.000	1.000	1.000
Yield stress of part (N/mm²)	[σFK]	715.457	715.457	413.069
Safety yield stress	[S]		2.507	
Required safety	[Smin]		1.200	
Result (%)	[S/Smin]		208.9	
Present safety for proof of avoiding incipient crack on hard surface layers:				
Safety against incipient crack	[S]		4.142	
Required safety	[Smin]		1.200	
Result (%)	[S/Smin]		345.2	

Remarks:
- The shearing force is not considered in the analysis specified in DIN 743.
- Cross section with interference fit:
  The notching factor for the light fit case is no longer defined in DIN 743.
  The values are imported from the FKM-Guideline..

KISSSOFT
Calculation programs for machine design

End of Report	lines:	792

THERMALLY SAFE OPERATING SPEED CALCULATION
(according to DIN ISO 15312 and DIN 732)

Lubricant	Castrol ATF Dex II Multivehicle		
Lubrication type:			
Immersion lubrication - Oil level up to the middle of the lowest rolling element.			
Mean bearing temperature	[T_m]	75.000	°C
Temperature of bearing environment	[T_u]	65.000	°C
Lubricant - service temperature	[T_B]	65.000	°C
Lubricant temperature - Reference conditions	[T_{ref}]	70.000	°C

Shaft 'Shaft 1', Rolling bearing 'Rolling bearing':

Thermal nominal speed according to DIN ISO 15312:

Type of support	Deep groove ball bearing (single row)		
Bearing number	SKF 6209		
Design series	62		
Speed	[n]	300.310	1/min
Coefficient	[f_{0r}]	2.000	
(Depends upon type of design and lubrication at reference conditions)			
Coefficient	[f_{1r}]	0.000200	
(Depends upon type of design and load at reference conditions)			
Heat sink reference surface	[A_S]	7759.734	mm²
Reference load	[P_{1r}]	1.080	kN
Bearing mean diameter	[d_m]	65.000	mm
Bearing-specific reference heat flow density	[q_r]	16.000	kW/m²
kinematic viscosity (for reference conditions)	[v_r]	12.000	mm²/s
Thermal nominal speed	[$n_{\theta r}$]	9306.785	1/min

Thermally safe operating speed according to DIN 732:

Coefficient	[f_0]	2.000	
(Depends upon type of design and lubrication)			
Coefficient	[f_1]	0.000330	
(Depends upon type of design and load)			
Heat flow (dissipated by the bearing support surface)	[Φ_S]	0.024	kW
Total heat flow	[Φ]	0.024	kW
Dynamic equivalent load	[P_1]	2909.075	N
kinematic viscosity at service temperature	[v]	17.134	mm²/s
Lubricant film parameter	[K_L]	6.544	
Charge parameter	[K_P]	2.530	
Speed ratio	[f_n]	0.209	
Thermally safe operating speed	[n_θ]	1942.700	1/min

Shaft 'Shaft 1', Rolling bearing 'Rolling bearing':

Thermal nominal speed according to DIN ISO 15312:

Type of support		Deep groove ball bearing (single row)		
Bearing number		SKF 6309		
Design series		63		
Speed	[n]	300.310	1/min	
Coefficient	[f_{0r}]		2.300	
(Depends upon type of design and lubrication at reference conditions)				
Coefficient	[f_{1r}]		0.000200	
(Depends upon type of design and load at reference conditions)				
Heat sink reference surface	[A_S]		11388.273	mm²
Reference load	[P_{1r}]		1.575	kN
Bearing mean diameter	[d_m]		72.500	mm
Bearing-specific reference heat flow density	[q_r]		16.000	kW/m²
kinematic viscosity (for reference conditions)	[v_r]		12.000	mm²/s
Thermal nominal speed	[$n_{\theta r}$]		8850.783	1/min

Thermally safe operating speed according to DIN 732:

Coefficient	[f_0]		2.300	
(Depends upon type of design and lubrication)				
Coefficient	[f_1]		0.000412	
(Depends upon type of design and load)				
Heat flow (dissipated by the bearing support surface)	[Φ_S]		0.035	kW
Total heat flow	[Φ]		0.035	kW
Dynamic equivalent load	[P_1]		6596.087	N
kinematic viscosity at service temperature	[v]		17.134	mm²/s
Lubricant film parameter	[K_L]		6.544	
Charge parameter	[K_P]		5.171	
Speed ratio	[f_n]		0.143	
Thermally safe operating speed	[n_θ]		1264.089	1/min

The reference conditions for calculating the thermal nominal speed are taken from the DIN ISO 15312 standard.

End of Report lines: 90

Analysis of shafts, axle and beams

Input data

Coordinate system shaft: see picture W-002

Label		Shaft 1
Drawing		
Initial position (mm)		0.000
Length (mm)		163.900
Speed (1/min)		14000.00
Sense of rotation: clockwise		
Material		18CrNiMo7-6
Young's modulus (N/mm²)		206000.000
Poisson's ratio nu		0.300
Density (kg/m³)		7830.000
Coefficient of thermal expansion	(10^-6/K)	11.500
Temperature (°C)		75.000
Weight of shaft (kg)		0.799
(Notice: Weight stands for the shaft only without considering the gears)		
Weight of shaft, including additional masses (kg)		0.839
Mass moment of inertia (kg*mm²)		100.120
Momentum of mass GD2 (Nm²)		0.004
Position in space (°)		0.000
Gears mounted with stiffness according to ISO		
Consider deformations due to shearing		
Shear correction coefficient		1.100
Contact angle of rolling bearings is considered		
Tolerance field: Mean value		
Housing material		G-AlSi10Mg
Coefficient of thermal expansion	(10^-6/K)	22.000
Temperature of housing (°C)		65.000
Thermal housing reference point (mm)		0.000
Reference temperature (°C)		20.000

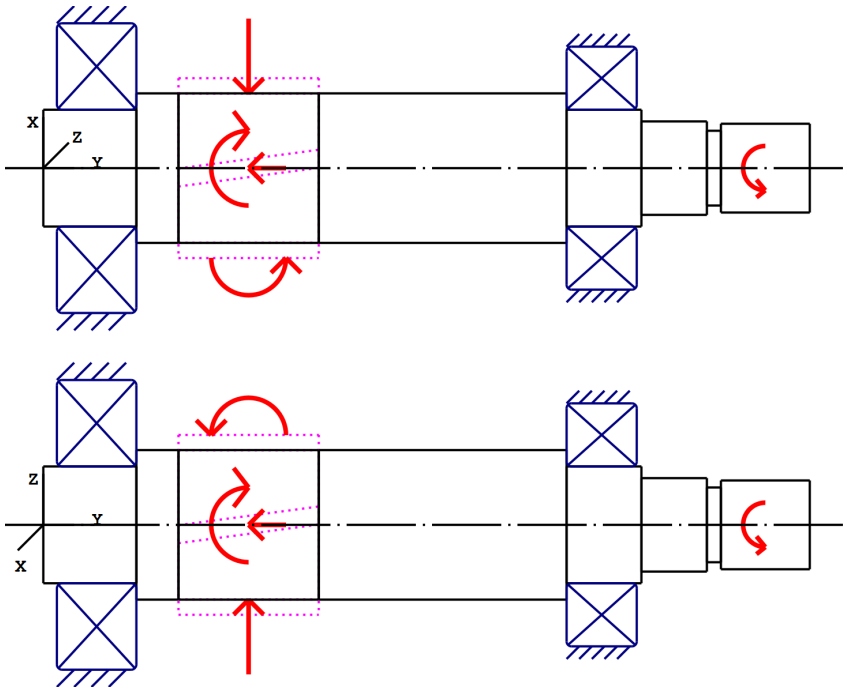

Figure: Load applications

Shaft definition (Shaft 1)

Outer contour

Cylinder (Cylinder)			0.000mm ... 19.900mm
Diameter (mm)	[d]	25.0000	
Length (mm)	[l]	19.9000	
Surface roughness (µm)	[Rz]	4.8000	

Relief groove right (Relief groove right)
r=0.80 (mm), t=0.30 (mm), l=2.50 (mm), Rz=8.0, Turned (Ra=3.2µm/125µin)
Form E (DIN 509), Series 1, with the usual stressing

Chamfer left (Chamfer left)
l=0.50 (mm), alpha=45.00 (°)

Square groove (Square groove)
b=1.30 (mm), t=0.55 (mm), r=0.10 (mm), Rz=8.0, Turned (Ra=3.2µm/125µin)

Cylinder (Cylinder)			19.900mm ... 111.900mm
Diameter (mm)	[d]	32.0000	
Length (mm)	[l]	92.0000	
Surface roughness (µm)	[Rz]	4.8000	

Cylinder (Cylinder)			111.900mm ... 127.900mm
Diameter (mm)	[d]	25.0000	
Length (mm)	[l]	16.0000	

Surface roughness (µm)	[Rz]	4.8000

Relief groove left (Relief groove left)
r=0.80 (mm), t=0.30 (mm), l=2.50 (mm), Rz=8.0, Turned (Ra=3.2µm/125µin)
Form E (DIN 509), Series 1, with the usual stressing

Chamfer right (Chamfer right)
l=0.50 (mm), alpha=45.00 (°)

Cylinder (Cylinder)			127.900mm ... 141.900mm
Diameter (mm)	[d]	20.0000	
Length (mm)	[l]	14.0000	
Surface roughness (µm)	[Rz]	8.0000	

Chamfer right (Chamfer right)
l=0.50 (mm), alpha=45.00 (°)

Radius left (Radius left)
r=0.10 (mm), Rz=8.0, Turned (Ra=3.2µm/125µin)

Cylinder (Cylinder)			141.900mm ... 144.900mm
Diameter (mm)	[d]	16.0000	
Length (mm)	[l]	3.0000	
Surface roughness (µm)	[Rz]	8.0000	

Radius left (Radius left)
r=0.10 (mm), Rz=8.0, Turned (Ra=3.2µm/125µin)

Cylinder (Cylinder)			144.900mm ... 163.900mm
Diameter (mm)	[d]	19.0000	
Length (mm)	[l]	19.0000	
Surface roughness (µm)	[Rz]	8.0000	

Chamfer right (Chamfer right)
l=0.50 (mm), alpha=45.00 (°)

Spline (Spline) 135.400mm ... 154.400mm
da=18.84 (mm), df=17.16 (mm), z=22, mn=0.80 (mm), l=19.00 (mm), Rz=8.0, Turned (Ra=3.2µm/125µin)

Forces

Type of force element		**Cylindrical gear**
Label in the model		Cylindrical gear
Position on shaft (mm)	[y_{local}]	43.9000
Position in global system (mm)	[y_{global}]	43.9000
Operating pitch diameter (mm)		38.4914
Helix angle (°)		12.0156 left
Working pressure angle at normal section (°)		20.2001
Position of contact (°)		20.0000
Length of load application (mm)		30.0000
Power (kW)		25.0000 driving (output)
Torque (Nm)		-17.0523
Axial force (N)		-188.5838

Shearing force X (N)		-616.2405
Shearing force Z (N)		718.6034
Bending moment X (Nm)		1.2413
Bending moment Z (Nm)		-3.4105

Type of force element		**Coupling**
Label in the model		Coupling
Position on shaft (mm)	[y_{local}]	154.4000
Position in global system (mm)	[y_{global}]	154.4000
Effective diameter (mm)		20.0000
Radial force factor (-)		0.0000
Direction of the radial force (°)		0.0000
Axial force factor (-)		0.0000
Length of load application (mm)		19.0000
Power (kW)		25.0000 driven (input)
Torque (Nm)		17.0523
Axial force (N)		0.0000
Shearing force X (N)		0.0000
Shearing force Z (N)		0.0000
Bending moment X (Nm)		0.0000
Bending moment Z (Nm)		0.0000
Mass (kg)		0.0000
Mass moment of inertia Jp (kg*m²)		0.0000
Mass moment of inertia Jxx (kg*m²)		0.0000
Mass moment of inertia Jzz (kg*m²)		0.0000
Eccentricity (mm)		0.0000

Bearing

Label in the model		Rolling bearing
Bearing type		SKF 6205 ETN9
Bearing type		Deep groove ball bearing (single row)

Bearing position (mm)	[y_{lokal}]	119.400
Bearing position (mm)	[y_{global}]	119.400
Attachment of external ring		Fixed bearing
Inner diameter (mm)	[d]	25.000
External diameter (mm)	[D]	52.000
Width (mm)	[b]	15.000
Corner radius (mm)	[r]	1.000
Basic static load rating (kN)	[C_0]	9.300
Basic dynamic load rating (kN)	[C]	17.800
Fatigue load rating (kN)	[C_u]	0.400
Values for approximated geometry:		
Basic dynamic load rating (kN)	[C_{theo}]	0.000
Basic static load rating (kN)	[C_{0theo}]	0.000

Label in the model		Rolling bearing
Bearing type		SKF 6305 ETN9
Bearing type		Deep groove ball bearing (single row)

Bearing position (mm)	[y_{lokal}]	11.400
Bearing position (mm)	[y_{global}]	11.400
Attachment of external ring		Free bearing
Inner diameter (mm)	[d]	25.000
External diameter (mm)	[D]	62.000

Width (mm)	[b]	17.000
Corner radius (mm)	[r]	1.100
Basic static load rating (kN)	[C_0]	13.400
Basic dynamic load rating (kN)	[C]	26.000
Fatigue load rating (kN)	[C_u]	0.570
Values for approximated geometry:		
Basic dynamic load rating (kN)	[C_{theo}]	0.000
Basic static load rating (kN)	[C_{0theo}]	0.000

Shaft 'Shaft 1': Cylindrical gear 'Cylindrical gear' (y= 43.9000 (mm)) is taken into account as component of the shaft.
EI (y= 28.9000 (mm)): 10603.2019 (Nm²), EI (y= 58.9000 (mm)): 10603.2019 (Nm²), m (yS= 43.9000 (mm)): 0.0403 (kg)
Jp: 0.0000 (kg*m²), Jxx: 0.0000 (kg*m²), Jzz: 0.0000 (kg*m²)

Results

Shaft

Maximum deflection (µm)	8.060
Position of the maximum (mm)	58.900
Mass center of gravity (mm)	72.807
Total axial load (N)	-188.584
Torsion under torque (°)	0.039

Bearing

Probability of failure	[n]	10.00	%
Axial clearance	[u_A]	10.00	µm
Lubricant	Castrol ATF Dex II Multivehicle		
Lubricant with additive, effect on bearing lifetime confirmed in tests.			
Oil lubrication, off-line/no filtration, ISO4406 -/15/12			
Lubricant - service temperature	[T_B]	75.00	°C
Limit for factor aISO	[a_{ISOmax}]	50.00	
Oil level	[h_{oil}]	0.00	mm
Oil bath lubrication			

Rolling bearings, classical calculation (contact angle considered)

Shaft 'Shaft 1' Rolling bearing 'Rolling bearing'

Position (Y-coordinate)	[y]	119.40	mm
Dynamic equivalent load	[P]	0.54	kN
Equivalent load	[P_0]	0.27	kN
Life modification factor for reliability	[a_1]	1.000	
Life modification factor	[a_{ISO}]	11.686	
Nominal bearing service life	[L_{nh}]	43545.93	h
Modified bearing service life	[L_{nmh}]	508885.43	h
Operating viscosity	[v]	12.72	mm²/s
Static safety factor	[S_0]	34.31	
Bearing reaction force	[Fx]	0.154	kN

Bearing reaction force	[Fy]	0.189	kN
Bearing reaction force	[Fz]	-0.223	kN
Bearing reaction force	[Fr]	0.271	kN (-55.41°)
Oil level	[H]	0.000	mm
Rolling moment of friction	[M_{rr}]	0.034	Nm
Sliding moment of friction	[M_{sl}]	0.004	Nm
Moment of friction, seals	[M_{seal}]	0.000	Nm
Moment of friction for seals determined according to SKF main catalog 10000/1 EN:2013			
Moment of friction flow losses	[M_{drag}]	0.000	Nm
Torque of friction	[M_{loss}]	0.038	Nm
Power loss	[P_{loss}]	55.255	W
The moment of friction is calculated according to the details in SKF Catalog 2013.			
The calculation is always performed with a coefficient for additives in the lubricant μbl=0.15.			
Displacement of bearing	[u_x]	-3.551	μm
Displacement of bearing	[u_y]	108.206	μm
Displacement of bearing	[u_z]	5.143	μm
Displacement of bearing	[u_r]	6.250	μm (124.62°)
Misalignment of bearing	[r_x]	-0.028	mrad (-0.1')
Misalignment of bearing	[r_y]	0.174	mrad (0.6')
Misalignment of bearing	[r_z]	-0.032	mrad (-0.11')
Misalignment of bearing	[r_r]	0.043	mrad (0.15')

Shaft 'Shaft 1' Rolling bearing 'Rolling bearing'

Position (Y-coordinate)	[y]	11.40	mm
Dynamic equivalent load	[P]	0.67	kN
Equivalent load	[P_0]	0.67	kN
Life modification factor for reliability	[a_1]	1.000	
Life modification factor	[a_{ISO}]	22.373	
Nominal bearing service life	[L_{nh}]	69051.76	h
Modified bearing service life	[L_{nmh}]	> 1000000	h
Operating viscosity	[v]	12.72	mm²/s
Static safety factor	[S_0]	19.95	
Bearing reaction force	[Fx]	0.462	kN
Bearing reaction force	[Fy]	0.000	kN
Bearing reaction force	[Fz]	-0.487	kN
Bearing reaction force	[Fr]	0.672	kN (-46.5°)
Bearing reaction moment	[Mx]	0.00	Nm
Bearing reaction moment	[My]	0.00	Nm
Bearing reaction moment	[Mz]	0.00	Nm
Bearing reaction moment	[Mr]	0.00	Nm (74.05°)
Oil level	[H]	0.000	mm
Rolling moment of friction	[M_{rr}]	0.021	Nm
Sliding moment of friction	[M_{sl}]	0.003	Nm
Moment of friction, seals	[M_{seal}]	0.000	Nm
Moment of friction for seals determined according to SKF main catalog 10000/1 EN:2013			
Moment of friction flow losses	[M_{drag}]	0.000	Nm
Torque of friction	[M_{loss}]	0.024	Nm
Power loss	[P_{loss}]	34.850	W
The moment of friction is calculated according to the details in SKF Catalog 2013.			
The calculation is always performed with a coefficient for additives in the lubricant μbl=0.15.			
Displacement of bearing	[u_x]	-4.313	μm
Displacement of bearing	[u_y]	39.807	μm
Displacement of bearing	[u_z]	4.523	μm
Displacement of bearing	[u_r]	6.250	μm (133.64°)
Misalignment of bearing	[r_x]	0.046	mrad (0.16')
Misalignment of bearing	[r_y]	0.000	mrad (0')

Misalignment of bearing	[r_Z]	0.024	mrad	(0.08')
Misalignment of bearing	[r_r]	0.052	mrad	(0.18')

Damage (%) [Lreq] (5000.000)

Bin no	B1	B2
1	0.98	0.50
Σ	0.98	0.50

Utilization (%) [Lreq] (5000.000)

B1	B2
21.42	17.10

Note: Utilization = (Lreq/Lh)^(1/k)
Ball bearing: k = 3, roller bearing: k = 10/3

B1: Rolling bearing
B2: Rolling bearing

Shaft '

Shaft 1', Dokumentationspunkt Meshing point

Y position (mm)	[y]	43.90
Equivalent stress (N/mm²)	[sigV]	6.30

	X	Y	Z	R
Displacement (mm)	-0.0051	0.0604	0.0060	0.0079
Rotation (mrad)	0.0254	0.0053	0.0055	0.0260
Force (kN)	-0.1543	0.0945	0.1303	0.2020
Torque (Nm)	-13.8041	8.5262	-11.0102	17.6572

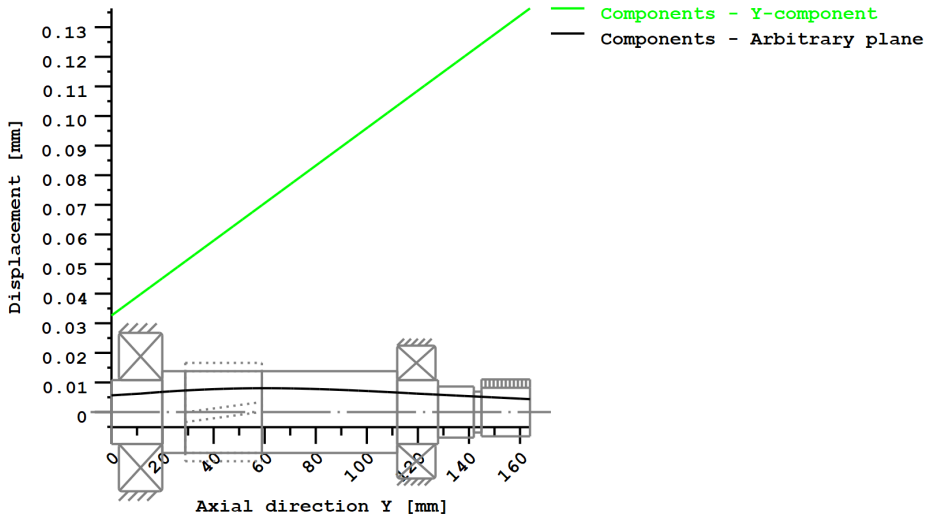

Figure: Deformation (bending etc.) (Arbitrary plane 129.0489259 121)

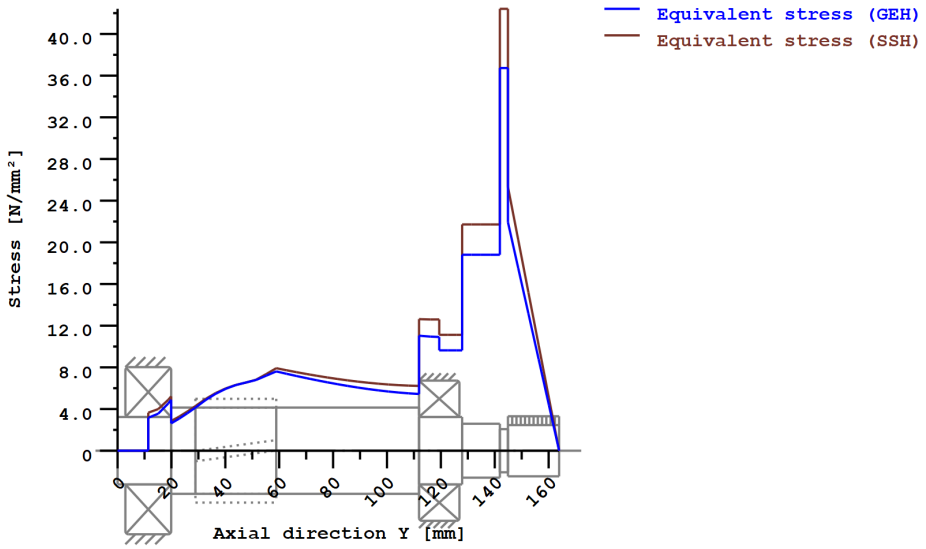

Nominal stresses, without taking into account stress concentrations
GEH(von Mises): sigV = ((sigB+sigZ,D)^2 + 3*(tauT+tauS)^2)^1/2
SSH(Tresca): sigV = ((sigB-sigZ,D)^2 + 4*(tauT+tauS)^2)^1/2

Figure: Equivalent stress

Eigenfrequencies/Critical speeds

1. Eigenfrequency:	0.00 Hz, Critical speed:	0.00 1/min	Rigid body rotation Y 'Shaft 1'
2. Eigenfrequency:	4559.70 Hz, Critical speed:	273581.98 1/min	Bending XY 'Shaft 1', Bending YZ 'Shaft 1'
3. Eigenfrequency:	7336.79 Hz, Critical speed:	440207.17 1/min	Bending XY 'Shaft 1', Bending YZ 'Shaft 1'
4. Eigenfrequency:	10674.69 Hz, Critical speed:	640481.54 1/min	Axial 'Shaft 1'
5. Eigenfrequency:	13739.13 Hz, Critical speed:	824347.98 1/min	Torsion 'Shaft 1'

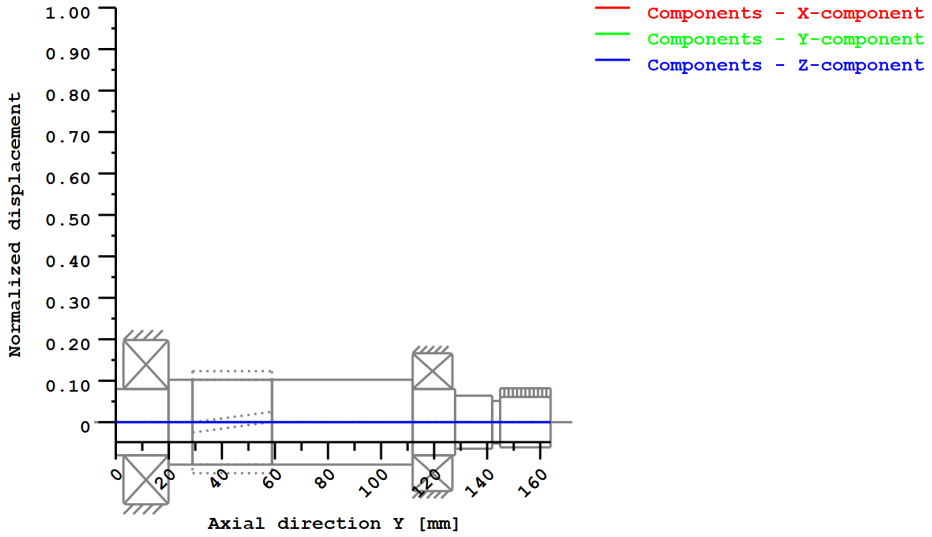

Figure: Eigenfrequencies (Normalized rotation) (Eigenfrequency: 1. (0 Hz))

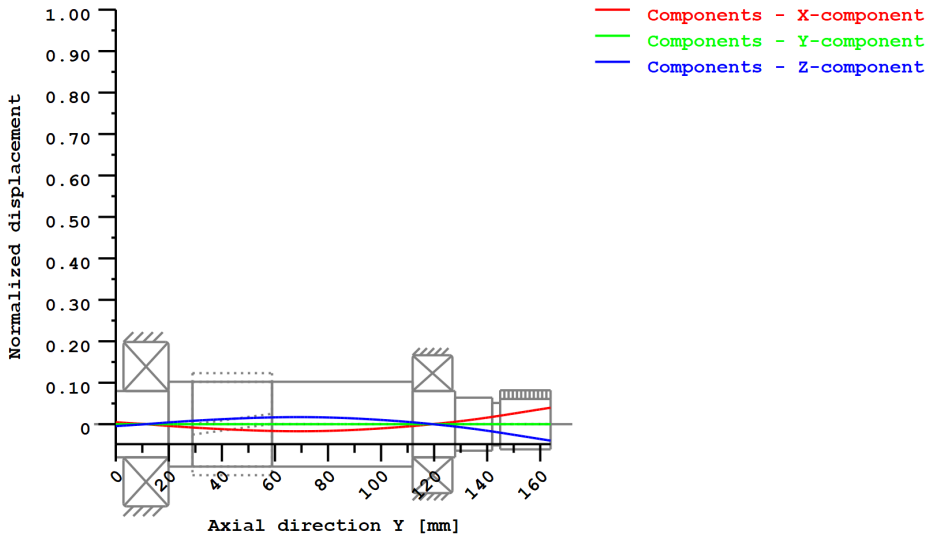

Figure: Eigenfrequencies (Normalized rotation) (Eigenfrequency: 2. (4559.7 Hz))

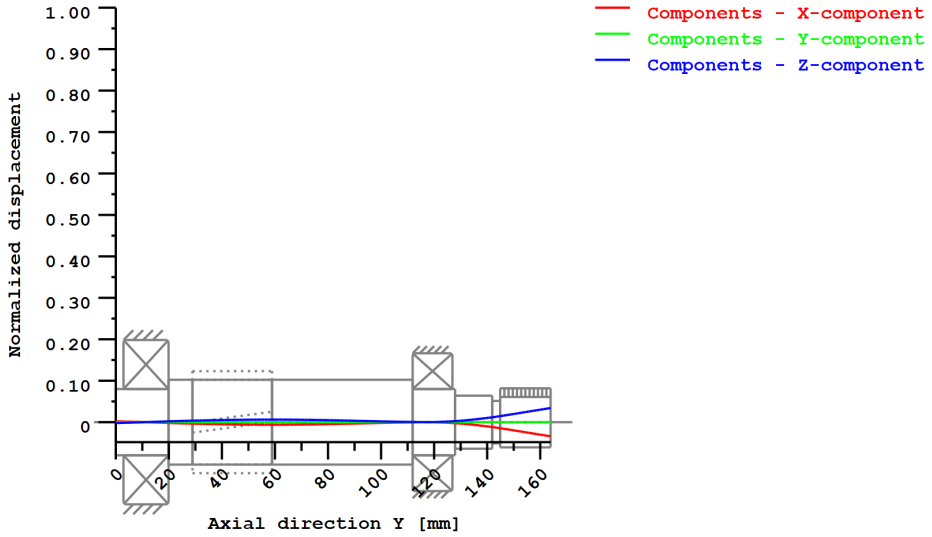

Figure: Eigenfrequencies (Normalized rotation) (Eigenfrequency: 3. (7336.79 Hz))

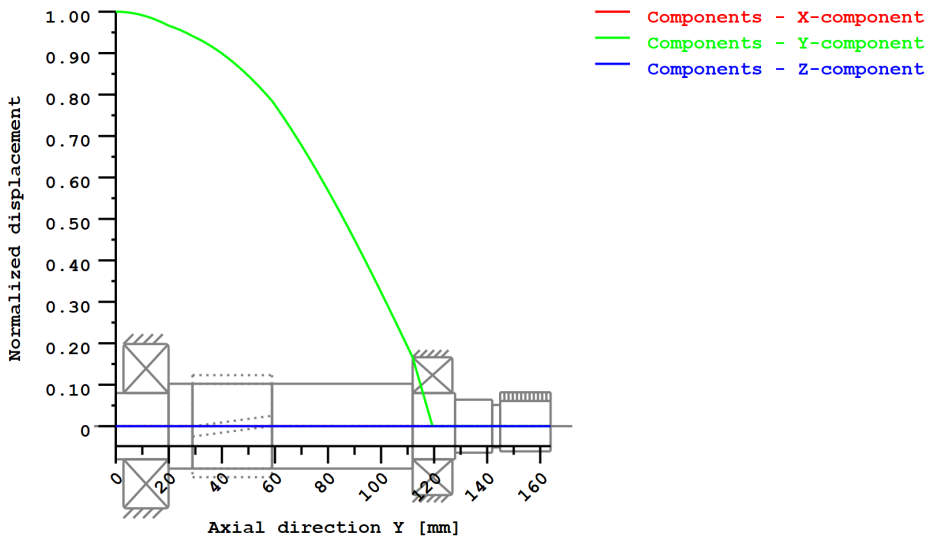

Figure: Eigenfrequencies (Normalized rotation) (Eigenfrequency: 4. (10674.69 Hz))

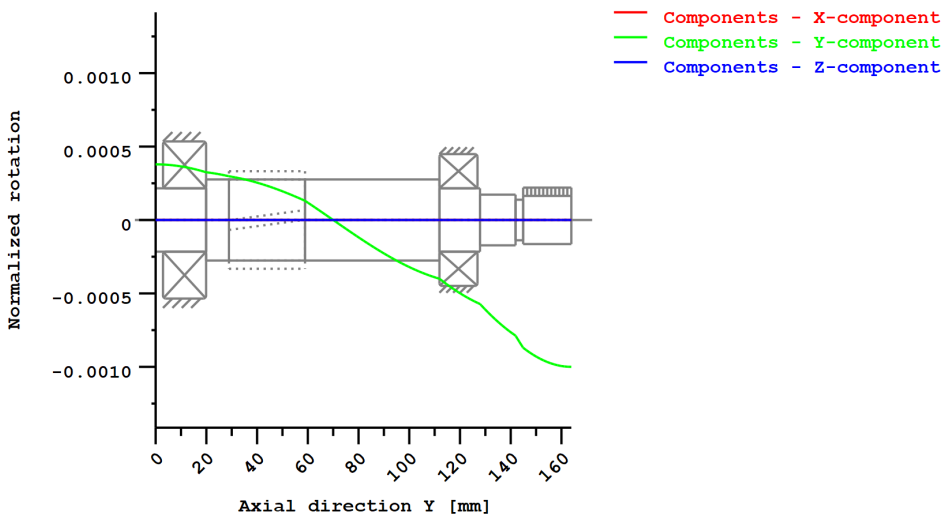

Figure: Eigenfrequencies (Normalized displacement) (Eigenfrequency: 5. (13739.13 Hz))

KISSSOFT
Calculation programs for machine design

Strength calculation according to DIN 743:2012
with finite life fatigue strength according to FKM standard and FVA draft

Summary

Shaft 1

Material	18CrNiMo7-6
Material type	Case-carburized steel
Material treatment	case-hardened
Surface treatment	No

Calculation of finite life fatigue strength and static strength

Calculation for load case 2 (σav/σmv = const)

Cross section	Position (Y-Coord) (mm)	
A-A Spline	144.91	Spline
B-B Shoulder	141.90	Shoulder
C-C Shoulder	127.90	Shoulder
E-E Smooth Shaft	131.40	Smooth shaft
F-F Shoulder with relief groove	111.90	Shoulder with relief groove

Results:

Cross section	Kfb	Kfs	K2d	SD	SS	SA
A-A Spline	1.00	1.00	0.94	23.29	15.32	78.74
B-B Shoulder	2.06	0.85	0.95	17.04	12.41	25.00
C-C Shoulder	2.25	0.85	0.93	31.27	24.24	45.46
E-E Smooth Shaft	1.00	0.85	0.93	36.85	24.24	124.54
F-F Shoulder with relief groove	1.72	0.85	0.92	47.70	43.33	108.32

Required safeties:	1.20	1.20	1.20

Abbreviations:
Kfb: Notch factor bending
Kfσ: Surface factor
K2d: size factor bending
SD: Safety endurance limit
SS: Safety against yield point
SA: Safety against incipient crack

Service life and damage

System service life (h)	[Hatt]	1000000.00
Damage to system (%)	[D]	0.00
Damage (%)	[H] (5000.0 h)	

Calculation of reliability R(t) using a Weibull distribution; t in (h):

R(t) = 100 * Exp(-((t*fac - t0)/(T - t0))^b) %

Welle	fac	b	t0	T

1	840000	1.5	7.66e+011	1.624e+012

Damage to cross sections (%)	[D]
A-A Spline:	0.00
B-B Shoulder:	0.00
C-C Shoulder:	0.00
E-E Smooth Shaft:	0.00
F-F Shoulder with relief groove:	0.00

Utilization (%) [Smin/S]

Cross section	Static	Endurance
A-A Spline	7.833	5.152
B-B Shoulder	9.668	7.044
C-C Shoulder	4.950	3.837
E-E Smooth Shaft	4.950	3.257
F-F Shoulder with relief groove	2.769	2.516

Maximum utilization (%)	[A]	9.668

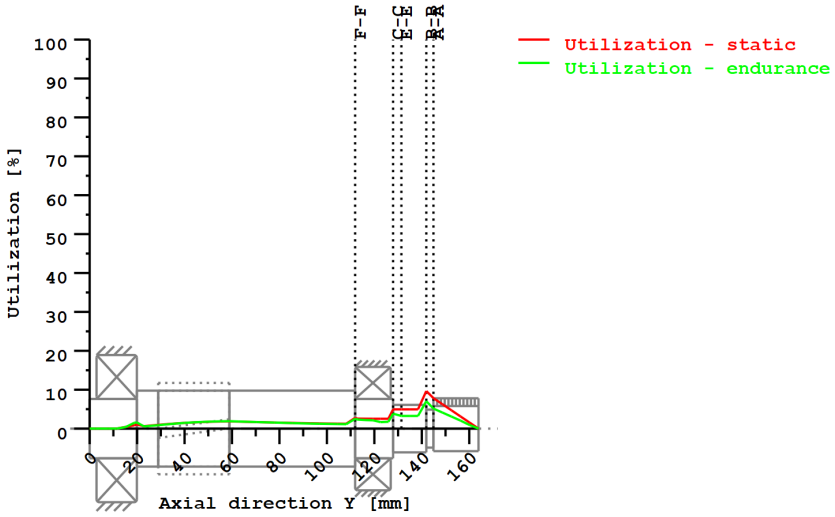

Utilization = Smin/S (%)

Figure: Strength

Calculation details

General statements

Label	Shaft 1		
Drawing			
Length (mm)		[l]	163.90
Speed (1/min)		[n]	14000.00

Material	18CrNiMo7-6
Material type	Case-carburized steel
Material treatment	case-hardened
Surface treatment	No

	Tension/Compression	Bending	Torsion	Shearing
Load factor static calculation	1.700	1.700	1.700	1.700
Load factor endurance limit	1.000	1.000	1.000	1.000

Reference diameter material (mm)	[dB]	16.00
σB according to DIN 743 (at dB) (N/mm²)	[σB]	1200.00
σS according to DIN 743 (at dB) (N/mm²)	[σS]	850.00
[σzdW] (bei dB) (N/mm²)		480.00
[σbW] (bei dB) (N/mm²)		600.00
[τtW] (bei dB) (N/mm²)		360.00
Thickness of raw material (mm)	[dWerkst]	35.00
Material data calculated according DIN743/3 with K1(d)		
Material strength calculated from size of raw material		
Geometric size factor K1d calculated from raw material diameter		
[σBeff] (N/mm²)		1093.94
[σSeff] (N/mm²)		774.87
[σbF] (N/mm²)		774.87
[τtF] (N/mm²)		447.37
[σBRand] (N/mm²)		2300.00
[σzdW] (N/mm²)		437.57

[σbW] (N/mm²)		546.97
[τtW] (N/mm²)		328.18

Fatigue strength for single stage use

Required life time	[H]	5000.00
Number of load cycles (Mio)	[NL]	4200.000

Data of S-N curve (Woehler line) analog to FKM standard:

[kσ, kτ]	15	25
[kDσ, kDτ]	0	0
[NDσ, NDτ]	1e+006	1e+006
[NDσII, NDτII]	0	0

Calculation for load case 2 (σ.av/σ.mv = const)

Cross section 'A-A Spline' Spline

Comment	Y= 144.90...163.90mm	
Position (Y-Coordinate) (mm)	[y]	144.910
External diameter (mm)	[da]	19.000
Inner diameter (mm)	[di]	0.000
Notch effect		Spline

ISO 4156:2005, DIN 5480:2005

[da, df, z, mn] (mm)	18.840	17.160	22	0.800
Mean roughness (µm)	[Rz]			8.000

		Tension/Compression	Bending	Torsion	Shearing
Load: (N) (Nm)					
Mean value	[Fzdm, Mbm, Tm, Fqm]	0.000	0.000	8.522	0.000
Amplitude	[Fzda, Mba, Ta, Fqa]	0.000	0.004	8.522	0.414
Maximum value	[Fzdmax, Mbmax, Tmax, Fqmax]	0.000	0.007	28.974	0.703
Cross section, moment of resistance: (mm²)					
[A, Wb, Wt, A]		231.273	496.080	992.160	231.273

Stresses: (N/mm²)				
[σzdm, σbm, τm, τqm] (N/mm²)	0.000	0.000	8.589	0.000
[σzda, σba, τa, τqa] (N/mm²)	0.000	0.008	8.589	0.002
[σzdmax,σbmax,τmax,τqmax] (N/mm²)	0.000	0.013	29.203	0.004

Technological size influence	[K1(σB)]	0.912	
	[K1(σS)]	0.912	

		Tension/Compression	Bending	Torsion
Notch effect coefficient	[ß(dB)]	1.000	1.000	1.000
[dB] (mm) = 29.0				
Geometrical size influence	[K3(d)]	1.000	1.000	1.000
Geometrical size influence	[K3(dB)]	1.000	1.000	1.000
Notch effect coefficient	[ß]	1.000	1.000	1.000
Geometrical size influence	[K2(d)]	1.000	0.938	0.938
Influence coefficient surface roughness	[KF]	1.000	1.000	1.000
Roughness factor is included into the notch effect coefficient				
Surface stabilization factor	[KV]	1.000	1.000	1.000
Total influence coefficient	[K]	1.000	1.066	1.066

Present safety for endurance limit:			
Equivalent mean stress (N/mm²)	[σmV]		14.877	
Equivalent mean stress (N/mm²)	[τmV]		8.589	
Fatigue limit of part (N/mm²)	[σWK]	437.574	513.025	307.815
Influence coefficient of mean stress sensitivity.				
	[ψσK]	0.250	0.306	0.164
Permissible amplitude (N/mm²)	[σADK]	0.052	0.412	223.686
Permissible amplitude (N/mm²)	[σANK]	0.052	0.412	223.686
Effective Miner sum	[DM]	0.300	0.300	0.300
Load spectrum factor	[fKoll]	1.000	1.000	1.000
Safety against fatigue	[S]		23.291	
Required safety against fatigue	[Smin]		1.200	
Result (%)	[S/Smin]		1940.9	

Present safety for proof against exceed of yield point:				
Static notch sensitivity factor	[K2F]	1.000	1.000	1.000
Increase coefficient	[γF]	1.000	1.000	1.000

KISSSOFT
Calculation programs for machine design

Yield stress of part (N/mm²)	[σFK]	774.871	774.871	447.372
Safety yield stress	[S]		15.320	
Required safety	[Smin]		1.200	
Result (%)	[S/Smin]		1276.6	

Present safety
for proof of avoiding incipient crack on hard surface layers:

Safety against incipient crack	[S]		78.742	
Required safety	[Smin]		1.200	
Result (%)	[S/Smin]		6561.8	

Cross section 'B-B Shoulder' **Shoulder**

Comment	Y= 141.90mm			
Position (Y-Coordinate) (mm)		[y]		141.900
External diameter (mm)		[da]		16.000
Inner diameter (mm)		[di]		0.000
Notch effect			Shoulder	
[D, r, t] (mm)	20.000	0.100	2.000	
Mean roughness (µm)		[Rz]		8.000

	Tension/Compression	Bending	Torsion	Shearing
Load: (N) (Nm)				
Mean value [Fzdm, Mbm, Tm, Fqm]	0.000	0.000	8.526	0.000
Amplitude [Fzda, Mba, Ta, Fqa]	0.000	0.005	8.526	0.460
Maximum value [Fzdmax, Mbmax, Tmax, Fqmax]	0.000	0.009	28.989	0.782
Cross section, moment of resistance: (mm²)				
[A, Wb, Wt, A]	201.062	402.124	804.248	201.062

Stresses: (N/mm²)				
[σzdm, σbm, τm, τqm] (N/mm²)	0.000	0.000	10.601	0.000
[σzda, σba, τa, τqa] (N/mm²)	0.000	0.013	10.601	0.003
[σzdmax,σbmax,τmax,τqmax] (N/mm²)	0.000	0.022	36.045	0.005

Technological size influence	[K1(σB)]	0.912	
	[K1(σS)]	0.912	

	Tension/Compression	Bending	Torsion
Stress concentration factor	[a]	4.631	4.081	2.551
References stress slope	[G']	24.156	24.156	11.500
Notch sensitivity factor	[n]	1.981	1.981	1.677
Notch effect coefficient	[ß]	2.338	2.060	1.522
Geometrical size influence	[K2(d)]	1.000	0.949	0.949
Influence coefficient surface roughness	[KF]	0.853	0.853	0.916
Surface stabilization factor	[KV]	1.000	1.133	1.133
Total influence coefficient	[K]	2.510	2.066	1.496

Present safety for endurance limit:

Equivalent mean stress (N/mm²)	[σmV]		18.362	
Equivalent mean stress (N/mm²)	[τmV]		10.601	
Fatigue limit of part (N/mm²)	[σWK]	174.339	264.684	219.446
Influence coefficient of mean stress sensitivity.				
	[ψσK]	0.087	0.138	0.111
Permissible amplitude (N/mm²)	[σADK]	0.042	0.550	197.435
Permissible amplitude (N/mm²)	[σANK]	0.042	0.550	197.435
Effective Miner sum	[DM]	0.300	0.300	0.300
Load spectrum factor	[fKoll]	1.000	1.000	1.000
Safety against fatigue	[S]		17.036	
Required safety against fatigue	[Smin]		1.200	
Result (%)	[S/Smin]		1419.7	

Present safety
for proof against exceed of yield point:

Static notch sensitivity factor	[K2F]	1.000	1.000	1.000
Increase coefficient	[γF]	1.000	1.000	1.000
Yield stress of part (N/mm²)	[σFK]	774.871	774.871	447.372
Safety yield stress	[S]		12.412	
Required safety	[Smin]		1.200	
Result (%)	[S/Smin]		1034.3	

Present safety
for proof of avoiding incipient crack on hard surface layers:

Safety against incipient crack	[S]	24.997
Required safety	[Smin]	1.200
Result (%)	[S/Smin]	2083.1

Cross section 'C-C Shoulder' **Shoulder**

Comment	Y= 127.90mm			
Position (Y-Coordinate) (mm)		[y]		127.900
External diameter (mm)		[da]		20.000
Inner diameter (mm)		[di]		0.000
Notch effect			Shoulder	
[D, r, t] (mm)	25.000	0.100	2.500	
Mean roughness (µm)		[Rz]		8.000

		Tension/Compression	Bending	Torsion	Shearing
Load: (N) (Nm)					
Mean value	[Fzdm, Mbm, Tm, Fqm]	0.000	0.000	8.526	0.000
Amplitude	[Fzda, Mba, Ta, Fqa]	0.000	0.014	8.526	0.798
Maximum value	[Fzdmax, Mbmax, Tmax, Fqmax]	0.000	0.024	28.989	1.356
Cross section, moment of resistance: (mm²)					
[A, Wb, Wt, A]		314.159	785.398	1570.796	314.159

Stresses: (N/mm²)					
[σzdm, σbm, τm, τqm] (N/mm²)		0.000	0.000	5.428	0.000
[σzda, σba, τa, τqa] (N/mm²)		0.000	0.018	5.428	0.003
[σzdmax,σbmax,τmax,τqmax] (N/mm²)		0.000	0.030	18.455	0.006
Technological size influence	[K1(σB)]	0.912			
	[K1(σS)]	0.912			

		Tension/Compression	Bending	Torsion
Stress concentration factor	[a]	5.065	4.451	2.738
References stress slope	[G']	24.045	24.045	11.500
Notch sensitivity factor	[n]	1.978	1.978	1.677
Notch effect coefficient	[ß]	2.560	2.250	1.633
Geometrical size influence	[K2(d)]	1.000	0.935	0.935
Influence coefficient surface roughness	[KF]	0.853	0.853	0.916
Surface stabilization factor	[KV]	1.000	1.133	1.133
Total influence coefficient	[K]	2.732	2.276	1.623

Present safety for endurance limit:				
Equivalent mean stress (N/mm²)	[σmV]		9.401	
Equivalent mean stress (N/mm²)	[τmV]		5.428	
Fatigue limit of part (N/mm²)	[σWK]	160.155	240.349	202.199
Influence coefficient of mean stress sensitivity.				
	[ψσK]	0.079	0.123	0.102
Permissible amplitude (N/mm²)	[σADK]	0.082	1.471	183.513
Permissible amplitude (N/mm²)	[σANK]	0.082	1.471	183.513
Effective Miner sum	[DM]	0.300	0.300	0.300
Load spectrum factor	[fKoll]	1.000	1.000	1.000
Safety against fatigue	[S]		31.271	
Required safety against fatigue	[Smin]		1.200	
Result (%)	[S/Smin]		2605.9	

Present safety				
for proof against exceed of yield point:				
Static notch sensitivity factor	[K2F]	1.000	1.000	1.000
Increase coefficient	[γF]	1.000	1.000	1.000
Yield stress of part (N/mm²)	[σFK]	774.871	774.871	447.372
Safety yield stress	[S]		24.241	
Required safety	[Smin]		1.200	
Result (%)	[S/Smin]		2020.1	

Present safety
for proof of avoiding incipient crack on hard surface layers:

Safety against incipient crack	[S]	45.459

KISSSOFT
Calculation programs for machine design

Required safety	[Smin]	1.200
Result (%)	[S/Smin]	3788.2

Cross section 'E-E Smooth Shaft' Smooth shaft

Comment		
Position (Y-Coordinate) (mm)	[y]	131.400
External diameter (mm)	[da]	20.000
Inner diameter (mm)	[di]	0.000
Notch effect		Smooth shaft
Mean roughness (µm)	[Rz]	8.000

	Tension/Compression	Bending	Torsion	Shearing
Load: (N) (Nm)				
Mean value [Fzdm, Mbm, Tm, Fqm]	0.000	0.000	8.526	0.000
Amplitude [Fzda, Mba, Ta, Fqa]	0.000	0.011	8.526	0.713
Maximum value [Fzdmax, Mbmax, Tmax, Fqmax]	0.000	0.019	28.989	1.213
Cross section, moment of resistance: (mm²)				
[A, Wb, Wt, A]	314.159	785.398	1570.796	314.159
Stresses: (N/mm²)				
[σzdm, σbm, τm, τqm] (N/mm²)	0.000	0.000	5.428	0.000
[σzda, σba, τa, τqa] (N/mm²)	0.000	0.015	5.428	0.003
[σzdmax,σbmax,τmax,τqmax] (N/mm²)	0.000	0.025	18.455	0.005

Technological size influence	[K1(σB)]	0.912	
	[K1(σS)]	0.912	

		Tension/Compression	Bending	Torsion
Notch effect coefficient	[ß]	1.000	1.000	1.000
Geometrical size influence	[K2(d)]	1.000	0.935	0.935
Influence coefficient surface roughness	[KF]	0.853	0.853	0.916
Surface stabilization factor	[KV]	1.000	1.133	1.133
Total influence coefficient	[K]	1.172	1.096	1.025
Present safety for endurance limit:				
Equivalent mean stress (N/mm²)	[σmV]		9.401	
Equivalent mean stress (N/mm²)	[τmV]		5.428	
Fatigue limit of part (N/mm²)	[σWK]	373.418	499.161	320.047
Influence coefficient of mean stress sensitivity.	[ψσK]	0.206	0.296	0.171
Permissible amplitude (N/mm²)	[σADK]	0.082	1.195	223.686
Permissible amplitude (N/mm²)	[σANK]	0.082	1.195	223.686
Effective Miner sum	[DM]	0.300	0.300	0.300
Load spectrum factor	[fKoll]	1.000	1.000	1.000
Safety against fatigue	[S]		36.848	
Required safety against fatigue	[Smin]		1.200	
Result (%)	[S/Smin]		3070.7	
Present safety for proof against exceed of yield point:				
Static notch sensitivity factor	[K2F]	1.000	1.000	1.000
Increase coefficient	[γF]	1.000	1.000	1.000
Yield stress of part (N/mm²)	[σFK]	774.871	774.871	447.372
Safety yield stress	[S]		24.241	
Required safety	[Smin]		1.200	
Result (%)	[S/Smin]		2020.1	
Present safety for proof of avoiding incipient crack on hard surface layers:				
Safety against incipient crack	[S]		124.545	
Required safety	[Smin]		1.200	
Result (%)	[S/Smin]		10378.7	

Cross section 'F-F Shoulder with relief groove' Shoulder with relief groove

Comment	Y= 111.90mm	

Position (Y-Coordinate) (mm)		[y]		111.900		
External diameter (mm)		[da]		25.000		
Inner diameter (mm)		[di]		0.000		
Notch effect			Shoulder with relief groove			
[D, d, D1, r, t1] (mm)	32.000	24.400	25.000	0.800	Qu[5].Geo.t	
Shape B						
Mean roughness (µm)		[Rz]		8.000		

		Tension/Compression	Bending	Torsion	Shearing
Load: (N) (Nm)					
Mean value	[Fzdm, Mbm, Tm, Fqm]	94.404	0.000	8.526	0.000
Amplitude	[Fzda, Mba, Ta, Fqa]	94.404	2.059	8.526	272.216
Maximum value	[Fzdmax, Mbmax, Tmax, Fqmax]		320.974	3.500	28.989	462.768
Cross section, moment of resistance: (mm²)					
[A, Wb, Wt, A]		467.595	1426.164	2852.327	467.595

Stresses: (N/mm²)				
[σzdm, σbm, τm, τqm] (N/mm²)	0.202	0.000	2.989	0.000
[σzda, σba, τa, τqa] (N/mm²)	0.202	1.444	2.989	0.776
[σzdmax,σbmax,τmax,τqmax] (N/mm²)	0.686	2.454	10.163	1.320

Technological size influence	[K1(σB)]	0.912
	[K1(σS)]	0.912

		Tension/Compression	Bending	Torsion
Stress concentration factor	[a]	2.599	2.332	1.680
References stress slope	[G']	3.143	3.143	1.437
Notch sensitivity factor	[n]	1.354	1.354	1.239
Notch effect coefficient	[ß]	1.920	1.722	1.355
Geometrical size influence	[K2(d)]	1.000	0.920	0.920
Influence coefficient surface roughness	[KF]	0.853	0.853	0.916
Surface stabilization factor	[KV]	1.000	1.133	1.133
Total influence coefficient	[K]	2.092	1.804	1.382
Present safety for endurance limit:				
Equivalent mean stress (N/mm²)	[σmV]		5.181	
Equivalent mean stress (N/mm²)	[τmV]		2.991	
Fatigue limit of part (N/mm²)	[σWK]	209.200	303.151	237.505
Influence coefficient of mean stress sensitivity.				
	[ψσK]	0.106	0.161	0.122
Permissible amplitude (N/mm²)	[σADK]	29.061	168.865	211.705
Permissible amplitude (N/mm²)	[σANK]	29.061	168.865	211.705
Effective Miner sum	[DM]	0.300	0.300	0.300
Load spectrum factor	[fKoll]	1.000	1.000	1.000
Safety against fatigue	[S]		47.699	
Required safety against fatigue	[Smin]		1.200	
Result (%)	[S/Smin]		3974.9	
Present safety for proof against exceed of yield point:				
Static notch sensitivity factor	[K2F]	1.000	1.000	1.000
Increase coefficient	[γF]	1.000	1.000	1.000
Yield stress of part (N/mm²)	[σFK]	774.871	774.871	447.372
Safety yield stress	[S]		43.334	
Required safety	[Smin]		1.200	
Result (%)	[S/Smin]		3611.2	
Present safety for proof of avoiding incipient crack on hard surface layers:				
Safety against incipient crack	[S]		108.321	
Required safety	[Smin]		1.200	
Result (%)	[S/Smin]		9026.8	

Remarks:
- The shearing force is not considered in the analysis specified in DIN 743.
- Cross section with interference fit:
  The notching factor for the light fit case is no longer defined in DIN 743.
  The values are imported from the FKM-Guideline..

KISSSOFT
Calculation programs for machine design

End of Report	lines:	852

File

Name : shaftASpeed
Changed by: Carlos Rodrigues on: 02.07.2018 at: 23:23:09

THERMALLY SAFE OPERATING SPEED CALCULATION
(according to DIN ISO 15312 and DIN 732)

Lubricant	Castrol ATF Dex II Multivehicle		
Lubrication type:			
Oil-groove lubrication			
Mean bearing temperature	[T_m]	85.000	°C
Temperature of bearing environment	[T_u]	75.000	°C
Lubricant - service temperature	[T_B]	75.000	°C
Lubricant temperature - Reference conditions	[T_{ref}]	70.000	°C

Shaft 'Shaft 1', Rolling bearing 'Rolling bearing':

Thermal nominal speed according to DIN ISO 15312:

Type of support	Deep groove ball bearing (single row)		
Bearing number	SKF 6205 ETN9		
Design series	62		
Speed	[n]	14000.000	1/min
Coefficient	[f_{0r}]	2.000	
(Depends upon type of design and lubrication at reference conditions)			
Coefficient	[f_{1r}]	0.000200	
(Depends upon type of design and load at reference conditions)			
Heat sink reference surface	[A_s]	3628.540	mm²
Reference load	[P_{1r}]	0.465	kN
Bearing mean diameter	[d_m]	38.500	mm
Bearing-specific reference heat flow density	[q_r]	16.000	kW/m²
kinematic viscosity (for reference conditions)	[v_r]	12.000	mm²/s
Thermal nominal speed	[$n_{\theta r}$]	15140.793	1/min

Thermally safe operating speed according to DIN 732:

Coefficient	[f_0]	2.000	
(Depends upon type of design and lubrication)			
Coefficient	[f_1]	0.000154	
(Depends upon type of design and load)			
Temperature difference	[$\Delta\theta=\theta_o-\theta_i$]	10.000	°C
Lubricant Oil-volume	[V_L]	0.300	l/min
Heat flow (dissipated by the lubricant)	[Φ_L]	0.086	kW
Heat flow (dissipated by the bearing support surface)	[Φ_S]	0.011	kW
Total heat flow	[Φ]	0.097	kW
Dynamic equivalent load	[P_1]	595.960	N
kinematic viscosity at service temperature	[v]	12.724	mm²/s
Lubricant film parameter	[K_L]	0.624	
Charge parameter	[K_P]	0.058	
Speed ratio	[f_n]	1.274	
Thermally safe operating speed	[n_θ]	19295.640	1/min

Shaft 'Shaft 1', Rolling bearing 'Rolling bearing':

Thermal nominal speed according to DIN ISO 15312:

Type of support		Deep groove ball bearing (single row)		
Bearing number		SKF 6305 ETN9		
Design series		63		
Speed	[n]	14000.000	1/min	
Coefficient	[f_{0r}]		2.300	
(Depends upon type of design and lubrication at reference conditions)				
Coefficient	[f_{1r}]		0.000200	
(Depends upon type of design and load at reference conditions)				
Heat sink reference surface	[A_S]		4646.416	mm²
Reference load	[P_{1r}]		0.670	kN
Bearing mean diameter	[d_m]		43.500	mm
Bearing-specific reference heat flow density	[q_r]		16.000	kW/m²
kinematic viscosity (for reference conditions)	[v_r]		12.000	mm²/s
Thermal nominal speed	[$n_{\theta r}$]		12963.076	1/min

Thermally safe operating speed according to DIN 732:

Coefficient	[f_0]	2.300	
(Depends upon type of design and lubrication)			
Coefficient	[f_1]	0.000201	
(Depends upon type of design and load)			
Temperature difference	[$\Delta\theta=\theta_o-\theta_i$]	10.000	°C
Lubricant Oil-volume	[V_L]	0.300	l/min
Heat flow (dissipated by the lubricant)	[Φ_L]	0.086	kW
Heat flow (dissipated by the bearing support surface)	[Φ_S]	0.014	kW
Total heat flow	[Φ]	0.100	kW
Dynamic equivalent load	[P_1]	671.669	N
kinematic viscosity at service temperature	[v]	12.724	mm²/s
Lubricant film parameter	[K_L]	0.773	
Charge parameter	[K_P]	0.080	
Speed ratio	[f_n]	1.099	
Thermally safe operating speed	[n_θ]	14241.661	1/min

The reference conditions for calculating the thermal nominal speed are taken from the DIN ISO 15312 standard.

End of Report lines: 96

Analysis of shafts, axle and beams

Input data

Coordinate system shaft: see picture W-002

Label		Shaft 1
Drawing		
Initial position (mm)		0.000
Length (mm)		145.550
Speed (1/min)		3556.80
Sense of rotation: counter clockwise		
Material		18CrNiMo7-6
Young's modulus (N/mm²)		206000.000
Poisson's ratio nu		0.300
Density (kg/m³)		7830.000
Coefficient of thermal expansion	(10^-6/K)	11.500
Temperature (°C)		75.000
Weight of shaft (kg)		1.552
(Notice: Weight stands for the shaft only without considering the gears)		
Weight of shaft, including additional masses (kg)		3.233
Mass moment of inertia (kg*mm²)		2451.291
Momentum of mass GD2 (Nm²)		0.096
Position in space (°)		0.000
Gears mounted with stiffness according to ISO		
Consider deformations due to shearing		
Shear correction coefficient		1.100
Contact angle of rolling bearings is considered		
Tolerance field: Mean value		
Housing material		G-AlSi10Mg
Coefficient of thermal expansion	(10^-6/K)	22.000
Temperature of housing (°C)		65.000
Thermal housing reference point (mm)		0.000
Reference temperature (°C)		20.000

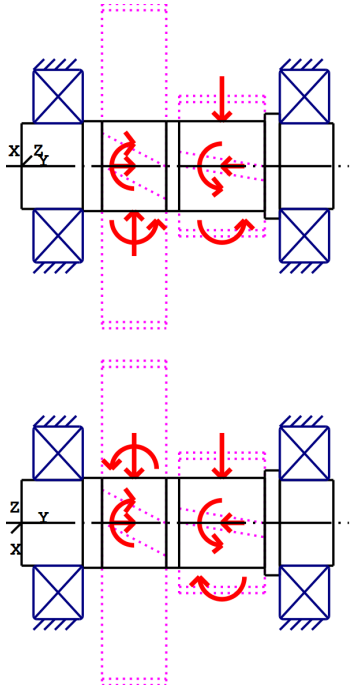

Figure: Load applications

Shaft definition (Shaft 1)

Outer contour

Cylinder (Cylinder)			0.000mm ... 28.550mm
Diameter (mm)	[d]	40.0000	
Length (mm)	[l]	28.5500	
Surface roughness (µm)	[Rz]	4.8000	

Relief groove right (Relief groove right)
r=0.80 (mm), t=0.30 (mm), l=2.50 (mm), Rz=8.0, Turned (Ra=3.2µm/125µin)
Form E (DIN 509), Series 1, with the usual stressing

Chamfer left (Chamfer left)
l=0.80 (mm), alpha=45.00 (°)

Square groove (Square groove)
b=1.85 (mm), t=1.25 (mm), r=0.01 (mm), Rz=8.0, Turned (Ra=3.2µm/125µin)

Cylinder (Cylinder)			28.550mm ... 113.550mm
Diameter (mm)	[d]	42.0000	
Length (mm)	[l]	85.0000	
Surface roughness (µm)	[Rz]	4.8000	

Key way (Key way) 38.550mm ... 66.550mm
l=28.00 (mm), i=1, Rz=8.0, Turned (Ra=3.2µm/125µin)

Radius right (Radius right)

r=0.10 (mm), Rz=8.0, Turned (Ra=3.2µm/125µin)

Cylinder (Cylinder)			113.550mm ...	120.550mm
Diameter (mm)	[d]	49.0000		
Length (mm)	[l]	7.0000		
Surface roughness (µm)	[Rz]	8.0000		

Cylinder (Cylinder)			120.550mm ...	145.550mm
Diameter (mm)	[d]	40.0000		
Length (mm)	[l]	25.0000		
Surface roughness (µm)	[Rz]	4.8000		

Relief groove left (Relief groove left)
r=0.80 (mm), t=0.30 (mm), l=2.50 (mm), Rz=8.0, Turned (Ra=3.2µm/125µin)
Form E (DIN 509), Series 1, with the usual stressing

Chamfer right (Chamfer right)
l=0.80 (mm), alpha=45.00 (°)

Forces

Type of force element		**Cylindrical gear**
Label in the model		Cylindrical gear
Position on shaft (mm)	[y_{local}]	52.5500
Position in global system (mm)	[y_{global}]	52.5500
Operating pitch diameter (mm)		151.5086
Helix angle (°)		12.0156 right
Working pressure angle at normal section (°)		20.2001
Position of contact (°)		200.0000
Length of load application (mm)		30.0000
Power (kW)		25.0000 driven (input)
Torque (Nm)		-67.1200
Axial force (N)		188.5815
Shearing force X (N)		616.2330
Shearing force Z (N)		-718.5946
Bending moment X (Nm)		4.8861
Bending moment Z (Nm)		-13.4243

Type of force element		**Cylindrical gear**
Label in the model		Cylindrical gear
Position on shaft (mm)	[y_{local}]	93.5500
Position in global system (mm)	[y_{global}]	93.5500
Operating pitch diameter (mm)		65.6436
Helix angle (°)		12.0839 right
Working pressure angle at normal section (°)		21.0503
Position of contact (°)		-25.0000
Length of load application (mm)		40.0000
Power (kW)		25.0000 driving (output)
Torque (Nm)		67.1200
Axial force (N)		-437.8049
Shearing force X (N)		-1593.7273
Shearing force Z (N)		-1513.2223
Bending moment X (Nm)		-6.0728
Bending moment Z (Nm)		-13.0232

KISSSOFT
Calculation programs for machine design

Bearing

Label in the model		Rolling bearing
Bearing type		SKF 6308
Bearing type		Deep groove ball bearing (single row)
		SKF Explorer
Bearing position (mm)	[y_{lokal}]	17.050
Bearing position (mm)	[y_{global}]	17.050
Attachment of external ring		Free bearing
Inner diameter (mm)	[d]	40.000
External diameter (mm)	[D]	90.000
Width (mm)	[b]	23.000
Corner radius (mm)	[r]	1.500
Basic static load rating (kN)	[C_0]	24.000
Basic dynamic load rating (kN)	[C]	42.300
Fatigue load rating (kN)	[C_u]	1.000
Values for approximated geometry:		
Basic dynamic load rating (kN)	[C_{theo}]	0.000
Basic static load rating (kN)	[C_{0theo}]	0.000

Label in the model		Rolling bearing
Bearing type		SKF 6308
Bearing type		Deep groove ball bearing (single row)
		SKF Explorer
Bearing position (mm)	[y_{lokal}]	132.050
Bearing position (mm)	[y_{global}]	132.050
Attachment of external ring		Fixed bearing
Inner diameter (mm)	[d]	40.000
External diameter (mm)	[D]	90.000
Width (mm)	[b]	23.000
Corner radius (mm)	[r]	1.500
Basic static load rating (kN)	[C_0]	24.000
Basic dynamic load rating (kN)	[C]	42.300
Fatigue load rating (kN)	[C_u]	1.000
Values for approximated geometry:		
Basic dynamic load rating (kN)	[C_{theo}]	0.000
Basic static load rating (kN)	[C_{0theo}]	0.000

Shaft 'Shaft 1': Cylindrical gear 'Cylindrical gear' (y= 52.5500 (mm)) is taken into account as component of the shaft.
EI (y= 37.5500 (mm)): 31465.4742 (Nm²), EI (y= 67.5500 (mm)): 31465.4742 (Nm²), m (yS= 52.5500 (mm)): 1.4016 (kg)
Jp: 0.0019 (kg*m²), Jxx: 0.0011 (kg*m²), Jzz: 0.0011 (kg*m²)

Shaft 'Shaft 1': Cylindrical gear 'Cylindrical gear' (y= 93.5500 (mm)) is taken into account as component of the shaft.
EI (y= 73.5500 (mm)): 31465.4742 (Nm²), EI (y= 113.5500 (mm)): 31465.4742 (Nm²), m (yS= 93.5500 (mm)): 0.2786 (kg)
Jp: 0.0002 (kg*m²), Jxx: 0.0001 (kg*m²), Jzz: 0.0001 (kg*m²)

Results

Shaft

Maximum deflection (µm)	7.506
Position of the maximum (mm)	80.217
Mass center of gravity (mm)	73.663
Total axial load (N)	-249.223
Torsion under torque (°)	0.002

Bearing

Probability of failure	[n]	10.00	%
Axial clearance	[u_A]	10.00	µm
Lubricant	Castrol ATF Dex II Multivehicle		
Lubricant with additive, effect on bearing lifetime confirmed in tests.			
Oil lubrication, off-line/no filtration, ISO4406 -/15/12			
Lubricant - service temperature	[T_B]	75.00	°C
Limit for factor aISO	[a_{ISOmax}]	50.00	
Oil level	[h_{oil}]	-54.94	mm
Oil bath lubrication			

Rolling bearings, classical calculation (contact angle considered)

Shaft 'Shaft 1' Rolling bearing 'Rolling bearing'

Position (Y-coordinate)	[y]	17.05	mm
Dynamic equivalent load	[P]	1.07	kN
Equivalent load	[P_0]	1.07	kN
Life modification factor for reliability	[a_1]	1.000	
Life modification factor	[a_{ISO}]	15.043	
Nominal bearing service life	[L_{nh}]	292752.00	h
Modified bearing service life	[L_{nmh}]	> 1000000	h
Operating viscosity	[v]	13.11	mm²/s
Static safety factor	[S_0]	22.51	
Bearing reaction force	[Fx]	0.338	kN
Bearing reaction force	[Fy]	0.000	kN
Bearing reaction force	[Fz]	1.011	kN
Bearing reaction force	[Fr]	1.066	kN (71.54°)
Bearing reaction moment	[Mx]	0.00	Nm
Bearing reaction moment	[My]	0.00	Nm
Bearing reaction moment	[Mz]	0.00	Nm
Bearing reaction moment	[Mr]	0.00	Nm (19.86°)
Oil level	[H]	0.000	mm
Rolling moment of friction	[M_{rr}]	0.033	Nm
Sliding moment of friction	[M_{sl}]	0.005	Nm
Moment of friction, seals	[M_{seal}]	0.000	Nm
Moment of friction for seals determined according to SKF main catalog 10000/1 EN:2013			
Moment of friction flow losses	[M_{drag}]	0.000	Nm
Torque of friction	[M_{loss}]	0.038	Nm
Power loss	[P_{loss}]	14.173	W
The moment of friction is calculated according to the details in SKF Catalog 2013.			
The calculation is always performed with a coefficient for additives in the lubricant µbl=0.15.			
Displacement of bearing	[u_x]	-2.073	µm
Displacement of bearing	[u_y]	47.980	µm
Displacement of bearing	[u_z]	-6.161	µm

Displacement of bearing	[u_r]	6.500	µm (-108.6°)
Misalignment of bearing	[r_x]	-0.014	mrad (-0.05')
Misalignment of bearing	[r_y]	0.000	mrad (0')
Misalignment of bearing	[r_z]	0.014	mrad (0.05')
Misalignment of bearing	[r_r]	0.020	mrad (0.07')

Shaft 'Shaft 1' Rolling bearing 'Rolling bearing'

Position (Y-coordinate)	[y]	132.05	mm
Dynamic equivalent load	[P]	1.41	kN
Equivalent load	[P_0]	1.41	kN
Life modification factor for reliability[a_1]		1.000	
Life modification factor	[a_{ISO}]	8.521	
Nominal bearing service life	[L_{nh}]	127515.66	h
Modified bearing service life	[L_{nmh}]	> 1000000	h
Operating viscosity	[v]	13.11	mm²/s
Static safety factor	[S_0]	17.07	
Bearing reaction force	[Fx]	0.640	kN
Bearing reaction force	[Fy]	0.250	kN
Bearing reaction force	[Fz]	1.252	kN
Bearing reaction force	[Fr]	1.406	kN (62.93°)
Bearing reaction moment	[Mx]	-0.00	Nm
Bearing reaction moment	[My]	0.00	Nm
Bearing reaction moment	[Mz]	0.00	Nm
Bearing reaction moment	[Mr]	0.00	Nm (180°)
Oil level	[H]	0.000	mm
Rolling moment of friction	[M_{rr}]	0.070	Nm
Sliding moment of friction	[M_{sl}]	0.015	Nm
Moment of friction, seals	[M_{seal}]	0.000	Nm

Moment of friction for seals determined according to SKF main catalog 10000/1 EN:2013

Moment of friction flow losses	[M_{drag}]	0.000	Nm
Torque of friction	[M_{loss}]	0.085	Nm
Power loss	[P_{loss}]	31.608	W

The moment of friction is calculated according to the details in SKF Catalog 2013.
The calculation is always performed with a coefficient for additives in the lubricant µbl=0.15.

Displacement of bearing	[u_x]	-2.958	µm
Displacement of bearing	[u_y]	120.730	µm
Displacement of bearing	[u_z]	-5.788	µm
Displacement of bearing	[u_r]	6.500	µm (-117.07°)
Misalignment of bearing	[r_x]	0.023	mrad (0.08')
Misalignment of bearing	[r_y]	0.039	mrad (0.13')
Misalignment of bearing	[r_z]	-0.004	mrad (-0.01')
Misalignment of bearing	[r_r]	0.023	mrad (0.08')

Damage (%) [Lreq] (5000.000)

Bin no	B1	B2
1	0.50	0.50
Σ	0.50	0.50

Utilization (%) [Lreq] (5000.000)

B1	B2
17.10	17.10

Note: Utilization = (Lreq/Lh)^(1/k)
Ball bearing: k = 3, roller bearing: k = 10/3

B1: Rolling bearing
B2: Rolling bearing

Shaft '

Shaft 1', Dokumentationspunkt Meshing point Z2

Y position (mm)	[y]	52.55
Equivalent stress (N/mm²)	[sigV]	7.05

	X	Y	Z	R
Displacement (mm)	-0.0026	0.0704	-0.0067	0.0072
Rotation (mrad)	-0.0066	0.0004	0.0119	0.0136
Force (kN)	-0.6457	-0.0936	-0.6398	0.9090
Torque (Nm)	30.5687	33.5600	-7.5775	31.4939

Shaft '

Shaft 1', Dokumentationspunkt Meshing point Z3

Y position (mm)	[y]	93.55
Equivalent stress (N/mm²)	[sigV]	7.78

	X	Y	Z	R
Displacement (mm)	-0.0031	0.0964	-0.0068	0.0074
Rotation (mrad)	0.0098	0.0335	0.0035	0.0104
Force (kN)	-0.1569	0.0310	0.4888	0.5133
Torque (Nm)	37.4563	33.5600	-23.1801	44.0488

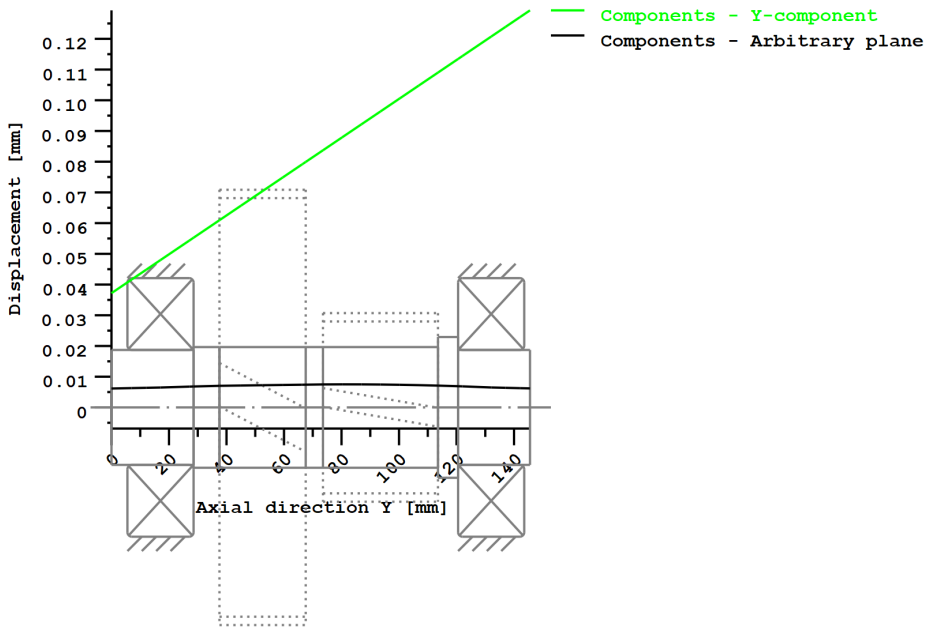

Figure: Deformation (bending etc.) (Arbitrary plane 246.2853138 121)

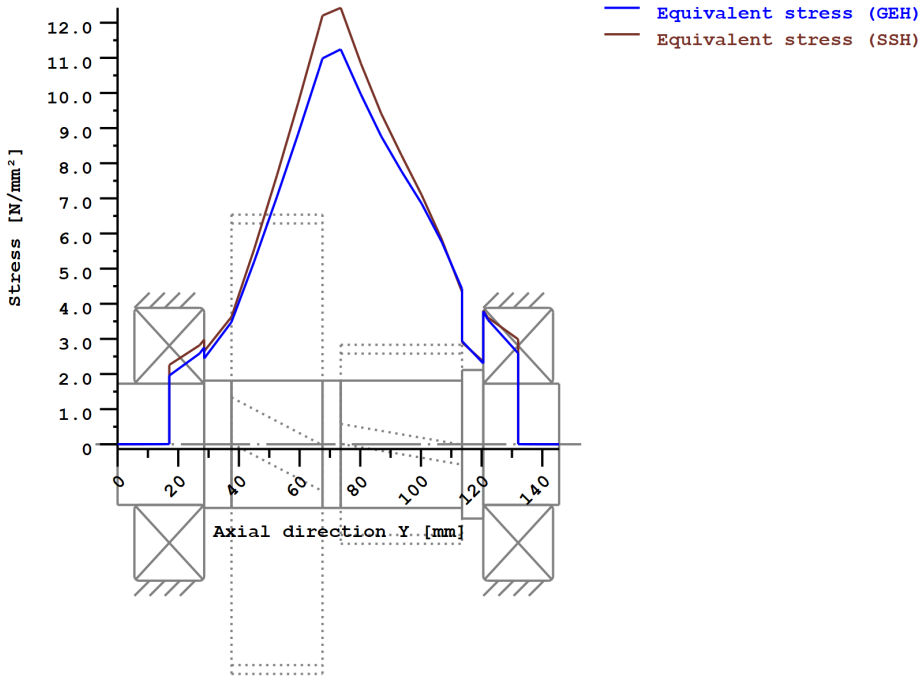

Nominal stresses, without taking into account stress concentrations
GEH(von Mises): sigV = ((sigB+sigZ,D)^2 + 3*(tauT+tauS)^2)^1/2
SSH(Tresca): sigV = ((sigB-sigZ,D)^2 + 4*(tauT+tauS)^2)^1/2

Figure: Equivalent stress

Eigenfrequencies/Critical speeds

1. Eigenfrequency:	0.00 Hz, Critical speed:	0.00 1/min	Rigid body rotation Y 'Shaft 1'
2. Eigenfrequency:	5024.56 Hz, Critical speed:	301473.36 1/min	Bending XY 'Shaft 1', Bending YZ 'Shaft 1'
3. Eigenfrequency:	7620.02 Hz, Critical speed:	457200.98 1/min	Bending XY 'Shaft 1'
4. Eigenfrequency:	12087.28 Hz, Critical speed:	725236.56 1/min	Bending XY 'Shaft 1'
5. Eigenfrequency:	12150.11 Hz, Critical speed:	729006.89 1/min	Torsion 'Shaft 1'

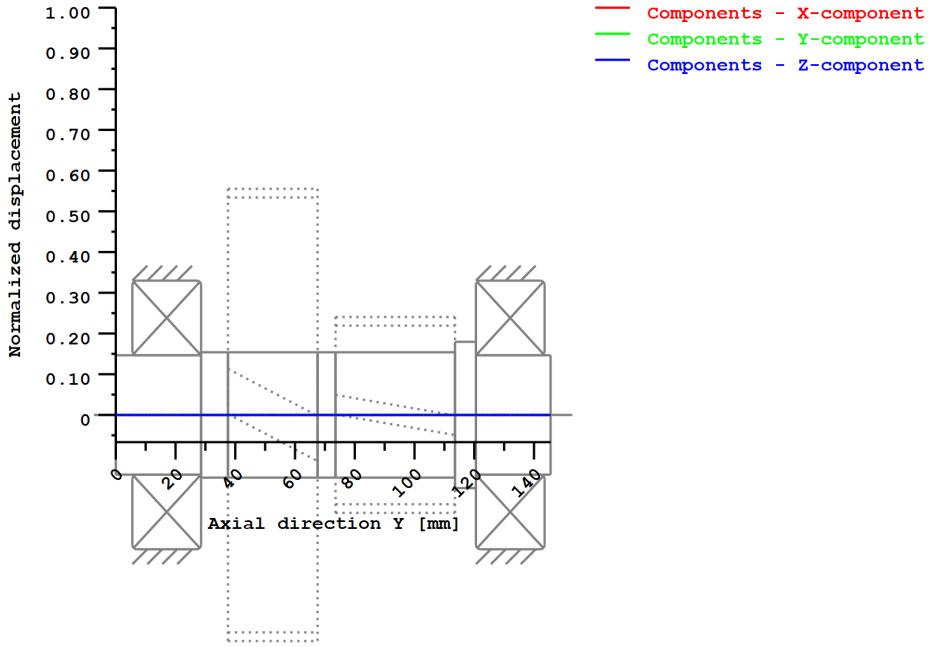

Figure: Eigenfrequencies (Normalized rotation) (Eigenfrequency: 1. (0 Hz))

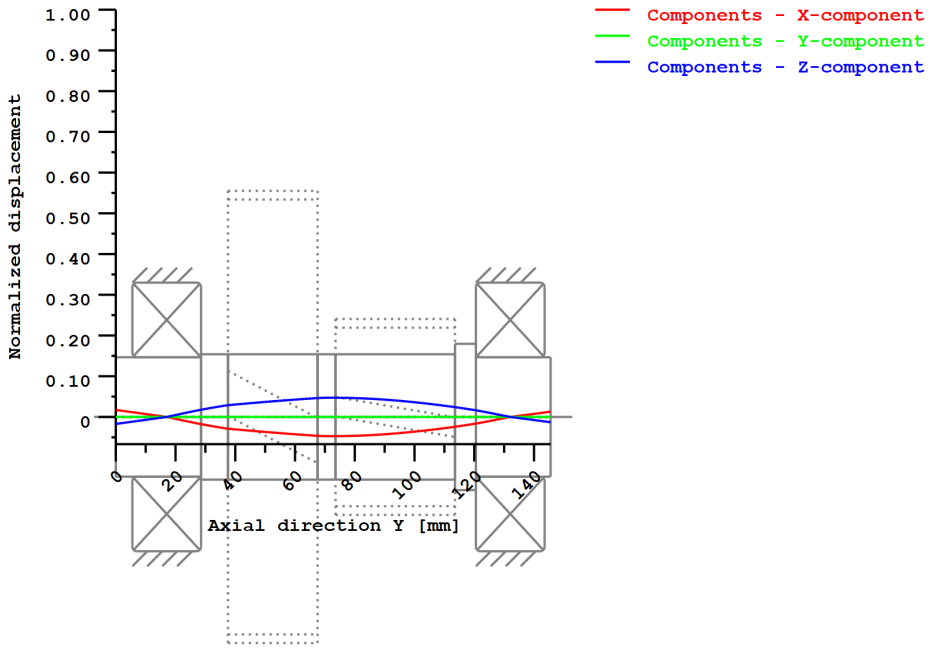

Figure: Eigenfrequencies (Normalized rotation) (Eigenfrequency: 2. (5024.56 Hz))

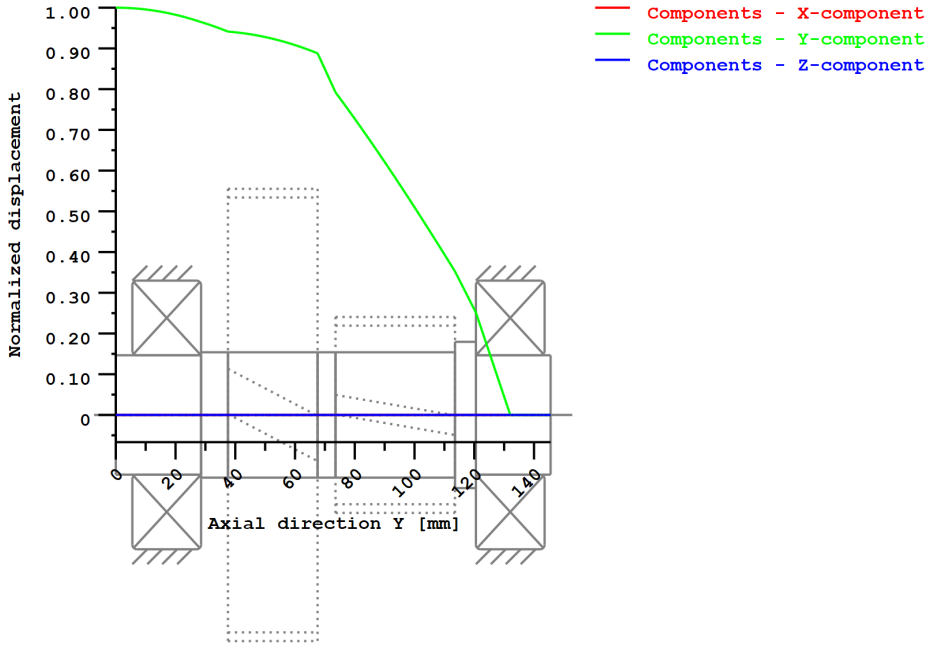

Figure: Eigenfrequencies (Normalized rotation) (Eigenfrequency: 3. (7620.02 Hz))

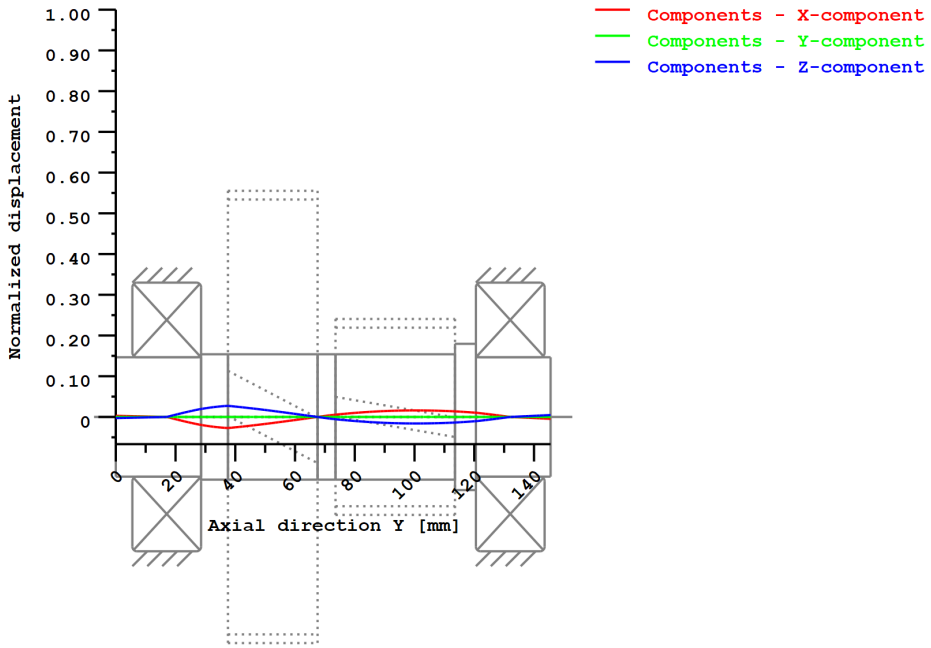

Figure: Eigenfrequencies (Normalized rotation) (Eigenfrequency: 4. (12087.28 Hz))

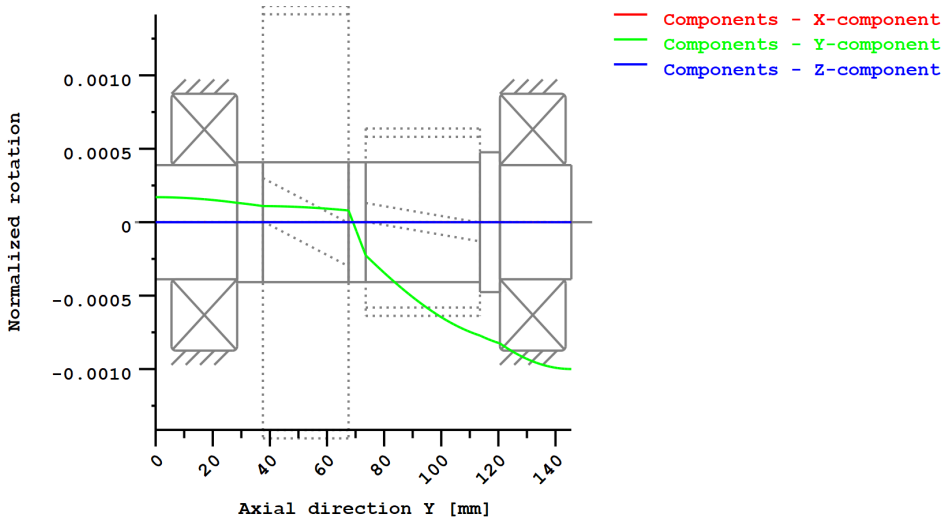

Figure: Eigenfrequencies (Normalized displacement) (Eigenfrequency: 5. (12150.11 Hz))

KISSSOFT
Calculation programs for machine design

Strength calculation according to DIN 743:2012
with finite life fatigue strength according to FKM standard and FVA draft

Summary

Shaft 1

Material	18CrNiMo7-6
Material type	Case-carburized steel
Material treatment	case-hardened
Surface treatment	No

Calculation of finite life fatigue strength and static strength

Calculation for load case 2 (σav/σmv = const)

Cross section	Position (Y-Coord) (mm)	
A-A Key way	66.54	Key
B-B Smooth shaft	73.55	Smooth shaft
C-C Shoulder	113.55	Shoulder

Results:

Cross section	Kfb	Kfs	K2d	SD	SS	SA
A-A Key way	3.05	1.00	0.88	22.82	47.49	72.24
B-B Smooth shaft	1.00	0.89	0.88	42.43	44.89	166.48
C-C Shoulder	2.88	0.86	0.88	42.71	116.14	63.10
Required safeties:				1.20	1.20	1.20

Abbreviations:
Kfb: Notch factor bending
Kfσ: Surface factor
K2d: size factor bending
SD: Safety endurance limit
SS: Safety against yield point
SA: Safety against incipient crack

Service life and damage

System service life (h)	[Hatt]	1000000.00
Damage to system (%)	[D]	0.00
Damage (%)	[H] (5000.0 h)	

Calculation of reliability R(t) using a Weibull distribution; t in (h):

R(t) = 100 * Exp(-((t*fac - t0)/(T - t0))^b) %

Welle	fac	b	t0	T
1	213408	1.5	1.946e+011	4.127e+011

Damage to cross sections (%)	[D]
A-A Key way:	0.00
B-B Smooth shaft:	0.00

C-C Shoulder: 0.00

Utilization (%) [Smin/S]

Cross section	Static	Endurance
A-A Key way	2.527	5.259
B-B Smooth shaft	2.673	2.828
C-C Shoulder	1.902	2.809

Maximum utilization (%) [A] 5.259

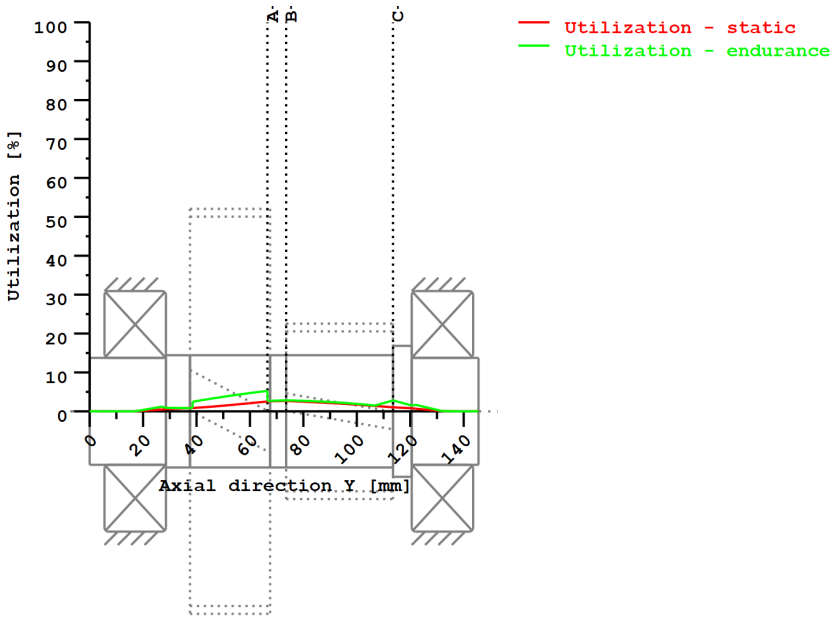

Utilization = Smin/S (%)

Figure: Strength

Calculation details

General statements

Label	Shaft 1		
Drawing			
Length (mm)	[l]	145.55	
Speed (1/min)	[n]	3556.80	
Material	18CrNiMo7-6		
Material type	Case-carburized steel		
Material treatment	case-hardened		
Surface treatment	No		

	Tension/Compression	Bending	Torsion	Shearing
Load factor static calculation	1.700	1.700	1.700	1.700
Load factor endurance limit	1.000	1.000	1.000	1.000

Reference diameter material (mm)	[dB]	16.00
σB according to DIN 743 (at dB) (N/mm²)	[σB]	1200.00
σS according to DIN 743 (at dB) (N/mm²)	[σS]	850.00
[σzdW] (bei dB) (N/mm²)		480.00
[σbW] (bei dB) (N/mm²)		600.00
[τtW] (bei dB) (N/mm²)		360.00
Thickness of raw material (mm)	[dWerkst]	50.00
Material data calculated according DIN743/3 with K1(d)		
Material strength calculated from size of raw material		
Geometric size factor K1d calculated from raw material diameter		
[σBeff] (N/mm²)		1045.61
[σSeff] (N/mm²)		740.64
[σbF] (N/mm²)		740.64
[τtF] (N/mm²)		427.61
[σBRand] (N/mm²)		2300.00
[σzdW] (N/mm²)		418.24

[σbW] (N/mm²)		522.80
[τtW] (N/mm²)		313.68

Fatigue strength for single stage use

Required life time	[H]	5000.00
Number of load cycles (Mio)	[NL]	1067.040

Data of S-N curve (Woehler line) analog to FKM standard:

[kσ, kτ]	15	25
[kDσ, kDτ]	0	0
[NDσ, NDτ]	1e+006	1e+006
[NDσII, NDτII]	0	0

Calculation for load case 2 (σ.av/σ.mv = const)

Cross section 'A-A Key way' Key

Comment	Y= 38.55... 66.55mm	
Position (Y-Coordinate) (mm)	[y]	66.540
External diameter (mm)	[da]	42.000
Inner diameter (mm)	[di]	0.000
Notch effect		Key
Number of keys	[n]	1

Groove with manufactured with end milling cutter

Standard:	DIN 6885.1:1968 Default	
[b, t] (mm)	12.000	5.100
Mean roughness (µm)	[Rz]	8.000

		Tension/Compression	Bending	Torsion	Shearing	
Load: (N) (Nm)						
Mean value	[Fzdm, Mbm, Tm, Fqm]	-90.8	0.0	32.4	0.0	
Amplitude	[Fzda, Mba, Ta, Fqa]	90.8	37.0	32.4	979.1	
Maximum value	[Fzdmax, Mbmax, Tmax, Fqmax]	-308.6	62.8	110.3		1664.5
Cross section, moment of resistance: (mm²)						
[A, Wb, Wt, A]		1385.4	7273.6	14547.1	1385.4	

Stresses: (N/mm²)

[σzdm, σbm, τm, τqm] (N/mm²)	-0.066	0.000	2.229	0.000
[σzda, σba, τa, τqa] (N/mm²)	0.066	5.083	2.229	0.942
[σzdmax,σbmax,τmax,τqmax] (N/mm²)	-0.223	8.640	7.580	1.602

Technological size influence	[K1(σB)]	0.871		
	[K1(σS)]	0.871		

		Tension/Compression	Bending	Torsion
Notch effect coefficient	[ß(dB)]	3.046	3.046	1.846
[dB] (mm) = 40.0				
Geometrical size influence	[K3(d)]	0.944	0.944	0.969
Geometrical size influence	[K3(dB)]	0.946	0.946	0.970
Notch effect coefficient	[ß]	3.051	3.051	1.847
Geometrical size influence	[K2(d)]	1.000	0.885	0.885
Influence coefficient surface roughness	[KF]	1.000	1.000	1.000
Roughness factor is included into the notch effect coefficient				
Surface stabilization factor	[KV]	1.000	1.000	1.000
Total influence coefficient	[K]	3.051	3.447	2.087

Present safety for endurance limit:

Equivalent mean stress (N/mm²)	[σmV]	3.861	
Equivalent mean stress (N/mm²)	[τmV]	2.229	
Fatigue limit of part (N/mm²)	[σWK]	137.098	151.662	150.279
Influence coefficient of mean stress sensitivity.				
	[ψσK]	0.070	0.078	0.077
Permissible amplitude (N/mm²)	[σADK]	12.360	143.159	139.481
Permissible amplitude (N/mm²)	[σANK]	12.360	143.159	139.481
Effective Miner sum	[DM]	0.300	0.300	0.300
Load spectrum factor	[fKoll]	1.000	1.000	1.000
Safety against fatigue	[S]		22.819	
Required safety against fatigue	[Smin]		1.200	
Result (%)	[S/Smin]		1901.6	

Present safety
for proof against exceed of yield point:

Static notch sensitivity factor	[K2F]	1.000	1.000	1.000
Increase coefficient	[γF]	1.000	1.000	1.000
Yield stress of part (N/mm²)	[σFK]	740.638	740.638	427.608
Safety yield stress	[S]		47.491	
Required safety	[Smin]		1.200	
Result (%)	[S/Smin]		3957.6	

Present safety
for proof of avoiding incipient crack on hard surface layers:

Safety against incipient crack	[S]		72.242	
Required safety	[Smin]		1.200	
Result (%)	[S/Smin]		6020.2	

Cross section 'B-B Smooth shaft' Smooth shaft

Comment					
Position (Y-Coordinate) (mm)	[y]		73.550		
External diameter (mm)	[da]		42.000		
Inner diameter (mm)	[di]		0.000		
Notch effect			Smooth shaft		
Mean roughness (µm)	[Rz]		4.800		

		Tension/Compression	Bending	Torsion	Shearing	
Load: (N) (Nm)						
Mean value	[Fzdm, Mbm, Tm, Fqm]	-93.9	0.0	33.6	0.0	
Amplitude	[Fzda, Mba, Ta, Fqa]	93.9	41.0	33.6	991.7	
Maximum value	[Fzdmax, Mbmax, Tmax, Fqmax]	-319.4	69.8	114.1		1685.8
Cross section, moment of resistance: (mm²)						
[A, Wb, Wt, A]		1385.4	7273.6	14547.1	1385.4	

Stresses: (N/mm²)					
[σzdm, σbm, τm, τqm] (N/mm²)	-0.068	0.000	2.307	0.000	
[σzda, σba, τa, τqa] (N/mm²)	0.068	5.643	2.307	0.954	
[σzdmax,σbmax,τmax,τqmax] (N/mm²)	-0.231	9.593	7.844	1.622	

Technological size influence	[K1(σB)]	0.871		
	[K1(σS)]	0.871		

		Tension/Compression	Bending	Torsion
Notch effect coefficient	[ß]	1.000	1.000	1.000
Geometrical size influence	[K2(d)]	1.000	0.885	0.885
Influence coefficient surface roughness	[KF]	0.892	0.892	0.938
Surface stabilization factor	[KV]	1.000	1.033	1.033
Total influence coefficient	[K]	1.121	1.210	1.157

Present safety for endurance limit:

Equivalent mean stress (N/mm²)	[σmV]		3.995	
Equivalent mean stress (N/mm²)	[τmV]		2.307	
Fatigue limit of part (N/mm²)	[σWK]	373.215	431.973	271.029
Influence coefficient of mean stress sensitivity.	[ψσK]	0.217	0.260	0.149
Permissible amplitude (N/mm²)	[σADK]	12.361	364.739	213.819
Permissible amplitude (N/mm²)	[σANK]	12.361	364.739	213.819
Effective Miner sum	[DM]	0.300	0.300	0.300
Load spectrum factor	[fKoll]	1.000	1.000	1.000
Safety against fatigue	[S]		42.425	
Required safety against fatigue	[Smin]		1.200	
Result (%)	[S/Smin]		3535.5	

Present safety
for proof against exceed of yield point:

Static notch sensitivity factor	[K2F]	1.000	1.000	1.000
Increase coefficient	[γF]	1.000	1.000	1.000
Yield stress of part (N/mm²)	[σFK]	740.638	740.638	427.608
Safety yield stress	[S]		44.890	
Required safety	[Smin]		1.200	
Result (%)	[S/Smin]		3740.8	

Present safety

for proof of avoiding incipient crack on hard surface layers:

Safety against incipient crack	[S]	166.482
Required safety	[Smin]	1.200
Result (%)	[S/Smin]	13873.5

Cross section 'C-C Shoulder' **Shoulder**

Comment	Y= 113.55mm			
Position (Y-Coordinate) (mm)		[y]		113.550
External diameter (mm)		[da]		42.000
Inner diameter (mm)		[di]		0.000
Notch effect			Shoulder	
[D, r, t] (mm)	49.000	0.100	3.500	
Mean roughness (µm)		[Rz]		8.000

		Tension/Compression	Bending	Torsion	Shearing
Load: (N) (Nm)					
Mean value	[Fzdm, Mbm, Tm, Fqm]	125.0	0.0	0.0	0.0
Amplitude	[Fzda, Mba, Ta, Fqa]	125.0	26.0	0.0	1403.3
Maximum value	[Fzdmax, Mbmax, Tmax, Fqmax]	424.8	44.2	0.0	2385.5
Cross section, moment of resistance: (mm²)					
[A, Wb, Wt, A]		1385.4	7273.6	14547.1	1385.4

Stresses: (N/mm²)					
[σzdm, σbm, τm, τqm] (N/mm²)		0.090	0.000	0.000	0.000
[σzda, σba, τa, τqa] (N/mm²)		0.090	3.571	0.000	1.350
[σzdmax,σbmax,τmax,τqmax] (N/mm²)		0.307	6.070	0.000	2.296
Technological size influence	[K1(σB)]	0.871			
	[K1(σS)]	0.871			

		Tension/Compression	Bending	Torsion
Stress concentration factor	[a]	6.381	5.683	3.299
References stress slope	[G']	23.896	23.896	11.500
Notch sensitivity factor	[n]	1.975	1.975	1.677
Notch effect coefficient	[ß]	3.230	2.877	1.968
Geometrical size influence	[K2(d)]	1.000	0.885	0.885
Influence coefficient surface roughness	[KF]	0.857	0.857	0.918
Surface stabilization factor	[KV]	1.000	1.033	1.033
Total influence coefficient	[K]	3.397	3.307	2.238
Present safety for endurance limit:				
Equivalent mean stress (N/mm²)	[σmV]		0.090	
Equivalent mean stress (N/mm²)	[τmV]		0.052	
Fatigue limit of part (N/mm²)	[σWK]	123.135	158.089	140.148
Influence coefficient of mean stress sensitivity.				
	[ψσK]	0.063	0.082	0.072
Permissible amplitude (N/mm²)	[σADK]	115.884	157.763	8.057
Permissible amplitude (N/mm²)	[σANK]	115.884	157.763	8.057
Effective Miner sum	[DM]	0.300	0.300	0.300
Load spectrum factor	[fKoll]	1.000	1.000	1.000
Safety against fatigue	[S]		42.714	
Required safety against fatigue	[Smin]		1.200	
Result (%)	[S/Smin]		3559.5	
Present safety for proof against exceed of yield point:				
Static notch sensitivity factor	[K2F]	1.000	1.000	1.000
Increase coefficient	[γF]	1.000	1.000	1.000
Yield stress of part (N/mm²)	[σFK]	740.638	740.638	427.608
Safety yield stress	[S]		116.145	
Required safety	[Smin]		1.200	
Result (%)	[S/Smin]		5257.9	
Present safety for proof of avoiding incipient crack on hard surface layers:				
Safety against incipient crack	[S]		63.095	
Required safety	[Smin]		1.200	
Result (%)	[S/Smin]		5257.9	

Remarks:
- The shearing force is not considered in the analysis specified in DIN 743.
- Cross section with interference fit:
  The notching factor for the light fit case is no longer defined in DIN 743.
  The values are imported from the FKM-Guideline..

End of Report lines: 698

THERMALLY SAFE OPERATING SPEED CALCULATION
(according to DIN ISO 15312 and DIN 732)

Lubricant	Castrol ATF Dex II Multivehicle		
Lubrication type:			
Oil-groove lubrication			
Mean bearing temperature	[T_m]	85.000	°C
Temperature of bearing environment	[T_u]	75.000	°C
Lubricant - service temperature	[T_B]	75.000	°C
Lubricant temperature - Reference conditions	[T_{ref}]	70.000	°C

Shaft 'Shaft 1', Rolling bearing 'Rolling bearing':

Thermal nominal speed according to DIN ISO 15312:

Type of support	Deep groove ball bearing (single row)		
Bearing number	SKF 6308		
Design series	63		
Speed	[n]	3556.800	1/min
Coefficient	[f_{0r}]	2.300	
(Depends upon type of design and lubrication at reference conditions)			
Coefficient	[f_{1r}]	0.000200	
(Depends upon type of design and load at reference conditions)			
Heat sink reference surface	[A_S]	9393.362	mm²
Reference load	[P_{1r}]	1.200	kN
Bearing mean diameter	[d_m]	65.000	mm
Bearing-specific reference heat flow density	[q_r]	16.000	kW/m²
kinematic viscosity (for reference conditions)	[v_r]	12.000	mm²/s
Thermal nominal speed	[$n_{\theta r}$]	9597.697	1/min

Thermally safe operating speed according to DIN 732:

Coefficient	[f_0]	2.300	
(Depends upon type of design and lubrication)			
Coefficient	[f_1]	0.000190	
(Depends upon type of design and load)			
Temperature difference	[$\Delta\theta=\theta_o-\theta_i$]	10.000	°C
Lubricant Oil-volume	[V_L]	0.300	l/min
Heat flow (dissipated by the lubricant)	[Φ_L]	0.086	kW
Heat flow (dissipated by the bearing support surface)	[Φ_S]	0.029	kW
Total heat flow	[Φ]	0.115	kW
Dynamic equivalent load	[P_1]	1066.032	N
kinematic viscosity at service temperature	[v]	13.108	mm²/s
Lubricant film parameter	[K_L]	1.390	
Charge parameter	[K_P]	0.115	
Speed ratio	[f_n]	0.776	
Thermally safe operating speed	[n_θ]	7451.337	1/min

Shaft 'Shaft 1', Rolling bearing 'Rolling bearing':

Thermal nominal speed according to DIN ISO 15312:

Type of support		Deep groove ball bearing (single row)		
Bearing number		SKF 6308		
Design series		63		
Speed	[n]	3556.800	1/min	
Coefficient	[f_{0r}]		2.300	
(Depends upon type of design and lubrication at reference conditions)				
Coefficient	[f_{1r}]		0.000200	
(Depends upon type of design and load at reference conditions)				
Heat sink reference surface	[A_S]		9393.362	mm²
Reference load	[P_{1r}]		1.200	kN
Bearing mean diameter	[d_m]		65.000	mm
Bearing-specific reference heat flow density	[q_r]		16.000	kW/m²
kinematic viscosity (for reference conditions)	[v_r]		12.000	mm²/s
Thermal nominal speed	[$n_{\theta r}$]		9597.697	1/min

Thermally safe operating speed according to DIN 732:

Coefficient	[f_0]	2.300	
(Depends upon type of design and lubrication)			
Coefficient	[f_1]	0.000218	
(Depends upon type of design and load)			
Temperature difference	[$\Delta\theta=\theta_o-\theta_i$]	10.000	°C
Lubricant Oil-volume	[V_L]	0.300	l/min
Heat flow (dissipated by the lubricant)	[Φ_L]	0.086	kW
Heat flow (dissipated by the bearing support surface)	[Φ_S]	0.029	kW
Total heat flow	[Φ]	0.115	kW
Dynamic equivalent load	[P_1]	1406.314	N
kinematic viscosity at service temperature	[v]	13.108	mm²/s
Lubricant film parameter	[K_L]	1.390	
Charge parameter	[K_P]	0.175	
Speed ratio	[f_n]	0.754	
Thermally safe operating speed	[n_θ]	7240.450	1/min

The reference conditions for calculating the thermal nominal speed are taken from the DIN ISO 15312 standard.

End of Report lines: 96

Analysis of shafts, axle and beams

Input data

Coordinate system shaft: see picture W-002

Label		Shaft 1
Drawing		
Initial position (mm)		0.000
Length (mm)		201.550
Speed (1/min)		1201.30
Sense of rotation: clockwise		
Material		18CrNiMo7-6
Young's modulus (N/mm²)		206000.000
Poisson's ratio nu		0.300
Density (kg/m³)		7830.000
Coefficient of thermal expansion	(10^-6/K)	11.500
Temperature (°C)		75.000
Weight of shaft (kg)		2.509
(Notice: Weight stands for the shaft only without considering the gears)		
Weight of shaft, including additional masses (kg)		5.566
Mass moment of inertia (kg*mm²)		7357.325
Momentum of mass GD2 (Nm²)		0.289
Position in space (°)		0.000
Gears mounted with stiffness according to ISO		
Consider deformations due to shearing		
Shear correction coefficient		1.100
Contact angle of rolling bearings is considered		
Tolerance field: Mean value		
Housing material		GK-AlSi7Mg wa
Coefficient of thermal expansion	(10^-6/K)	22.000
Temperature of housing (°C)		65.000
Thermal housing reference point (mm)		0.000
Reference temperature (°C)		20.000

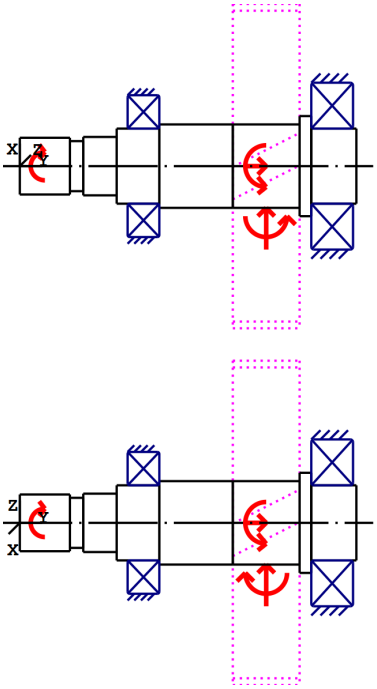

Figure: Load applications

Shaft definition (Shaft 1)

Outer contour

Cylinder (Cylinder)			0.000mm ... 30.000mm
Diameter (mm)	[d]	34.0000	
Length (mm)	[l]	30.0000	
Surface roughness (µm)	[Rz]	8.0000	

Spline (Spline) -15.000mm ... 15.000mm
da=33.84 (mm), df=32.16 (mm), z=41, mn=0.80 (mm), l=30.00 (mm), Rz=8.0, Turned (Ra=3.2µm/125µin)

Chamfer left (Chamfer left)
l=0.80 (mm), alpha=45.00 (°)

Cylinder (Cylinder)			30.000mm ... 38.000mm
Diameter (mm)	[d]	30.0000	
Length (mm)	[l]	8.0000	
Surface roughness (µm)	[Rz]	8.0000	

Radius left (Radius left)
r=0.10 (mm), Rz=8.0, Turned (Ra=3.2µm/125µin)

Radius right (Radius right)
r=0.10 (mm), Rz=8.0, Turned (Ra=3.2µm/125µin)

Cylinder (Cylinder) 38.000mm ... 58.000mm

Diameter (mm)	[d]	35.0000
Length (mm)	[l]	20.0000
Surface roughness (µm)	[Rz]	4.8000

Chamfer left (Chamfer left)
l=0.80 (mm), alpha=45.00 (°)

Radius right (Radius right)
r=0.10 (mm), Rz=8.0, Turned (Ra=3.2µm/125µin)

Cylinder (Cylinder) 58.000mm ... 83.550mm

Diameter (mm)	[d]	45.0000
Length (mm)	[l]	25.5500
Surface roughness (µm)	[Rz]	8.0000

Chamfer left (Chamfer left)
l=0.80 (mm), alpha=45.00 (°)

Square groove (Square groove)
b=1.75 (mm), t=1.25 (mm), r=0.20 (mm), Rz=8.0, Turned (Ra=3.2µm/125µin)

Relief groove right (Relief groove right)
r=0.80 (mm), t=0.30 (mm), l=2.50 (mm), Rz=8.0, Turned (Ra=3.2µm/125µin)
Form E (DIN 509), Series 1, with the usual stressing

Cylinder (Cylinder) 83.550mm ... 167.550mm

Diameter (mm)	[d]	50.0000
Length (mm)	[l]	84.0000
Surface roughness (µm)	[Rz]	4.8000

Key way (Key way) 129.550mm ... 165.550mm
l=36.00 (mm), i=1, Rz=8.0, Turned (Ra=3.2µm/125µin)

Radius right (Radius right)
r=0.10 (mm), Rz=8.0, Turned (Ra=3.2µm/125µin)

Cylinder (Cylinder) 167.550mm ... 174.550mm

Diameter (mm)	[d]	60.0000
Length (mm)	[l]	7.0000
Surface roughness (µm)	[Rz]	8.0000

Cylinder (Cylinder) 174.550mm ... 201.550mm

Diameter (mm)	[d]	45.0000
Length (mm)	[l]	27.0000
Surface roughness (µm)	[Rz]	4.8000

Relief groove left (Relief groove left)
r=0.80 (mm), t=0.30 (mm), l=2.50 (mm), Rz=8.0, Turned (Ra=3.2µm/125µin)
Form E (DIN 509), Series 1, with the usual stressing

Chamfer right (Chamfer right)
l=0.80 (mm), alpha=45.00 (°)

KISSSOFT
Calculation programs for machine design

Forces

Type of force element		**Cylindrical gear**
Label in the model		Cylindrical gear
Position on shaft (mm)	[y_{local}]	147.5500
Position in global system (mm)	[y_{global}]	147.5500
Operating pitch diameter (mm)		194.3564
Helix angle (°)		12.0839 left
Working pressure angle at normal section (°)		21.0503
Position of contact (°)		160.0000
Length of load application (mm)		40.0000
Power (kW)		25.0000 driven (input)
Torque (Nm)		198.7284
Axial force (N)		437.8062
Shearing force X (N)		1455.7807
Shearing force Z (N)		1646.3710
Bending moment X (Nm)		-14.5513
Bending moment Z (Nm)		-39.9794

Type of force element		**Coupling**
Label in the model		Coupling
Position on shaft (mm)	[y_{local}]	15.0000
Position in global system (mm)	[y_{global}]	15.0000
Effective diameter (mm)		40.0000
Radial force factor (-)		0.0000
Direction of the radial force (°)		0.0000
Axial force factor (-)		0.0000
Length of load application (mm)		30.0000
Power (kW)		25.0000 driving (output)
Torque (Nm)		-198.7284
Axial force (N)		0.0000
Shearing force X (N)		0.0000
Shearing force Z (N)		0.0000
Bending moment X (Nm)		0.0000
Bending moment Z (Nm)		0.0000
Mass (kg)		0.0000
Mass moment of inertia Jp (kg*m²)		0.0000
Mass moment of inertia Jxx (kg*m²)		0.0000
Mass moment of inertia Jzz (kg*m²)		0.0000
Eccentricity (mm)		0.0000

Bearing

Label in the model		Rolling bearing
Bearing type		SKF 6209
Bearing type		Deep groove ball bearing (single row)
		SKF Explorer
Bearing position (mm)	[y_{lokal}]	74.050
Bearing position (mm)	[y_{global}]	74.050
Attachment of external ring		Free bearing
Inner diameter (mm)	[d]	45.000
External diameter (mm)	[D]	85.000
Width (mm)	[b]	19.000
Corner radius (mm)	[r]	1.100
Basic static load rating (kN)	[C_0]	21.600
Basic dynamic load rating (kN)	[C]	35.100

Fatigue load rating (kN)	[C_u]	0.915
Values for approximated geometry:		
Basic dynamic load rating (kN)	[C_{theo}]	0.000
Basic static load rating (kN)	[C_{0theo}]	0.000

Label in the model		Rolling bearing
Bearing type		SKF 6309
Bearing type		Deep groove ball bearing (single row)
		SKF Explorer
Bearing position (mm)	[y_{lokal}]	187.050
Bearing position (mm)	[y_{global}]	187.050
Attachment of external ring		Fixed bearing
Inner diameter (mm)	[d]	45.000
External diameter (mm)	[D]	100.000
Width (mm)	[b]	25.000
Corner radius (mm)	[r]	1.500
Basic static load rating (kN)	[C_0]	31.500
Basic dynamic load rating (kN)	[C]	55.300
Fatigue load rating (kN)	[C_u]	1.300
Values for approximated geometry:		
Basic dynamic load rating (kN)	[C_{theo}]	0.000
Basic static load rating (kN)	[C_{0theo}]	0.000

Shaft 'Shaft 1': Cylindrical gear 'Cylindrical gear' (y= 147.5500 (mm)) is taken into account as component of the shaft.
EI (y= 127.5500 (mm)): 63200.0085 (Nm²), EI (y= 167.5500 (mm)): 63200.0085 (Nm²), m (yS= 147.5500 (mm)): 3.0570 (kg)
Jp: 0.0067 (kg*m²), Jxx: 0.0037 (kg*m²), Jzz: 0.0037 (kg*m²)

Results

Shaft

Maximum deflection (µm)	8.068
Position of the maximum (mm)	0.000
Mass center of gravity (mm)	114.120
Total axial load (N)	437.806
Torsion under torque (°)	0.070

Bearing

Probability of failure	[n]	10.00	%
Axial clearance	[u_A]	10.00	µm
Lubricant	Castrol ATF Dex II Multivehicle		
Lubricant with additive, effect on bearing lifetime confirmed in tests.			
Oil lubrication, off-line/no filtration, ISO4406 -/15/12			
Lubricant - service temperature	[T_B]	75.00	°C
Limit for factor aISO	[a_{ISOmax}]	50.00	
Oil level	[h_{oil}]	0.00	mm
Oil bath lubrication			

KISSSOFT
Calculation programs for machine design

Rolling bearings, classical calculation (contact angle considered)

Shaft 'Shaft 1' Rolling bearing 'Rolling bearing'

Position (Y-coordinate)	[y]	74.05	mm
Dynamic equivalent load	[P]	0.70	kN
Equivalent load	[P_0]	0.70	kN
Life modification factor for reliability[a_1]		1.000	
Life modification factor	[a_{ISO}]	4.773	
Nominal bearing service life	[L_{nh}]	> 1000000	h
Modified bearing service life	[L_{nmh}]	> 1000000	h
Operating viscosity	[v]	13.11	mm²/s
Static safety factor	[S_0]	31.06	
Bearing reaction force	[Fx]	-0.155	kN
Bearing reaction force	[Fy]	0.000	kN
Bearing reaction force	[Fz]	-0.678	kN
Bearing reaction force	[Fr]	0.695	kN (-102.89°)
Bearing reaction moment	[Mx]	-0.00	Nm
Bearing reaction moment	[My]	0.00	Nm
Bearing reaction moment	[Mz]	0.00	Nm
Bearing reaction moment	[Mr]	0.00	Nm (179.21°)
Oil level	[H]	37.500	mm
Rolling moment of friction	[M_{rr}]	0.015	Nm
Sliding moment of friction	[M_{sl}]	0.005	Nm
Moment of friction, seals	[M_{seal}]	0.000	Nm
Moment of friction for seals determined according to SKF main catalog 10000/1 EN:2013			
Moment of friction flow losses	[M_{drag}]	0.006	Nm
Torque of friction	[M_{loss}]	0.026	Nm
Power loss	[P_{loss}]	3.288	W
The moment of friction is calculated according to the details in SKF Catalog 2013.			
The calculation is always performed with a coefficient for additives in the lubricant μbl=0.15.			
Displacement of bearing	[u_x]	1.910	μm
Displacement of bearing	[u_y]	123.733	μm
Displacement of bearing	[u_z]	6.994	μm
Displacement of bearing	[u_r]	7.250	μm (74.73°)
Misalignment of bearing	[r_x]	-0.014	mrad (-0.05')
Misalignment of bearing	[r_y]	0.980	mrad (3.37')
Misalignment of bearing	[r_z]	-0.039	mrad (-0.13')
Misalignment of bearing	[r_r]	0.042	mrad (0.14')

Shaft 'Shaft 1' Rolling bearing 'Rolling bearing'

Position (Y-coordinate)	[y]	187.05	mm
Dynamic equivalent load	[P]	1.82	kN
Equivalent load	[P_0]	1.59	kN
Life modification factor for reliability[a_1]		1.000	
Life modification factor	[a_{ISO}]	2.705	
Nominal bearing service life	[L_{nh}]	390439.03	h
Modified bearing service life	[L_{nmh}]	> 1000000	h
Operating viscosity	[v]	13.11	mm²/s
Static safety factor	[S_0]	19.82	
Bearing reaction force	[Fx]	-1.301	kN
Bearing reaction force	[Fy]	-0.438	kN
Bearing reaction force	[Fz]	-0.914	kN
Bearing reaction force	[Fr]	1.590	kN (-144.91°)
Oil level	[H]	43.125	mm

Rolling moment of friction	[M_{rr}]	0.060	Nm
Sliding moment of friction	[M_{sl}]	0.033	Nm
Moment of friction, seals	[M_{seal}]	0.000	Nm

Moment of friction for seals determined according to SKF main catalog 10000/1 EN:2013

Moment of friction flow losses	[M_{drag}]	0.008	Nm
Torque of friction	[M_{loss}]	0.101	Nm
Power loss	[P_{loss}]	12.649	W

The moment of friction is calculated according to the details in SKF Catalog 2013.
The calculation is always performed with a coefficient for additives in the lubricant μbl=0.15.

Displacement of bearing	[u_x]	5.863	μm
Displacement of bearing	[u_y]	195.180	μm
Displacement of bearing	[u_z]	4.264	μm
Displacement of bearing	[u_r]	7.250	μm (36.03°)
Misalignment of bearing	[r_x]	-0.033	mrad (-0.11')
Misalignment of bearing	[r_y]	1.221	mrad (4.2')
Misalignment of bearing	[r_z]	-0.032	mrad (-0.11')
Misalignment of bearing	[r_r]	0.046	mrad (0.16')

Damage (%) [Lreq] (5000.000)

Bin no	B1	B2
1	0.50	0.50
Σ	0.50	0.50

Utilization (%) [Lreq] (5000.000)

B1	B2
17.10	17.10

Note: Utilization = (Lreq/Lh)^(1/k)
Ball bearing: k = 3, roller bearing: k = 10/3

B1: Rolling bearing
B2: Rolling bearing

Shaft '

Shaft 1', Dokumentationspunkt Documentation point

Y position (mm)	[y]	147.55
Equivalent stress (N/mm²)	[sigV]	8.50

	X	Y	Z	R
Displacement (mm)	0.0047	0.1702	0.0056	0.0073
Rotation (mrad)	-0.0302	1.2204	-0.0355	0.0466
Force (kN)	-0.5728	-0.2189	-0.1135	0.5839
Torque (Nm)	-35.4909	99.3642	24.1091	42.9052

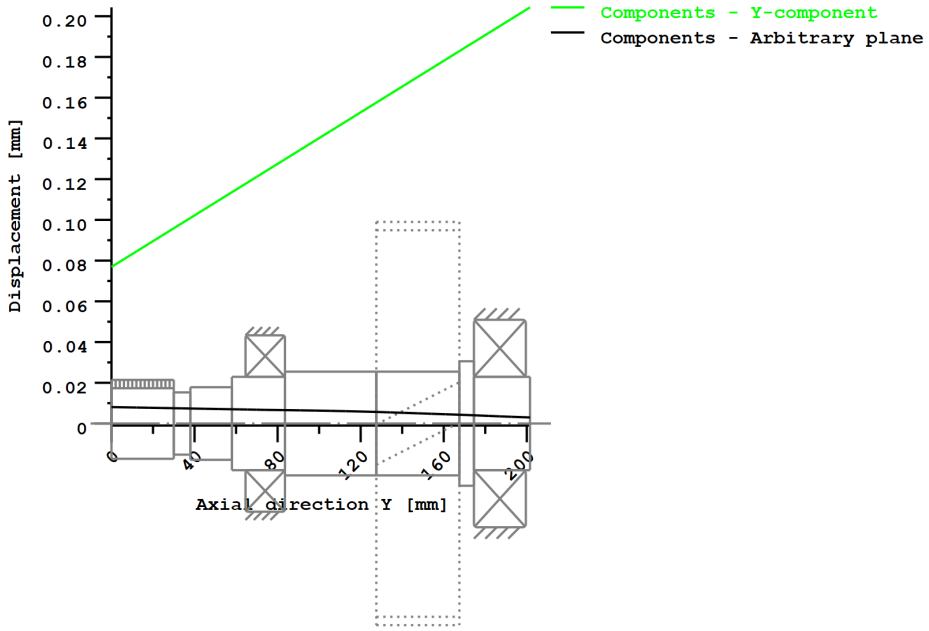

Figure: Deformation (bending etc.) (Arbitrary plane 97.09668381 121)

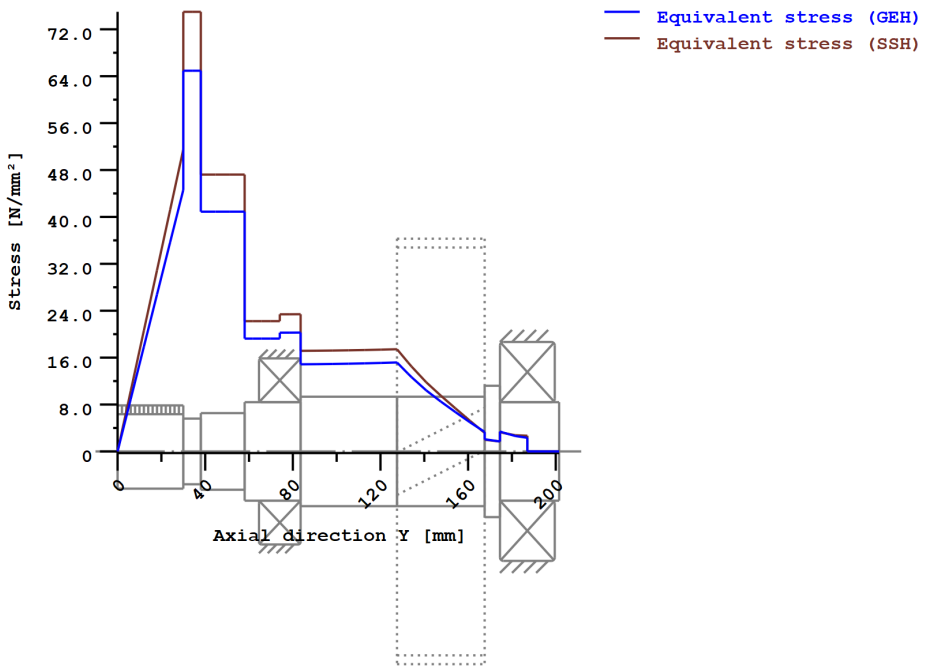

Nominal stresses, without taking into account stress concentrations
GEH(von Mises): sigV = ((sigB+sigZ,D)^2 + 3*(tauT+tauS)^2)^1/2
SSH(Tresca): sigV = ((sigB-sigZ,D)^2 + 4*(tauT+tauS)^2)^1/2

Figure: Equivalent stress

Eigenfrequencies/Critical speeds

1. Eigenfrequency:	0.00 Hz, Critical speed:	0.00 1/min	Rigid body rotation Y 'Shaft 1'
2. Eigenfrequency:	3684.74 Hz, Critical speed:	221084.43 1/min	Bending XY 'Shaft 1', Bending YZ 'Shaft 1'
3. Eigenfrequency:	5214.44 Hz, Critical speed:	312866.44 1/min	Bending YZ 'Shaft 1', Bending XY 'Shaft 1'
4. Eigenfrequency:	8439.39 Hz, Critical speed:	506363.47 1/min	Bending XY 'Shaft 1'
5. Eigenfrequency:	9325.02 Hz, Critical speed:	559501.01 1/min	Torsion 'Shaft 1'

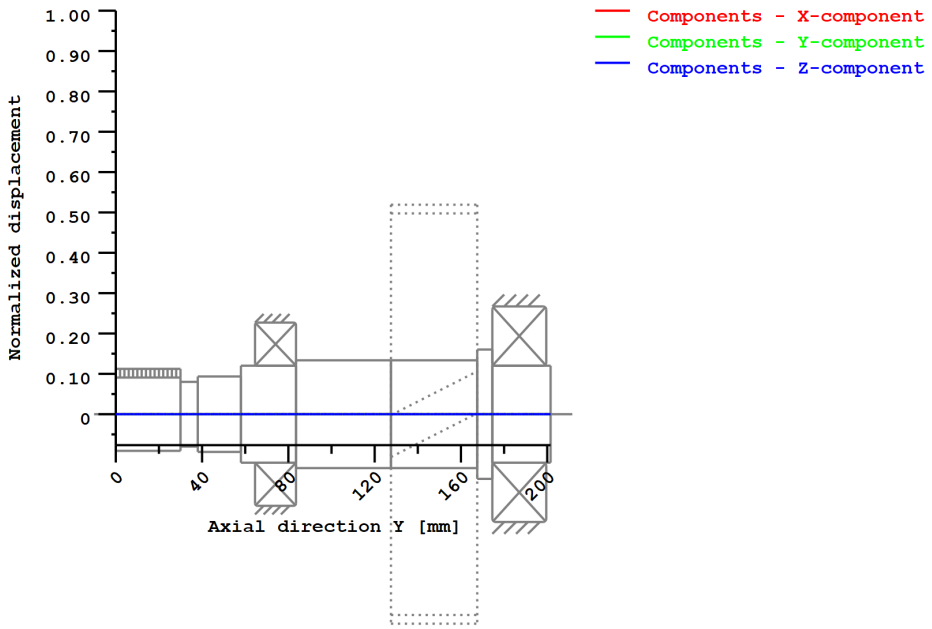

Figure: Eigenfrequencies (Normalized rotation) (Eigenfrequency: 1. (0 Hz))

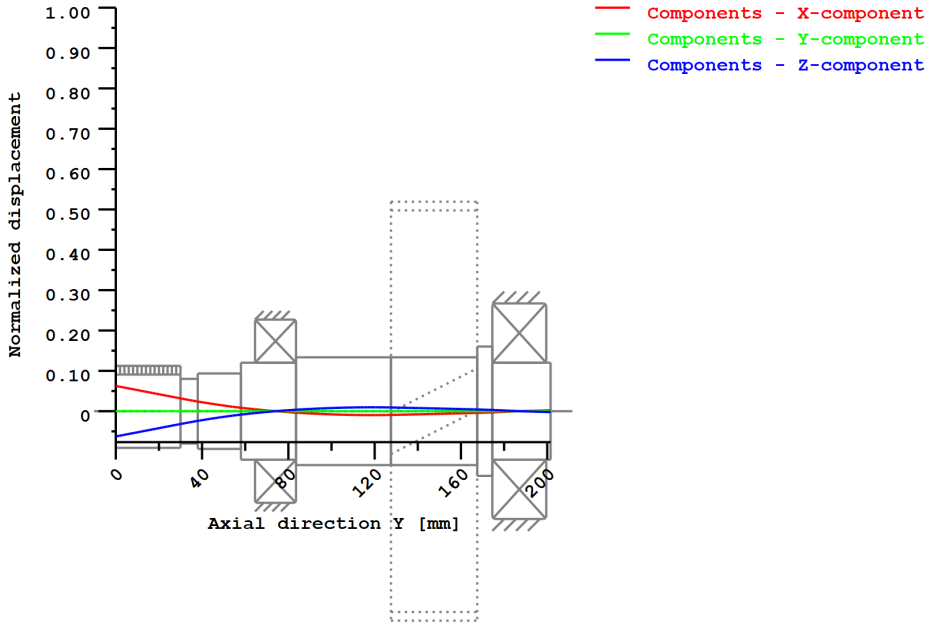

Figure: Eigenfrequencies (Normalized rotation) (Eigenfrequency: 2. (3684.74 Hz))

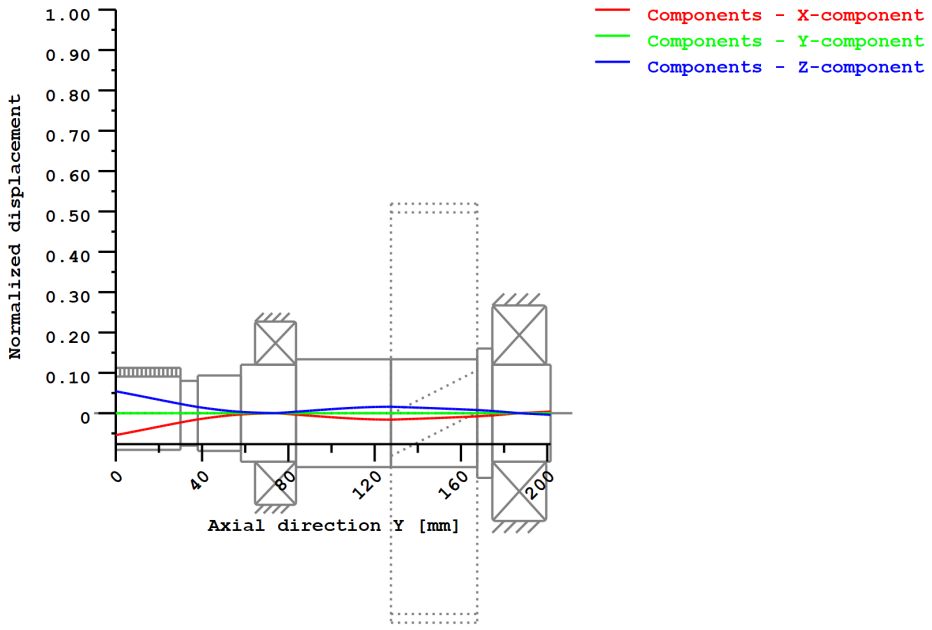

Figure: Eigenfrequencies (Normalized rotation) (Eigenfrequency: 3. (5214.44 Hz))

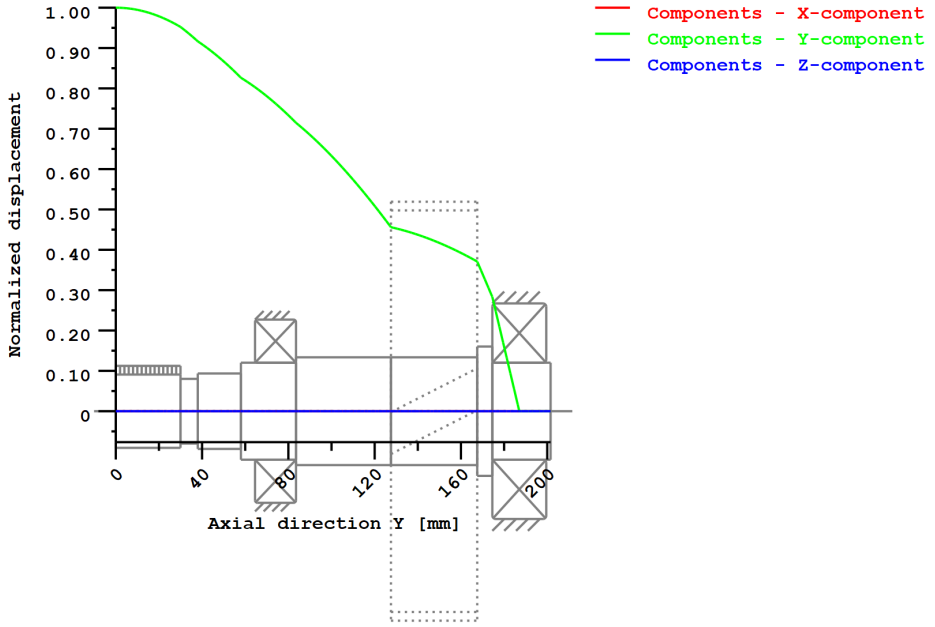

Figure: Eigenfrequencies (Normalized rotation) (Eigenfrequency: 4. (8439.39 Hz))

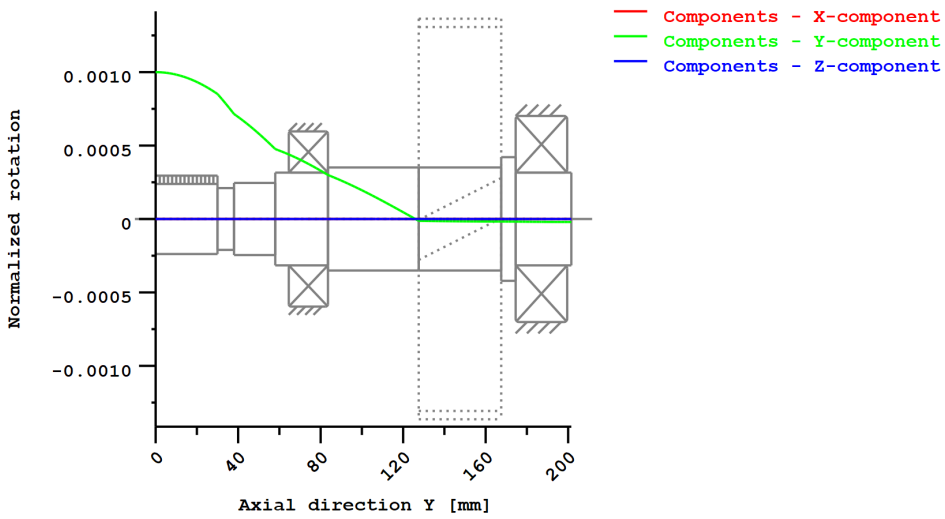

Figure: Eigenfrequencies (Normalized displacement) (Eigenfrequency: 5. (9325.02 Hz))

KISSSOFT
Calculation programs for machine design

Strength calculation according to DIN 743:2012
with finite life fatigue strength according to FKM standard and FVA draft

Summary

Shaft 1

Material	18CrNiMo7-6
Material type	Case-carburized steel
Material treatment	case-hardened
Surface treatment	No

Calculation of finite life fatigue strength and static strength

Calculation for load case 2 (σav/σmv = const)

Cross section	Position (Y-Coord) (mm)	
A-A Shoulder	38.00	Shoulder
B-B Shoulder	30.00	Shoulder
C-C Smooth shaft	34.00	Smooth shaft
D-D Shoulder	58.00	Shoulder

Results:

Cross section	Kfb	Kfs	K2d	SD	SS	SA
A-A Shoulder	2.50	0.86	0.91	7.02	6.48	12.27
B-B Shoulder	2.41	0.86	0.91	7.25	6.48	12.78
C-C Smooth shaft	1.00	0.86	0.91	9.86	6.48	36.08
D-D Shoulder	2.87	0.86	0.90	9.90	10.29	16.99
Required safeties:				1.20	1.20	1.20

Abbreviations:
Kfb: Notch factor bending
Kfσ: Surface factor
K2d: size factor bending
SD: Safety endurance limit
SS: Safety against yield point
SA: Safety against incipient crack

Service life and damage

System service life (h) [Hatt] 1000000.00

Damage to system (%) [D] 0.00

Damage (%) [H] (5000.0 h)

Calculation of reliability R(t) using a Weibull distribution; t in (h):

R(t) = 100 * Exp(-((t*fac - t0)/(T - t0))^b) %

Welle	fac	b	t0	T
1	72078	1.5	6.573e+010	1.394e+011

Damage to cross sections (%) [D]

A-A Shoulder:	0.00
B-B Shoulder:	0.00
C-C Smooth shaft:	0.00
D-D Shoulder:	0.00

Utilization (%) [Smin/S]

Cross section	Static	Endurance
A-A Shoulder	18.513	17.086
B-B Shoulder	18.513	16.554
C-C Smooth shaft	18.513	12.177
D-D Shoulder	11.658	12.124

Maximum utilization (%)	[A]	18.513

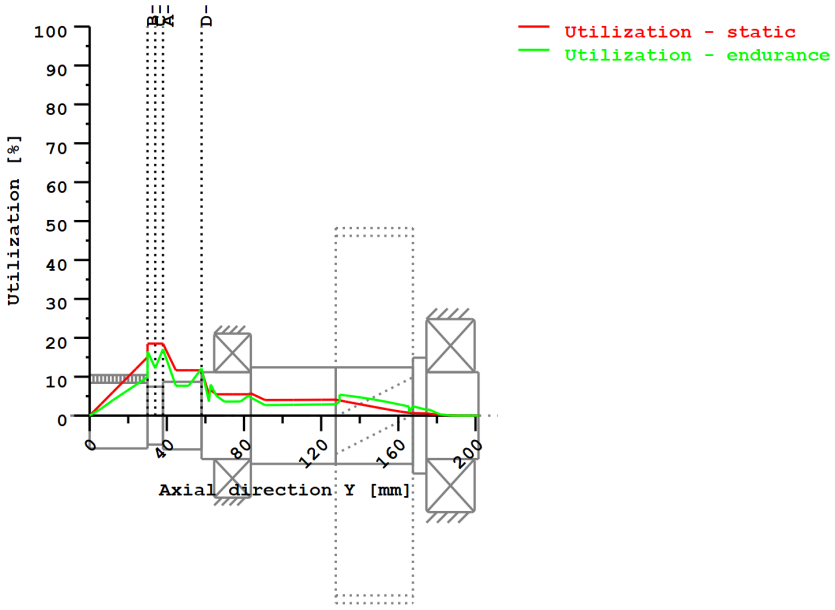

Utilization = Smin/S (%)

Figure: Strength

Calculation details

General statements

Label	Shaft 1		
Drawing			
Length (mm)		[l]	201.55
Speed (1/min)		[n]	1201.30
Material	18CrNiMo7-6		
Material type	Case-carburized steel		
Material treatment	case-hardened		
Surface treatment	No		

	Tension/Compression	Bending	Torsion	Shearing
Load factor static calculation	1.700	1.700	1.700	1.700
Load factor endurance limit	1.000	1.000	1.000	1.000

Reference diameter material (mm)	[dB]	16.00
σB according to DIN 743 (at dB) (N/mm²)	[σB]	1200.00
σS according to DIN 743 (at dB) (N/mm²)	[σS]	850.00
[σzdW] (bei dB) (N/mm²)		480.00
[σbW] (bei dB) (N/mm²)		600.00
[τtW] (bei dB) (N/mm²)		360.00
Thickness of raw material (mm)	[dWerkst]	65.00
Material data calculated according DIN743/3 with K1(d)		
Material strength calculated from size of raw material		
Geometric size factor K1d calculated from raw material diameter		
[σBeff] (N/mm²)		1010.06
[σSeff] (N/mm²)		715.46
[σbF] (N/mm²)		715.46
[τtF] (N/mm²)		413.07
[σBRand] (N/mm²)		2300.00
[σzdW] (N/mm²)		404.02

[σbW] (N/mm²)		505.03
[τtW] (N/mm²)		303.02

Fatigue strength for single stage use

Required life time	[H]	5000.00
Number of load cycles (Mio)	[NL]	360.390

Data of S-N curve (Woehler line) analog to FKM standard:

[kσ, kτ]	15	25
[kDσ, kDτ]	0	0
[NDσ, NDτ]	1e+006	1e+006
[NDσII, NDτII]	0	0

Calculation for load case 2 (σ.av/σ.mv = const)

Cross section 'A-A Shoulder' **Shoulder**

Comment	Y= 38.00mm			
Position (Y-Coordinate) (mm)		[y]		38.000
External diameter (mm)		[da]		30.000
Inner diameter (mm)		[di]		0.000
Notch effect			Shoulder	
[D, r, t] (mm)	35.000	0.100	2.500	
Mean roughness (µm)		[Rz]		8.000

		Tension/Compression	Bending	Torsion	Shearing
Load: (N) (Nm)					
Mean value	[Fzdm, Mbm, Tm, Fqm]	0.0	0.0	99.4	0.0
Amplitude	[Fzda, Mba, Ta, Fqa]	0.0	0.0	99.4	2.5
Maximum value	[Fzdmax, Mbmax, Tmax, Fqmax]	0.0	0.1	337.8	4.3
Cross section, moment of resistance: (mm²)					
[A, Wb, Wt, A]		706.9	2650.7	5301.4	706.9

Stresses: (N/mm²)					
[σzdm, σbm, τm, τqm] (N/mm²)		0.000	0.000	18.743	0.000
[σzda, σba, τa, τqa] (N/mm²)		0.000	0.019	18.743	0.005
[σzdmax,σbmax,τmax,τqmax] (N/mm²)		0.000	0.032	63.726	0.008
Technological size influence	[K1(σB)]	0.842			
	[K1(σS)]	0.842			

		Tension/Compression	Bending	Torsion
Stress concentration factor	[a]	5.543	4.953	2.940
References stress slope	[G']	24.045	24.045	11.500
Notch sensitivity factor	[n]	1.978	1.978	1.677
Notch effect coefficient	[ß]	2.802	2.504	1.753
Geometrical size influence	[K2(d)]	1.000	0.907	0.907
Influence coefficient surface roughness	[KF]	0.860	0.860	0.920
Surface stabilization factor	[KV]	1.000	1.000	1.000
Total influence coefficient	[K]	2.964	2.921	2.020
Present safety for endurance limit:				
Equivalent mean stress (N/mm²)	[σmV]		32.464	
Equivalent mean stress (N/mm²)	[τmV]		18.743	
Fatigue limit of part (N/mm²)	[σWK]	136.294	172.877	150.034
Influence coefficient of mean stress sensitivity.	[ψσK]	0.072	0.094	0.080
Permissible amplitude (N/mm²)	[σADK]	0.022	0.414	138.891
Permissible amplitude (N/mm²)	[σANK]	0.022	0.414	138.891
Effective Miner sum	[DM]	0.300	0.300	0.300
Load spectrum factor	[fKoll]	1.000	1.000	1.000
Safety against fatigue	[S]		7.023	
Required safety against fatigue	[Smin]		1.200	
Result (%)	[S/Smin]		585.3	
Present safety for proof against exceed of yield point:				
Static notch sensitivity factor	[K2F]	1.000	1.000	1.000
Increase coefficient	[γF]	1.000	1.000	1.000
Yield stress of part (N/mm²)	[σFK]	715.457	715.457	413.069
Safety yield stress	[S]		6.482	
Required safety	[Smin]		1.200	

KISSSOFT
Calculation programs for machine design

Result (%)	[S/Smin]	540.2

Present safety
for proof of avoiding incipient crack on hard surface layers:

Safety against incipient crack	[S]	12.272
Required safety	[Smin]	1.200
Result (%)	[S/Smin]	1022.6

Cross section 'B-B Shoulder' **Shoulder**

Comment	Y= 30.00mm			
Position (Y-Coordinate) (mm)		[y]		30.000
External diameter (mm)		[da]		30.000
Inner diameter (mm)		[di]		0.000
Notch effect			Shoulder	
[D, r, t] (mm)	34.000	0.100	2.000	
Mean roughness (µm)		[Rz]		8.000

		Tension/Compression	Bending	Torsion	Shearing
Load: (N) (Nm)					
Mean value	[Fzdm, Mbm, Tm, Fqm]	0.0	0.0	99.4	0.0
Amplitude	[Fzda, Mba, Ta, Fqa]	0.0	0.0	99.4	2.1
Maximum value	[Fzdmax, Mbmax, Tmax, Fqmax]	0.0	0.1	337.8	3.6
Cross section, moment of resistance: (mm²)					
[A, Wb, Wt, A]		706.9	2650.7	5301.4	706.9

Stresses: (N/mm²)					
[σzdm, σbm, τm, τqm] (N/mm²)		0.000	0.000	18.743	0.000
[σzda, σba, τa, τqa] (N/mm²)		0.000	0.012	18.743	0.004
[σzdmax,σbmax,τmax,τqmax] (N/mm²)		0.000	0.020	63.726	0.007
Technological size influence	[K1(σB)]	0.842			
	[K1(σS)]	0.842			

		Tension/Compression	Bending	Torsion
Stress concentration factor	[a]	5.278	4.774	2.824
References stress slope	[G']	24.156	24.156	11.500
Notch sensitivity factor	[n]	1.981	1.981	1.677
Notch effect coefficient	[ß]	2.665	2.410	1.684
Geometrical size influence	[K2(d)]	1.000	0.907	0.907
Influence coefficient surface roughness	[KF]	0.860	0.860	0.920
Surface stabilization factor	[KV]	1.000	1.000	1.000
Total influence coefficient	[K]	2.827	2.819	1.944
Present safety for endurance limit:				
Equivalent mean stress (N/mm²)	[σmV]		32.464	
Equivalent mean stress (N/mm²)	[τmV]		18.743	
Fatigue limit of part (N/mm²)	[σWK]	142.910	179.175	155.913
Influence coefficient of mean stress sensitivity.	[ψσK]	0.076	0.097	0.084
Permissible amplitude (N/mm²)	[σADK]	0.022	0.261	143.880
Permissible amplitude (N/mm²)	[σANK]	0.022	0.261	143.880
Effective Miner sum	[DM]	0.300	0.300	0.300
Load spectrum factor	[fKoll]	1.000	1.000	1.000
Safety against fatigue	[S]		7.249	
Required safety against fatigue	[Smin]		1.200	
Result (%)	[S/Smin]		604.1	
Present safety for proof against exceed of yield point:				
Static notch sensitivity factor	[K2F]	1.000	1.000	1.000
Increase coefficient	[γF]	1.000	1.000	1.000
Yield stress of part (N/mm²)	[σFK]	715.457	715.457	413.069
Safety yield stress	[S]		6.482	
Required safety	[Smin]		1.200	
Result (%)	[S/Smin]		540.2	

Present safety
for proof of avoiding incipient crack on hard surface layers:

Safety against incipient crack	[S]	12.777
Required safety	[Smin]	1.200
Result (%)	[S/Smin]	1064.8

Cross section 'C-C Smooth shaft' Smooth shaft

Comment		
Position (Y-Coordinate) (mm)	[y]	34.000
External diameter (mm)	[da]	30.000
Inner diameter (mm)	[di]	0.000
Notch effect		Smooth shaft
Mean roughness (µm)	[Rz]	8.000

	Tension/Compression	Bending	Torsion	Shearing	
Load: (N) (Nm)					
Mean value [Fzdm, Mbm, Tm, Fqm]	0.0	0.0	99.4	0.0	
Amplitude [Fzda, Mba, Ta, Fqa]	0.0	0.0	99.4	2.3	
Maximum value [Fzdmax, Mbmax, Tmax, Fqmax]	0.0	0.1	337.8		3.9
Cross section, moment of resistance: (mm²)					
[A, Wb, Wt, A]	706.9	2650.7	5301.4	706.9	

Stresses: (N/mm²)					
[σzdm, σbm, τm, τqm] (N/mm²)	0.000	0.000	18.743	0.000	
[σzda, σba, τa, τqa] (N/mm²)	0.000	0.015	18.743	0.004	
[σzdmax,σbmax,τmax,τqmax] (N/mm²)	0.000	0.026	63.726	0.007	
Technological size influence [K1(σB)]	0.842				
[K1(σS)]	0.842				

		Tension/Compression	Bending	Torsion
Notch effect coefficient	[ß]	1.000	1.000	1.000
Geometrical size influence	[K2(d)]	1.000	0.907	0.907
Influence coefficient surface roughness	[KF]	0.860	0.860	0.920
Surface stabilization factor	[KV]	1.000	1.000	1.000
Total influence coefficient	[K]	1.162	1.264	1.189
Present safety for endurance limit:				
Equivalent mean stress (N/mm²)	[σmV]		32.464	
Equivalent mean stress (N/mm²)	[τmV]		18.743	
Fatigue limit of part (N/mm²)	[σWK]	347.567	399.414	254.774
Influence coefficient of mean stress sensitivity.				
	[ψσK]	0.208	0.246	0.144
Permissible amplitude (N/mm²)	[σADK]	0.022	0.334	206.535
Permissible amplitude (N/mm²)	[σANK]	0.022	0.334	206.535
Effective Miner sum	[DM]	0.300	0.300	0.300
Load spectrum factor	[fKoll]	1.000	1.000	1.000
Safety against fatigue	[S]		9.855	
Required safety against fatigue	[Smin]		1.200	
Result (%)	[S/Smin]		821.3	
Present safety for proof against exceed of yield point:				
Static notch sensitivity factor	[K2F]	1.000	1.000	1.000
Increase coefficient	[γF]	1.000	1.000	1.000
Yield stress of part (N/mm²)	[σFK]	715.457	715.457	413.069
Safety yield stress	[S]		6.482	
Required safety	[Smin]		1.200	
Result (%)	[S/Smin]		540.2	
Present safety for proof of avoiding incipient crack on hard surface layers:				
Safety against incipient crack	[S]		36.085	
Required safety	[Smin]		1.200	
Result (%)	[S/Smin]		3007.1	

Cross section 'D-D Shoulder' Shoulder

KISSSOFT
Calculation programs for machine design

Comment	Y= 58.00mm			
Position (Y-Coordinate) (mm)		[y]	58.000	
External diameter (mm)		[da]	35.000	
Inner diameter (mm)		[di]	0.000	
Notch effect			Shoulder	
[D, r, t] (mm)	45.000	0.100	5.000	
Mean roughness (µm)		[Rz]	8.000	

	Tension/Compression	Bending	Torsion	Shearing
Load: (N) (Nm)				
Mean value [Fzdm, Mbm, Tm, Fqm]	0.0	0.0	99.4	0.0
Amplitude [Fzda, Mba, Ta, Fqa]	0.0	0.1	99.4	4.0
Maximum value [Fzdmax, Mbmax, Tmax, Fqmax]		0.0	0.2	337.8	6.8
Cross section, moment of resistance: (mm²)				
[A, Wb, Wt, A]	962.1	4209.2	8418.5	962.1

Stresses: (N/mm²)					
[σzdm, σbm, τm, τqm] (N/mm²)		0.000	0.000	11.803	0.000
[σzda, σba, τa, τqa] (N/mm²)		0.000	0.027	11.803	0.006
[σzdmax,σbmax,τmax,τqmax] (N/mm²)		0.000	0.047	40.131	0.009
Technological size influence	[K1(σB)]	0.842			
	[K1(σS)]	0.842			

		Tension/Compression	Bending	Torsion
Stress concentration factor	[a]	6.536	5.666	3.369
References stress slope	[G']	23.759	23.759	11.500
Notch sensitivity factor	[n]	1.973	1.973	1.677
Notch effect coefficient	[ß]	3.313	2.873	2.010
Geometrical size influence	[K2(d)]	1.000	0.897	0.897
Influence coefficient surface roughness	[KF]	0.860	0.860	0.920
Surface stabilization factor	[KV]	1.000	1.000	1.000
Total influence coefficient	[K]	3.476	3.364	2.327
Present safety for endurance limit:				
Equivalent mean stress (N/mm²)	[σmV]		20.444	
Equivalent mean stress (N/mm²)	[τmV]		11.803	
Fatigue limit of part (N/mm²)	[σWK]	116.236	150.113	130.198
Influence coefficient of mean stress sensitivity.				
	[ψσK]	0.061	0.080	0.069
Permissible amplitude (N/mm²)	[σADK]	0.035	0.956	121.807
Permissible amplitude (N/mm²)	[σANK]	0.035	0.956	121.807
Effective Miner sum	[DM]	0.300	0.300	0.300
Load spectrum factor	[fKoll]	1.000	1.000	1.000
Safety against fatigue	[S]		9.897	
Required safety against fatigue	[Smin]		1.200	
Result (%)	[S/Smin]		824.8	
Present safety for proof against exceed of yield point:				
Static notch sensitivity factor	[K2F]	1.000	1.000	1.000
Increase coefficient	[γF]	1.000	1.000	1.000
Yield stress of part (N/mm²)	[σFK]	715.457	715.457	413.069
Safety yield stress	[S]		10.293	
Required safety	[Smin]		1.200	
Result (%)	[S/Smin]		857.8	
Present safety for proof of avoiding incipient crack on hard surface layers:				
Safety against incipient crack	[S]		16.993	
Required safety	[Smin]		1.200	
Result (%)	[S/Smin]		1416.1	

Remarks:
- The shearing force is not considered in the analysis specified in DIN 743.
- Cross section with interference fit:
  The notching factor for the light fit case is no longer defined in DIN 743.
  The values are imported from the FKM-Guideline..

End of Report lines: 788

KISSsoft Release 03/2017 F

KISSsoft University license - Universidade do Porto

File

Name : shaftCSpeed

Changed by: Carlos Rodrigues on: 02.07.2018 at: 14:51:47

THERMALLY SAFE OPERATING SPEED CALCULATION

(according to DIN ISO 15312 and DIN 732)

Lubricant	Castrol ATF Dex II Multivehicle		
Lubrication type:			
Immersion lubrication - Oil level up to the middle of the lower bearing.			
Mean bearing temperature	$[T_m]$	85.000	°C
Temperature of bearing environment	$[T_u]$	75.000	°C
Lubricant - service temperature	$[T_B]$	75.000	°C
Lubricant temperature - Reference conditions	$[T_{ref}]$	70.000	°C

Shaft 'Shaft 1', Rolling bearing 'Rolling bearing':

Thermal nominal speed according to DIN ISO 15312:

Type of support	Deep groove ball bearing (single row)		
Bearing number	SKF 6209		
Design series	62		
Speed	$[n]$	1201.300	1/min
Coefficient	$[f_{0r}]$	2.000	
(Depends upon type of design and lubrication at reference conditions)			
Coefficient	$[f_{1r}]$	0.000200	
(Depends upon type of design and load at reference conditions)			
Heat sink reference surface	$[A_S]$	7759.734	mm²
Reference load	$[P_{1r}]$	1.080	kN
Bearing mean diameter	$[d_m]$	65.000	mm
Bearing-specific reference heat flow density	$[q_r]$	16.000	kW/m²
kinematic viscosity (for reference conditions)	$[v_r]$	12.000	mm²/s
Thermal nominal speed	$[n_{\theta r}]$	9306.785	1/min

Thermally safe operating speed according to DIN 732:

Coefficient	$[f_0]$	4.000	
(Depends upon type of design and lubrication)			
Coefficient	$[f_1]$	0.000161	
(Depends upon type of design and load)			
Heat flow (dissipated by the bearing support surface)	$[\Phi_S]$	0.024	kW
Total heat flow	$[\Phi]$	0.024	kW
Dynamic equivalent load	$[P_1]$	695.422	N
kinematic viscosity at service temperature	$[v]$	13.108	mm²/s
Lubricant film parameter	$[K_L]$	10.948	
Charge parameter	$[K_P]$	0.296	
Speed ratio	$[f_n]$	0.227	
Thermally safe operating speed	$[n_\theta]$	2113.113	1/min

Shaft 'Shaft 1', Rolling bearing 'Rolling bearing':

Thermal nominal speed according to DIN ISO 15312:

Type of support		Deep groove ball bearing (single row)		
Bearing number		SKF 6309		
Design series		63		
Speed	[n]	1201.300	1/min	
Coefficient	[f_{0r}]		2.300	
(Depends upon type of design and lubrication at reference conditions)				
Coefficient	[f_{1r}]		0.000200	
(Depends upon type of design and load at reference conditions)				
Heat sink reference surface	[A_S]		11388.273	mm²
Reference load	[P_{1r}]		1.575	kN
Bearing mean diameter	[d_m]		72.500	mm
Bearing-specific reference heat flow density	[q_r]		16.000	kW/m²
kinematic viscosity (for reference conditions)	[v_r]		12.000	mm²/s
Thermal nominal speed	[$n_{\theta r}$]		8850.783	1/min

Thermally safe operating speed according to DIN 732:

Coefficient	[f_0]		4.600	
(Depends upon type of design and lubrication)				
Coefficient	[f_1]		0.000202	
(Depends upon type of design and load)				
Heat flow (dissipated by the bearing support surface)	[Φ_S]		0.035	kW
Total heat flow	[Φ]		0.035	kW
Dynamic equivalent load	[P_1]		1589.647	N
kinematic viscosity at service temperature	[v]		13.108	mm²/s
Lubricant film parameter	[K_L]		10.948	
Charge parameter	[K_P]		0.612	
Speed ratio	[f_n]		0.218	
Thermally safe operating speed	[n_θ]		1928.546	1/min

The reference conditions for calculating the thermal nominal speed are taken from the DIN ISO 15312 standard.

End of Report lines: 90

Appendix E

Deep groove rolling bearings

The following appendix consists of the rolling bearings product sheets from the SKF catalogue. A total of six bearings are present in the transmission, two in each shaft, where:

- Shaft A - 6205 ETN9 and 6305 ETN9;
- Shaft B - 2 x 6308;
- Shaft C - 6209 and 6309.

SKF

6205 ETN9

Dimensions

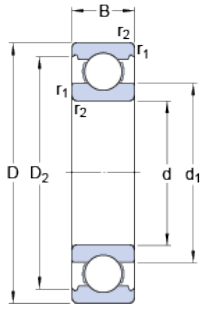

d		25	mm
D		52	mm
B		15	mm
d_1	≈	33.1	mm
D_2	≈	46.21	mm
$r_{1,2}$	min.	1	mm

Abutment dimensions

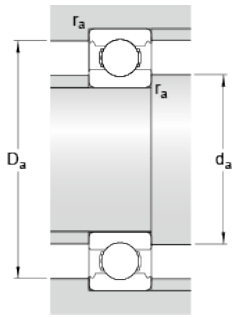

d_a	min.	30.6	mm
D_a	max.	46.4	mm
r_a	max.	1	mm

Calculation data

Basic dynamic load rating	C	17.8	kN
Basic static load rating	C_0	9.3	kN
Fatigue load limit	P_u	0.4	kN
Reference speed		28000	r/min
Limiting speed		18000	r/min
Calculation factor	k_r	0.025	
Calculation factor	f_0	13	

Mass

Mass bearing		0.12	kg

6305 ETN9

Dimensions

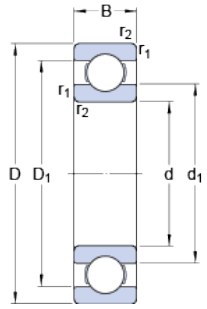

d		25	mm
D		62	mm
B		17	mm
d_1	≈	36.35	mm
D_1	≈	51.62	mm
$r_{1,2}$	min.	1.1	mm

Abutment dimensions

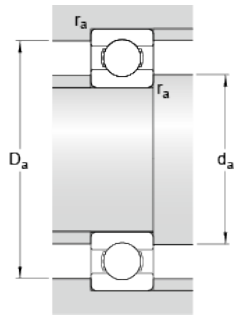

d_a	min.	32	mm
D_a	max.	55	mm
r_a	max.	1	mm

Calculation data

Basic dynamic load rating	C	26	kN
Basic static load rating	C_0	13.4	kN
Fatigue load limit	P_u	0.57	kN
Reference speed		24000	r/min
Limiting speed		16000	r/min
Calculation factor	k_r	0.03	
Calculation factor	f_0	12	

Mass

Mass bearing	0.22	kg

SKF

6308

SKF Explorer

Dimensions

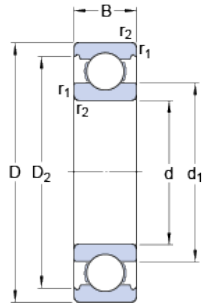

d		40	mm
D		90	mm
B		23	mm
d_1	≈	56.11	mm
D_2	≈	77.7	mm
$r_{1,2}$	min.	1.5	mm

Abutment dimensions

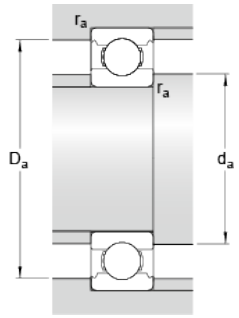

d_a	min.	49	mm
D_a	max.	81	mm
r_a	max.	1.5	mm

Calculation data

Basic dynamic load rating	C	42.3	kN
Basic static load rating	C_0	24	kN
Fatigue load limit	P_u	1.02	kN
Reference speed		17000	r/min
Limiting speed		11000	r/min
Calculation factor	k_r	0.03	
Calculation factor	f_0	13.2	

Mass

Mass bearing	0.63	kg

6209

SKF Explorer

Dimensions

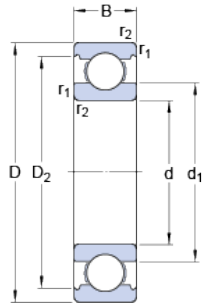

d		45	mm
D		85	mm
B		19	mm
d_1	≈	57.6	mm
D_2	≈	75.19	mm
$r_{1,2}$	min.	1.1	mm

Abutment dimensions

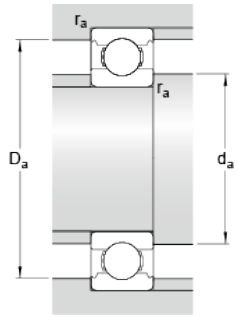

d_a	min.	52	mm
D_a	max.	78	mm
r_a	max.	1	mm

Calculation data

Basic dynamic load rating	C	35.1	kN
Basic static load rating	C_0	21.6	kN
Fatigue load limit	P_u	0.915	kN
Reference speed		17000	r/min
Limiting speed		11000	r/min
Calculation factor	k_r	0.025	
Calculation factor	f_0	14.2	

Mass

Mass bearing	0.42	kg

SKF

6309

SKF Explorer

Dimensions

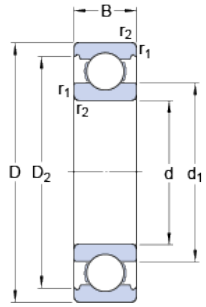

d		45	mm
D		100	mm
B		25	mm
d_1	≈	62.18	mm
D_2	≈	86.7	mm
$r_{1,2}$	min.	1.5	mm

Abutment dimensions

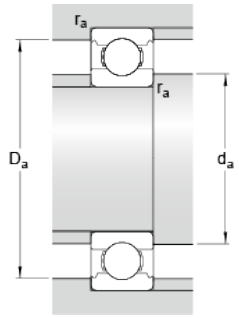

d_a	min.	54	mm
D_a	max.	91	mm
r_a	max.	1.5	mm

Calculation data

Basic dynamic load rating	C	55.3	kN
Basic static load rating	C_0	31.5	kN
Fatigue load limit	P_u	1.34	kN
Reference speed		15000	r/min
Limiting speed		9500	r/min
Calculation factor	k_r	0.03	
Calculation factor	f_0	13	

Mass

Mass bearing	0.83	kg

Appendix F

Radial shaft seals

In this appendix, the product sheets of the radial shaft seals, selected from the SKF catalogue, with the respective specifications are listed. The final transmission has two radial shaft seals, one in the input shaft (A) and the other in the output shaft (C), with the following designation:

- Input shaft seal - 20x30x7 CRW1 R;
- Output shaft seal - 35x47x7 CRW1 R.

20x30x7 CRW1 R

US stock number	7905
Design	CRW1
Lip material	R

Dimensions

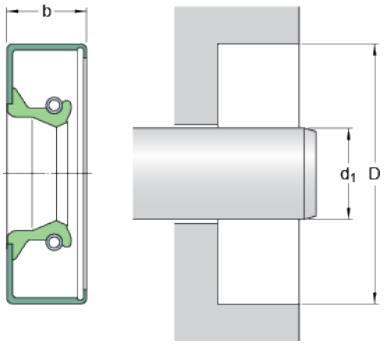

d_1	20	mm
D	30	mm
b	7	mm

Application and operating conditions

Pressure differential	max.	0.07	MPa
Operating temperature	min.	-40	°C
Operating temperature	max.	100	°C
Operating temperature, short period	max.	120	°C
Rotational speed	max.	17189	r/min
Shaft surface speed	max.	18	m/s

35x47x7 CRW1 R

US stock number	13938
Design	CRW1
Lip material	R

Dimensions

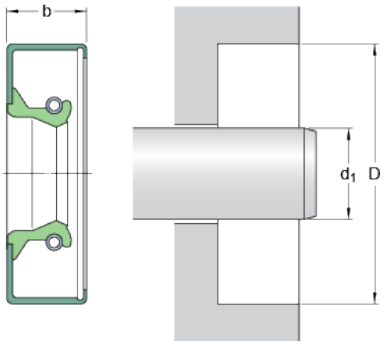

d_1	35	mm
D	47	mm
b	7	mm

Application and operating conditions

Pressure differential	max.	0.07	MPa
Operating temperature	min.	-40	°C
Operating temperature	max.	100	°C
Operating temperature, short period	max.	120	°C
Rotational speed	max.	9822	r/min
Shaft surface speed	max.	18	m/s